TECNOLÓGICO NACIONAL DE MÉXICO

INSTITUTO TECNOLÓGICO DE TEPIC

UNIVERSIDAD POLITÉCNICA DE VALENCIA

DESARROLLO DE MICRO Y NANOFIBRAS ANTIFÚNGICAS PARA EL CONTROL DE ANTRACNOSIS EN AGUACATE "HASS" (*Persea americana* Mill. cv. Hass) OBTENIDAS POR PROCESADO ELECTROHIDRODINÁMICO Y AEROHIDRODINÁMICO.

Por:

M.C.A YULIANA VÁZQUEZ GONZÁLEZ

TESIS EN COTUTELA PROPUESTA A LA:

DIVISIÓN DE ESTUDIOS DE POSGRADO E INVESTIGACIÓN

<<DEPARTAMENTO DE TECNOLOGÍA DE ALIMENTOS>>

COMO REQUISITO PARCIAL PARA OBTENER EL GRADO DE

DOCTOR EN CIENCIAS EN ALIMENTOS

<< DOCTOR EN CIENCIA, TECNOLOGÍA Y GESTIÓN ALIMENTARIA>>

Directores:

Dra. Montserrat Calderón Santoyo

Dr. José María Lagarón Cabello

Co-Directora:

Dra. Cristina Prieto López

Tepic, Nayarit, México Marzo, 2024

Tepic, Nayarit, 24/enero/2024
H. CLAUSTRO DOCTORAL DEL DOCTORADO EN CIENCIAS EN ALIMENTOS
No. Oficio CDCA: 001-2024

M.C. LUZ DEL CARMEN ROMERO ISLAS
JEFA DE LA DIV. DE EST. DE POSF. E INV.
INSTITUTO TECNOLÓGICO DE TEPIC
P R E S E N T E

Por este conducto comunico a usted que el H. Claustro Doctoral en Ciencias en Alimentos ha designado como revisores de la tesis de la alumna **M.C. Yuliana Vázquez González** con número de control **D17400101**, cuyo título es "Desarrollo de micro y nanofibras antifúngicas para el control de antracnosis en aguacate "Hass" (*Persea americana* Mill. cv. Hass) obtenidas por procesado electrohidrodinámico y aerohidrodinámico, a los miembros que a continuación se enlistan, mismos que han evaluado y aprobado el contenido del manuscrito para obtener el grado de Doctora en Ciencias en Alimentos y que firman de conformidad.

Dra. Montserrat Calderón Santoyo
(Presidente)

Dr. José María Lagarón Cabello
(Secretario)

Dra. Cristina Prieto López
(Vocal)

Dr. Juan Arturo Ragazzo Sánchez
(Vocal)

Dra. María de Lourdes García Magaña
(Vocal)

Por lo anterior, le solicito se sirva a elaborar el oficio correspondiente para **autorizar la impresión de tesis**. Agradeciendo de antemano la atención prestada a la presente, aprovecho la ocasión para enviarle un cordial saludo.

A T E N T A M E N T E
Excelencia en Educación Tecnológica®
"Sabiduría tecnológica, pasión de nuestro espíritu" ®

DRA. EFIGENIA MONTALVO GONZÁLEZ
PRESIDENTE DEL H. CLAUSTRO DOCTORAL

ccp. Expediente

Tepic, Nayarit, 20/junio/2023
Oficio No. 25/478/2023
Asunto: Constancia de Originalidad de Trabajo de Tesis

A QUIEN CORRESPONDA:
P R E S E N T E

Por medio de la presente se CERTIFICA que una vez analizado mediante el uso del Software PLAGIARISM v. 1740, el trabajo de tesis ***"DESARROLLO DE MICRO Y NANOFIBRAS ANTIFÚNGICAS PARA EL CONTROL DE ANTRACNOSIS EN AGUACATE "HASS" (Persea americana Mill. Cv. Hass) OBTENIDAS POR PROCESADO ELECTROHIDRODINÁMICO Y AEROHIDRODINÁMICO"*** para obtener el grado de Doctor (a) en Ciencias en Alimentos de la **M.C.A. YULIANA VÁZQUEZ GONZÁLEZ** con número de control **D17400101**, cuenta con un nivel de **Originalidad EXCELENTE** según lo definido en el Procedimiento para la Verificación de Originalidad, por lo cual se determina que no constituye un plagio.

Es importante mencionar que los trabajos de Tesis estan constituidos por artículos publicados en revistas Indizadas y/o arbitradas por lo que las técnicas utilizadas son citadas frecuentemente.
Se extiende la presente para los fines que mejor convengan al interesado.

Sin mas por el momento envío saludos cordiales

A T E N T A M E N T E
Excelencia en Educación Tecnológica®
Sabiduría Tecnológica, Pasión de nuestro espíritu®

MANUEL ÁNGEL URIBE VÁZQUEZ
DIRECTOR

EDUCACIÓN | TECNOLÓGICO NACIONAL DE MÉXICO
INSTITUTO TECNOLÓGICO DE TEPIC
DIRECCIÓN

OGTM/lcr
Ccp: Coordinación de Doctorado en Ciencias en Alimentos

Detector de plagio v. 2118 - Informe de originalidad 16/6/2023 14:05:04

Documento analizado: TESIS 2023_Yuliana VG-para antiplagio.docx Licenciado para: Roberto Enriquez_License2

Preajuste de comparación: Palabra a palabra Idioma detectado: Es

Tipo de verificación: Control de internet

TEE y codificación: DocX n/a

Análisis detallado del cuerpo del documento:

Tabla de relaciones:

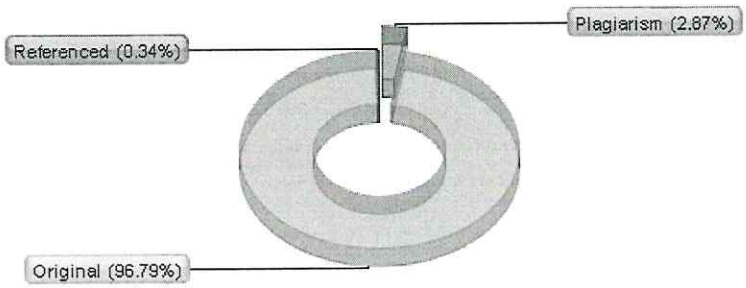

Gráfico de distribución:

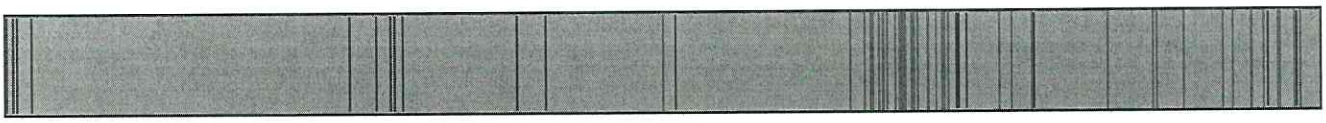

Principales fuentes de plagio: 75

1%	ABC	383	1. https://shsfeapi1.pdc-gate2.com/get_doc.php?id=7619/MTAuMzM4OS9mbWljYi4yMDE5LjAxMjcz.txt
1%	ABC	320	2. https://shsfeapi1.pdc-gate2.com/get_doc.php?id=5053/MTAuMTA4MC8wNzM3MzkzNy4yMDE2LjExNjI3OTc=.txt
0.8%	ABC	193	3. https://shsfeapi1.pdc-gate2.com/get_doc.php?id=4732/MTAuMTAxNi9qLmFyYWJqYy4yMDE1LjExLjAxNQ==.txt

Detalles de recursos procesados: 412 - Okay / 51 - Ha fallado

Notas importantes:

Wikipedia:	Libros de Google:	Servicios de escritura fantasma:	Anti-trampa:
[no detectado]	[no detectado]	[no detectado]	[no detectado]

Informe anti trampas de UACE:

1. Estado: Analizador **Encendido** Normalizador **Encendido** similitud de caracteres establecida en **100%**
2. Porcentaje de contaminación UniCode detectado: **0.2%** con límite de: 4%
3. Documento no normalizado: porcentaje no alcanzado 5%
4. Todos los símbolos sospechosos se marcarán en color violeta: Abcd...
5. Símbolos invisibles encontrados: 0

Recomendación de evaluación:

No se requiere ninguna acción especial. El documento está bien.

Tepic, Nayarit, 29/enero/2024
No. Oficio: 25-108-2024
Asunto: Autorización de impresión de Trabajo de Tesis

MCA YULIANA VÁZQUEZ GONZÁLEZ
CANDIDATO AL GRADO DE DOCTOR EN CIENCIAS EN ALIMENTOS
P R E S E N T E

De acuerdo con los Lineamientos para la Operación de los Estudios de Posgrado en el Tecnológico Nacional de México y las disposiciones en este Instituto, habiendo cumplido con todas las indicaciones que la Comisión Revisora realizó con respecto a su Trabajo de Tesis titulado "*DESARROLLO DE MICRO Y NANOFIBRAS ANTIFÚNGICAS PARA EL CONTROL DE ANTRACNOSIS EN AGUACATE "HASS" (Persea americana Mill. Cv. Hass) OBTENIDAS POR PROCESADO ELECTROHIDRODINÁMICO Y AEROHIDRODINÁMICO*", la División de Estudios de Posgrado e Investigación de este Instituto, concede la Autorización para que proceda a la impresión del mismo.

Sin otro particular, quedo de Usted.

SECRETARIA DE EDUCACIÓN PÚBLICA
INSTITUTO TECNOLÓGICO
DE TEPIC
DIVISIÓN DE ESTUDIOS DE
POSGRADO E INVESTIGACIÓN

A T E N T A M E N T E
Excelencia en Educación Tecnológica®
"Sabiduría tecnológica, pasión de nuestro espíritu"®

LUZ DEL CARMEN ROMERO ISLAS
JEFA DE LA DIVISIÓN DE ESTUDIOS DE POSGRADO E INVESTIGACIÓN

ccp. Coordinación del Doctorado en Ciencias en Alimentos
Archivo

TECNOLÓGICO NACIONAL DE MÉXICO

INSTITUTO TECNOLÓGICO DE TEPIC
DIVISIÓN DE ESTUDIOS DE POSGRADO E INVESTIGACIÓN
POSGRADO EN CIENCIAS EN ALIMENTOS

ASUNTO: CARTA DE SESIÓN DE DERECHOS

En la ciudad de Tepic, Nayarit., a treinta días del mes de enero de 2024, la que suscribe alumna **YULIANA VÁZQUEZ GONZÁLEZ** del Programa de **DOCTORADO EN CIENCIAS EN ALIMENTOS** con número de control **D17400101**, manifiesta que todos los resultados derivados de sus estudios de posgrado y realizados bajo la dirección de la **DRA. MONTSERRAT CALDERÓN SANTOYO** pertenece al TECNOLÓGICO NACIONAL DE MÉXICO/INSTITUTO TECNOLÓGICO DE TEPIC, por lo que cedo los derechos de los mismos a este instituto con fines académicos y de investigación. Así mismo manifiesto que es de mi conocimiento que si de estos resultados se originan patentes o publicaciones, participaré como coautor y de los beneficios que se deriven.

YULIANA VÁZQUEZ GONZÁLEZ

Dra. Montserrat Calderón Santoyo, Profesora del Laboratorio Integral de Investigación en Alimentos del Tecnológico Nacional de México/Instituto Tecnológico de Tepic (TecNM/ITTepic), Dr. Jose María Lagarón Cabello, Investigador Científico del Consejo Superior de Investigaciones Científicas (CSIC) en el Instituto de Agroquímica y Tecnología de Alimentos (IATA) y Dra. Cristina Prieto López, Investigadora Postdoctoral del Consejo Superior de Investigaciones Científicas (CSIC) en el Instituto de Agroquímica y Tecnología de Alimentos (IATA)

CERTIFICAN

Que la presente tesis titulada "Desarrollo de micro y nanofibras antifúngicas para el control de antracnosis en aguacate "Hass" (*Persea americana* Mill. cv. Hass) obtenidas por procesado electrohidrodinámico y aerohidrodinámico" constituye la tesis doctoral de Yuliana Vázquez González y reúne las condiciones adecuadas para su presentación. Asimismo, certifican haber dirigido y supervisado tanto los distintos aspectos del trabajo como la redacción.

Y para que así conste a los efectos oportunos, firmamos la presente.

Montserrat Calderón Santoyo

Firmado digitalmente por Montserrat Calderón Santoyo
Fecha: 2024.03.13 08:14:37 -07'00'

Fdo. Montserrat Calderón Santoyo

Fdo. José María Lagarón Cabello

Firmado por PRIETO LOPEZ, CRISTINA (FIRMA) el día 13/03/2024 con un certificado emitido por AC DNIE 004

Fdo. Cristina Prieto López

"Pregúntate si lo que estás haciendo hoy te acerca al lugar en el que quieres estar mañana"
Walt Disney

A mis padres
Teresa y Laureano

AGRADECIMIENTOS

Agradezco a **Dios** por hacer posible este proceso, permitirme llegar a este momento de mi vida, cuatro años de gran aprendizaje y de aventuras. **Hoy**, logro una de las metas que me propuse hace cuatro años y que me llena de gran satisfacción. Quiero dar un enorme agradecimiento **a mis padres** quienes me han apoyado y guiado en cada una de las decisiones tomadas, por sus enseñanzas y valores que me forjaron e hicieron de mí una persona exitosa. Tomando en cuenta, que para mí el concepto de éxito concuerda con las palabras dichas por Ralph Waldo Emerson: ¿Qué es el éxito? reír mucho y con regularidad; ganarse el respeto de personas inteligentes y el cariño de los niños; ganar el aprecio de críticos sinceros y soportar la traición de amigos falsos; apreciar la belleza; encontrar lo mejor de los demás; dejar el mundo un poco mejor, un trozo de jardín o el rescate de un grupo social; saber que por lo menos una vida respiró mejor por haber vivido tú.

Agradezco al Consejo Nacional de Ciencia y Tecnología (CONACyT) por la beca número 754518 concedida para hacer posible el desarrollo de este proyecto de investigación.

A mis directores de tesis, Montserrat Calderón Santoyo, por brindarme esta gran oportunidad de participar en un proceso de doble titulación entre el Laboratorio Integral de Investigación de Alimentos y la Universidad Politécnica de Valencia, asimismo, agradezco por la dirección y apoyo en la realización de este proyecto. A José María Lagarón Cabello por el recibimiento y gran hospitalidad en el Instituto de Agroquímica y Tecnología de Alimentos (IATA-CSIC), por su dirección, comprensión y apoyo en el desarrollo de este trabajo. A Cristina Prieto López por su acogida en el Grupo de Nuevos Materiales y Nanotecnología para Aplicaciones Alimentarias, por su apoyo constante, su dirección y por ser una guía en el desarrollo de este trabajo.

Agradezco a los revisores, Juan Arturo Ragazzo Sánchez y María de Lourdes García Magaña integrantes de mi comité tutorial, por sus conocimientos y aportaciones brindadas para el desarrollo de este trabajo.

El concepto propio es un conjunto de creencias, valores, actitudes, ideas y sentimientos almacenados en el fondo de nosotros y son el resultado de casi todas las experiencias que hemos tenido en la vida, el concepto propio "precede, predice y determina los niveles de eficacia en casi todas las áreas de nuestra vida". En este sentido, quiero agradecer a cada una de las personas que estuvieron presentes durante este periodo, de ellos/ellas aprendí cosas invaluables que me hicieron crecer personal y académicamente modificando "mi concepto propio".

Un agradecimiento especial a Milan Stojanovic, quien fue una persona trascendental e influyó en mi crecimiento personal y académico durante mi estancia en España.

Agradezco a los amigos que estuvieron presentes, en especial a Maricarmen Iñiguez por brindarme esa inolvidable amistad, sus consejos, su apoyo y sus conocimientos. También quiero agradecer a Surelys Ramos por su valiosa amistad y su apoyo desde el primer momento que nos conocimos. Agradezco a Yokaterine Lebron y a Daniela Arango, dos seres llenos de luz que me acompañaron durante mis casi dos años de estancia en Valencia. Agradezco a Octavio García, quien hizo que mi estancia en España fuera más amena enviándome productos mexicanos.

Por otro lado, quiero agradecer a todos mis compañeros del Laboratorio de Microbiología de Alimentos por todas las convivencias, Jerusalén Betancourt, Karla Ayón y Rafael López agradezco su energía positiva y todo su apoyo brindado haciendo más ameno este proceso. Agradezco también a mis compañeros del Laboratorio 502, Zoran, Alberto, Mattia, Carmen y Kelly, quienes me apoyaron en todo momento desde el primer día de mi estancia.

RESUMEN

La pérdida y desperdicio de alimentos supone un problema global de gran magnitud con implicaciones significativas en los ámbitos ambiental, económico y social. Una fracción importante de dichas pérdidas está producida por las enfermedades postcosecha causadas por fitopatógenos. De forma convencional, estas enfermedades se combaten con pesticidas químicos, pero en la actualidad se están buscando alternativas más sostenibles, como los agentes de biocontrol naturales, entre los que destacan los microorganismos antagonistas. Para garantizar su efectividad y proporcionar protección y estabilidad a dichos microorganismos, su combinación con matrices biopoliméricas en forma de recubrimientos podría ser una alternativa. Sin embargo, las técnicas convencionales de producción de dichos recubrimientos no garantizan la homogeneidad del tratamiento sobre el alimento, pudiendo afectar a su efectividad. En este sentido, las nanofibras hiladas mediante procesos electro y aerohidrodinámicos pueden actuar como una matriz biopolimérica para atrapar dichos microorganismos, y pueden ser depositadas homogéneamente en la superficie de los alimentos, y esto, junto a que son estructuras con una gran superficie-volumen, las hace más activas y eficientes. Por tanto, el objetivo general de esta investigación fue el desarrollo de recubrimientos comestibles antifúngicos basados en micro o nanofibras biopoliméricas producidas mediante procesos electro y aerohidrodinámicos, conteniendo la levadura biocontrol *Meyerozyma caribbica*, para el control de antracnosis en aguacate "Hass" (*Persea americana* Mill. cv. Hass) y garantizando además los parámetros de calidad en el fruto.

Para lograr este objetivo, el estudio se dividió en cuatro etapas. Las etapas 1 y 2, consistieron en la realización de un estudio sobre la formación de micro y nanoestructuras biopoliméricas mediante procesos electrohidrodinámicos y aerohidrodinámicos. Para ello, se llevó a cabo el desarrollo y caracterización fisicoquímica de las disoluciones poliméricas de goma de anacardo (CG) y FucoPol (FP) como polímeros principales, y poli (óxido de etileno) (PEO) y pululano (Pul) como polímeros de soporte. De tal modo, se desarrollaron formulaciones de CG, FP, FP:PEO y FP:Pul capaces de formar estructuras mediante *electrospray* y *electrospining*. La etapa 1 se centró en el estudio de la CG, mientras que la etapa 2 se centró en el estudio del FP. Las estructuras obtenidas mediante *electrospray* y

electrospinning fueron caracterizadas mediante microscopía electrónica de barrido (SEM), espectroscopía de infrarrojo (ATR-FTIR), dispersión de rayos X (WAXS), análisis termogravimétrico (TGA) y calorimetría diferencial de barrido (DSC). Las microestructuras obtenidas a partir de la disolución de CG, resultaron ser cápsulas esféricas y sin depresiones irregulares. El TGA y el análisis de exposición a la luz UV mostraron que las cápsulas de CG brindaron protección térmica y fotoestabilidad al compuesto modelo encapsulado (β-caroteno). El análisis ATR-FTIR mostró indirectamente la presencia del β-caroteno en las cápsulas de CG. Por otro lado, FP, FP:Pul y FP:PEO mostraron fibras helicoidales cilíndricas, lisas y gruesas. Los análisis de DSC y WAXS mostraron que las nanofibras de FP:PEO presentaban naturaleza cristalina reducida en comparación con PEO puro. Finalmente, mediante WAXS, en las nanofibras de FP:Pul y FP:PEO se detectaron nuevos picos a ángulos por debajo de los 10º, lo que sugiere que FucoPol podría afectar la estructura polimérica de otros materiales con una estructura secundaria helicoidal.

La etapa 3 consistió en la encapsulación de *M. caribbica* en nanofibras de pululano, CG:PEO y FP:PEO obtenidas mediante *electrospinning*. Las nanofibras se caracterizaron mediante SEM, ATR-FTIR y TGA. Se determinó la viabilidad de *M. caribbica* a 6 ºC y 26 ºC durante 25 días y se evaluó la actividad antifúngica de las nanofibras frente a seis hongos de interés comercial (*Fusarium oxysporum*, *Colletotrichum gloeosporioides*, *Penicillium italicum*, *Penicillium digitatum*, *Trichothecium roseum* y *Botrytis cinerea*). Las nanofibras de pululano, CG:PEO y FP:PEO con *M. caribbica* mostraron nanofibras cilíndricas, lisas y homogéneas. El análisis ATR-FTIR mostró que no hubo interacciones químicas entre la levadura y los polímeros. Las fibras con *M. caribbica* mostraron un efecto fungistático en la germinación de esporas de los seis hongos de interés comercial, las nanofibras de pululano mostraron la viabilidad más alta de *M. caribbica,* así como el mayor porcentaje de inhibición en el crecimiento de los seis hongos evaluados.

Finalmente, la etapa 4 consistió en la encapsulación de *M. caribbica* en nanofibras de pululano, CG:PEO y FP:PEO obtenidas mediante *Solution Blow Spinning* (SBS) y su posterior evaluación *in vivo* en frutos de aguacate almacenados a temperaturas de almacenamiento y de comercialización. La estructura de las nanofibras se caracterizó mediante SEM, obteniéndose fibras homogéneas, continuas y rizadas. Posteriormente, se determinó la viabilidad de *M. caribbica* en las nanofibras, se evaluó la actividad antifúngica

in vitro e *in vivo* como tratamientos preventivos y curativos frente a *C. gloeosporioides*. Se observó una alta viabilidad de *M. caribbica* en las nanofibras aplicadas en la superficie de los aguacates mediante SBS bajo las diferentes condiciones evaluadas. Las nanofibras de pululano con *M. caribbica* como tratamiento preventivo inhibieron por completo el crecimiento de *C. gloeosporioides* en los frutos de aguacate. Finalmente, se evaluó el efecto de las nanofibras sobre los parámetros de calidad de los aguacates (sólidos solubles totales, pH, contenido de materia seca, pérdida de peso, acidez titulable, firmeza, color). La aplicación de las nanofibras de pululano sobre los aguacates no afectó a los parámetros de calidad con respecto al control.

El pululano, la CG y el FP en combinación con PEO y pululano se han estudiado por primera vez para formar estructuras mediante *electrospray*, *electrospinning* y SBS. Estos resultados, sugieren un alto potencial de las nanofibras para su uso en la industria alimentaria y representan una alternativa interesante para el tratamiento postcosecha de frutos en el control de enfermedades fúngicas, contribuyendo de esta manera a reducir la pérdida en la producción de alimentos.

Palabras clave: FucoPol, goma de anacardo, pululano, *electrospinning*, *solution blown spinning*, *Meyerozyma caribbica*, control postcosecha.

ABSTRACT

Food loss and waste is a large global problem with significant implications for the environment, the economy, and society. An important fraction of these losses is caused by postharvest diseases caused by phytopathogens. Conventionally, these diseases were fought with chemical pesticides, but more sustainable alternatives are currently being sought, such as natural biocontrol agents, among which antagonistic microorganisms stand out. To guarantee its effectiveness and provide protection and stability to these microorganisms, its combination with biopolymeric matrices in the form of coatings could be an alternative. However, the production techniques of these coatings do not guarantee the homogeneity of the treatment on the food, which may affect its effectiveness. In this sense, nanofibers spun using electro- and aerohydrodynamic processes can act as a biopolymeric matrix to trap microorganisms and be deposited homogeneously on the surface of food, in addition to being structures with a large surface-volume ratio, which makes them more active and efficient. Therefore, the general objective of this research was the development of antifungal coatings based on biopolymeric micro or nanofibers produced by electro- and aerohydrodynamic processes and loaded with the biocontrol yeast *Meyerozyma caribbica* for the control of anthracnose in "Hass" avocado (*Persea Americana* Mill. cv. Hass) and guaranteeing quality parameters in the fruit.

To achieve this objective, the study was divided into four stages. Stages 1 and 2 consisted of a study on the formation of biopolymeric micro and nanostructures via electrohydrodynamic and aerohydrodynamic processes. For this, the development and physicochemical characterization of the polymer solutions using cashew gum (CG) and FucoPol (FP) as main polymers, and polyethylene oxide (PEO) and pullulan (Pul) as supporting polymers were performed. In this manner, formulations of CG, FP, FP:PEO, and FP:Pul capable of forming structures by electrospray and electrospinning were developed. Stage 1 focused on the study of CG, whereas stage 2 focused on the study of FP. The structures developed by electrospray and electrospinning were characterized by scanning electron microscopy (SEM), infrared spectroscopy (ATR-FTIR), wide angle x-ray scattering (WAXS), thermogravimetric analysis (TGA) and differential scanning calorimetry (DSC). The microstructures obtained from the CG solution resulted to be spherical capsules without

irregular depressions. TGA and UV light exposure analysis showed that CG capsules provided thermal protection and photostability to the encapsulated model compound (β-carotene). The ATR-FTIR analysis indirectly showed the presence of β-carotene in CG capsules. On the other hand, FP, FP:Pul and FP:PEO showed cylindrical, smooth, and thick helical fibers. DSC and WAXS analysis demonstrated that FP:PEO nanofibers had a reduced crystalline nature compared to pure PEO. Finally, using WAXS, new peaks at angles below 10º were detected in FP:Pul and FP:PEO nanofibers, suggesting that FucoPol could affect the polymer structure of other materials with a secondary helical structure.

Stage 3 consisted of the *M. caribbica* encapsulation in nanofibers of pullulan, CG:PEO, and FP:PEO obtained by electrospinning. Nanofibers were characterized by SEM, ATR-FTIR and TGA. The viability of *M. caribbica* was determined at 6 ºC and 26 ºC for 25 days and the antifungal activity of nanofibers was evaluated against six fungi of commercial interest (*Fusarium oxysporum*, *Colletotrichum gloeosporioides*, *Penicillium italicum*, *Penicillium digitatum*, *Trichothecium roseum* and *Botrytis cinerea*). Nanofibers of pullulan, CG:PEO and FP:PEO loaded with *M. caribbica* showed cylindrical, smooth and homogeneous nanofibers. The ATR-FTIR analysis showed no chemical interactions between yeast and polymers. Fibers loaded with *M. caribbica* showed a fungistatic effect on the germination of spores of the six fungi of commercial interest, pullulan nanofibers showed the highest viability of *M. caribbica*, as well as the highest percentage of inhibition in the growth of the six fungi evaluated.

Finally, stage 4 consisted of the encapsulation of *M. caribbica* in nanofibers of pullulan, CG:PEO and FP:PEO obtained via Solution Blow Spinning (SBS) and its subsequent *in vivo* evaluation in avocado fruits stored at storage and commercialization temperatures. The structure of the nanofibers was characterized by SEM. Subsequently, the viability of *M. caribbica* in nanofibers was determined, and the antifungal activity *in vitro* and *in vivo* was evaluated as preventive and curative treatments against *C. gloeosporioides*. Finally, the effect of the developed nanofibers loaded with *M. caribbica* on avocado quality parameters (total soluble solids, pH, dry matter content, weight loss, titratable acidity, firmness, and color) was evaluated. Homogeneous, continuous, and curly fibers were obtained. SBS ensured a high viability of *M. caribbica* in nanofibers applied on the surface of avocados under different evaluated conditions. Nanofibers of pullulan loaded with *M. caribbica* as a preventive

treatment completely inhibited the growth of *C. gloeosporioides* in avocado fruits. The pullulan nanofibers application on avocados did not affect the quality parameters concerning the control.

Pullulan, CG, and FP in combination with PEO and pullulan have been studied for the first time to form structures by electrospray, electrospinning, and SBS. These results suggest a high potential of nanofibers for use in the food industry and represent an interesting alternative for the post-harvest treatment of fruits in the control of fungal diseases, thereby contributing to reducing loss in food production.

Keywords: FucoPol, cashew gum, pullulan, electrospinning, solution blown spinning, *Meyerozyma caribbica*, post-harvest control.

RESUM

La pèrdua i malbaratament alimentari suposa un problema global de gran magnitud amb implicacions significatives en els àmbits ambiental, econòmic i social. Una part important d'aquestes pèrdues està produïda per les malalties post collita causades per fitopatògens. Normalment, aquestes malalties es combaten amb pesticides químics, però en l'actualitat s'estan fent recerques alternatives més sostenibles, com els agents de biocontrol naturals, entre els quals destaquen els microorganismes antagonistes. Per a garantir la seua efectivitat i proporcionar protecció i estabilitat a aquests microorganismes, la seua combinació amb matrius bio-polimèriques en forma de recobriments comestibles podria ser una alternativa. No obstant això, les tècniques convencionals de producció d'aquests recobriments no garanteixen l'homogeneïtat del tractament sobre l'aliment, podent afectar la seua efectivitat. En aquest sentit, les nanofibres filades mitjançant processos electre i aerohidrodinámics poden actuar com una matriu bio-polimèrica per a atrapar aquests microorganismes, i poden ser dipositades homogèniament en la superfície dels aliments, i això, al costat de què són estructures amb una gran superfície-volum, les fa més actives i eficients. Per tant, l'objectiu general d'aquesta recerca va ser el desenvolupament de recobriments comestibles antifúngics basats en micro o nanofibres bio-polimèriques produïdes mitjançant processos electre i aerohidrodinámics, contenint el llevat biocontrol *Meyerozyma caribbica*, per al control d' antracnosis en alvocat "Hass" (*Persea americana* Mill. cv. Hass) i garantint a més els paràmetres de qualitat en el fruit.

Per a aconseguir aquest objectiu, l'estudi es va dividir en quatre etapes. Les etapes 1 i 2, van consistir en la realització d'un estudi sobre la formació de micro i nanoestructures bio-polimèriques mitjançant processos electrehidrodinámicos i aerohidrodinámics. Per a això, es va dur a terme el desenvolupament i caracterització fisicoquímica de les dissolucions polimèriques de goma d'anacard (CG) i FucoPol (FP) com a polímers principals, i poli (òxid d'etilè) (PEO) i pululan (Pul) com a polímers de suport. Així, es van desenvolupar formulacions de CG, FP, FP:PEO i FP:Pul capaços de formar estructures mitjançant *electrospray* i *electrospining*. L'etapa 1 es va centrar en l'estudi de la CG, mentre que l'etapa 2 es va centrar en l'estudi del FP. Les estructures obtingudes mitjançant *electrospray* i *electrospinning* van ser caracteritzades mitjançant microscòpia electrònica d'escombratge

(SEM), espectroscopía d'infraroig (ATR-FTIR), dispersió de raigs X (WAXS), anàlisis termogravimétrica (TGA) i calorimetria diferencial d'escombratge (DSC). Les microestructures obtingudes a partir de la dissolució de CG, van resultar ser càpsules esfèriques i sense depressions irregulars. El TGA i l'anàlisi d'exposició a la llum UV van mostrar que les càpsules de CG van brindar protecció tèrmica i foto estabilitat al compost model encapsulat (β-carotè). L'anàlisi ATR-FTIR va mostrar indirectament la presència del β-carotè en les càpsules de CG. D'altra banda, FP, FP:Pul i FP:PEO van mostrar fibres helicoïdals cilíndriques, llises i gruixudes. Les anàlisis de DSC i WAXS van mostrar que les nanofibres d'FP:PEO presentaven naturalesa cristal·lina reduïda en comparació amb PEO pur. Finalment, mitjançant WAXS, en les nanofibres d'FP:Pul i FP:PEO es van detectar nous pics a angles per sota dels 10°, la qual cosa suggereix que FucoPol podria afectar l'estructura polimèrica d'altres materials amb una estructura secundària helicoïdal.

L'etapa 3 va consistir en l'encapsulació de *M. caribbica* en nanofibres de pululan, CG:PEO i FP:PEO obtingudes mitjançant *electrospinning*. Les nanofibras es van caracteritzar mitjançant SEM, ATR-FTIR i TGA. Es va determinar la viabilitat de *M. caribbica* a 6 °C i 26 °C durant 25 dies i es va avaluar l'activitat antifúngica de les nanofibres front a sis fongs d'interès comercial (*Fusarium oxysporum, Colletotrichum gloeosporioides, Penicillium italicum, Penicillium digitatum, Trichothecium roseum i Botrytiscinerea*).

Les nanofibres de pululano, CG:PEO i FP:PEO amb *M. caribbica* van mostrar nanofibres cilíndriques, llises i homogènies. L'anàlisi ATR-FTIR va mostrar que no va haver-hi interaccions químiques entre el llevat i els polímers. Les fibres amb *M. caribbica* van mostrar un efecte fungistàtic en la germinació d'espores dels sis fongs d'interès comercial, les nanofibres de pululan van mostrar la viabilitat més alta de *M. caribbica*, així com el percentatge més gran d'inhibició en el creixement dels sis fongs avaluats.

Finalment, l'etapa 4 va consistir en l'encapsulació de *M. caribbica* en nanofibres de pululan, CG:PEO I FP:PEO obtingudes mitjançant *Solution Blow Spinning* (SBS) i la seua posterior avaluació *in vivo* en fruits d'alvocat emmagatzemats a temperatures d'emmagatzematge i de comercialització. L'estructura de les nanofibres es va caracteritzar mitjançant SEM, obtenint-se fibres homogènies, contínues i arrissades. Posteriorment, es va determinar la viabilitat de *M. caribbica* en les nanofibres, es va avaluar l'activitat antifúngica

in vitro i *in vivo* com a tractaments preventius i curatius enfront de *C. gloeosporioides*. Es va observar una alta viabilitat de *M. caribbica* en les nanofibres aplicades en la superfície dels alvocats mitjançant SBS sota les diferents condicions avaluades. Les nanofibres de pululan amb *M. caribbica* com a tractament preventiu van inhibir per complet el creixement de *C. gloeosporioides* en els fruits d'alvocat. Finalment, es va avaluar l'efecte de les nanofibres sobre els paràmetres de qualitat dels alvocats (sòlids solubles totals, pH, contingut de matèria seca, pèrdua de pes, acidesa titulable, fermesa, color). L'aplicació de les nanofibres de pululan sobre els alvocats no va afectar els paràmetres de qualitat respecte al control.

El pululan, la CG i l'FP en combinació amb PEO i pululan s'han estudiat per primera vegada per a formar estructures mitjançant *electrospray*, *electrospinning* i SBS. Aquests resultats suggereixen un alt potencial de les nanofibres per al seu ús en la indústria alimentària i representen una alternativa interessant per al tractament post collita de fruits en el control de malalties fúngiques, contribuint d'aquesta manera a reduir la pèrdua en la producció d'aliments.

Paraules clau: FucoPol, goma d'anacard, pululan, *electrospinning*, *solution blown spinning*, *Meyerozyma caribbica*, control post collita.

CONTENIDO

LISTA DE CUADROS

LISTA DE FIGURAS

LISTA DE ABREVIATURAS

BCA	*Biocontrol agents*
CECT	*Spanish Type Culture Collection*
CG	*Cashew gum*
CG:PEO	*Cashew gum: Polyethylene oxide*
DMC	*Dry matter content*
DSC	*Differential Scanning Calorimetry*
EPS	*Exopolysaccharides*
FP	*FucoPol*
FP:PEO	*FucoPol: Polyethylene oxide*
FTIR-ATR	*Fourier Transform Infrared Spectroscopy-Attenuated Total Reflection*
GRAS	*Generally Recognized As Safe*
NMR	*Nuclear magnetic resonance*
PBS	*Phosphate-buffered saline*
PDA	*Potato Dextrose Agar*
PEO	*Polyethylene oxide*
PLA	*Polylactic acid*
PLG	*Poly (d,l-lactide-co-glycolide)*
Pul	*Pullulan*
PVA	*Poly (vinyl alcohol)*
RH	*Relative Humidity*
ROS	*Reactive Oxygen Species*
SBS	*Solution Blow Spinning*
SEM	*Scanning Electron Microscopy*
TA	*Titratable acidity*
Tc	*Crystallization temperature*
TGA	*Thermogravimetric analysis*
Tm	*Melting point*
TSS	*Total Solids Soluble*
VOC	*Volatile Organic Compounds*
WAXS	*Wide-angle X-ray scattering*
YPD	*Yeast extract Peptone Dextrose*
ΔHc	*Enthalpy of cristallization*
ΔH	*Relaxation enthalpy*
ΔHm	*Enthalpy of melting*
%LC	*Loading Capacity Percentage*
EβC	*Extractable β-carotene*

CAPÍTULO 1. INTRODUCCIÓN

1. INTRODUCCIÓN

La pérdida y desperdicio de alimentos supone un problema global de gran magnitud con implicaciones significativas en los ámbitos ambiental, económico y social, repercutiendo negativamente en la seguridad alimentaria y la nutrición, en las emisiones de gases de efecto invernadero (GEI), la contaminación del medio ambiente, la degradación de los ecosistemas naturales y la pérdida de biodiversidad. De acuerdo con estimaciones de Naciones Unidas, este problema se manifiesta a lo largo de diversas etapas de la cadena de suministro de alimentos. Globalmente, alrededor de un 13% de los alimentos producidos se pierden en producción y procesamiento, mientras que el 17% se pierden en las etapas de distribución y venta, o durante el consumo (ONU, 2023a), alimentos que de acuerdo con estimaciones de la Organización de las Naciones Unidas para la Alimentación y la Agricultura (FAO) podrían alimentar a 1260 millones de personas hambrientas cada año (FAO, 2023). Es por tanto necesario llamar a la acción tanto al sector público (autoridades nacionales o locales) como al sector privado (empresas e individuos), para priorizar acciones que permitan reducir la pérdida y el desperdicio de alimentos y así restaurar y reconstruir sistemas alimentarios mejores y más resilientes. Esta problemática constituye uno de los Objetivos de Desarrollo Sostenible de la Agenda 2030 de Naciones Unidas, está presente en las estrategias europeas "*European Green Deal*" y "*Farm to fork*". El gobierno estadounidense, a través del Departamento de Agricultura de los Estados Unidos (USDA); tiene programas que apoyan prácticas agrícolas para reducir el impacto ambiental y promueven la salud del suelo, así como la promoción de sistemas de alimentos locales y regionales (USDA, 2023). Por otro lado, México ha implementado diversas estrategias y políticas en términos de economía circular reduciendo el desperdicio de alimentos y fomentando prácticas sostenibles en la producción y el consumo. También se han implementado programas de agricultura sostenible, incluyendo el apoyo a la agricultura orgánica y la implementación de prácticas agrícolas que reduzcan el impacto ambiental (ONU, 2023b).

Centrando la atención sobre la producción agrícola, el conjunto de causas que ocasionan la pérdida de alimentos se pueden clasificar en factores medioambientales y biológicos (fenomenología extrema, enfermedades y plagas), factores tecnológicos (herramientas, técnicas o instalaciones inadecuadas), factores económicos y sociales (variabilidad de los precios, normas y estándares de calidad, desajustes en la oferta y la

demanda), y factores humanos (programación inadecuada, abandono, mala gestión) (Magalhães y cols., 2021).

Entre los anteriores factores, las enfermedades postcosecha representan una importante amenaza para los cultivos, hortalizas y frutas cosechados, durante su transporte, manipulación y almacenamiento; además son consideradas como el factor más importante de daño del alimento a nivel cosmético, organoléptico y nutricional induciendo una reducción en la percepción de calidad multifuncional (Ramírez-Gil y cols.., 2021). Por lo tanto, ha surgido un interés creciente en prevenir las enfermedades postcosecha causadas por microorganismos fitopatógenos en los alimentos frescos.

Tradicionalmente, la principal medida para el control de los fitopatógenos ha sido el uso de pesticidas químicos, los cuales generalmente se aplican por aspersión sobre los frutos, previo al almacenamiento en los envases. Sin embargo, el uso desmedido y en concentraciones subletales ha incrementado la presencia de especies resistentes a estos compuestos, y esto, aunado al creciente interés por tener bajos riesgos toxicológicos, el menor riesgo a especies endógenas, la necesidad de contar con alimentos inocuos y disminuir el impacto negativo al medio ambiente (Sharma, Singh y Singh, 2009), ha llevado a la búsqueda de medidas alternativas que minimicen el uso de agentes químicos.

CAPÍTULO 2. ANTECEDENTES

2. ANTECEDENTES

2.1 El aguacate

El aguacate es una fruta conocida por su alto contenido nutricional y los beneficios que confiere a salud (Alvarez y cols.., 2012), cuyas características como tamaño (entre los 120 g y los 2.5 kg), tipo de piel (lisa o rugosa, delgada o gruesa), número de semillas, dependen de la variedad, de las condiciones climáticas y de las prácticas agrícolas durante su cultivo (Morton, 2004).

2.2 Producción de aguacate

El aguacate (*Persea americana* Mill. cv. Hass) es un cultivo de gran importancia económica a nivel mundial, siendo uno de los diez principales cultivos en México. En 2021, la producción global de aguacates osciló en torno a los 8.1 millones de toneladas (STATISTA, 2023), principalmente debido a la creciente demanda de este fruto causada por su versatilidad y los beneficios nutricionales que éste presenta. México es el primer productor y exportador mundial de aguacate, con una producción nacional en el 2021 de 2.44 millones de toneladas métricas (STATISTA, 2023), de los cuales alrededor del 50% se exporta a aproximadamente 26 países entre los que se encuentra China, Estados Unidos, o la Unión Europea. Los principales estados productores de aguacate son Michoacán, Jalisco, Estado de México, Nayarit y Morelos. En el año 2021, Nayarit tuvo una producción nacional de 75, 013.41 toneladas de aguacate (SIAP, 2021). A pesar de la alta producción de este fruto, el aguacate es un fruto climatérico, hecho que dificulta su conservación y comercialización a mercados distantes, disminuyendo su calidad, vida útil y su valor comercial (Ramírez-Gil y cols., 2021), además es altamente susceptible a enfermedades postcosecha, factores que generan importantes pérdidas de la producción y consecuentemente económicas.

2.3 Causas que afectan a la pérdida de valor comercial del aguacate

Durante el proceso de maduración, los frutos de aguacate son susceptibles a magulladuras y pudriciones. Las primeras generalmente son provocadas por algunas lesiones mecánicas, ya sea por impacto, compresión o vibración de los frutos al momento de su manipulación.

Mientras que, las pudriciones son el resultado de algunos patógenos fúngicos que pueden atacar al fruto en la etapa de floración o durante la cosecha del fruto (Cuadro 1), siendo la antracnosis y la pudrición del tallo, las dos enfermedades más importantes que atacan a este fruto, causando grandes pérdidas económicas.

Cuadro 1. Enfermedades postcosecha más comunes en aguacate

Nombre común	**Agente causal**
Antracnosis	*Colletotrichum gloeosporioides*
Pudrición del tallo	*Botryodiploidia theobromae* Pat *Dothiorella* spp.
	Thyronectria pseudotrichia
Pudrición por *Alternaria*	*Alternaria* spp.
Pudrición por *Rhizopus*	*Rhizopus stolonifer*
Pudrición por *Fusarium*	*Fusarium* spp.
Podredumbre rosa	*Trichothecium roseum* Link.
Tizón de halo	*Colletotrichum gloeosporioides*
Moho azul	*Penicillium expansum* Link.

Fuente: (Bill y cols., 2014)

2.3.1 La enfermedad de la antracnosis

Esta enfermedad es causada principalmente por hongos dentro del complejo de *Colletotrichum gloeosporioides*, aunque en algunos países también es causada por hongos de las especies *C. acutatum* y *C. boninense* (Bill y cols., 2014). Este patógeno se presenta en temporada de lluvias y en condiciones de alta humedad relativa, causando daños en hojas y frutos en cualquier etapa fenológica, y también en postcosecha.

El suelo, el agua de riego y los restos vegetales forman una fuente importante de infección debido a la posibilidad de acumulación de esporas, las cuales pueden ser transportadas mediante corrientes de aire o lluvias, o dispersadas por insectos, a las flores y a las frutas jóvenes.

Cuando las esporas germinan forman apresorios que penetran en la cutícula de la fruta y produce una hifa subcuticular latente. El crecimiento de la hifa usualmente se activa cuando el fruto comienza a madurar fisiológicamente, provocando lesiones circulares de color marrón claro, las cuales se agrandan y producen áreas hundidas de color marrón oscuro o

negro en la superficie del fruto, causando lesiones severas en el mismo (Dahn y cols., 2013). Como consecuencia de dichas lesiones se producen grandes pérdidas postcosecha y por ende pérdidas económicas. Por lo que se requieren estrategias que ayuden a controlar este tipo de enfermedades. La siguiente sección describe los métodos convencionales e introduce los métodos más innovadores en el control de enfermedades.

2.4 Métodos de control de enfermedades postcosecha en frutos

Para evitar o disminuir este tipo de enfermedades postcosecha, se han utilizado tratamientos físicos, químicos o biológicos. Dentro de los tratamientos físicos, destaca la conservación empleando frío o calor, este tipo de conservación disminuye o aumenta la producción de C_2H_4 y CO_2, y con ello se retrasa o acelera el proceso de maduración, provocando cambios en las propiedades organolépticas. Otro método es la aplicación de ceras como recubrimiento comestible, sin embargo, en aguacates ya se ha demostrado que tienen una mayor incidencia de decoloración del mesocarpio, retrasos prolongados en la maduración y mayor desarrollo de más pudriciones que aguacates no tratados.

Entre los tratamientos químicos, se encuentra la aplicación de fungicidas químicos, los más utilizados en postcosecha han sido: imazalil, tiabendazol, difenoconazol, propiconazol, captan, oxicloruro de cobre e hidróxido de cobre (Agrios, 2005). Algunos fungicidas actúan en múltiples sitios de acción, por ejemplo, en la desnaturalización no específica de enzimas y otras proteínas, otros actúan en sitios específicos como en la tubulina de huso acromático, en la mitosis o interfiriendo en la respiración celular de los hongos. Este tipo de fungicidas ya han sido evaluados frente a diferentes microorganismos, por ejemplo, *C. gloeosporioides*, *C. acutatum* y *Penicillium* spp (Gaviria-Hernández y cols., 2013). No obstante, han generado preocupación en la opinión pública, respecto al total de los residuos generados, así como también al impacto potencial sobre el medio ambiente y la salud humana. Sin embargo, algunos de ellos no son completamente efectivos. Principalmente los fungicidas químicos, representan un riesgo para la salud humana, contaminan el ambiente ya que existe un exceso de residuos químicos, además del desarrollo de resistencia por parte de los microorganismos (Damasceno y cols., 2019).

A pesar de que estos métodos han demostrado cierta efectividad en el control de enfermedades, se han buscado alternativas que ayuden a controlarlas, disminuyendo el

impacto ambiental, el daño al fruto y los posibles efectos adversos a la salud que los métodos convencionales pudieran mostrar, por lo que se están explorado nuevas alternativas, algunas de las cuales se discuten a continuación.

2.5 Agentes de control naturales

Dentro de los agentes de origen natural se encuentran los extractos vegetales, aceites esenciales y microorganismos antagonistas. Generalmente, estos agentes de origen natural son biodegradables, no muestran toxicidad, no son específicos en su mecanismo de acción, lo que implica baja probabilidad de desarrollo de resistencia por parte de los microorganismos y, además, tienen mínima permanencia en el medio ambiente (Rodriguez y cols., 2015; Tripathi y Dubey, 2004).

2.5.1 Extractos vegetales

Los extractos vegetales pueden obtenerse a partir de plantas o parte de ellas, mediante varios procedimientos tales como la maceración, la extracción supercrítica, la extracción asistida con ultrasonidos o microondas, empleando disolventes como agua, etanol, hexano, y metanol, entre otros (Pérez, 2012). Algunos de los metabolitos que pueden estar presentes en los extractos vegetales, son terpenoides, compuestos fenólicos, fenilpropanoides, estilbenos, alcaloides, y saponinas, entre otros (Rodriguez y cols., 2015). Estos extractos, han mostrado tener amplio espectro frente a algunos fitopatógenos, por ejemplo, *C. gloeosporioides* y *P. italicum* (Vázquez-González y cols., 2020), *Fusarium oxysporum, Alternaria alternata* o *Botrytis cinerea* (Rodriguez y cols., 2015).

El uso de extractos de plantas puede ser una opción viable para sustituir las medidas actuales del control de hongos, basadas en las propiedades antifúngicas y la baja o nula toxicidad que tales extractos presentan; sin embargo, su efectividad dependerá del tiempo de contacto, la concentración utilizada, factores ambientales, así como la susceptibilidad del microorganismo.

2.5.2 Aceites esenciales

Los aceites esenciales son una mezcla compleja de compuestos orgánicos volátiles y aromáticos producidos en diferentes partes de las plantas como flores, raíces, semillas, corteza, etc. Actualmente existen 3000 aceites esenciales reconocidos, algunos de los cuales

ya son utilizados en la industria farmacéutica, cosmética, agronómica y alimentaria, principalmente debido a sus conocidas propiedades antibacterianas, antifúngicas, insecticidas y antivirales (Tariq y cols., 2019). Los compuestos presentes en cada uno de los aceites esenciales como aldehídos, cetonas, alcoholes, ésteres o hidrocarburos definirán sus propiedades, puesto que son resultado de las interacciones complejas de los compuestos.

El mecanismo de acción de estos aceites frente a los hongos se basa en establecer un potencial de membrana a través de la pared celular que interrumpe el ensamblaje de ATP, dañando la pared celular. Además, pueden desintegrar la membrana mitocondrial interfiriendo con la vía del sistema de transporte de electrones. Sin embargo, la eficacia de los aceites esenciales dependerá del microorganismo que se esté evaluando y la concentración de los compuestos presentes en los aceites, entre otros factores (Faleiro, 2011). De este modo, algunos aceites esenciales han mostrado actividad antifúngica frente a *Botrytis*, *Fusarium*, *Cladosporium*, *Candida acutus*, *Candida albicans*, entre otros (Calderón-Santoyo y cols., 2022; González-Estrada y cols., 2017; Iñiguez-Moreno y cols., 2022; Tariq y cols., 2019).

No obstante, al igual que los extractos vegetales, su efectividad dependerá de su composición, del tiempo de contacto, la concentración utilizada, factores ambientales, así como la susceptibilidad del microorganismo.

2.5.3 Microorganismos antagonistas

Los microorganismos antagonistas, generalmente levaduras, mohos y bacterias (Damasceno y cols., 2019), se han utilizado desde 1977, para el control de algunas enfermedades postcosecha. Por ejemplo, ha sido reportado el uso de *Trichoderma* para controlar *Botrytis* en fresas (Tronsmo y Dennis, 1977), o el uso de *Bacillus subtilis* para controlar *Monilinia fructicola* en duraznos (Wilson y Pusey, 1985). Sin embargo, se ha avanzado poco hacia una implementación comercial más amplia de productos de biocontrol eficaces y económicamente viables.

Entre los mecanismos de acción más importantes que presentan los agentes de biocontrol (BCA) se encuentran la colonización y competencia por nutrientes, exudación de enzimas específicas, capacidad de inducir resistencia al huésped frente a algunos fitopatógenos, capacidad de regular la densidad de población en sitios específicos, secreción

de sustancias antimicrobianas (solubles en agua o volátiles) y quizás producción de metabolitos activos específicos inducidos por la interacción con tejidos de las frutas o plantas (Droby y cols., 2009; Liu y cols., 2010).

Algunas levaduras que han mostrado actividad antifúngica para inhibir el crecimiento del género *Colletotrichum*, se muestran en el Cuadro 2. En general, dentro de las diversas cepas que se han estudiado como agentes de biocontrol, recibe atención *Meyerozyma caribbica*, puesto que esta cepa es efectiva como control biológico en mango (Bautista-Rosales y cols., 2013), en papaya (Aguirre-Güitrón y cols., 2022) y recientemente en frutos de aguacate (González-Gutiérrez y cols., 2021; Iñiguez-Moreno y cols., 2020).

Cuadro 2. Levaduras antagonistas frente a *Colletotrichum gloeosporioides*.

Levadura antagonista	**Fruto**	**Referencia**
Yamadazyma mexicana	Aguacate	González-Gutérrez y cols. (2023)
M. caribbica	Mango y papaya	Aguirre-Güitrón y cols. (2022)
M. caribbica	Aguacate	González-Gutiérrez y cols. (2021)
M. guilliermondii	Mango	López-Cruz y cols. (2020)
M. caribbica	Aguacate	Iñiguez-Moreno y cols. (2020)
Debaryomyces nepalensis	Mango	Zhou y cols. (2018)

2.5.3.1 *Meyerozyma caribbica*

La levadura *M. caribbica* (*GenBank ID*: JQ398674) fue previamente aislada del mango "Ataulfo" e identificada por Bautista-Rosales y cols. (2013). *M caribbica* tiene un genoma pequeño (10.6 Mb, 8 cromosomas) no produce hifas y forman consorcios celulares adheridos por biopelículas (Herrera-Balandrano y cols., 2023).

Bautista-Rosales y cols. (2013) evaluaron los mecanismos de acción y la actividad antifúngica de *M. caribbica* en el control de *C. gloeosporioides* en mango variedad "Ataulfo". Reportaron que *M. caribbica* redujo significativamente la lesión causada por el hongo en las frutas heridas en un 86.7% en comparación con el control. Por lo que es considerada como un antagonista efectivo de *C. gloeosporioides* al aplicarlo en concentraciones de 1×10^7 o 1×10^8 células/mL.

Respecto a los mecanismos que esta levadura utiliza en la inhibición, se reportan principalmente competencia por nutrientes, como sacarosa y fructosa, producción de enzimas hidrolíticas (glucanasa, nagasa y quitinasa), parasitismo y producción de biopelículas.

No obstante, para aumentar la efectividad de *M. caribbica*, algunos autores han reportado el uso de estrés hídrico y térmico (González-Gutiérrez y cols., 2021), así como la inducción de enzimas hidrolíticas en las levaduras (Iñiguez-Moreno y cols., 2020) con el objetivo de su posible aplicación en tratamientos pre y postcosecha en frutos de aguacate Hass.

De acuerdo con lo reportado por Ocampo-Suarez y cols. (2017) esta cepa no ha mostrado toxicidad ni patogenicidad en modelos murinos, embriones de pollo ni irritación dérmica en conejos. Por lo tanto, su uso como agente de biocontrol es una alternativa segura.

2.6 Encapsulación de agentes de control

Para el uso comercial de los agentes de biocontrol, se requiere desarrollar métodos de producción que permitan mantener la viabilidad celular de los microorganismos, tener una vida útil de al menos 6 meses a temperatura ambiente o en refrigeración, mostrar estabilidad genética, además de mantener su metabolismo y fisiología celular (Droby y cols., 2009; Wiyono y Widodo, 2013). Este tipo de microorganismos deben cumplir con algunas características que permitan desarrollarlos de manera comercial (Cuadro 3).

Cuadro 3. Características de BCA para su desarrollo comercial

*Genéticamente estable
*Efectivo a bajas concentraciones
*No exigente en sus requerimientos de nutrientes
*Habilidad para sobrevivir en condiciones ambientales adversas
*No debe ser perjudicial para la salud humana
*Disponible para la producción en medios de crecimiento económico
*Disponible para la formulación con una vida larga de anaquel
*Compatible con procesos comerciales

Fuente: (Droby y cols., 2009)

Sin embargo, algunas levaduras son susceptibles a condiciones de estrés abiótico (contaminación, desecación) y su viabilidad puede verse comprometida (González-Estrada y cols., 2017) cuando se aplican directamente en las matrices vegetales. Por este motivo, se ha propuesto la incorporación de levaduras biocontrol en matrices poliméricas con la finalidad de brindarles protección y estabilidad, con el fin de mantener su actividad y eficacia contra los patógenos (Sharma y cols., 2009).

Una de las tecnologías actualmente empleadas para tal fin, ha sido la encapsulación. Por ejemplo, Aguirre-Güitrón y cols. (2019) encapsularon *M. caribbica* mediante secado por aspersión y posteriormente evaluaron la efectividad de esta formulación, observando una reducción de la incidencia y la severidad de la enfermedad hasta en un 53.4% y un 23.9%, respectivamente, en mangos almacenados a 25 °C. López-Cruz y cols. (2020) encapsularon mediante secado por aspersión a *M. guilliermondii* para controlar la antracnosis en mango, mostrando una inhibición de 86.4 ± 1.1% del crecimiento micelial de *C. gloeosporioides*.

Por otro lado, el atrapamiento de estos agentes antifúngicos en matrices poliméricas es una estrategia eficiente para facilitar su almacenamiento, la manipulación y el transporte de este tipo de microorganismos, además de brindarles protección frente a factores ambientales y alargar su vida útil. La aplicación de este tipo de matrices poliméricas sobre los frutos puede realizarse mediante métodos convencionales y actualmente mediante métodos emergentes.

2.6.1 Métodos convencionales

2.6.1.1 Biopelículas o recubrimientos comestibles

Son matrices formuladas a base de lípidos, proteínas y carbohidratos o mezclas de estos componentes (Rohasmizah y Azizah, 2022), que les confieren diferentes propiedades fisicoquímicas y sirven como vehículos para incorporar aditivos específicos que refuerzan su funcionalidad (Aayush y cols., 2022).

Las propiedades de barrera, mecánicas y de transporte dependerán del material con que se formulen, no obstante, los materiales más utilizados han sido los polisacáridos, ya que estos presentan mayor adherencia y flexibilidad en la superficie de los productos hortofrutícolas (Aayush y cols., 2022; Iñiguez-Moreno y cols., 2021; Rohasmizah y Azizah, 2022; Romero y cols., 2022).

2.6.1.2 Aplicación de recubrimientos por inmersión

Este método es el más empleado para el recubrimiento de los alimentos, generalmente se usa en alimentos de superficie irregular. El tiempo de inmersión dependerá de la humedad, concentración o viscosidad de la solución, de la superficie y de la posible penetración de la dispersión de recubrimiento en el alimento. Los alimentos recubiertos por inmersión deben someterse posteriormente a etapas de escurrido y secado con el fin de obtener una película adherida a la superficie del alimento. El espesor de la película estará determinado por la viscosidad del material del recubrimiento y/o por la velocidad con la cual la viscosidad cambia después de la aplicación (Moncayo-Martínez, 2013).

2.6.1.3 Aplicación de recubrimientos por aspersión

La aplicación mediante aspersión evita el consumo excesivo de recubrimiento; sin embargo, la aplicación manual no es homogénea, provocando una disminución en el total del área del fruto recubierta (Aayush y cols., 2022; Moncayo-Martínez, 2013). En la aplicación automatizada se deben controlar principalmente la velocidad de flujo y el tipo de boquilla.

Debido a las limitaciones de las técnicas convencionales se han investigado técnicas que sean más eficientes, permitan una liberación controlada del agente activo y a su vez, permitan una aplicación directa sobre el fruto. Tal es el caso de las tecnologías emergentes de encapsulación mediante procesos electrohidrodinámicos y aerohidrodinámicos que permiten obtener cápsulas y micro o nanofibras que puedan ser aplicadas directamente sobre el fruto.

2.6.2 Métodos emergentes

2.6.2.1 Nanocápsulas

Actualmente, la encapsulación está siendo ampliamente estudiada, puesto que sirve como alternativa para brindar protección al agente activo frente a factores ambientales (luz, oxígeno, radiación humedad, entre otros), permitir una liberación controlada, así como para mejorar y mantener la viabilidad, durante su almacenamiento (Ningtyas y cols., 2019). Una gran variedad de materiales pueden ser usados para la encapsulación de agentes activos, polisacáridos, maltodextrina, trehalosa, almidón de maíz, proteínas (Aguirre-Güitrón y cols., 2018), goma arábiga (Ballesteros y cols., 2017), dextrano (Moncayo-Martínez, 2013), suero

de leche, zeína, gelatina o lípidos, aceites, ácidos grasos insaturados o poliinsaturados (Khan y cols., 2012), entre otros. Se han encapsulado exitosamente extractos vegetales (Ballesteros y cols., 2017), algunos productos lácteos (O'Sullivan y cols., 2019), probióticos (Zaeim y cols., 2018), β-caroteno (Ramos-Hernández y cols., 2018), entre otros. No obstante, se están buscando alternativas para el atrapamiento de compuestos que permitan nuevas aplicaciones, como son las nanofibras.

2.6.2.2 Nanofibras

Las nanofibras son estructuras nanométricas en forma de fibras, tubos, cintas, varillas y cables, que debido a su escala presentan propiedades nuevas que no están presentes en estructuras de igual composición y tamaño macroscópico. Características como el diámetro submicrométrico, elevada relación superficie-volumen (50 m^2 por gramo de material), baja densidad, flexibilidad en la superficie, porosidad variable, poros interconectados y un rendimiento mecánico superior comparado con otras estructuras, las hacen aptas para desarrollar nuevas aplicaciones (Andrady, 2008).

Entre las aplicaciones más estudiadas se encuentran dispositivos biomédicos, tales como sistemas de tejidos, prendas de vestir, productos de limpieza y de cuidado personal, hasta productos industriales de filtrado, barrera y aislamiento. Actualmente, la aplicación en el área de los alimentos está siendo explorada, por ejemplo en la encapsulación de compuestos bioactivos (Aceituno-Medina y cols., 2013; Cruz-Salas y cols., 2019), envases comestibles (Pérez-Masiá y cols., 2013), modificadores, aplicación de chocolate, sabor ahumado a la carne, productos de confitería y aditivos alimentarios (Khan y cols., 2012).

Los polímeros más utilizados para la elaboración de nanofibras han sido generalmente polímeros sintéticos tales como poli (alcohol vinílico), poli (óxido de etileno), poli (Ɛ-caprolactona), polihidroxialcanoatos, polivinilpirrolidona, nylon, polilactida, poliamida o poliestireno (Ricaurte y Quintanilla-Carvajal, 2019). También se han estudiado algunos biopolímeros, los cuáles son comúnmente comestibles, tales como pululano (García-Moreno y cols., 2017), proteína de zeína (Pérez-Masiá y cols., 2013), gelatina (Deng y cols., 2017), proteína de amaranto (Aceituno-Medina y cols., 2013), ciclodextrina (Aytac y cols., 2017), entre otros polisacáridos (Ricaurte y Quintanilla-Carvajal, 2019). Estos materiales han mostrado buenas propiedades para ser utilizados principalmente en la industria alimentaria.

Algunos procesos para la obtención de micro y nanoestructuras, son los procesos electro y aerohidrodinámicos (Sousa y cols., 2015), los cuales ya se han utilizado en diferentes aplicaciones.

2.7 Procesos electrohidrodinámicos y aerohidrodinámicos

Los procesos electro y aerohidrodinámicos más usados en nanotecnología de materiales involucran las técnicas de electropulverizado (*Electrospraying*), electrohilado (*Electrospinning*), hilado mediante soplado por fusión (*Meltblown*) y actualmente hilado por soplado (*Solution Blow Spinning*).

2.7.1 Elaboración de nanofibras por *Electrospinning*

El electrohilado es un proceso sencillo, que requiere de un suministro de energía de alto voltaje, una bomba de jeringa, una jeringa, un tubo, un inyector con una aguja o punta capilar (hilera) y un colector (Fig. 1). Durante el proceso de electrohilado, se genera un campo eléctrico entre dos electrodos, uno formado por una aguja que es parte del sistema de inyección y otro por un plato metálico (colector). La solución polimérica se coloca dentro de una jeringa, ésta es inyectada mediante una bomba y por el efecto de la polarización causada por el campo eléctrico, la solución se estira formando hilos con diferentes características, los cuales tras la evaporación del disolvente a temperatura ambiente da lugar a las fibras electroestiradas (Olvera-Gracia y cols., 2013; Ricaurte y Quintanilla-Carvajal, 2019; Sousa y cols., 2015). Esta tecnología ha demostrado ser altamente respetuosa con los compuestos bioactivos, sin disminuir su efectividad.

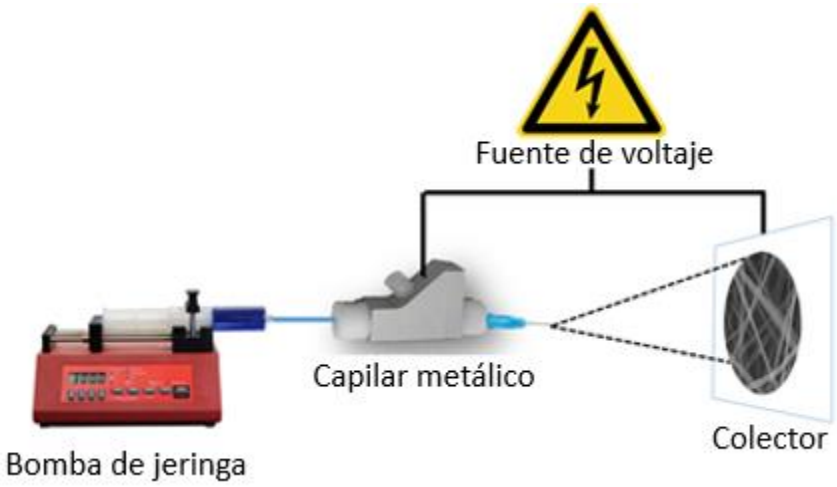

Figura 1. Parámetros del proceso de ***electrospinning*** basado en (Ricaurte y Quintanilla-Carvajal, 2019).

Sin embargo, la necesidad de una fuente de voltaje y de un sustrato conductivo dificulta la aplicación directa sobre los frutos. Por lo que se está migrando a la búsqueda de otras técnicas que permitan lograrlo, como el hilado mediante soplado por fusión y el hilado mediante soplado.

2.7.2 Hilado mediante soplado por fusión (*Meltblown*)

Meltblown es una tecnología no tejida que produce fibras finas (1–5 µm) generalmente a partir de polímeros formadores de fibras termoplásticas. Las fibras se producen por extrusión del polímero fundido a través de una matriz que contiene pequeños orificios. Luego, las fibras son atenuadas rápidamente por corrientes convergentes de aire caliente y posteriormente son transportadas por aire a alta velocidad hacia un colector (Hassan y cols., 2013). Este proceso fue originalmente desarrollado en su forma comercial por la firma Exxon a fines de la década de 1970.

La tecnología es muy útil y sus productos se utilizan en muchas aplicaciones técnicas, higiénicas y médicas, como medios de filtración, almohadillas de sorción, pañales, máscaras de respiración, paños desechables y otros. Sin embargo, hay pocas aplicaciones en la industria alimentaria. Los polímeros básicos utilizados para la producción de materiales no tejidos, soplados por fusión son polipropileno, polietileno, poliestireno, tereftalato de polietileno, ácido poliláctico, tereftalato de polibutileno, poli-ε-caprolactona (Erben y cols., 2016). Con la excepción del ácido poliláctico, estos polímeros no son biodegradables y no

pueden usarse para consumo humano. Adicionalmente, el uso de altas temperaturas podría afectar a la efectividad de la levadura biocontrol.

Por tanto, una alternativa prometedora que permita encapsular estos agentes antifúngicos utilizando polímeros de origen natural, sin uso de temperatura y que además permita aplicarlos directamente al fruto, es la elaboración de nanofibras mediante hilado por soplado.

2.7.3 Elaboración de nanofibras mediante hilado por soplado (*Solution Blow Spinning*)

Este método es una técnica simple y rápida para producir nanofibras, esta técnica fue desarrollada utilizando una combinación de las tecnologías *electrospinning* y *meltblown*, con el fin de tener una mayor producción (Medeiros y cols., 2009), utiliza una corriente de aire a presión (1-80 psi) como fuerza impulsora para la formación de fibras (Daristotle y cols., 2016). Esta técnica supera algunos inconvenientes asociados con *electrospinning* como el uso del campo eléctrico (Santos y cols., 2016). Además, la principal ventaja radica en su gran potencial para su uso en la deposición *in situ*.

Este sistema utiliza una bomba de jeringa para suministrar una solución de polímero a un inyector que consiste en boquillas concéntricas por las cuales la solución de polímero se bombea a través de la boquilla interna mientras se mantiene un flujo de gas comprimido (N, Ar o Aire) constante y de alta velocidad a través de la boquilla externa (Fig. 2) (Medeiros y cols., 2009). La diferencia de presión y el cizallamiento en la interfase gas/disolución provocan la generación de múltiples hebras de solución polimérica las cuales vuelan hacia un colector. Durante el vuelo, el disolvente se evapora rápidamente a temperatura ambiente formando una red de micro y nanofibras. Los principales parámetros de proceso son velocidad de inyección, la presión del flujo de gas, la concentración de polímero, la distancia de trabajo y la distancia de protrusión de la boquilla interior. Estos parámetros pueden determinar la facilidad de procesamiento, así como el diámetro de la fibra y la morfología de estas.

Esta técnica se ha utilizado exitosamente para obtener nanofibras con aplicación en materiales de construcción (polímeros reforzados), producción, conversión y almacenamiento de energía (celdas solares, baterías), mejora y protección ambiental

(filtración de aire, tratamiento de aguas residuales), aplicaciones biomédicas (dosificación de medicamentos, ingeniería de tejidos, cicatrización de heridas) (Barhoum y cols.., 2019), sin embargo, su aplicación en alimentos apenas está siendo explorada.

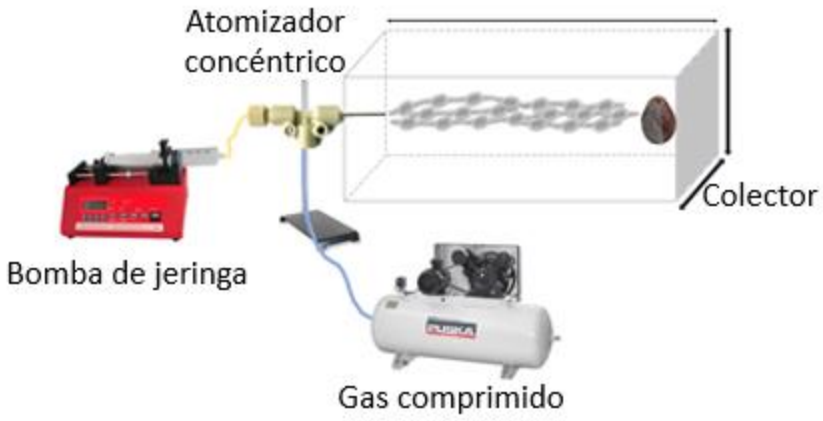

Figura 2. Esquema de *Solution Blow Spinning* basado en Medeiros y cols. (2009).

Para la elaboración de estas nanofibras, se han utilizado diversos polímeros sintéticos. No obstante, los biopolímeros han demostrado no ser nocivos para la salud humana y los ecosistemas acuáticos, no son tóxicos ni corrosivos y son biodegradables (Freitas y cols., 2017), además de mostrar alta estabilidad bajo diferentes condiciones (Lim y cols., 2018).

2.8 Polímeros usados

Para el desarrollo de diferentes nanofibras, ya se han utilizado diversos polímeros como metaloceno, polipropileno isotáctico (Hassan y cols., 2013), fructanos de agave (Cruz-Salas y cols., 2019), óxido de polietileno, polivinilpolipirrolidona (Benavides y cols., 2012), poli metacrilato de metilo, poliestireno, ácido poliláctico (Medeiros y cols., 2009), polialcohol vinílico, propilenglicol, entre otros (Daristotle y cols., 2016).

Actualmente se han buscado otras alternativas de origen natural, o biopolímeros, con la finalidad de ampliar sus aplicaciones, por ejemplo, en la industria alimentaria, además de que son bastante accesibles y muestran menores costes de producción.

La goma de anacardo es un polisacárido exudado obtenido de los árboles *Anacardium occidentale*, es un heteropolisacárido ácido ramificado de baja viscosidad (Das y cols., 2014). La goma contiene 9.8–13.2% de humedad, 1.9–4.8% de materia insoluble, 0.5–1.2% de

ceniza total, 1.27–1.80% de proteína, 9.6–21.0% de azúcar y 0.21–2.26% de fenol (Olorunsola y cols., 2016), está compuesta de β-D-galactosa (72%), α-D-glucosa (14%), arabinosa (4.6%), ramnosa (3.2%) y ácido glucurónico (4.7%) (Silva y cols., 2006), ha mostrado buenas propiedades térmicas (Olorunsola y cols., 2016), fisicoquímicas (Gyedu-Akoto y cols., 2008), así como propiedades emulsificantes (Abdulsamad y cols., 2006).

También han sido estudiados algunos otros polisacáridos, por ejemplo, los exopolisacáridos (EPS), estos no son tóxicos y están ampliamente disponibles, los EPS son biopolímeros complejos que presentan diversas propiedades fisicoquímicas, su producción depende de los microorganismos, las fuentes de carbono y nitrógeno, así como los nutrientes que se les suministren, además de la vía metabólica que estos microorganismos experimenten (Shukla y cols., 2019).

Este tipo de polisacáridos son ecológicos y biodegradables, algunas bacterias productoras de EPS ya han sido ampliamente estudiadas como: *Leuconostoc mesenteroides* (Nwodo y cols., 2012), *Xanthomonas campestris* (Shukla y cols.., 2019), *Acinetobacter calcoaceticus* (Kumar y cols., 2007), así como también, algunos exopolisacáridos fúngicos producidos por: *Aureobasidium pullulans* (Singh y cols., 2006), *Fusarium solani* (Mahapatra y Banerjee, 2012), *Coriolus versicolor* (Ooi y Liu, 2000), para aplicaciones farmacéuticas, agrícolas, alimentarias y cosméticas.

Un EPS que ha llamado la atención por sus características hidrofílicas, alta permeabilidad al vapor de agua (1.01×10^{-11} mol / ms Pa), buenas propiedades de barrera al oxígeno y al dióxido de carbono (0.7×10^{-16} mol m / m^2 s Pa y 42.7×10^{-16} mol m / m^2 s Pa, respectivamente) y excelentes propiedades mecánicas (Ferreira y cols., 2014), es el FucoPol recientemente reportado producido por *Enterobacter* A47 (DSM23139) utilizando glicerol como fuente de carbono (Torres y cols., 2011). Es un heteropolisacárido de alto peso molecular (4.19×10^6 -5.80×10^6 Da), compuesto de residuos de azúcar (fucosa, galactosa, glucosa y ácido glucorónico) y grupos acilo (piruvato, succinato, acetato) (Freitas y cols., 2011). Tiene un carácter aniónico y tiene propiedades funcionales como buena capacidad de emulsión y formación de película (Freitas y cols., 2014).

El pululano también es un exopolisacárido producido por el hongo *Aureobasidium pullulans* tiene un peso molecular de 2×10^5 Da. Su estructura consiste en un α-glucano

lineal, hecho de tres unidades de glucosa unidos por un enlace α-(1,4) en unidades de maltotriosa unidas a su vez en un enlace α-(1,6). Esta formación hace que el pululano muestre dos importantes características, flexibilidad estructural y solubilidad mejorada. Debido a sus propiedades, el pululano se ha usado como agente gelificante, material de recubrimiento y envasado para alimentos y medicamentos, entre otras aplicaciones (Karim y cols., 2009; Kong y Ziegler, 2014; Singh y cols., 2008).

CAPÍTULO 3. JUSTIFICACIÓN

3. JUSTIFICACIÓN

A nivel mundial el aguacate es un cultivo de gran importancia económica, debido a su versatilidad y a los beneficios nutricionales que este fruto presenta. En el 2017, Nayarit ocupó el cuarto lugar en la producción nacional con 49 mil toneladas. Sin embargo, debido a la susceptibilidad que muestran estos frutos a enfermedades causadas por fitopatógenos se generan grandes pérdidas alimentarias y económicas. Dentro de estas enfermedades, la antracnosis es la principal enfermedad que ataca a este fruto, causando un daño severo en el mismo. Para su control, se han utilizado algunos tratamientos físicos, químicos y biológicos, como el uso de temperatura, recubrimientos comestibles y fungicidas químicos, sin embargo, pese a su efectividad, han generado preocupación, respecto a los residuos generados, así como al impacto potencial sobre el medio ambiente y la salud humana, por lo que se han buscado medidas alternativas que disminuyan estos efectos, tal es el caso del uso de microorganismos antagonistas. *M. caribbica* es un microorganismo que ha demostrado ser efectivo en el control de antracnosis generada por *C. gloeosporioides* en frutos de mango, papaya y aguacate, por lo que su uso puede ser una alternativa viable. Recientemente se aplicó estrés hídrico y térmico, así como la inducción en la síntesis de enzimas hidrolíticas en *M. caribbica* con el fin de aumentar su efectividad. Para facilitar la manipulación, transporte, almacenamiento y aplicación de este agente de biocontrol, se ha agregado a matrices poliméricas, ya sea en recubrimientos comestibles, cápsulas o micro y nanofibras. Sin embargo, las técnicas convencionales de proceso y de aplicación no permitirían aplicarlas directamente, puesto que son generalmente aplicadas de forma manual y no proporcionan homogeneidad en el tratamiento, es por ello que los procesos electrohidrodinámicos y aerohidrodinámicos podrían permitir la aplicación directa de fibras a frutos de aguacate "Hass", ya que estos procesos son más eficientes para lograr una cobertura superficial homogénea, al mismo tiempo que proporcionan una liberación controlada y protección a los agentes antifúngicos ante factores ambientales.

CAPÍTULO 4. OBJETIVOS

4. OBJETIVOS

4.1 Objetivo general

Desarrollar recubrimientos antifúngicos basados en micro o nanofibras biopoliméricas adicionadas con *M. caribbica* producidos mediante procesos electro y aerohidrodinámicos para el control de antracnosis en aguacate "Hass" (*Persea americana* Mill. cv. Hass) garantizando además los parámetros de calidad en el fruto.

4.2 Objetivos específicos

1. Desarrollar las formulaciones poliméricas de pululano, goma de anacardo y FucoPol procesables mediante procesado electro y aerohidrodinámico.
2. Estudiar las condiciones de proceso para la obtención de micro y nanoestructuras biopoliméricas mediante *electrospraying*, *electrospinning* y *Solution Blow Spinning*.
3. Estudiar la encapsulación de *M. caribbica* mediante *electrospinning* y *Solution Blow Spinning*.
4. Caracterizar las micro y nanoestructuras con y sin *M. caribbica* en términos de morfología, estructura y propiedades térmicas.
5. Evaluar la viabilidad *in vitro* de *M. caribbica* en las fibras obtenidas mediante *Electrospinning* y SBS.
6. Evaluar la actividad antifúngica *in vitro* de las fibras con *M. caribbica* obtenidas mediante *Electrospinning* y SBS.
7. Evaluar la viabilidad *in vivo* de *M. caribbica* como tratamiento preventivo y curativo frente a *C. gloeosporioides*.
8. Evaluar el efecto de las nanofibras sobre los parámetros de calidad y las propiedades organolépticas de frutos de aguacate "Hass".

CAPÍTULO 5. HIPÓTESIS

5. HIPÓTESIS

Las condiciones idóneas del procesado electrohidrodinámico y aerohidrodinámico permitirán aplicar directamente nanofibras biopoliméricas cargadas con la levadura biocontrol *Meyerozyma caribbica* sobre los frutos de aguacate, capaces de controlar la enfermedad de antracnosis en aguacate "Hass" (*Persea americana* Mill. cv. Hass), sin afectar los parámetros de calidad y las características organolépticas del fruto.

CAPÍTULO 6. MATERIALES Y MÉTODOS

6. MATERIALES Y MÉTODOS

6.1. Etapa 1. Formación de microestructuras de goma de anacardo mediante procesado electrohidrodinámico

6.1.1. Materiales

La goma de anacardo (CG) fue proporcionado por Embrapa (Fortaleza, CE, Brasil). El β-caroteno, el aceite de ricino y el tensioactivo Span® 20 se adquirieron en Sigma Aldrich (St. Louis, MO, EE. UU.). El cloroformo se adquirió en Panreac AppliChem (Barcelona, España). Durante todo el estudio se utilizó agua destilada. Todos los productos químicos se utilizaron tal como se recibieron sin ninguna purificación adicional.

6.1.2. Preparación de disoluciones

En primer lugar, se prepararon disoluciones de goma de anacardo a diferentes concentraciones en agua destilada para estudiar la formación de microestructuras mediante procesado electrohidrodinámico. Se consideró también la posibilidad de añadir un surfactante para estabilizar el proceso.

Para la obtención de microcápsulas, la solución de goma de anacardo se preparó con una concentración del 50% (p/p) en agua destilada y una concentración de Span 20 del 1% (p/p). La solución se homogenizó agitando magnéticamente durante 36 h a temperatura ambiente.

Para la preparación de emulsiones que contenían β-caroteno, inicialmente se preparó una solución concentrada de β-caroteno en aceite de ricino (5 % p/p). Se preparó una emulsión añadiendo lentamente la fase orgánica a la fase acuosa en una relación de volumen de 20:80 y 10:90, posteriormente fue homogeneizada utilizando un homogeneizador Vórtex Mixer IR Digital (VELP SCIENTÍFICA, Usmate Velate, Italia) durante 5 minutos.

6.1.3 Determinación de la viscosidad

La viscosidad aparente, se determinó mediante un viscosímetro rotatorio Visco Basic Plus L (Fungilab S.A., San Feliu de Llobregat, España) con un husillo L1 (regularmente usado para altas viscosidades). El husillo L1 se colocó en el viscosímetro y 25 mL de muestra se

colocaron en un tubo de ensayo cónico y ambos se pusieron en contacto para obtener el valor de viscosidad aparente.

6.1.4 Determinación de la tensión superficial

La tensión superficial se midió usando el método Wilhemy plate en un tensiómetro EasyDyne K20 (Krüss GmbH, Hamburgo, Alemania). Se colocaron 25 mL de muestra en un cristalizador, se procedió a la limpieza de la placa Wilhelmy mediante pirólisis y se colocó en el soporte, posteriormente se procedió al análisis de cada una de las muestras (Ramos-Hernández y cols., 2018).

6.1.5 Determinación de la conductividad

La conductividad se determinó usando un medidor de conductividad Hanna Instruments HI-4521 (Melrose, MA, USA). La sonda se sumergió en 10 mL de muestra en un tubo cónico hasta cubrir y estabilizar los sensores.

6.1.6 Determinación de la distribución del tamaño de gota en las emulsiones

La distribución del tamaño de gota en las emulsiones empleadas para encapsular β-caroteno fue observada mediante un microscopio óptico convencional (Nikon Eclipse 90i, Nikon Instruments Inc., New York, USA), para esto se tomó una alícuota y se colocó sobre un portaobjetos para ser vista en el microscopio. La distribución del tamaño de partícula en las emulsiones fue determinada mediante espectroscopía de correlación fotónica empleando un Mastersizer 2000 (Malvern Instruments, Malvern, Reino Unido). Se colocaron alícuotas de emulsión en el equipo y mediante el software de Malvern Instruments, se obtuvo el reporte de los resultados.

6.1.7 Obtención de microestructuras mediante procesado electrohidrodinámico

El procesado electrohidrodinámico se realizó en un equipo Fluidnatek LE-10 de Bioinicia S.L. (Valencia, España). Las disoluciones o emulsiones preparadas se colocaron en una jeringa de plástico de 5 mL, posteriormente fueron colocadas en una bomba de jeringa y se conectó por tubo de PTFE a un inyector en el que se colocó una aguja de acero inoxidable del calibre 27. Un electrodo positivo de una fuente de alimentación de alta tensión fue acoplado a la aguja. Las soluciones fueron procesadas a un caudal constante de 200 μL/h y

el voltaje de 25 kV. La distancia entre la punta de la aguja y el colector plano fue de 28 cm. El proceso se realizó en condiciones ambientales.

6.1.8 Microscopía Electrónica de Barrido (SEM)

La morfología de las microestructuras obtenidas fue determinada mediante SEM en un equipo Hitachi-S-4800 FE-SEM (Hitachi High-Technologies Corporation, Tokio, Japón) con una aceleración del haz de electrones de 10 kV. Las muestras se fijaron con cinta de doble cara en el porta muestras, posteriormente fueron recubiertas con una capa de oro-paladio. La determinación de la distribución del tamaño de partículas basada en los diámetros de las estructuras se realizó usando el software Image J Launcher v1.41 (National Institutes of Health, Bethesda, MD, USA) con 100 mediciones por muestra.

6.1.9 Capacidad de carga y eficiencia de encapsulación

El porcentaje de capacidad de carga (%CC) se estimó midiendo la cantidad de β-caroteno en las partículas. Para ello, se disolvieron aproximadamente 0.05 g de partículas en agua y se realizó una extracción del β-caroteno con cloroformo. Las mediciones cuantitativas de β-caroteno fueron realizadas por espectrofotometría UV-vis en un espectrofotómetro UV UV4000 (Dinko Instruments, Barcelona, España). La absorbancia de β-caroteno se midió a 461 nm. Se usaron soluciones estándar de β-caroteno en cloroformo a 0.1 g/mL para construir la curva de calibrado (y= 0.8433x + 0.0012, R^2=0.9986), a partir de la cual se determinó la cantidad de β-caroteno presente en el volumen recuperado. Se calculó el porcentaje de CC mediante la Ecuación 1.

$$\%\, CC = \left(\frac{Masa\ del\ \beta-caroteno}{Masa\ de\ las\ partículas}\right) x\ 100 \qquad \text{Eq. 1}$$

La eficiencia de encapsulación se estimó midiendo el β-caroteno en la superficie de las partículas mediante el lavado del polvo con un disolvente orgánico. Aproximadamente 0.025 g de muestra se lavaron con cloroformo durante 30 s y se centrifugaron durante 5 min a 7000 rpm. La absorbancia del filtrado se midió a 461 nm en un espectrofotómetro UV4000 y se determinó la concentración de β-caroteno presente en el filtrado. El porcentaje de la eficiencia de encapsulación se calculó de acuerdo con la Ecuación 2.

$$\% EE = \frac{(\beta-caroteno\ total)-(\beta-caroteno\ superficial)}{\beta-caroteno\ total}\ x\ 100 \qquad \text{Eq. 2}$$

6.1.10 Espectroscopía infrarroja con transformada de Fourier en modo de reflectancia total atenuada (ATR-FTIR)

Para determinar los espectros infrarrojos de las muestras se usó un equipo ATR-FTIR (Bruker FTIR Tensor 37, Rheinstetten, Alemania). Las muestras se colocaron sobre el cristal de diamante y se aseguró un buen contacto mediante el uso del accesorio de ATR. Todos los espectros se obtuvieron dentro del rango de números de onda de 4000 a 600 cm^{-1} promediando 10 escaneos a 4 cm^{-1} de resolución. El análisis de los datos se llevó a cabo usando Origin Pro, Version 2019 (OriginLab Corporation, Northampton, MA, EE. UU.).

6.1.11 Análisis termogravimétrico (TGA)

Se realizó un análisis termogravimétrico del β-caroteno, y de las cápsulas con y sin β-caroteno usando un equipo TGA-STDA 1600 (Mettler Toledo, Columbus, OH, USA). Los análisis fueron hechos bajo las siguientes condiciones: 1-5 mg de muestra, un calentamiento de 25 ºC a 600 ºC, una rampa de calentamiento de 5 ºC/min bajo un flujo de nitrógeno (50 mL/min).

6.1.12 Ensayo de fotooxidación

Las partículas encapsulando β-caroteno, se compararon con la tasa de degradación de β-caroteno libre colocando las muestras bajo una lámpara de simulación de luz solar, a temperatura ambiente. Se utilizó una lámpara Osram Ultra-vitalux (300 W) (OSRAM, Munich, Alemania), que genera una mezcla de radiación, utilizando un tubo de descarga de cuarzo y un filamento de tungsteno. La distancia entre la lámpara y las muestras fue de 20 cm. Las muestras se recogieron durante periodos de tiempo de iluminación (0 min, 30 min, 45 min, 60 min, 75 min, 90 min y 105 min) y la concentración del β-caroteno se determinó usando un espectrofotómetro UV4000 a 461 nm.

Las muestras control de β-caroteno se disolvieron en 1 mL de cloroformo y las partículas primero se disolvieron en 1 mL de agua destilada para abrir la matriz polimérica, y posteriormente se agregó 1 mL de cloroformo para extraer el β-caroteno presente. La

mezcla fue agitada en un vórtex y centrifugada a 10,000 rpm durante 2 minutos. La fase orgánica fue separada y la concentración de β-caroteno fue determinada por espectrofotometría UV-vis.

6.2 Etapa 2. Formación de micro y nanofibras de FucoPol mediante procesado electrohidrodinámico

6.2.1 Materiales

FucoPol (Mw ~ 4,4 x 10^6 Da) fue proporcionado por el Grupo de Ingeniería Bioquímica de la Facultad de Ciencias y Tecnología de la Universidad Nova de Lisboa (Caparica, Portugal). El pululano (Mw ~ 2 x 10^5 Da) se adquirió de Hayashibara Co., Ltd. (Tokio, Japón), y el óxido de polietileno (PEO) (Mw ~ 100 000 Da), 2,2,2-trifluoroetanol y Span 20 se adquirieron de Sigma Aldrich (St. Louis, MO, EE. UU.). El etanol absoluto (EPR. Ph.Eur.) se obtuvo de Labkem (Vilassar de Dalt, España). Se utilizó agua destilada durante todo el estudio.

6.2.2 Preparación de disoluciones

Primeramente, se prepararon disoluciones de FucoPol con una concentración de 0.015 g/mL en agua destilada, posteriormente para mejorar la formación de fibras, se prepararon mezclas con otros polímeros ampliamente estudiados en diferentes proporciones (Cuadro 4). Para ello, se prepararon disoluciones de FucoPol con pululano (concentración: 0.015 g/mL) y FucoPol con PEO (concentración: 0.015 g/mL) en etanol:agua (30:70, v/v), la concentración usada en este estudio fue ajustada de acuerdo con ensayos previos. En cada una de las disoluciones se agregó Span 20 al 5% (w/w). Las disoluciones se homogenizaron agitando magnéticamente durante 15 h a temperatura ambiente. Las disoluciones que mostraron mejor formación de fibras fueron caracterizadas de acuerdo con la metodología propuesta en el apartado 6.1.3 Determinación de la viscosidad, el apartado 6.1.4 Determinación de la tensión superficial y el apartado 6.1.5 Determinación de la conductividad.

Cuadro 4. Proporciones de la mezcla de polímeros FucoPol, Pululano y PEO para la preparación de las nanofibras mediante *electrospinning*.

FucoPol/PEO (p/p)	FucoPol/Pululano (p/p)	Tensoactivo Span 20 (%)
3:1	3:1	3
2:1	2:1	3
1:1	1:1	3
1:0	1:0	3
0:1	0:1	3
1:2	1:2	3
1:3	1:3	3

6.2.3 Obtención de fibras mediante *Electrospinning*

El procesado electrohidrodinámico se realizó en el equipo Fluidnatek LE-500 de Bioinicia S.L. (Valencia, España) siguiendo la metodología anteriormente descrita en el apartado 6.1.7 Obtención de microestructuras mediante procesado electrohidrodinámico. Las soluciones fueron procesadas de acuerdo con condiciones establecidas en ensayos previos. Para la solución de FucoPol, se establecieron las siguientes condiciones, un caudal de 250 µL y un voltaje de 20 kV y -2 kV. Las disoluciones de FucoPol con pululano se electroestiraron bajo un caudal de 250 µL y un voltaje de 23 kV y -2 kV. Finalmente, las disoluciones de FucoPol con PEO, se procesaron empleando un caudal de 300 µL, un voltaje de 22 kV y -3 kV. La distancia de trabajo empleada fue de 28 cm, la temperatura osciló desde los 30 a los 35 °C y una humedad relativa desde 23% hasta 28%.

6.2.4 Caracterización de las nanofibras

Se caracterizó la morfología de las estructuras mediante SEM, de acuerdo con la metodología propuesta en el apartado 6.1.8 Microscopía Electrónica de Barrido (SEM), ATR-FTIR (6.1.10 Espectroscopía infrarroja con transformada de Fourier en modo de reflectancia total atenuada (ATR-FTIR) y TGA de acuerdo con el apartado 6.1.11 Análisis termogravimétrico (TGA).

6.2.5 Calorimetría Diferencial de Barrido (DSC)

Las transiciones térmicas se analizaron en un equipo DSC-8000 equipado con el accesorio de refrigeración Intracooler 2, todo de PerkinElmer, Inc. (Waltham, MA, USA). Se realizaron

3 barridos: un primer barrido de calentamiento de 30 ºC a 250 ºC, seguido de un enfriamiento de 250 ºC a 25 ºC y completado por un segundo calentamiento de 25 a 300 ºC. La velocidad de calentamiento y enfriamiento se establecieron en 10 ºC/min, y la masa de la muestra fue de alrededor 3 mg. Se utilizó una cápsula de aluminio vacía como referencia, mientras que la calibración se realizó utilizando una muestra de indio. Los valores del punto de fusión y entalpía de fusión se obtuvieron del barrido de calentamiento, mientras que la temperatura de cristalización y entalpía de cristalización se determinó a partir del barrido de enfriamiento.

6.2.6 Dispersión de Rayos X de ángulo amplio (WAXS)

La cristalinidad de las fibras y de los polímeros puros fue evaluada por WAXS utilizando un difractómetro Bruker AXS D4 Endeavor (Bruker, Ettlingen, Alemania). Se registraron los escaneos radiales de intensidad con respecto a los ángulos de dispersión (2θ) a temperatura ambiente en el rango de 2 a 40° (2θ) (tamaño del paso = 0.02°, velocidad del escaneo = 4 s/paso) con radiación CuKα filtrada (λ = 1.54 Å), una tensión de funcionamiento de 40 kV y un filamento de 40 mA.

6.3 Etapa 3. Nanofibras antifúngicas de goma de anacardo, FucoPol y pululano hiladas por *electrospinning*

6.3.1 Materiales

El pululano (Pul) (Mw ~ 2 x 10^5 g/mol) se adquirió de Hayashibara CO., LTD. (Tokio, Japón). Se adquirieron PEO (Mw ~ 4 × 10^5 g/mol), PEO (Mw ~ 5 × 10^6 g/mol), solución salina tamponada con fosfato (PBS), medio de cultivo YPD (extracto de levadura peptona dextrosa) y Span 20 de Sigma Aldrich (St. Louis, MO, EE. UU.). Se empleó glicerol de PanReac AppliChem (Barcelona, España). FucoPol (FP) (1.1 x 10^7 g/mol) fue proporcionado por el Grupo de Ingeniería Bioquímica de la Facultad de Ciencias y Tecnología de la Universidad Nova de Lisboa (Caparica, Portugal). La goma de anacardo (CG) (2.13 × 10^4 g/mol) fue proporcionado por Embrapa (Fortaleza, CE, Brasil).

6.3.2 Preparación de disoluciones

Para encapsular a *M. caribbica* (*GenBank ID*: JQ398674) en las nanofibras poliméricas, primero se optimizaron las condiciones de *electrospinning*. Se utilizaron cuatro polímeros, pululano (Pul), óxido de polietileno (PEO), FucoPol (FP) y goma de anacardo (CG). La

solución de Pul se preparó a una concentración del 15% (p/p). La solución de FP se preparó con PEO (Mw ~ 4×10^5 Da). La solución de FP:PEO se preparó con una concentración de 0.015 g/mL (relación 1:2, p/p) con un 5% de Span 20 (p/v). La tercera solución de CG también se preparó con PEO (Mw ~ 5×10^6 Da). La solución de CG:PEO se preparó con una concentración de 0.15 g/mL (relación 5.6:1 p/p) con 1% de Span 20 (p/v). Para todas las soluciones, se usó agua destilada estéril y para evitar un tratamiento agresivo, Pul y CG:PEO fueron irradiados bajo UV durante 30 min. Mientras que, FP fue esterilizado (autoclave 4001759, J.P. SELECTA, SA, Barcelona, España) a 120 ºC durante 20 min, ya que FP contenía algunos residuos de *Enterobacter* A47, y no era posible esterilizarlo usando solo radiación UV. Posteriormente, cada solución polimérica fue ajustada con *M. caribbica* a una concentración final de 1×10^8 células/mL.

6.3.3 Proceso de *electrospinning*

El proceso de electrohilado se realizó en un equipo Fluidnatek LE-500 de Bioinicia S.L. (Valencia, España). Para obtener las nanofibras, se evaluaron diferentes condiciones de proceso. Una vez logradas las condiciones óptimas, se procesaron todas las soluciones tanto en presencia como en ausencia de *M. caribbica*. La solución de Pul, fue procesada a la velocidad de flujo constante de 500 µL/h, la distancia de trabajo fue de 20 cm, y el voltaje fue de 9.7 kV en el inyector y -3 kV en el colector. La solución de FP:PEO, fue procesada a la velocidad de flujo constante de 600 µL/h, una distancia de trabajo de 15 cm y el voltaje fue de 19 y -1 kV para inyector y colector, respectivamente. La solución de CG:PEO fue procesada según los parámetros optimizados reportados por Grumi (2021) con ligeras modificaciones. Para ello se utilizó un caudal de 400 µL/h, la distancia de trabajo fue de 28 cm y la tensión fue de 20 y -7 kV para inyector y colector, respectivamente. Para todas las soluciones se utilizó una aguja del calibre 23. Las condiciones ambientales fueron monitoreadas y mantenidas a 33 ºC y 28% HR.

6.3.4 Caracterización de las nanofibras

Se caracterizó la morfología de las estructuras mediante SEM, de acuerdo con la metodología propuesta en el apartado 6.1.8 Microscopía Electrónica de Barrido (SEM), ATR-FTIR como se mencionó en el apartado 6.1.10 Espectroscopía infrarroja con transformada de Fourier en

modo de reflectancia total atenuada (ATR-FTIR) y TGA de acuerdo con el apartado 6.1.11 Análisis termogravimétrico (TGA).

6.3.5 Microscopía óptica convencional

Las nanofibras fueron encapsuladas en resina LR-White en cápsulas de gelatina y polimerizadas en estufa de secado convencional entre 55-60 ºC durante 24 h. Los bloques se cortaron a 2 µm con la cuchilla de diamante DIATOME en un ultramicrotomo (UC7, Leica, Wetclar, Alemania). Para observar los cortes, fueron teñidos con azul de toluidina y las muestras fueron visualizadas mediante un microscopio convencional (Eclipse 90i, Nikon Instruments Inc., Nueva York, USA).

6.3.6 Cepas fúngicas y condiciones de cultivo

En este estudio se emplearon: *Colletotrichum gloeosporioides* Pa14 (GenBank ID: MN477464) aislado de aguacate en descomposición en Nayarit, México (Bautista-Rosales y cols.., 2013), *Botrytis cinerea* CECT 20973 (BC03 Persoon 1794) aislado de uvas, *Penicillium digitatum* CECT 21108 (NAV-7 (Persoon) Saccardo 1881) y *Penicillium italicum* CECT 21109 (MAV-1 Wehmer 1894) aislados de cítricos cosechados, *Fusarium oxysporum* CECT 20967 (Schlechtendal 1824) aislado de la raíz de *Citrus macrophylla*, *Trichothecium roseum* CECT 20223 (Persoon) Link 1809) aislado de *Diospyros kaki*. Todas estas cepas se obtuvieron de la Colección Española de Cultivo Tipo (CECT) de la Universidad de Valencia, y se cultivaron en placas de agar de papa y dextrosa (PDA, Scharlau, Barcelona, España). Las cepas obtenidas por la CECT se incubaron según sus condiciones óptimas de cultivo para cepas, es decir, 24 ~ 26 ºC durante 7-10 días. Mientras que *Colletotrichum gloeosporioides* se cultivó a 28 ºC durante 7-10 días.

6.3.7 Viabilidad de *M. caribbica* después del proceso de *electrospinning*

Las nanofibras se recogieron en tubos estériles después del proceso de *electrospinning*. La cantidad empleada de nanofibras se calculó de acuerdo con el porcentaje de sólidos contenidos en la solución polimérica incluidos el peso del polímero y la levadura. Las nanofibras se mezclaron con agua destilada estéril en matraces y se agitaron durante 1 h. Posterior a ello, se prepararon diluciones seriadas y se distribuyeron 100 µL de muestra en las placas YPD. Los recuentos de *M. caribbica* se realizaron después de 48 h de incubación

a 28 ºC. Los análisis se realizaron por triplicado para cada tratamiento y el experimento se repitió tres veces.

6.3.8 Inhibición *in vitro* de germinación de esporas

La inhibición de la germinación de esporas se determinó de acuerdo con González-Estrada y cols. (2017). Se utilizó PBS para hacer la suspensión de esporas. Luego, se agregaron 10 mL a cada placa para cosechar el hongo, y las suspensiones de esporas se hicieron frotando la superficie del agar con un bucle de inoculación estéril. Luego, la suspensión se filtró en gasa estéril y se recuperó en un tubo cónico. La concentración de esporas se ajustó a 1×10^5 esporas/mL mediante conteo microscópico en un hemocitómetro. Cincuenta microlitros de esporas fúngicas (1×10^5 esporas/mL) se esparcieron en discos PDA (1.4 cm) y luego se dejaron secar durante 5 min en un cámara de seguridad. Después de este tiempo, los discos fueron cubiertos con nanofibras que contenían a *M. caribbica* (Pul, FP:PEO, y CG:PEO). Consecutivamente, los discos se incubaron según las condiciones de cultivo de las cepas de CECT (24 ~ 26 ºC) durante 7-10 días. Después del tiempo de incubación, las nanofibras fueron absorbidas por los discos de PDA. El porcentaje de germinación de cada hongo evaluado se determinó mediante microscopía convencional. El porcentaje de esporas germinadas se midió después de 24 h (26 ºC) para *B. cinerea*, después de 9 h (25 ºC) para *P. digitatum*, después de 9 h (25 ºC) para *P. italicum*, después de 6 h (26 ºC) para *F. oxysporum*, después de 6 h (25 ºC) para *T. roseum* y después de 9.5 h (25 ºC) para *C. gloeosporioides*. En el control se tuvieron en cuenta un mínimo de 200 esporas germinadas. Las esporas se consideraban germinadas cuando la longitud del tubo germinal era igual o mayor que el diámetro de la espora.

6.3.9 Inhibición *in vitro* del crecimiento micelial de las nanofibras con *M. caribbica*

Se evaluó la efectividad de las nanofibras contra las diferentes cepas de hongos, los ensayos se realizaron en cajas de PDA. 100 µL de esporas fúngicas (1×10^5 esporas/mL) se esparcieron en el centro de las placas de Petri y luego se dejaron secar durante 5 min en una cámara de seguridad. Luego, las placas inoculadas fueron cubiertas con las nanofibras que contenían *M. caribbica* (fibras de Pululano, FP:PEO y CG:PEO). El diámetro de crecimiento se registró durante 6 días (24 ºC) para *B. cinerea*, durante 8 días (25 ºC) para *P. digitatum*,

durante 8 días (25 ºC) para *P. italicum*, durante 6 días (26 ºC) para *F. oxysporum*, durante 8 días (25 ºC) para *T. roseum* y durante 7 días (28 ºC) para *C. gloeosporioides*. El porcentaje de inhibición del crecimiento micelial se calculó según la Ecuación 3:

$$\% \text{ Inhibición} = [(dc - dt)/dc] \times 100 \qquad \text{Eq. 3}$$

Donde *dc* (cm) es la media del diámetro de la colonia del control y *dt* (cm) es la media del diámetro de la colonia de los tratamientos. Todas las pruebas se realizaron por triplicado. Todas las placas de Petri se cubrieron con papel *Parafilm* para evitar la deshidratación.

Tanto para el ensayo de inhibición de germinación de esporas como el ensayo de inhibición de crecimiento micelial, se usaron como control placas de PDA inoculadas y sin nanofibras y placas de PDA inoculadas con nanofibras sin *M. caribbica*.

6.4 Etapa 4. Nanofibras antifúngicas de goma de anacardo, FucoPol y pululano hiladas por *Solution Blow Spinning*

6.4.1 Materiales

El pululano (Mw ~ 2 x 10^5 g/mol) se adquirió de Hayashibara CO., LTD. (Tokio, Japón). Se adquirió PEO (Mw ~ 4 × 10^5 g/mol), solución salina tamponada con fosfato y medio de cultivo YPD de Sigma Aldrich (St. Louis, MO, EE. UU.). FucoPol (1.1 x 10^7 g/mol) fue proporcionado por el Grupo de Ingeniería Bioquímica de la Facultad de Ciencias y Tecnología de la Universidad Nova de Lisboa (Caparica, Portugal). La goma de anacardo (CG) (2.13 × 10^4 g/mol) fue proporcionada por el Departamento de Agricultura, Servicio de Investigación Agrícola (Peoria, Illinois, EE.UU.). El fungicida Azoxystrobin se adquirió de AMISTAR® (Syngenta, Zeneca, Frankfurt, Alemania). Se obtuvieron aguacates sanos en etapa de madurez fisiológica y de tamaño uniforme (~120 g, con un contenido de materia seca aproximado del 24%) de la empresa Leb Trading Products (Guacamodely S. de R.L. de C.V., Xalisco, México).

6.4.2 Preparación de disoluciones

Para obtener las nanofibras con *M. caribbica* mediante SBS, se prepararon previamente disoluciones poliméricas de pululano (Pul), poli (óxido de etileno) (PEO), FucoPol (FP) y goma de anacardo (CG). Estas soluciones poliméricas fueron preparadas como se describe en la sección 2.3 del manuscrito titulado "A new method for antifungal nanofibers production and its potential post-harvest application on avocado fruit".

6.4.3 Proceso de *Solution Blow Spinning*

El procesado aerohidrodinámico fue llevado a cabo en un equipo Fluidnatek LE-10 *electrospray* (Bioinicia S.L. Valencia, Spain) con una adaptación de aire comprimido de 1 bar de presión (14.50 psi) a 8 bares (116.03 psi). Las soluciones fueron puestas en jeringas de plástico conectadas a un tubo PTFE y a un inyector de boquillas concéntricas conectadas a la toma de aire comprimido. Para obtener las nanofibras se evaluaron diferentes condiciones (solución de pululano [flujo: 5 mL/h, presión: 3 bar, distancia de trabajo: 42.5 cm], solución de FP:PEO [flujo: 2 mL/h; presión: 1 bar; distancia de trabajo; 36.5 cm], y para la solución de CG:PEO [flujo: 3 mL/h; presión: 2 bar; distancia de trabajo; 36.5 cm]. Para los ensayos *in vitro* las nanofibras fueron colectadas sobre papel aluminio y se cortaron círculos de 2 y de 8 cm para posterior análisis. Para los análisis *in vivo* se colocaron 20 aguacates en una cámara de acrílico para la aplicación de las nanofibras. Las nanofibras fueron depositadas sobre la superficie de los aguacates durante diferentes periodos de tiempo de acuerdo a las diferentes concentraciones de las soluciones (Pul 1 h, FP:PEO 4 h y 10 min y CG:PEO 3h y 46 min).

6.4.4 Microscopía Electrónica de Barrido

La morfología de las estructuras obtenidas mediante SBS con y sin *M. caribbica* fue caracterizada de acuerdo con la metodología mencionada en el apartado 6.1.9 de la presente tesis.

6.4.5 Ensayos *in vitro* de las nanofibras con *M. caribbica* obtenidas mediante SBS en la inhibición de *C. gloeosporioides*

Los ensayos se llevaron a cabo de acuerdo con la metodología propuesta en el apartado 6.3.8 Inhibición *in vitro* de germinación de esporas y en el apartado 6.3.9 Inhibición *in vitro* del crecimiento micelial de las nanofibras con *M. caribbica* de la presente tesis. Se usaron como controles placas de Petri con PDA o en su caso discos de PDA inoculados sin recubrir e inoculados recubiertos con las nanofibras sin *M. caribbica* (Pul, FP:PEO, CG:PEO).

6.4.6 Viabilidad de *M. caribbica* en las nanofibras aplicadas sobre la superficie del aguacate

La viabilidad de *M. caribbica* fue evaluada a dos diferentes condiciones de almacenamiento: 1) 25 ºC durante 15 d, y 2) 6 ºC durante 10 d y madurada a 25 ºC durante 5 d para simular las condiciones de comercialización del aguacate. Los aguacates fueron puestos dentro de bolsas estériles que contenía 50 mL de PBS. Las levaduras fueron removidas de la superficie del aguacate mediante sonicación (90 s, KENDAL, Model CD 48-20, Middletown, USA). Posterior a ellos, se hicieron diluciones seriadas que fueron esparcidas en placas de Petri con YPD. Las colonias fueron incubadas por 48 h a 28 ºC (Iñiguez-Moreno y cols., 2020).

6.4.7 Evaluación de las nanofibras de Pululano, FP:PEO y CG:PEO como tratamientos curativos y preventivos en la inhibición de *C. gloeosporioides*

Se tomaron frutos sanos con un tamaño homogéneo (~120 g). Los frutos fueron lavados y desinfectados con hipoclorito de sodio al 2% durante 2 min, posterior a ello fueron lavados con agua destilada estéril y se secaron con una corriente de aire estéril. Para llevar a cabo el tratamiento curativo se hicieron dos agujeros en los aguacates, y se dejaron secar para permitir al patógeno infectar antes de aplicar los tratamientos. Para llevar a cabo el tratamiento preventivo primero se aplicaron los tratamientos y posterior a ello se inoculó la suspensión de *C. gloeosporioides*. Los aguacates fueron almacenados en una cámara (Novatech, Model CA-550; Kingwood, USA) bajo dos diferentes condiciones 1) 25 ºC durante 15 d (75 % RH), y 2) 6 ºC durante 10 d (95% RH) durante 10 d y madurados a 25 ºC (75 % RH) durante 5 d. Se evaluó la incidencia (porcentaje de frutos infectados), las heridas infectadas (porcentaje) y la severidad (diámetro de la lesión, mm). Los tratamientos aplicados fueron: (1) control (agua destilada), (2) azoxystrobin (800 mg/L), (3) nanofibras de Pul,

FP:PEO y CG:PEO sin *M. caribbica* y (4) nanofibras de Pul, FP:PEO y CG:PEO con *M. caribbica*.

6.4.8 Efecto de las nanofibras de Pululano, CG:PEO y FP:PEO sobre los parámetros de calidad en los aguacates.

Se evaluaron los parámetros de calidad en los aguacates después de la aplicación de los tratamientos; control (agua destilada), (2) azoxystrobin (800 mg/L), (3) nanofibras de Pul, FP:PEO y CG:PEO sin *M. caribbica* y (4) nanofibras de Pul, FP:PEO y CG:PEO con *M. caribbica*. Las determinaciones se hicieron de acuerdo con la metodología descrita en los apartados 2.8.1 Pérdida de peso, 2.8.2 Sólidos solubles totales, 2.8.3 Acidez titulable y pH, 2.8.4 Firmeza, 2.8.5 Contenido de materia seca y 2.8.6 Color del manuscrito titulado "A new method for antifungal nanofibers production and its potential post-harvest application on avocado fruit".

6.5 Análisis estadístico

Se realizó un análisis de varianza (ANOVA) y pruebas LSD para evaluar diferencia entre las medias de los tratamientos ($P = 0.05$) utilizando el software STATISTICA 10 (Statsoft Inc., Tulsa, OK, USA).

CAPÍTULO 7. RESULTADOS Y DISCUSIÓN

7. RESULTADOS Y DISCUSIÓN

7.1 Estudio de la goma de anacardo como polisacárido para la encapsulación de compuestos mediante *electrospraying*

Los resultados correspondientes a la etapa 1 de este proyecto de tesis están contenidos en la siguiente publicación:

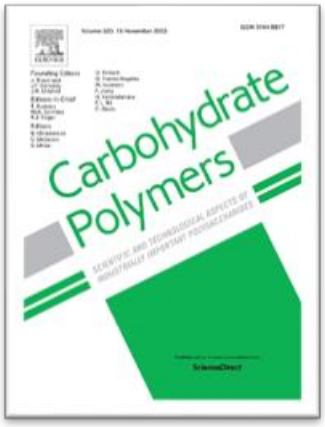

Electrosprayed cashew gum microparticles for the encapsulation of highly sensitive bioactive materials

Vázquez-González, Y., Prieto, C., Filizoglu, M. F., Ragazzo-Sánchez, J. A., Calderón-Santoyo, M., Furtado, R. F., Cheng, H. N., Biswas, A., Lagaron, J.M.

Carbohydrate Polymers 264 (2021) 118060, DOI:10.1016/j.carbpol.2021.118060.

Factor de impacto (2021): 10.723

Número de citas: 17

7.1.1 Introducción al tema

De entre las técnicas de encapsulación disponibles, el *electrospraying* surge como una nueva tecnología en donde las nano o las micropartículas son producidas a temperatura ambiente mediante la aplicación de alto voltaje a una disolución polimérica. En este proceso están involucrados parámetros tales como propiedades fisicoquímicas como viscosidad, tensión superficial, y la conductividad de la solución polimérica, y parámetros del proceso como la distancia de trabajo, el voltaje y el flujo, los cuales afectan a la formación y las características de las nano o micropartículas obtenidas. En la encapsulación de compuestos bioactivos mediante la técnica de *electrospraying*, no hay limitaciones acerca de la naturaleza del material polimérico, así pueden emplearse polímeros naturales como polisacáridos, proteínas o lípidos. De esta manera, los polisacáridos han jugado un papel importante en la encapsulación. En particular, algunos recubrimientos a base de gomas proporcionan una barrera semipermeable en la superficie del producto que permite reducir la tasa de respiración, la pérdida de peso y además permite mantener el valor nutricional de los productos. Las gomas han sido reconocidas como GRAS (*Generally Recognized As Safe*) por la Administración de Alimentos y Medicamentos de los Estados Unidos (FDA), por lo que su uso es seguro para el consumidor. En particular, la goma de anacardo (CG) es un exudado gomoso obtenido a partir del árbol *Anacardium occidentale,* el cual está ampliamente distribuido en la parte nororiental de Brasil. Existe un alto potencial para explorar la CG ya que se trata de una materia prima económica, biocompatible, ecológica y altamente biodisponible. Sin embargo, hasta abril 2021, no existían reportes de su uso en procesos de encapsulación mediante procesos electrohidrodinámicos. Por lo que el objetivo de la presente investigación fue evaluar la factibilidad de emplear la CG como una matriz protectora para encapsular al compuesto modelo β-caroteno mediante el proceso de *electrospraying* para su potencial aplicación en alimentos y productos farmacéuticos. Para ello se prepararon cuatro diferentes disoluciones, la disolución 1 (D1) fue preparada a una concentración del 50% (w/w) en agua destilada. La disolución 2 (D2) fue preparada a la misma concentración junto con el 1% de Span 20 como surfactante. La disolución 3 (D3) consistió en una disolución de goma de anacardo con β-caroteno en aceite de ricino (5% w/w) en proporciones de 20:80 (v/v). Mientras que, la disolución 4 (D4) fue preparada en proporciones de 10:80 (v/v). Posteriormente las diferentes disoluciones fueron caracterizadas fisicoquímicamente, en

cuanto a la conductividad, la tensión superficial y la viscosidad, además, en las disoluciones D3 y D4 se determinó la distribución del tamaño y la morfología de las partículas que conformaron las disoluciones. Todas las disoluciones fueron procesadas mediante un equipo de *electrospray* LE-10 con la finalidad de obtener partículas.

Las partículas obtenidas fueron caracterizadas mediante microscopía electrónica de barrido (SEM), espectroscopía de transformada de Fourier (ATR-FTIR) y análisis termogravimétrico (TGA). También se determinó la capacidad de carga de β-caroteno y el β-caroteno extraíble. Finalmente se evalúo la fotoestabilidad de las cápsulas de β-caroteno frente a la luz UV.

Se obtuvieron partículas esféricas de superficie lisa y tamaño medio entre 3 y 6 µm. Las partículas producidas a partir de la emulsión 90:10 (v/v) mostraron capacidad de carga de 0.075 ± 0.006% y una pequeña cantidad de β-caroteno extraíble, 10.75 ± 2.42%. La goma de anacardo demostró ofrecer fotoprotección durante cortos periodos de tiempo.

Este estudio fue el primer reporte del uso de la goma de anacardo como material encapsulante usando un proceso electrohidrodinámico, y además fue la base para tomar decisiones en el desarrollo de los siguientes objetivos de la tesis.

Electrosprayed cashew gum microparticles for the encapsulation of highly sensitive bioactive materials

Y. Vázquez-González[1,2], C. Prieto[1*], M.F. Filizoglu[1,3], J.A. Ragazzo-Sánchez[2], M. Calderón-Santoyo[2], R.F. Furtado[4], H.N. Cheng[5], A. Biswas[6] and J.M. Lagaron[1]

[1] Novel Materials and Nanotechnology Group, IATA-CSIC, Calle Catedrático Agustín Escardino Benlloch 7, 46980 Paterna, Spain; cprieto@iata.csic.es (C.P.); lagaron@iata.csic.es (J.M.L.); yuliana.vg04@gmail.com (Y.V.-G); filizoglumf@gmail.com (M.F.F.)

[2] Laboratorio Integral de Investigación en Alimentos, Tecnológico Nacional de México – Instituto Tecnológico de Tepic, Av. Tecnológico de Tepic, Av. Tecnológico # 2595, C.P. 63195, Tepic, Nayarit, Mexico; yuliana.vg04@gmail.com (Y.V.-G.); montserratcalder@gmail.com (M.C.-S.); arturoragazzo@hotmail.com (J.A.R.-S)

[3] Department of Biology, Faculty of Science, İstanbul University, 34134 Vezneciler, İstanbul – Turkey; filizoglumf@gmail.com (M.F.F.)

[4] Embrapa Agroindústria Tropical, Rua Dra. Sara Mesquita 2270, CEP 60511-110 Fortaleza, CE, Brazil, roselayne.furtado@embrapa.br (R.F.F.)

[5] U.S. Department of Agriculture, Agriculture Research Service, Southern Regional Research Center, 1100 Robert E. Lee Blvd., New Orleans, LA 70124, USA, hn.cheng@usda.gov (H.N.C)

[6] U.S. Department of Agriculture, Agricultural Research Service, National Center for Agricultural Utilization Research, 1815 N. University St, Peoria, IL 61604, USA; atanu.biswas@usda.gov (A.B.)

***** Corresponding author: Tel.: (+34) 963 900 022 ext.2515; fax: +34 963 636 301
E-mail address: cprieto@iata.csic.es (C. Prieto)

Abstract:

This study focuses on the production and characterization of electrosprayed cashew gum (CG) microparticles that encapsulate β-carotene. CG is an inexpensive, non-toxic polysaccharide obtained from *Anacardium occidentale* trees. Encapsulation of β-carotene in CG was performed by electrospraying from two emulsion formulations (water : oil ratios 80:20 and 90:10 (v/v)) in which the dispersed phase consisted of β-carotene dissolved in castor oil, and the continuous phase was a CG aqueous solution. Spherical particles with smooth surface and medium size between 3 and 6 μm were obtained. The particles produced from the 90:10 (v/v) emulsion showed a loading capacity of 0.075±0.006% and a minor amount of extractable β-carotene, 10.75±2.42%. ATR-FTIR confirmed the absence of interaction between the particles' components. CG demonstrated to offer thermoprotection, and photoprotection for short periods of time. These results make CG a viable candidate to encapsulate bioactive compounds via electrospraying for agricultural, food and pharmaceutical applications.

Keywords: Cashew gum polysaccharide; β-carotene; electrospray; microparticles; encapsulation.

Abbreviations: CG: Cashew gum, LC: Loading capacity, EβC: Extractable β-carotene.

Highlights:

- Cashew gum microparticles encapsulating β-carotene were produced by electrospraying.
- Smooth and spherical microparticles with sizes between 3 and 6 µm were obtained.
- 11% of extractable β-carotene confirmed the efficiency of the encapsulation process.
- Cashew gum demonstrated to offer thermoprotection to β-carotene.
- Photoprotection for β-carotene was observed for short periods of time.

Graphical abstract

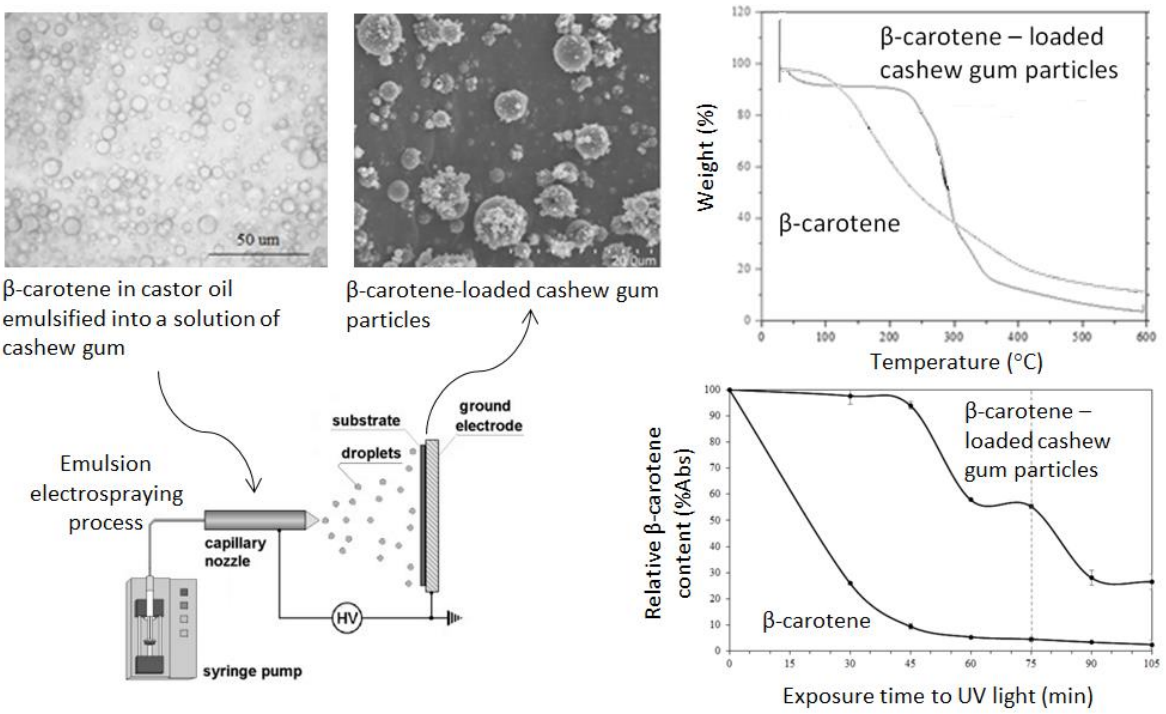

1. Introduction

Encapsulation may be defined as the process that entraps a bioactive compound into a wall material in order to protect it from different physico-chemical factors (temperature, oxygen, humidity, pH, among others), which may engender its degradation and loss of bioavailability (Sobel, Versic, & Gaonkar, 2014). This technology is of significant interest to the pharmaceutical, cosmetic, and biotechnological sectors but has special relevance for the food industry (Nedovic et al., 2011). Multiple encapsulation technologies have been developed so far; the efficiency of the encapsulation process not only depends on the selected technology but also on the characteristics of the wall material. Together, they can improve the core material stability and reduce its volatility, mask undesirable aromas and flavors, avoid migration of the core material to the particle surface, and provide controlled release (Botrel, Borges, Fernandez, et al., 2017). The wall material must be biocompatible and biodegradable, form a barrier between the internal phase and its surroundings, provide its release at the desired time, and is approved for use in the final product. In addition, the availability and cost of the wall material are also important (Fernandez et al., 2016). Wall materials can be selected from a wide variety of natural or synthetic polymers. Most of the natural polymers are water soluble and non-toxic, which makes them highly appropriate for the encapsulation of sensitive bioactives (Nedovic et al., 2011). Among the natural polymers, polysaccharides and proteins are the most often used in encapsulation processes. In view of their relevance and utility, it is useful to study newly emerging and non-conventional biopolymers for this application (Botrel, Borges, Fernandes, et al., 2017).

Polysaccharides appear to be appropriate for preparing micro- and nanoparticles due to their unique physicochemical properties and excellent biocompatibility. Moreover, they are safe, low-cost, highly biodegradable, and abundant in nature (Abreu et al., 2016). Polysaccharides include cellulose, chitin and chitosan, glucans, gums, pectins, and starch. Gum-biobased compounds are used mainly in food and bioproducts, because they are film-forming and able to stabilize emulsions (Porto & Cristianini, 2018). They are derived from different sources such as microbial (e.g., dextran, pullulan), plant and seed (e.g., starch, pectin, cellulose), algal (e.g., alginate, carrageenan), and animal (e.g., chitosan, chondroitin) (Valencia, Zare, Makvandi, & Gutiérrez, 2019; Yang, Han, Zheng, Dong, & Liu, 2015).

Cashew gum (CG), an exudate gum, is a complex water-soluble heteropolysaccharide extracted from *Anacardium occidentale* tree, which is widely distributed in northeastern Brazil but can also be found in India, Mozambique, Tanzania, and Kenya among other countries (Dias et al., 2016; Mothé, Souza, & Calazans, 2008). This gum has a high availability, as an average 700 gram of gum is being produced per tree annually with a potential global production of 50,000 tons per year (Cunha, Paula, & Feitosa, 2009). Regarding its composition, purified CG is mainly composed of galactose (59.4-73%), glucose (6.4-14%), arabinose (4.2-5.3%), rhamnose (2.4-4%) and glucuronic acid (6.3-13.5%) (Silva et al., 2016). CG is an inexpensive, non-toxic, biocompatible, biodegradable polymer with good rheological and mechanical properties (Botrel, Borges, Fernandes, et al., 2017; Silva et al., 2012), readily soluble in water, and with good emulsifying, adhesive and stabilizing properties (Botrel, Borges, Yoshida, et al., 2017). CG has also pharmaceutical attributes, since earlier publications have reported its mucoadhesive, anti-inflammatory (Nicolau et al., 2019; Souza Filho et al., 2018), anti-microbial, antidiarrheal, antitumor and hypoglycemic effects (Silva et al., 2018). CG can be used pure or chemically modified to improve viscosity, functionality and bioactive retention (Das, Dutta, Nayak, & Nanda, 2014; Leite et al., 2017; Vasconselos Silva et al., 2019). All these properties make CG a suitable candidate as a wall material in order to encapsulate bioactive compounds for food and pharmaceutical industry. However, thus far, CG has not often been used for microencapsulation (Abreu et al., 2016; Botrel, Borges, Fernandes, et al., 2017; Fernandes et al., 2016; Porto & Cristianini, 2018).

Electrohydrodynamic spraying or electrospraying is a simple and highly versatile method of liquid atomization by means of electrical forces which allows the production of particles in the micro, submicro and nano range (Jaworek & Sobczyk, 2008). In this process, the liquid flowing out of a capillary nozzle, within a high electrical potential, is forced by the electrostatic forces to be dispersed into fine droplets, which after drying, generate the capsules at room temperature (Gómez-Mascaraque, Ambrosio-Martín, Fabra, Perez-Masia, & López-Rubio, 2016; Torres-Giner, Martinez-Abad, Ocio, & Lagaron, 2010). This technology is very suitable for the encapsulation of bioactive compounds due to its mild operating conditions. In addition, this technology presents more advantages compared to other encapsulation techniques, such as high encapsulation efficiency and reduced particle

size. It does not require a subsequent step to separate the particles from the medium, and a wide range of polymeric wall materials can be used (Echegoyen, Fabra, Castro-Mayorga, Cherpinski, & Lagaron, 2017; Gómez-Mascaraque & López-Rubio, 2016). This technology has been involved in the encapsulation of multiple bioactive compounds with applications in the food, pharmaceutical and cosmetic industries, such as β-carotene (de Freitas Zômpero, López-Rubio, de Pinho, Lagaron, & de la Torre, 2015), and folic acid (Aceituno-Medina, Mendoza, Lagaron, & López-Rubio, 2015; Pérez-Masiá et al., 2015).

The objective of this study was to evaluate the feasibility of CG as a protective matrix to encapsulate β-carotene (a challenging model bioactive compound) through the electrospraying process for potential use in food and pharmaceutical products. The particles produced were characterized via morphology, particle size, loading capacity and extractable β-carotene. Stability studies against thermo and photo-oxidation were also included in this investigation.

2. Experimental

2.1. Materials

CG was collected from native *Anacardium occidentale* L trees in the Experimental Field of Embrapa Tropical Agroindustry (Fortaleza, CE, Brazil). The polysaccharide isolation from CG was performed using the methodology previously described by Silva et al. (2018). The centesimal composition of the CG was 94.09% carbohydrate, 4.43% water, 0.76% protein, 0.63% ash and 0.09% of ether extract, with a content of phenolic compounds of 143.85 mg per 100 g of product; being the molar mass of the CG 2.13 x 10^4 g/mol with a PDI of 2.61 (Melo et al., 2020). The ratio of monosaccharides present in cashew gum was 9.85: 4.19: 4.74: 1 of galactose: arabinose: glucose: rhamnose, respectively, as determined by NMR analysis using a 600 MHz Agilent DD2 equipment (Santa Clara, CA, USA) with a probe of 5 mm inside diameter (HF / 15N-31P), reverse detection and gradient field on the "z" axis. The samples were prepared by dissolving 9.5 mg of purified cashew gum in 550 µL of D_2O. One-dimensional spectrum of 13C was performed at 80 °C with a time between each acquisition of 1s, acquisition of 15k of transients in a spectral window of 251.1 ppm and 32k

of number of points. The 13C signals related to anomeric carbons were integrated to obtain the relative percentage of monosaccharides in the samples.

β-carotene, castor oil and Span® 20 surfactant were purchased from Sigma Aldrich (St. Louis, MO, USA), and chloroform from Panreac AppliChem (Barcelona, Spain). Distilled water was used throughout the study. All chemicals were used as received without any further purification.

2.2. Preparation of solutions and emulsions

The CG solution (D1) was prepared at a concentration of 50% (*w*/*w*) in distilled water. CG solution was also prepared containing 1% (*w*/*w*) of Span 20 as a surfactant (D2). Aqueous solutions were homogenized under magnetic stirring for 36 h at room temperature, and immediately used for the preparation of emulsions or for solution characterization.

For encapsulation of β-carotene in CG, initially a concentrated solution of β-carotene in castor oil (5 % w/w) was prepared. An emulsion was then prepared by slowly adding the organic phase to the aqueous solution with Span 20 (D2) in a volume ratio of 20:80 (D3) or 10:90 (D4) and homogenized using an IR Digital Vortex Mixer (Velp Scientifica, Usmate Velate, Italy) for 5 min. Emulsions were denominated 80:20 and 90:10 in relation to the proportion of aqueous and organic phase volumes. After homogenization, emulsions were immediately processed or characterized.

2.3. Characterization of the solutions and distribution of particle size in the emulsions

The characterization of the solutions was performed in terms of electrical conductivity, viscosity and surface tension. The electrical conductivity was analyzed with a multiparameter potentiometer, Hanna Instruments HI-4521 (Melrose, MA, USA). The probe was immersed in 20 mL of sample in a Falcon tube until sensors were covered and stabilized, and the conductivity value was read. The viscosity was measured using a rotational viscosimeter, Visco Basic Plus L (Fungilab S.A., Sant Feliu de Llobregat, Spain). The L1 spindle was positioned in the viscosimeter, and 20 mL of samples were placed in a Falcon tube and put in contact with the spindle to obtain the viscosity value. The surface tension was measured with the Force tensiometer model K20 EasyDyne (Krüss GmbH, Hamburg, Germany), with the Wilhelmy plate method. 20 mL of sample were placed in a crystallizer, then the Wilhelmy plate was cleaned by pyrolysis and suspended from the pendulum; the crystallizer with the

sample was then placed on the platform for sample analysis. These measurements were made in triplicate at room temperature.

2.3.1 Morphology and emulsion particle size distribution

The prepared emulsions were observed by conventional optical microscopy (Nikon Eclipse 90i, Nikon Instruments Inc., New York, USA), whilst its particle size distribution was determined by photon correlation spectroscopy using a Master Sizer 2000 (Malvern Instruments, Malvern, United Kingdom). Emulsions were diluted with recirculating water (3000 rpm) until it reached a dilution of 12%. The refractive indices of sunflower oil (1.469) and water (1.330) were used as references. Results were given as droplet mean diameter (D0.5). Measurements were made in triplicate.

2.4. Obtaining particles by electrospray

The electrospray process was performed in a high-throughput Fluinatek® LE-50 equipment from Bioinicia S.L. (Valencia, Spain). The freshly prepared solutions or emulsions were drawn in a 5 mL plastic syringe that was placed on a syringe pump and connected by PTFE tube to a stainless-steel needle (27 gauge). A positive electrode of a high voltage power supply was coupled to the needle. The solutions were electrosprayed at the constant flow rate of 200 µL/h and a voltage of 25 kV. The distance between the needle tip and the flat collector was 28 cm. The process was performed under room conditions. Empty CG capsules were also prepared as a control using the same operating conditions.

2.5. Morphological analysis of the obtained particles through SEM

The morphology of the particles obtained was determined using scanning electron microscopy (SEM) in a Hitachi-S-4800 FE-SEM (Hitachi High-Technologies Corporation, Tokyo, Japan) with an electron beam acceleration of 10 kV. Approximately 1.5 mg of sample were affixed with double-sided tape on the sample holder and coated with a gold-palladium layer. The determination of the particle size distribution based on the diameters of the structures was made using the Image J Launcher v1.41 software (National Institutes of Health, Bethesda, MD, USA) with at least 100 measurements per sample.

2.6. Loading capacity and extractable β-carotene

Loading capacity (LC) was estimated by measuring the total amount of β-carotene in the particles. About 0.05 g of the particles were dissolved in water. 1.5 mL of chloroform were

added to the aqueous solution to extract the β-carotene. The aqueous-chloroform mixture was stirred on the vortex for 1 min and centrifuged at 10,000 rpm for 2 min for phase separation. Quantitative measurements of β-carotene in the chloroform phase were performed by UV-vis spectrophotometry. The absorbance of β-carotene was measured at 461 nm in a UV4000 spectrophotometer (Dinko Instruments, Barcelona, Spain). Standard solutions made of β-carotene in chloroform at 0.1 mg/mL were used to build the standard curve (y = 0.8433x + 0.0012, R^2=0.9986), from which the amount of β-carotene present in the filtrate was determined (Equation 1).

$$\boldsymbol{LC}\ (\%) = \left(\frac{\boldsymbol{Mass\ of\ \beta - carotene}}{\boldsymbol{Mass\ of\ particle}}\right) \times \mathbf{100} \quad (1)$$

The extractable β-carotene (EβC) was estimated by measuring the readily soluble β-carotene by washing the particles with an organic solvent. 25 mg of the particles were thoroughly washed with chloroform for 30 s and centrifuged for 5 min at 7000 rpm. The absorbance of the filtrate was measured at 461 nm in a UV4000 spectrophotometer (Dinko Instruments, Barcelona, Spain). The same standard curve was used (y = 0.8433x + 0.0012, R^2=0.9986) to determine the amount of β-carotene present in the filtrate. The extractable β-carotene was then calculated according to Equation 2.

$$\boldsymbol{E\beta C}\ (\%) = \frac{(\boldsymbol{surface\ \beta - carotene})}{\boldsymbol{total\ \beta - carotene}} \times \mathbf{100} \quad (2)$$

2.7. Fourier Transform Infrared Spectroscopy (ATR-FTIR)

Attenuated Total Reflectance Fourier Transform Infrared Spectroscopy (ATR-FTIR) (Bruker FTIR Tensor 37 equipment, Rheinstetten, Germany) was used to evaluate possible changes that occurred within the selected samples, e.g., CG, β-carotene, castor oil, empty CG capsules and β-carotene-loaded CG capsules. The samples were placed on top of the diamond crystal and appropriate contact was assured by using the low temperature ATR Sampling Golden Gate accessory (Specac Ltd., Orpington, UK). All the spectra were obtained at 4000-600 cm^{-1} by averaging 10 scans at 4 cm^{-1} resolution. Analysis of spectral data was carried out using Origin Pro, Version 2019 (OriginLab Corporation, Northampton, MA, USA).

2.8. Thermogravimetric analysis (TGA)

Thermogravimetric analyses of CG polymer, β-carotene, castor oil, empty CG capsules and β-carotene-loaded CG capsules were done in triplicate using TGA-STDA 1600 equipment (Mettler Toledo, Columbus, OH, USA). The analyses were carried out under the following conditions: 1-5 mg of sample, heating from 25 °C to 600 °C, heating rate 5 °C/min, and nitrogen flow (50 mL/min).

2.9. UV photostability

Stability against photo-oxidation of the β-carotene-loaded CG capsule*s* was compared with the degradation rate of pure β-carotene by placing the samples under a simulator of sunlight at room temperature. An Osram Ultra-vitalux lamp (300 W) (OSRAM, Munich, Germany) was used, which generated a mixture of radiation, using a quartz discharge tube and a tungsten filament OSRAM (Fernandez, Torres-Giner, & Lagaron, 2009). The distance between the lamp and the samples was 20 cm. Samples were collected over periods of illumination times (0 min, 30 min, 45 min, 60 min, 75 min, 90 min, and 105 min), and the intact β-carotene concentration was determined using a UV4000 spectrophotometer (Dinko Instruments, Barcelona, Spain) at 461 nm. For β-carotene concentration determination, a control sample was prepared by dissolving β-carotene in 1.5 mL chloroform. The samples consisting of encapsulated CG particles with β-carotene were dissolved first in 0.5 mL of distilled water, and then β-carotene was extracted with 1.5 mL of chloroform. The mixture was stirred on a vortex and centrifuged at 10,000 rpm for 1 min. The organic phase was separated, and the β-carotene concentration was determined by spectrophotometry.

2.10. Statistic analysis

Data were analyzed by ANOVA with a P-value < 0.05. Fisher Test was used for the comparison of means with STATISTICA 10 software (StatSoft, Inc., Tulsa, OK, USA).

3. Results and Discussion

3.1. Physicochemical Characterization of Solution

First, the physicochemical properties of the solutions and emulsions were evaluated in terms of viscosity, conductivity and surface tension, since the stability of the electrohydrodynamic process and the morphology of the structures obtained are highly related to them. Two

solutions and two emulsions were prepared. The aqueous CG solution was identified as D1, and the aqueous CG + Span 20 solution was designated D2. With respect to emulsions, the 80:20 (v/v) emulsion was called D3, and the 90:10 (v/v) emulsion was named D4. Results of their characterization are shown in Table 1. The aqueous solutions, D1 and D2, showed viscosity values around 400 cP, whereas the viscosity of the emulsions, D3 and D4, were around 1000 cP, probably due to the incorporation of castor oil in the emulsion formulation (μ=1000 cP at 24 °C). The electrospraying of solutions with high viscosities tended to produce particles with an increased particle size and could alter the shape of the particles from spherical to spindle or fiber-like, making difficult the formation of homogeneous particles (Ghorani & Tucker, 2015; Shenoy, Bates, Frisch, & Wnek, 2005).

The CG showed a surface tension of 54.80 ± 0.20 mN/m, probably due to its solubilization in water. However, the surface tension was reduced to 27.10 ± 0.10 mN/m by adding 1% (w/w) of Span 20 to the CG solution. It is well-known that the action of surfactants decreases the surface tension of the liquids (Lin, Wang, Wang, & Wang, 2004; Manee-in, Nithitanakul, & Supaphol, 2006). A slight increase of surface tension was observed in the emulsion, 30.30 ± 0.10 and 29.50 ± 0.10 mN/m, respectively for the 80:20 and 90:10 (v/v) emulsions, probably due to the presence of β-carotene and castor oil (surface tension of 36.10 mN/m) and to the role of Span 20 decreasing the interfacial tension between emulsion phases. Nevertheless, this value was beneath the maximum limit of 50 mN/m, which was suggested for a stable electrohydrodynamic process (Jaworek, 2007).

All the samples showed low conductivity values as shown in Table 1. These values are adequate, since they are lower than the maximum values recommended for an electrospraying process (<2.20 mS / cm) (Librán, Castro, & Lagaron, 2017).

Table 1. Physico-chemical properties* of the solutions of CG, CG with Span 20 (1% w/w), emulsion ratio 80:20 (v/v), and emulsion ratio 90:10 (v/v).

Sample	Viscosity (cP)	Surface tension (mN/m)	Conductivity (mS/cm)
D1-CG	425.85 ± 9.69c	54.80 ± 0.20a	1.35 ± 0.00b
D2-CG + Span 20	428.30 ± 9.13c	27.10 ± 0.10d	1.41 ± 0.00a
D3-Emulsion 80:20	1034.16 ± 29.97a	30.30 ± 0.10b	1.01 ± 0.01d
D4-Emulsion 90:10	918.86 ± 2.10b	29.50 ± 0.10c	1.17 ± 0.00c

*Each column represents the mean ± standard deviation of three independent replicas. Different letters in each column indicate significant difference ($p < 0.05$).

3.1.1. Distribution of particle size in the emulsions

Fig. 1 shows the morphology and particle size distribution of the droplets of the 80:20 and 90:10 (v/v) emulsions. The particle size distribution in both emulsions was wide, covering a range between 0.8 to 100 μm. The 90:10 (v/v) emulsion (Fig. 1a) showed a higher proportion (~2.5 %) of small particles (1 – 8 μm) in comparison to the 80:20 (v/v) emulsion (~1.5 %, Fig. 1b), whereas the 80:20 (v/v) emulsion showed a larger proportion of particles with larger diameters (~8 %, 10 – 100 μm). This wide distribution is probably due to the use of a vortex to homogenize the emulsions. The alternate use of ultrasound instead (or together with the vortex) probably would help to obtain a more homogeneous distribution. Normally, the ultrasound gives smaller droplet sizes (600 to 1000 nm) due to the cavitation effect transmitted through waves that compress and expand the contents of the emulsions (Cabrera-Trujillo, Filomena-Ambrosio, Quintanilla-Carvajal, & Sotelo-Díaz, 2018). Nevertheless, other inherent characteristics such as the stability of the emulsion could also be involved. Since the high volume of organic phase in the 80:20 (v/v) emulsion could not have allowed Span 20 to form an interfacial layer with enough thickness to stabilize the droplets, and consequently they could tend to aglomerate, thereby contributing to the formation of larger droplets (Cai et al., 2018; Tadros, 2015). However, both emulsions remained apparently stable during the whole electrospraying process, since no phase separation was observed.
Regarding the micrographs, they corroborated the observed difference between the particles size in the emulsions. The 90:10 (v/v) emulsion (Fig. 1a), showed smaller particles with

homogeneous sizes, while the 80:20 (v/v) emulsion (Fig. 1b) exhibited larger particles (30 – 50 µm) of different sizes.

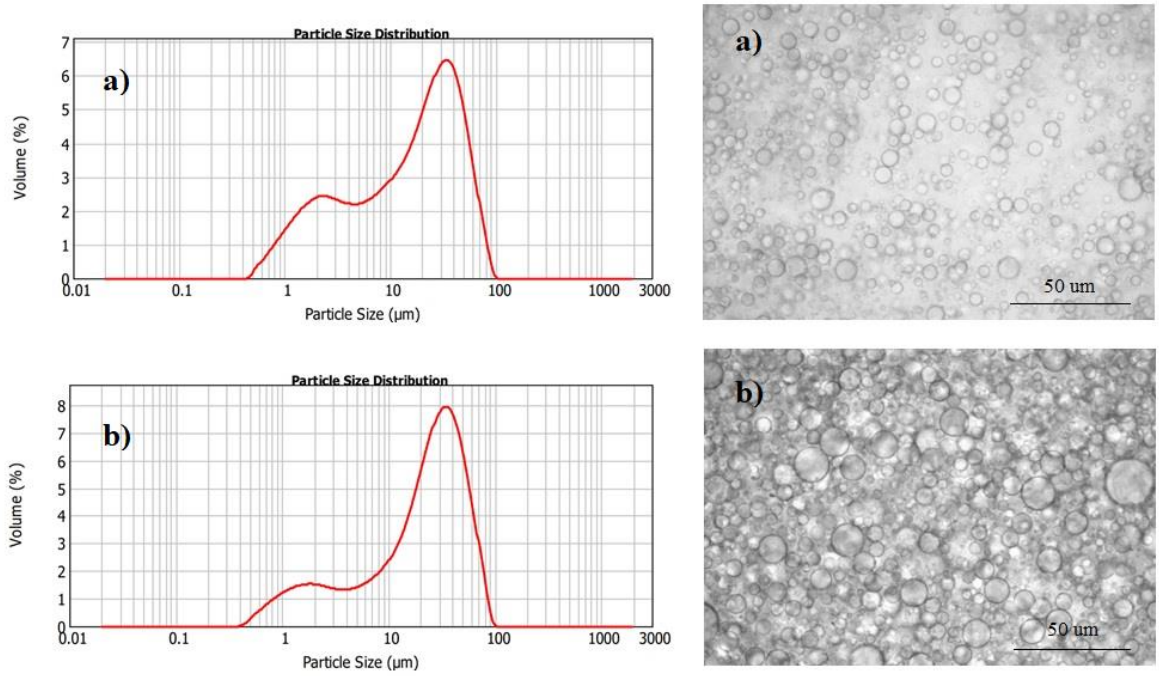

Fig. 1. Particle size distribution and morphology of the droplets of the emulsions: a) 90:10 (v/v) emulsion, b) 80:20 (v/v) emulsion.

3.2. Morphology

The morphology of the capsules was studied by SEM. This is an important characteristic since a good morphology is an assurance of high protection and retention of the encapsulated compound (Silva et al., 2018). Overall, CG capsules and β-carotene-loaded CG capsules produced with the 80:20 and 90:10 (v/v) emulsions showed completely spherical morphologies with smooth surface, without the presence of cracks, fissures or breaks as shown in Fig. 2. The incorporation of the oil with the β-carotene did not alter the morphology. In contrast, Silva et al. (2018) encapsulated green tea extract with CG + maltodextrin by spray drying and obtained microparticles that showed dents, cracked and concave surfaces. The irregular surface obtained by Silva et al. (2018) could be due to the combination of the CG with other polymeric matrices as well as the fast-drying process during spray drying.

Botrel et al. encapsulated fish oil into CG by spray drying and obtained microparticles with a raisin shape (Botrel, Borges, Fernandes et al., 2017).

In our samples, the particles obtained showed different mean particle sizes, being smaller for the β-carotene-loaded CG capsules prepared with the 80:20 (v/v) emulsion (3.34 ± 1.42 μm). The empty and β-carotene-loaded CG capsules prepared with the 90:10 (v/v) emulsion showed similar particle size, around 5.76 ± 3.65 μm and 5.09 ± 2.03 μm, respectively, as shown in Fig. 2. Busolo et al. (2019) also observed that the incorporation of fish oil to the encapsulating matrix led to capsules with a similar morphology but smaller in size (Busolo, Torres-Giner, Prieto, & Lagaron, 2019). All of them showed wide particle size distributions. Smaller particle size implies a large surface area, which may lead to a higher amount of non-encapsulated material (Anwar & Kunz, 2011).

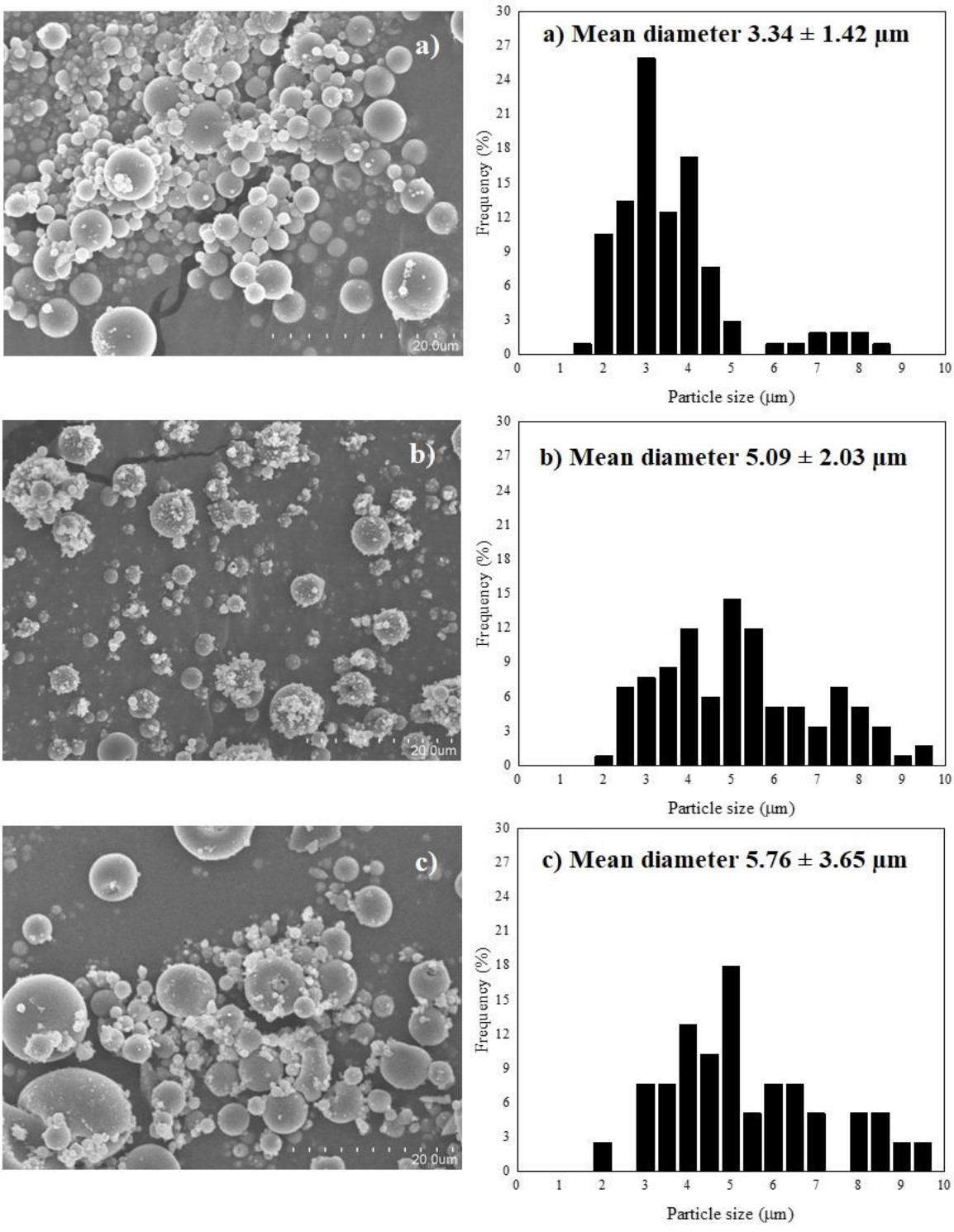

Fig. 2. Scanning electron microscopy (SEM) images and particle size distribution of a), and b) β-carotene-loaded CG capsules with emulsion ratio, 80:20 and 90:10 (v/v), respectively; and c) CG capsules.

3.3. Loading Capacity and extractable β-carotene

The β-carotene-loaded CG microcapsules prepared with emulsion ratios of 90:10 and 80:20 (v/v) presented loading capacities that were statistically different ($p < 0.05$), i.e., 0.075 ± 0.006 % and 0.165 ± 0.023 %, respectively, as shown in Table 2. This behavior could be attributed to the limited solubility of β-carotene (Flaxbart, 1999), and to the low viscosity of CG, because of the paucity of intra- and inter-molecular interactions (de Paula & Rodrigues, 1995). The values obtained were relatively low compared to the results obtained by other authors using other polymeric matrixes, for example, casein, PLG, PLA, and PVA (Rezaeinia, Ghorani, Emadzadeh, & Tucker, 2019). For instance, Kumari et al. (Kumari, Yadav, Pakade, Singh, & Yadav, 2010) obtained a loading capacity of 96.7% using PLA for the encapsulation of quercetin via the solvent evaporation method. However, an enhancement in loading capacity is observed if results are compared with the obtained by other authors encapsulating β-carotene. Basar et al. obtained loading capacities of 0.037 % using whey protein concentrate and deep eutectic solvents for the encapsulation of β-carotene via electrospraying (Basar et al., 2020). The low loading capacity obtained with CG could limit its application; however, chemical modification of the CG molecule, such as carboxylation (Leite et al., 2017), oxidation (Das et al., 2014) or acetylation (Vasconcelos Silva et al., 2019), can be used to improve the interactions between the bioactive compound and the polymeric matrix and, hence enhance the retention. In addition, chemical modifications can improve the emulsifying properties, since substitution by acetyl groups can lead to a reduction of surface tension, thus promoting the improvement of surface properties (Lima Cardial et al., 2019). In addition to chemical modifications, blending CG with other matrices could be an alternative to improve the loading capacity of the particles.

As regards extractable β-carotene, the capsules prepared with the 90:10 (v/v) emulsion showed low amount of extractable β-carotene (10.75 ± 2.42%) in comparison with the values obtained with the capsules produced with the 80:20 (v/v) emulsion, 75.47 ± 5.48 %. The emulsion with ratio 90:10 (v/v) had a lower content of castor oil, and this could ease the incorporation of the dispersed phase in the continuous phase, being the highest amount of β-carotene placed inside the microcapsule. With respect to the 80:20 (v/v) emulsion, the extractable β-carotene results corroborated the finding that most of β-carotene was positioned on the surface of the capsules. The high concentration of castor oil together with greater

heterogeneity in the particle size, could have contributed to the increased extraction of β-carotene. Likewise, a higher viscosity of the 80:20 (v/v) emulsion could contribute to increase emulsion stability and decrease the extractable β-carotene. Indeed, Rezaeinia et al. (Rezaeinia et al., 2019) attributed the high loading capacity and encapsulation efficiency to the high values of viscosity (5480 ± 3 cP) obtained for their samples.

Table 2. Loading capacity and extractable β-carotene * of the electrosprayed β-carotene-loaded CG microcapsules.

β-carotene-loaded CG microcapsules	**Loading Capacity (%)**	**Extractable β-carotene (%)**
Emulsion ratio 90:10	0.075 ± 0.006a	10.75 ± 2.42a
Emulsion ratio 80:20	0.165 ± 0.023b	75.47 ± 5.48b

*Different letters within the same column indicate significant differences ($p \geq 0.05$).

3.4. ATR-FTIR Analysis

ATR-FTIR analysis was carried out in order to detect changes in the bioactive molecule during the encapsulation process. β-carotene-loaded CG capsules produced with emulsion ratios 80:20 and 90:10 (v/v), neat CG capsules, β-carotene, and castor oil were analyzed by ATR-FTIR. The CG spectrum showed a broad band at 3300 cm^{-1} due to the stretching vibration of O-H, a small peak at 2912 cm^{-1}, attributed to the C-H stretching vibration, an absorption peak at 1635 cm^{-1}, due to O-H vibrations from bound water molecules, and a band at ca. 1620 cm^{-1}, attributed to the carboxylate group. The peaks at 1137, 1060 and 1010 cm^{-1} were due to stretching vibrations of C-O-C from glycosidic bonds and O-H bending of alcohols (da Silva, Feitosa, Paula, & de Paula, 2009; Silva et al., 2018), as shown in Fig. 3c. β-carotene showed bands at 1442 and 1367 cm^{-1}, attributed to the – CH stretch of the alkene (Niu, Shao, Feng, Qiu, & Sun, 2020) (Fig. 3d). Castor oil showed a wide band at 3450 cm^{-1} for hydroxyl groups, 2920 and 2850 cm^{-1} for CH_2 and CH_3 scissoring, 1743 cm^{-1} for C-O ester groups, 1711 cm^{-1} for the stretching of C-O in free fatty acids, 1281 cm^{-1} for asymmetric C-O stretching, and 1413 and 941 cm^{-1} for O-H bending vibrations (Alves, Maia, Fernandes, Feitosa, & de Sant'Ana, 2020; Khaskheli et al., 2015).

β-carotene-loaded CG capsules produced with emulsion ratios 80:20 and 90:10 (v/v) (Fig. 3a and 3b) showed peaks at 2920, 2850 cm^{-1} (peak 1), and a peak at 1740 cm^{-1} (peak 2), attributed to the presence of castor oil, and characteristic peaks of CG around 1000 cm^{-1}, as shown in Fig. 3c. We could not identify peaks of β-carotene in the electrosprayed capsules, since the main absorption bands of the β-carotene were masked by the main bands of the castor oil, and CG. However, the presence of β-carotene in the capsules can be indirectly inferred from the presence of the castor oil in which it was dissolved.

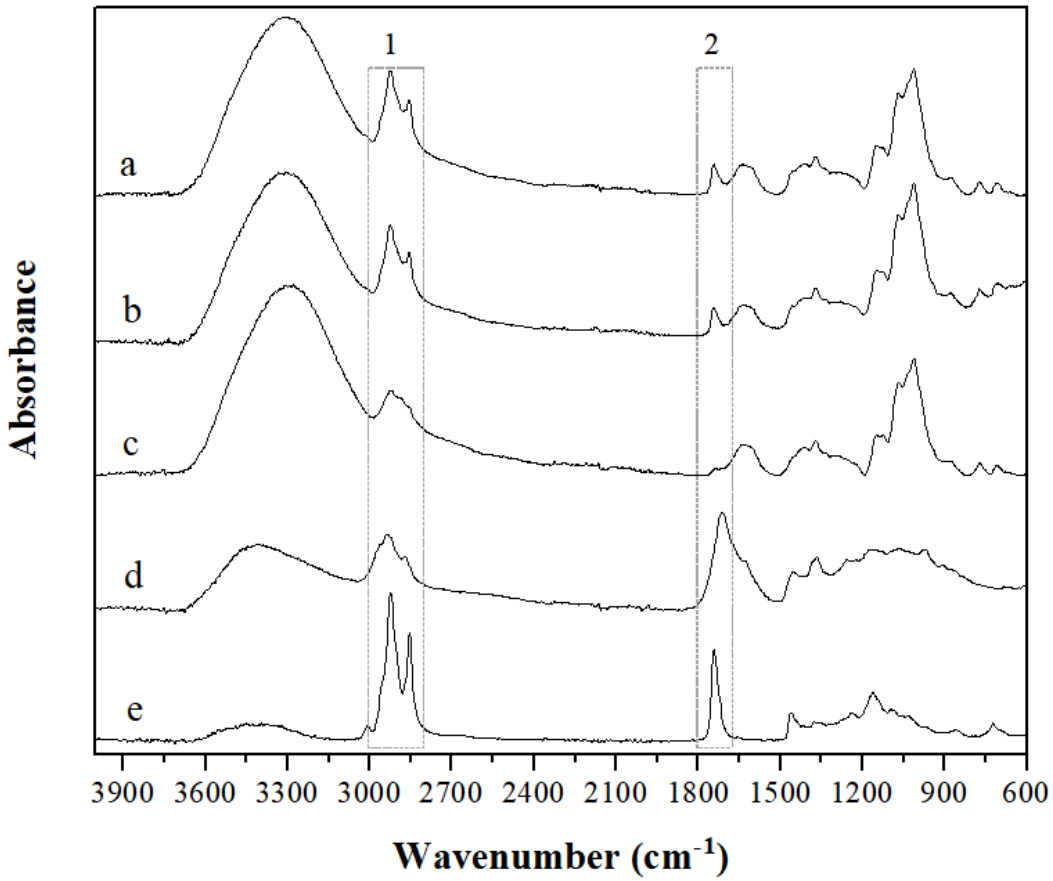

Fig. 3. ATR-FTIR spectra of a) and b) CG capsules with β-carotene (emulsion ratio, 80:20 (v/v), and 90:10 (v/v), respectively), c) neat CG capsules, d) pure β-carotene, and e) pure castor oil. Peaks 1 and 2 are attributed to the presence of castor oil in the β-carotene-loaded CG capsules.

3.5. Thermogravimetric analysis

For the evaluation of the thermoprotective effect of CG on the β-carotene-loaded electrosprayed particles, thermogravimetric analysis at different storage temperatures was performed. Results of this analysis are shown in Fig. 4. β-carotene showed an important mass loss around 70% between 130 °C and 450 °C (Fig. 4d). Similar observation was reported by Ramos-Hernández et al. (Ramos-Hernández et al., 2018), Cruz-Salas et al. (Cruz-Salas, Prieto, Calderón-Santoyo, Lagaron, & Ragazzo-Sánchez, 2019), and Rostamabadi et al. (Rostamabadi, Sadeghi Mahoonak, Allafchian, & Ghorbani, 2019). CG capsules showed three weight loss steps as shown in Fig. 4c. The first weight loss step between 31 and 120 °C of 10 % could correspond to the desorption of moisture of the polysaccharide; the second of 27% between 200 and 276 °C and the third of 43 % between 276 and 376 °C were due to depolymerization of CG into water, CO_2, and CH_4 as demonstrated by Klein et al. (Klein et al., 2018) during the preparation of CG-based flocculants by microwave- and ultrasound-assisted methods. β-carotene-loaded CG capsules produced with emulsion ratios 80:20 and 90:10 (v/v) showed three similar weight loss steps (Fig. 4a, and 4b, respectively). The capsules prepared with emulsion ratios 80:20 (v/v) and 90:10 (v/v) in the second weight loss step showed a lower mass loss of 19 %, and 23 %, respectively in comparison with the neat CG capsules (Fig. 4c). In addition, the weight loss step at 130 °C was not observed. In other words, the CG maintained the thermal stability of β-carotene, since both β-carotene-loaded capsules started the decomposition at 200 °C. This thermal protection could be due to high inorganic composition of the polymer as observed by Olorunsola et al. (Olorunsola, Bhatia, Tytler, & Adikwu, 2016), who demonstrated that the CG contains Na^+, K^+, Mg^+, Ca^+, and Cu^+.

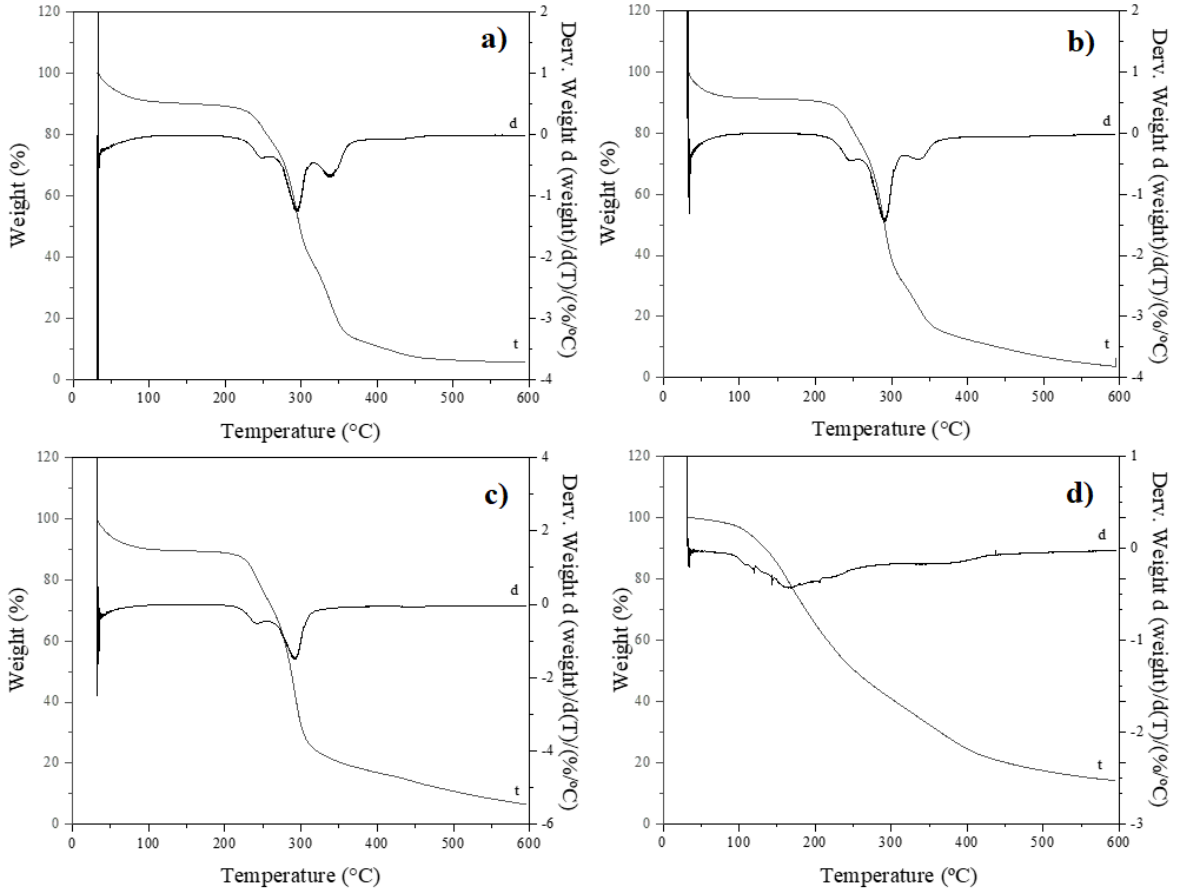

Fig. 4. Thermogravimetric analysis of a) and b) β-carotene-loaded CG capsules produced with emulsion ratios 80:20 and 90:10 (v/v), respectively), c) neat CG capsules, and d) pure β-carotene. Curve t represents the thermogram, and curve d represents the thermogram derivative.

3.6. Stability of β-carotene-loaded cashew gum capsules against photooxidation

β-carotene is a well-known natural compound that is highly unstable in the presence of light (Gutiérrez et al., 2013); therefore, it is an excellent model to evaluate the photoprotective properties of CG. In this study, the photooxidation rate of pure β-carotene and β-carotene-loaded capsules prepared with the emulsion ratio 90:10 (v/v) were compared. This emulsion formulation was selected because of the improved characteristics of the capsules. Results of the study are shown in Fig. 5. While 95 % of pure β-carotene was degraded after 75 min of UV light exposure, β-carotene-loaded capsules showed a 45 % degradation. The pattern observed for the degradation of the β-carotene in the capsules was related to the degradation

of the cashew gum under the UV light. This phenomenon was corroborated by ATR-FTIR (results not shown), where an increase in the intensity of the characteristic band at ca. 1620 cm^{-1}, attributed to the carboxylate group and due to cashew gum degradation (Cunha, Maciel, Sierakowski, Paula, & Feitosa, 2007), was observed at the same time points where a decrease in concentration of β-carotene was observed. The degradation of the polysaccharide could leave β-carotene unprotected and favor its UV degradation.

These UV stability results corroborated our finding that CG encapsulation via electrospraying can provide some stability to highly light-sensitive compounds. Other encapsulating materials such as whey protein concentrate (Basar et al., 2020) or polysaccharides such as high molecular weight agave fructans (Cruz-Salas et al., 2019; Ramos-Hernández et al., 2018) demonstrated the ability of providing larger photostability to β-carotene. However, the CG polysaccharide did not show absorption in the range of UVA (320-400 nm) and UVB (290-320 nm) which reduced its capacity as photoprotective wall material (Jesumami, Du, Pei, Aslam, & Huang, 2020). Nevertheless, even if small, this protection could be useful for some food, pharmaceutical or post-harvest agricultural applications.

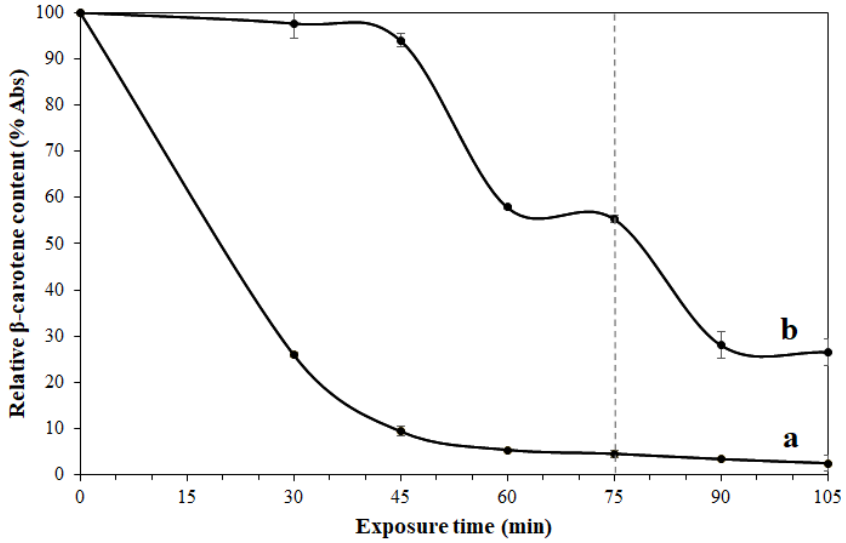

Fig. 5. Relative β-carotene content after of different exposure time to UV, a) β-carotene and b) CG microcapsules with β-carotene (emulsion ratio 90:10 (v/v)).

4. Conclusions

To the best of our knowledge, this is the first report of the use of CG as a wall material to achieve encapsulation using electrohydrodynamic processing. The CG capsules and the β-

carotene-loaded capsules produced with emulsion ratios of 80:20 and 90:10 (v/v) showed completely spherical morphology and smooth surfaces without cracks and breaks, with sizes between 3 and 6 μm. The capsules obtained via emulsion electrospraying at room temperature demonstrated high retention ability of the encapsulated compound as well as thermal and photoprotection. These favorable results make CG microcapsules produced by the electrospray technique a viable candidate as protective matrix to be used in the food and pharmaceutical industry. The low cost and ready availability of CG as a wall material along with other positive properties such as its biocompatibility, natural origin and high bioavailability make this polysaccharide a promising material for future investigations regarding encapsulation of different bioactive compounds and for possible industrial applications.

Author Contributions: Conceptualization by A.B. and J.M.L.; methodology, validation, and formal analysis was carried out by Y.V.G., M.F.F., C.P., and J.M.L.; investigation, resources, data curation, writing—original draft preparation and writing—review and editing was performed by Y.V.G., M.F.F., C.P., M.C.S., J.A.R.S., R.F.F., H.N.C., and J.M.L.; visualization, supervision, project administration, funding acquisition was carried out by A.B. and J.M.L

Funding: This study was supported in part by an OECD Co-operative Research Programme fellowship (A.B.), the H2020 EU FODIAC project (reference number 778388), and the H2020 EU project CAPSULTEK (reference number 873827), the CYTED thematic network code 319RT0576.

Acknowledgments: Yuliana Vázquez González thank Consejo Nacional de Ciencia y Tecnología for the scholarship awarded with number 862248, Mert F. Filizoglu acknowledges the EIT fellowship. The authors would also like to thank Milan Stojanovic for his collaboration editing this document. A. Biswas acknowledges the receipt of a fellowship from the OECD Co-operative Research Programme: Biological Resource Management for Sustainable Agricultural Systems in 2019. This work was supported in part by the U.S. Department of Agriculture, Agricultural Research Service. Mention of trade names or commercial products is solely for the purpose of providing specific information and does not

imply recommendation or endorsement by USDA. USDA is an equal opportunity provider and employer.

Conflicts of Interest: The authors declare no conflict of interest.

References

Abreu, C. M. W. S., Paula, H. C. B., Seabra, V., Feitosa, J. P. A., Sarmento, B., & de Paula, R. C. M. (2016). Synthesis and characterization of non-toxic and thermo-sensitive poly(N-isopropylacrylamide)-grafted cashew gum nanoparticles as a potential epirubicin delivery matrix. Carbohydrate Polymers, 154, 77-85. doi:https://doi.org/10.1016/j.carbpol.2016.08.031

Aceituno-Medina, M., Mendoza, S., Lagaron, J. M., & López-Rubio, A. (2015). Photoprotection of folic acid upon encapsulation in food-grade amaranth (Amaranthus hypochondriacus L.) protein isolate – Pullulan electrospun fibers. LWT - Food Science and Technology, 62(2), 970-975. doi:https://doi.org/10.1016/j.lwt.2015.02.025

Alves, R. S., Maia, D. L. H., Fernandes, F. A. N., Feitosa, F. X., & de Sant'Ana, H. B. (2020). Synthesis and application of castor oil maleate and castor oil maleate-styrene copolymers as demulsifier for water-in-oil emulsions. Fuel, 269, 117429. doi:https://doi.org/10.1016/j.fuel.2020.117429

Anwar, S. H., & Kunz, B. (2011). The influence of drying methods on the stabilization of fish oil microcapsules: Comparison of spray granulation, spray drying, and freeze drying. Journal of Food Engineering, 105(2), 367-378. doi:https://doi.org/10.1016/j.jfoodeng.2011.02.047

Basar, A. O., Prieto, C., Durand, E., Villeneuve, P., Sasmazel, H. T., & Lagaron, J. (2020). Encapsulation of β-Carotene by Emulsion Electrospraying Using Deep Eutectic Solvents. Molecules, 25(4). doi:10.3390/molecules25040981

Botrel, D. A., Borges, S. V., Fernandes, R. V. d. B., Antoniassi, R., de Faria-Machado, A. F., Feitosa, J. P. d. A., & de Paula, R. C. M. (2017). Application of cashew tree gum on the production and stability of spray-dried fish oil. Food Chemistry, 221, 1522-1529. doi:https://doi.org/10.1016/j.foodchem.2016.10.141

Botrel, D. A., Borges, S. V., Yoshida, M. I., Feitosa, J. P. d. A., Fernandes, R. V. d. B., de Souza, H. J. B., & de Paula, R. C. M. (2017). Properties of spray-dried fish oil with different carbohydrates as carriers. Journal of food science and technology, 54(13), 4181-4188. doi:10.1007/s13197-017-2877-0

Busolo, M. A., Torres-Giner, S., Prieto, C., & Lagaron, J. M. (2019). Electrospraying assisted by pressurized gas as an innovative high-throughput process for the microencapsulation and stabilization of docosahexaenoic acid-enriched fish oil in zein prolamine. Innovative Food Science & Emerging Technologies, 51, 12-19. doi:https://doi.org/10.1016/j.ifset.2018.04.007

Cabrera-Trujillo, M. A., Filomena-Ambrosio, A., Quintanilla-Carvajal, M. X., & Sotelo-Díaz, L. I. (2018). Stability of low-fat oil in water emulsions obtained by ultra turrax, rotor-stator and ultrasound homogenization methods. International Journal of Gastronomy and Food Science, 13, 58-64. doi:https://doi.org/10.1016/j.ijgfs.2018.06.002

Cai, Y., Deng, X., Liu, T., Zhao, M., Zhao, Q., & Chen, S. (2018). Effect of xanthan gum on walnut protein/xanthan gum mixtures, interfacial adsorption, and emulsion properties. Food Hydrocolloids, 79, 391-398. doi:https://doi.org/10.1016/j.foodhyd.2018.01.006

Carvalho da Silva, L., Alves do Nascimento, M., Guabiraba Mendes, L., Ferro Furtado, R., Correia da Costa, J. M., & Luiz Herzog Cardoso, A. (2018). Optimization of cashew gum and chitosan for microencapsulation of pequi oil by complex coacervation. Journal of Food Processing and Preservation, 42(3), e13538. doi:10.1111/jfpp.13538

Cruz-Salas, C. N., Prieto, C., Calderón-Santoyo, M., Lagarón, J. M., & Ragazzo-Sánchez, J. A. (2019). Micro- and Nanostructures of Agave Fructans to Stabilize Compounds of High Biological Value via Electrohydrodynamic Processing. Nanomaterials (Basel, Switzerland), 9(12), 1659. doi:10.3390/nano9121659

Cunha, P., Paula, R., & Feitosa, J. (2009). Polissacarídeos da biodiversidade brasileira: UMA oPortunidade de transformar conhecimento em valor econômico. Quimica Nova - QUIM NOVA, 32. doi:10.1590/S0100-40422009000300009

Cunha, P. L. R., Maciel, J. S., Sierakowski, M. R., Paula, R. C. M. d., & Feitosa, J. P. A. (2007). Oxidation of cashew tree gum exudate polysaccharide with TEMPO reagent. Journal of the Brazilian Chemical Society, 18, 85-92.

da Silva, D. A., Feitosa, J. P. A., Paula, H. C. B., & de Paula, R. C. M. (2009). Synthesis and characterization of cashew gum/acrylic acid nanoparticles. Materials Science and Engineering: C, 29(2), 437-441. doi:https://doi.org/10.1016/j.msec.2008.08.029

da Silva, D. P. B., Florentino, I. F., da Silva Moreira, L. K., Brito, A. F., Carvalho, V. V., Rodrigues, M. F., . . . Costa, E. A. (2018). Chemical characterization and pharmacological assessment of polysaccharide free, standardized cashew gum extract (Anacardium

occidentale L.). Journal of Ethnopharmacology, 213, 395-402. doi:https://doi.org/10.1016/j.jep.2017.11.021

Das, B., Dutta, S., Nayak, A. K., & Nanda, U. (2014). Zinc alginate-carboxymethyl cashew gum microbeads for prolonged drug release: Development and optimization. International Journal of Biological Macromolecules, 70, 506-515. doi:https://doi.org/10.1016/j.ijbiomac.2014.07.030

de Freitas Zômpero, R. H., López-Rubio, A., de Pinho, S. C., Lagaron, J. M., & de la Torre, L. G. (2015). Hybrid encapsulation structures based on β-carotene-loaded nanoliposomes within electrospun fibers. Colloids and Surfaces B: Biointerfaces, 134, 475-482. doi:https://doi.org/10.1016/j.colsurfb.2015.03.015

de Paula, R. C. M., & Rodrigues, J. F. (1995). Composition and rheological properties of cashew tree gum, the exudate polysaccharide from Anacardium occidentale L. Carbohydrate Polymers, 26(3), 177-181. doi:https://doi.org/10.1016/0144-8617(95)00006-S

Dias, S. F. L., Nogueira, S. S., de França Dourado, F., Guimarães, M. A., de Oliveira Pitombeira, N. A., Gobbo, G. G., . . . da Silva, D. A. (2016). Acetylated cashew gum-based nanoparticles for transdermal delivery of diclofenac diethyl amine. Carbohydrate Polymers, 143, 254-261. doi:https://doi.org/10.1016/j.carbpol.2016.02.004

Echegoyen, Y., Fabra, M. J., Castro-Mayorga, J. L., Cherpinski, A., & Lagaron, J. M. (2017). High throughput electro-hydrodynamic processing in food encapsulation and food packaging applications: Viewpoint. Trends in Food Science & Technology, 60, 71-79. doi:https://doi.org/10.1016/j.tifs.2016.10.019

Fernandes, R. V. d. B., Botrel, D. A., Silva, E. K., Borges, S. V., Oliveira, C. R. d., Yoshida, M. I., . . . de Paula, R. C. M. (2016). Cashew gum and inulin: New alternative for ginger essential oil microencapsulation. Carbohydrate Polymers, 153, 133-142. doi:https://doi.org/10.1016/j.carbpol.2016.07.096

Fernandez, A., Torres-Giner, S., & Lagaron, J. M. (2009). Novel route to stabilization of bioactive antioxidants by encapsulation in electrospun fibers of zein prolamine. Food Hydrocolloids, 23(5), 1427-1432. doi:https://doi.org/10.1016/j.foodhyd.2008.10.011

Flaxbart, D. (1999). Kirk-Othmer Encyclopedia of Chemical Technology, Fourth Edition, 27-Volume Set Wiley Interscience; New York, 1992-1998. ISBN 0-471-52704-1. In J. o. t. A. C. Society (Ed.), (Vol. 121, pp. 2339): American Chemical Society.

Ghorani, B., & Tucker, N. (2015). Fundamentals of electrospinning as a novel delivery vehicle for bioactive compounds in food nanotechnology. Food Hydrocolloids, 51, 227-240. doi:https://doi.org/10.1016/j.foodhyd.2015.05.024

Gómez-Mascaraque, L., Ambrosio-Martín, J., Fabra, M., Perez-Masia, R., & López-Rubio, A. (2016). Novel nanoencapsulation structures for functional foods and nutraceutical applications (pp. 373-395).

Gómez-Mascaraque, L. G., & López-Rubio, A. (2016). Protein-based emulsion electrosprayed micro- and submicroparticles for the encapsulation and stabilization of thermosensitive hydrophobic bioactives. Journal of Colloid and Interface Science, 465, 259-270. doi:https://doi.org/10.1016/j.jcis.2015.11.061

Gutiérrez, F. J., Albillos, S. M., Casas-Sanz, E., Cruz, Z., García-Estrada, C., García-Guerra, A., . . . Mussons, M.-L. (2013). Methods for the nanoencapsulation of β-carotene in the food sector. Trends in Food Science & Technology, 32(2), 73-83. doi:https://doi.org/10.1016/j.tifs.2013.05.007

Jaworek, A. (2007). Electrospray droplet sources for thin film deposition. Journal of Materials Science, 42(1), 266-297. doi:10.1007/s10853-006-0842-9

Jaworek, A., & Sobczyk, A. T. (2008). Electrospraying route to nanotechnology: An overview. Journal of Electrostatics, 66(3), 197-219. doi:https://doi.org/10.1016/j.elstat.2007.10.001

Jesumani, V., Du, H., Pei, P., Aslam, M., & Huang, N. (2020). Comparative study on skin protection activity of polyphenol-rich extract and polysaccharide-rich extract from Sargassum vachellianum. PLOS ONE, 15(1), e0227308. doi:10.1371/journal.pone.0227308

Khaskheli, A. A., Talpur, F. N., Ashraf, M. A., Cebeci, A., Jawaid, S., & Afridi, H. I. (2015). Monitoring the Rhizopus oryzae lipase catalyzed hydrolysis of castor oil by ATR-FTIR spectroscopy. Journal of Molecular Catalysis B: Enzymatic, 113, 56-61. doi:https://doi.org/10.1016/j.molcatb.2015.01.002

Klein, J. M., de Lima, V. S., da Feira, J. M. C., Camassola, M., Brandalise, R. N., & Forte, M. M. d. C. (2018). Preparation of cashew gum-based flocculants by microwave- and ultrasound-assisted methods. International Journal of Biological Macromolecules, 107, 1550-1558. doi:https://doi.org/10.1016/j.ijbiomac.2017.09.118

Kumari, A., Yadav, S. K., Pakade, Y. B., Singh, B., & Yadav, S. C. (2010). Development of biodegradable nanoparticles for delivery of quercetin. Colloids and Surfaces B: Biointerfaces, 80(2), 184-192. doi:https://doi.org/10.1016/j.colsurfb.2010.06.002

Leite, Á. J., Costa, R. R., Costa, A. M. S., Maciel, J. S., Costa, J. F. G., de Paula, R. C. M., & Mano, J. F. (2017). The potential of cashew gum functionalization as building blocks for layer-by-layer films. Carbohydrate Polymers, 174, 849-857. doi:https://doi.org/10.1016/j.carbpol.2017.06.055

Librán, C. M., Castro, S., & Lagaron, J. M. (2017). Encapsulation by electrospray coating atomization of probiotic strains. Innovative Food Science & Emerging Technologies, 39, 216-222. doi:https://doi.org/10.1016/j.ifset.2016.12.013

Lima Cardial, M. R., Paula, H. C. B., da Silva, R. B. C., da Silva Barros, J. F., Richter, A. R., Sombra, F. M., & de Paula, R. C. M. (2019). Pickering emulsions stabilized with cashew gum nanoparticles as indomethacin carrier. International Journal of Biological Macromolecules, 132, 534-540. doi:https://doi.org/10.1016/j.ijbiomac.2019.03.198

Lin, T., Wang, H., Wang, H., & Wang, X. (2004). The charge effect of cationic surfactants on the elimination of fibre beads in the electrospinning of polystyrene. Nanotechnology, 15(9), 1375-1381. doi:10.1088/0957-4484/15/9/044

Manee-in, J., Nithitanakul, M., & Supaphol, P. (2006). Effects of Solvent Properties, Solvent System, Electrostatic Field Strength, and Inorganic Salt Addition on Electrospun Polystyrene Fibres. Iranian Polymer Journal (English Edition), 15.

Melo, A. M. A., Oliveira, M. R. F., Furtado, R. F., de Fatima Borges, M., Biswas, A., Cheng, H. N., & Alves, C. R. (2020). Preparation and characterization of carboxymethyl cashew gum grafted with immobilized antibody for potential biosensor application. Carbohydrate Polymers, 228, 115408. doi:https://doi.org/10.1016/j.carbpol.2019.115408

Mothé, C., Souza, I., & Calazans, G. (2008). Antitumor activity of cashew gum from Anacardium Occidentale L. Agro Food Industry Hi Tech, 19.

Nedovic, V., Kalusevic, A., Manojlovic, V., Levic, S., & Bugarski, B. (2011). An overview of encapsulation technologies for food applications. Procedia Food Science, 1, 1806-1815. doi:https://doi.org/10.1016/j.profoo.2011.09.265

Nicolau, L. A. D., Batista-Lima, F. J., Santana, A. P. M., Sales, T. M. A. L., Carmo-Neto, J. P., Freitas, G. B., . . . Souza, M. H. L. P. (2019). Cashew gum, a biopolymer, topically protects oesophageal mucosa in non erosive reflux disease: A promising translational study. Carbohydrate Polymers, 226, 115205. doi:https://doi.org/10.1016/j.carbpol.2019.115205

Niu, B., Shao, P., Feng, S., Qiu, D., & Sun, P. (2020). Rheological aspects in fabricating pullulan-whey protein isolate emulsion suitable for electrospraying: Application in improving β-carotene stability. LWT, 129, 109581. doi:https://doi.org/10.1016/j.lwt.2020.109581

Olorunsola, E. O., Bhatia, P. G., Tytler, B. A., & Adikwu, M. U. (2016). Thermochemical Properties of Hydrophilic Polymers from Cashew and Khaya Exudates and Their Implications on Drug Delivery. Journal of Drug Delivery, 2016, 7496585. doi:10.1155/2016/7496585

OSRAM. OSRAM ultra-vitalux. Retrieved from https://www.osram.com/pia/ecat/ULTRA-VITALUXUltraviolet%20lamps-Specialty%20lamps/com/en/GPS01_1028569/PP_EUROPE_Europe_eCat/ZMP_60829/

Pérez-Masiá, R., López-Nicolás, R., Periago, M. J., Ros, G., Lagaron, J. M., & López-Rubio, A. (2015). Encapsulation of folic acid in food hydrocolloids through nanospray drying and electrospraying for nutraceutical applications. Food Chemistry, 168, 124-133. doi:https://doi.org/10.1016/j.foodchem.2014.07.051

Porto, B. C., & Cristianini, M. (2018). Effect of dynamic high pressure on emulsifying and encapsulant properties of cashew tree gum. Carbohydrate Polymers, 186, 350-357. doi:https://doi.org/10.1016/j.carbpol.2018.01.019

Ramos-Hernández, J. A., Ragazzo-Sánchez, J. A., Calderón-Santoyo, M., Ortiz-Basurto, R. I., Prieto, C., & Lagaron, J. M. (2018). Use of Electrosprayed Agave Fructans as Nanoencapsulating Hydrocolloids for Bioactives. Nanomaterials (Basel, Switzerland), 8(11), 868. doi:10.3390/nano8110868

Rezaeinia, H., Ghorani, B., Emadzadeh, B., & Tucker, N. (2019). Electrohydrodynamic atomization of Balangu (Lallemantia royleana) seed gum for the fast-release of Mentha longifolia L. essential oil: Characterization of nano-capsules and modeling the kinetics of release. Food Hydrocolloids, 93, 374-385. doi:https://doi.org/10.1016/j.foodhyd.2019.02.018

Rostamabadi, H., Sadeghi Mahoonak, A., Allafchian, A., & Ghorbani, M. (2019). Fabrication of β-carotene loaded glucuronoxylan-based nanostructures through electrohydrodynamic processing. International Journal of Biological Macromolecules, 139, 773-784. doi:https://doi.org/10.1016/j.ijbiomac.2019.07.182

Shenoy, S. L., Bates, W. D., Frisch, H. L., & Wnek, G. E. (2005). Role of chain entanglements on fiber formation during electrospinning of polymer solutions: good solvent, non-specific polymer–polymer interaction limit. Polymer, 46(10), 3372-3384. doi:https://doi.org/10.1016/j.polymer.2005.03.011

Silva, B. D. S., Ulhoa, C. J., Batista, K. A., Di Medeiros, M. C., Filho, R. R. d. S., Yamashita, F., & Fernandes, K. F. (2012). Biodegradable and bioactive CGP/PVA film for fungal growth inhibition. Carbohydrate Polymers, 89(3), 964-970. doi:https://doi.org/10.1016/j.carbpol.2012.04.052

Silva, F., Torres, L., Silva, L., Figueiredo, R., Garruti, D., Araújo, T., . . . Ricardo, N. (2018). Cashew gum and maltrodextrin particles for green tea (Camellia sinensis var Assamica) extract encapsulation. Food Chemistry, 261, 169-175. doi:https://doi.org/10.1016/j.foodchem.2018.04.028

Silva, F. E. F., Batista, K. A., Di-Medeiros, M. C. B., Silva, C. N. S., Moreira, B. R., & Fernandes, K. F. (2016). A stimuli-responsive and bioactive film based on blended polyvinyl alcohol and cashew gum polysaccharide. Materials Science and Engineering: C, 58, 927-934. doi:https://doi.org/10.1016/j.msec.2015.09.064

Sobel, R., Versic, R., & Gaonkar, A. G. (2014). Chapter 1 - Introduction to Microencapsulation and Controlled Delivery in Foods. In A. G. Gaonkar, N. Vasisht, A. R. Khare, & R. Sobel (Eds.), Microencapsulation in the Food Industry (pp. 3-12). San Diego: Academic Press.

Souza Filho, M. D., Medeiros, J. V. R., Vasconcelos, D. F. P., Silva, D. A., Leódido, A. C. M., Fernandes, H. F., . . . Pinto, G. R. (2018). Orabase formulation with cashew gum polysaccharide decreases inflammatory and bone loss hallmarks in experimental periodontitis. International Journal of Biological Macromolecules, 107, 1093-1101. doi:https://doi.org/10.1016/j.ijbiomac.2017.09.087

Tadros, T. (2015). Viscoelastic properties of sterically stabilised emulsions and their stability. Advances in Colloid and Interface Science, 222, 692-708. doi:https://doi.org/10.1016/j.cis.2015.03.001

Torres-Giner, S., Martinez-Abad, A., Ocio, M. J., & Lagaron, J. M. (2010). Stabilization of a Nutraceutical Omega-3 Fatty Acid by Encapsulation in Ultrathin Electrosprayed Zein Prolamine. Journal of Food Science, 75(6), N69-N79. doi:10.1111/j.1750-3841.2010.01678.x

Valencia, G. A., Zare, E. N., Makvandi, P., & Gutiérrez, T. J. (2019). Self-Assembled Carbohydrate Polymers for Food Applications: A Review. Comprehensive Reviews in Food Science and Food Safety, 18(6), 2009-2024. doi:10.1111/1541-4337.12499

Vasconcelos Silva, E. d. L., Oliveira, A. C. d. J., Patriota, Y. B. G., Ribeiro, A. J., Veiga, F., Hallwass, F., . . . Soares-Sobrinho, J. L. (2019). Solvent-free synthesis of acetylated cashew gum for oral delivery system of insulin. Carbohydrate Polymers, 207, 601-608. doi:https://doi.org/10.1016/j.carbpol.2018.11.071

Yang, J., Han, S., Zheng, H., Dong, H., & Liu, J. (2015). Preparation and application of micro/nanoparticles based on natural polysaccharides. Carbohydrate Polymers, 123, 53-66. doi:https://doi.org/10.1016/j.carbpol.2015.01.029

7.2. Preparación y caracterización de nanofibras de FucoPol mediante *electrospinning*

Los resultados correspondientes a la etapa 2 de este proyecto de tesis están contenidos en la siguiente publicación:

Preparation and Characterization of Electrospun Polysaccharide FucoPol-Based Nanofiber Systems

Vázquez-González, Y., Prieto, C., Stojanovic, M., Torres, C. A., Freitas, F., Ragazzo-Sánchez, J.A., Calderón-Santoyo, M., Lagaron, J.M.

Nanomaterials, 12 (2022) 498, DOI: 10.3390/nano12030498

Factor de impacto (2022): 5.3

Número de citas: 9

7.2.1. Introducción al tema

Las nanofibras electrohiladas muestran múltiples ventajas ya que son estructuras con una gran superficie-volumen, porosidad controlable, además pueden aumentar la estabilidad y la biodisponibilidad de los compuestos bioactivos, y proporcionar su liberación controlada. Los materiales de pared para generar este tipo de nanoestructuras pueden ser seleccionados de entre una amplia variedad de polímeros naturales o sintéticos. Los polisacáridos han demostrado propiedades fisicoquímicas únicas y, además, excelente biocompatibilidad. Estos pueden ser de origen vegetal como almidón, celulosa, pectina, gomas, y quitosano, entre otros, de origen animal como gelatina, quitina y quitosano, entre otros, o de origen microbiano generalmente conocidos como exopolisacáridos, como por ejemplo alginato, pululano, gelano y FucoPol, los cuales son biopolímeros producidos por bacterias u hongos filamentosos que están compuestos principalmente por carbohidratos y son altamente solubles en agua, no son tóxicos y generalmente de alto peso molecular.

FucoPol es un exopolisacárido producido por la bacteria *Enterobacter* A47, está compuesto por fucosa, galactosa, glucosa y ácido glucurónico, así como grupos acilo (piruvato, succinato y acetato), es de carácter aniónico y presenta propiedades funcionales interesantes (emulsificante, formador de película, floculante, actividad antitumoral y antiinflamatoria, así como propiedades adhesivas y fotoprotectoras). Por lo que surge el interés de evaluar este exopolisacárido como material formador de nanofibras para su posible aplicación en envases alimentarios, industria alimentaria, agricultura, biomedicina, farmacia, y aplicaciones cosméticas.

En este sentido, el objetivo de esta investigación fue estudiar por primera vez la posibilidad de producir fibras de FucoPol mediante *electrospinning*. Para llevar a cabo este objetivo se prepararon disoluciones de FucoPol a una concentración de 0.015 g/mL y para mejorar la formación de las fibras de FucoPol se mezcló con polímeros electrohilables conocidos, como pululano y óxido de polietileno en diferentes ratios. Todas las disoluciones preparadas, fueron caracterizadas fisicoquímicamente. Posterior a ello, las disoluciones fueron procesadas en un equipo de *electrospray* LE-10. Finalmente, las estructuras obtenidas se caracterizaron mediante SEM, FTIR-ATR, Calorimetría Diferencial de Barrido (DSC), TGA y Dispersión de Rayos X de Gran Angular (WAXS).

FucoPol, cuando estaba solo en las disoluciones, fue incapaz de formar fibras mediante *electrospinning*, esto debido a la baja solubilidad en agua y a sus bajos enredos moleculares. Sin embargo, cuando FucoPol se encontraba en mezcla con PEO o pululano, fue factible la obtención de las nanofibras. La solución de FucoPol:PEO mostró fibras con estructura cilíndrica bien definida. Los análisis WAXS, DSC and TGA mostraron que FucoPol es un biopolímero amorfo estable hasta 220 ºC, mientras que las fibras de FucoPol:PEO y FucoPol:pululano fueron estables hasta los 140 ºC y los 130 ºC, respectivamente. Mediante WAXS se observaron nuevos picos asociados a conjuntos jerárquicos intermoleculares generados por los componentes de las nanofibras.

De forma inesperada, los componentes de la mezcla influyeron entre sí en el orden intermolecular, ya que WAXS para FucoPol reveló nuevos picos adscritos a conjuntos jerárquicos intermoleculares.

De acuerdo con los resultados obtenidos, este estudio abre una nueva línea de investigación sobre las posibles aplicaciones de las fibras electrohiladas de FucoPol en diferentes sectores.

En esta tesis, el conocimiento obtenido se empleó para la encapsulación de la levadura *M. caribbica* en nanofibras electroestiradas de FucoPol para ser empleadas como tratamiento antifúngico en aguacates, objetivo correspondiente a la etapa 3 y la etapa 4.

Electrospun antifungal nanofibers from innovative biopolymers

Yuliana Vázquez-González[1,2], Cristina Prieto[1,*], Milan Stojanovic, Cristiana A.V. Torres, Filomena Freitas, Juan Arturo Ragazzo-Sánchez, Montserrat Calderón-Santoyo[2,*], José M. Lagarón[1,*].

[1] Novel Materials and Nanotechnology Group, Institute of Agrochemistry and Food Technology (IATA), Spanish Council for Scientific Research (CSIC), Calle Catedrático Agustín Escardino Benlloch 7, 46980 Paterna, Spain; cprieto@iata.csic.es (C.P.); lagaron@iata.csic.es (J.M.L.); yuliana.vg04@gmail.com (Y.V.-G)

[2] Laboratorio Integral de Investigación de Alimentos, Tecnológico Nacional de México - Instituto Tecnológico de Tepic, Av. Tecnológico de Tepic, Av. Tecnológico #2595, C.P. 63175, Tepic, Nayarit, México; yuliana.vg04@gnail.com (Y.V.-G); montserratcalder@gmail.com (M.C.-S); arturoragazzo@hotmail.com (J.A.R.-S).

[3] UCIBIO-REQUIMTE, Chemistry Department, Faculty of Sciences and Technology, NOVA University of Lisbon, Portugal; c.torres@fct.unl.pt (C.T.), filomenafreitas@fct.unl.pt (F.F.)

[†] On leave from the Department of Food Technology and Biochemistry, Faculty of Agriculture, University of Belgrade, Belgrade, Serbia; milan87stojanovic@gmail.com (M.S.)

* Correspondence: cprieto@iata.csic.es (C.P.), montserratcalder@gmail.com (M.C.S.) and lagaron@iata.csic.es (J.M.L.); Tel.: +34 963 900 022

*Corresponding author: mcalderon@tepic.tecnm.mx, cprieto@iata.csic.es and lagaron@iata.csic.es

Abstract: The electrospinnability of FucoPol, a bacterial exopolysaccharide, is presented for the first time, being evaluated alone and in combination with other polymers such as polyethylene oxide (PEO) and pullulan. The obtained fibers were characterized in terms of its morphological, structural and thermal properties. Pure FucoPol fibers could not be obtained due to its low water solubility and the lack of enough molecular entanglements. Nanofibers were obtained via blending with PEO and pullulan. FucoPol:PEO (1:3 w/w) showed fibers with well-defined cylindrical structure, since the higher molecular weight of PEO helps the continuity of the erupted jet towards the collector, hence forming stable fibers. WAXS, DSC and TGA showed that FucoPol is an amorphous biopolymer, stable until 220°C, whereas, FucoPol-PEO fibers were stable until 140°C and FucoPol:Pullulan fibers until 130°C. Interestingly, blending components influenced each other in the intermolecular order, since new peaks associated to intermolecular hierarchical assemblies were seen by WAXS. These results make FucoPol-based systems, viable candidates to produce nanofibers for packaging, agriculture, biomedicine, pharmacy, and cosmetic applications.

Keywords: FucoPol, exopolysaccharide, electrospinning process, nanofibers, characterization.

1. Introduction

Exopolysaccharides (EPS) are water-soluble, non-toxic, high-molecular-weight polymeric carbohydrate structures composed monosaccharide units joined together by glycosidic bonds [1]. EPS can be homopolysaccharides when composed of a single type of monosaccharide, for example, pullulan; or heteropolysaccharides if they are composed of two or more sugars with different ratios, such as FucoPol [2].

FucoPol is an EPS produced by *Enterobacter* A47, using glycerol as the sole carbon source [3]. It is a high molecular-weight (4.19×10^6–5.80×10^6 Da) heteropolysaccharide composed of sugar residues [fucose (32–36 mol %), galactose (25–26 mol %), glucose (28–34 mol %) and glucuronic acid (9–10 mol %)], as well as acyl groups [pyruvate (13–14 wt.%), succinate (3 wt.%) and acetate (3–5 wt.%)] [4]. It has an anionic character, with interesting functional properties, including emulsion, film-forming [5], thickening, and flocculating capacity; biological activity and adhesive photoprotective properties [6,7]. All these properties make FucoPol an interesting candidate for food packaging, agriculture, biomedicine, pharmacy, food and cosmetics applications. Hence, up to now, several research works have studied the potential of FucoPol. For instance, Lourenço et al. evaluated the ability of FucoPol to be used as encapsulation matrix of some bioactive compounds by spray drying [8]. Concordio-Reis et al. [9] studied the stabilization properties of FucoPol in the production of a FucoPol/AgNP biocomposite for wound-healing applications. Additionally, Ferreira et al. [10–13] studied the development of FucoPol films by casting. These films have shown to be transparent and hydrophilic, with high permeability to water vapor, but presented good barrier properties against oxygen and carbon dioxide. Electrohydrodynamic processes are commonly used for the formation of micro, submicro and nanostructures. This technology utilizes electrical forces to produce ultrathin fiber-based morphologies from different polymers (natural and synthetic) with diameters ranging from 2 nm to several micrometers. In the electrospinning process, a polymer solution in a capillary tube is subjected to an electric field [14,15]. When the applied electric field reaches a critical value, the repulsive electrical forces overcome the surface tension forces. Eventually, a charged jet of the solution is ejected from the tip of the Taylor cone, and an unstable and rapid whipping jet occurs in the space between the capillary tip and the collector, which leads to evaporation of the solvent at room temperature

[14,16,17]. The produced micro and nanostructures may offer many functional advantages, such as superior mechanical properties, flexibility, large surface-to-mass ratio, tailored morphology, tunable porosity and the capability of encapsulation and subsequent release of active and bioactive compounds [18–23]. In addition, mechanical properties, thermal stability, electrical conductivity, photocatalytic activity and bioactivity can be tuned by controlling the diameter [23]. These unique characteristics make electrospun micro and nanostructures attractive for novel applications in drug delivery, agriculture, food packaging, biomedical engineering, air filtration, energy production and storage, environmental protection and improvement, photonic and electronic devices [23,24]. To the best of our knowledge, the formation of non-woven FucoPol-based structures by electrospinning has not been reported yet. For this reason, the aim of this research was to study, for the first time, the possibility of producing FucoPol fibers via electrospinning, since the combination of characteristics of the electrospun fibers together with the interesting functional properties of FucoPol could be of great interest for potential applications in food packaging, agriculture, biomedicine, pharmaceutics, food and cosmetics, among others. The electrospinnability of FucoPol was characterized alone and in combination with well-known electrospinnable polymers, such as polyethylene oxide (PEO) and pullulan. The obtained fibers were characterized in terms of their morphological, structural, and thermal properties.

2. Materials and Methods

2.1. Materials

FucoPol (Mw ~ 4.4×10^6 Da) was provided by the Biochemical Engineering Group of Nova School of Sciences and Technology (Caparica, Portugal). FucoPol was produced and purified using the same procedures described by Ferreira et al. and Alves et al. [10,25]. The obtained FucoPol was characterized in terms of its chemical composition, as described by Alves et al. [25]. This heteropolysaccharide was composed of neutral sugars: fucose, galactose and glucose. The relative proportion of sugar monomers was 38% glucose, 25% fucose and 32% galactose. Regarding the content of acyl groups, it reached 12% of the polymer mass, with acetyl, pyruvil and succinyl groups in greatest abundance. The obtained sample also contained non-sugar contaminants, such as proteins and inorganic residues. The

protein content was 12 wt.%, and the total content of inorganic residues, determined by pyrolysis at 550 ◦C, was 32.5%. Regarding the purified polymer's average molecular weight and polydispersity index, they were determined by size-exclusion chromatography combined with multiple-angle laser light scattering (SEC-MALLS), as described in the work of Hilliou et al. [26]. The average molecular weight was around $1.1 \times 10^7 \pm 2.3 \times 10^5$ g/mol, with an average polydispersity index of 1.85 ± 0.14. Pullulan (Mw ~ 2×10^5 Da) was purchased from Hayashibara Co., Ltd. (Tokyo, Japan), and polyethylene oxide (PEO) (Mw ~ 100,000 Da), 2,2,2-trifluoroethanol and Span 20 were purchased from Sigma Aldrich (St. Louis, MO, USA). Absolute ethanol (EPR. Ph.Eur.) was obtained from Labkem (Vilassar de Dalt, Spain). Distillated water was used throughout the study.

2.2. Preparation and Characterization of Polymeric Solutions

Solutions of FucoPol were prepared with a concentration of 0.015 g/mL in distilled water, as well as in a mixture of ethanol:water (30:70 v/v) at the same concentration. Solubility tests were conducted in absolute ethanol and 2,2,2-trifluoroethanol; however, FucoPol was not soluble in these solvents (results not shown), and consequently, these formulations were not tested in electrospinning. After that, in order to improve the formation of fibers, blends with two well-known electrospinnable polymers were also studied, i.e., PEO and pullulan. Different ratios were studied to find the minimum amount of polymer of high molecular weight required to generate the molecular entanglements necessary to obtain the sought fibers. In order to reduce surface tension and to make the process more stable to obtain suitable fibers, ethanol–water solution (30:70 v/v) was used for the solutions with PEO and pullulan. The concentration of FucoPol in the solutions was maintained at 0.015 g/mL, and different ratios were explored, as shown in Table 1. Span 20 was used as a surfactant at a concentration of 3% (w/w). All formulations were proper solutions without solid residues.

Table 1. Polymer ratio employed for the preparation of the nanofibers via electrospinning. All solutions contained 3% of Span 20 as a surfactant.

FucoPol/PEO (w/w)	FucoPol/Pullulan (w/w)
3:1	3:1
2:1	2:1
1:0	1:0
0:1	0:1
1:2	1:2
1:3	1:3

Characterization of the solutions with the best electrospinning processing was made in terms of viscosity, conductivity, and surface tension. Viscosity was measured using a Visco Basic Plus L rotational viscometer (Fungilab S.A., Sant Feliu de Llobregat, Spain). Surface tension was determined in an Easy Dyne K20 tensiometer (Krüss GmbH, Hamburg, Germany) following the Wilhelmy plate method. Conductivity was measured using a conductivity meter (HI-4521 portable meter, Hanna Instruments, Gothenburg, Sweden). Measurements were taken in triplicate at room temperature.

2.3. Electrospinning Process

The electrospinning process was performed in a high-throughput Fluidnatek® LE-500 from Bioinicia S.L. (Valencia, Spain). The solutions of FucoPol in water and FucoPol in ethanol:water (30:70 v/v) were processed using different processing conditions in order to obtain fibers. The studied range of operation parameters was: flow rate between 250 and 500 µL/h, work distance between 15 and 30 cm, and voltage between 16 and 23 kV. Temperature and relative humidity (RH) were controlled at 35 °C and 28%, respectively.

2.4. Characterization of Electrospinning Fibers

2.4.1. Scanning Electron Microscopy (SEM)

The morphology of the obtained fibers was determined using a Hitachi-S-4800 FE-SEM scanning electron microscope (Hitachi High-Technologies Corporation, Tokyo, Japan) with an electron-beam acceleration of 10 kV. Approximately 1.5 mg of sample was placed using double-sided tape on the sample holder and coated with a gold-palladium layer. Fiber sizes were analyzed using Image J Launcher v1.41 software (National Institutes of Health, Bethesda, MD, USA). The presented data are based on measurements from a minimum of 100 fibers.

2.4.2. Attenuated Total Reflectance Fourier Transform Infrared Spectroscopy (ATR-FTIR)

To evaluate possible interactions between the different polymers that integrated the fibers, ATR-FTIR (Bruker FTIR Tensor 37 equipment, Rheinstetten, Germany) was used. The samples were placed on top of the diamond crystal, and appropriate contact was assured by using the Golden Gate low-temperature ATR sampling accessory (Specac Ltd., Orpington, UK). All spectra were obtained within the wavenumber range of 4000–600 cm^{-1} by averaging 10 scans at 4 cm^{-1} resolution. Analysis of spectral data was carried out using Origin Pro, Version 2019 (OriginLab Corporation, Northampon, MA, USA).

2.4.3. Differential Scanning Calorimetry (DSC)

Thermal transitions were studied by differential scanning calorimetry (DSC) on a DSC-8000 analyzer equipped with the Intracooler 2 cooling accessory from PerkinElmer, Inc. (Waltham, MA, USA). Three sweeps were done: a first heating step from 30 °C to 250 °C, followed by a cooling step from 250 to −25 °C and completed by a second heating from −25 to 300 °C. The heating and cooling rates were both set at 10 °C/min, and the sample weight was around 3 mg. An empty aluminum pan was used as reference, whereas calibration was performed using an indium sample. The values of melting point (Tm) and enthalpy of melting (ΔHm) were obtained from the heating scan, while the crystallization temperature from melt (Tc) and enthalpy of crystallization (ΔHc) was determined from the cooling scan.

2.4.4. Wide-Angle X-ray Scattering (WAXS)

The crystallinity of the fibers and pure polymers were assessed by WAXS using a Bruker AXS D4 Endeavor diffractometer (Bruker, Ettlingen, Germany), similarly to a previous work [27]. Radial scans of intensity versus scattering angle (2θ) were recorded at room temperature in the range of 2 to 40° (2θ) (step size = 0.02° (2θ), scanning rate = 4 s/step) with filtered CuKα radiation (λ = 1.54 Å), an operating voltage of 40 kV and a filament current of 40 mA.

2.4.5. Thermogravimetric Analysis (TGA)

Thermogravimetric analysis of all polymers and fibers was done in triplicate using a 550-TA thermogravimetric analyzer (New Castle, DE, USA). The analyses were carried out under the following conditions: 1–5 mg of sample, heating from 25 °C to 600 °C, at a heating rate 10 °C/min under nitrogen flow (50 mL/min).

2.5. Statistical Analysis

Data were analyzed by ANOVA with a $p\text{-value} < 0.05$. Fisher test was used for the comparison of means. STATISTICA 10 software (Statsoft Inc., Tulsa, OK, USA) was used for statistical analysis.

3. Results and Discussion

The aim of this work was to assess the electrospinnability of FucoPol and its blends with PEO and pullulan.

3.1. Physicochemical Characterization of Solutions

A fundamental step before electrospinning is to physicochemically characterize the solutions. These parameters govern the behavior of the solution throughout the process. Solutions of FucoPol in different solvents and FucoPol with complementary polymers were characterized in terms of viscosity, surface tension and conductivity. Table 2 shows the characterization of the solutions of pure FucoPol, as well as the solutions of FucoPol:pullulan (2:1 ratio, w/w) and FucoPol:PEO (1:3 ratio, w/w). Viscosity is an important parameter in the electrospinning process in terms of good fiber formation, since

below a critical value, the polymeric fibers break up the jet and form droplets on their way to the collector. However, a high viscosity makes it difficult to pass through the syringe needle of the equipment and stabilize the electrospinning process [28,29]. FucoPol water solutions showed a viscosity of 24.8 ± 0.3 Pa·s. This value is low in comparison with values reported in the literature. Araújo et al. [6], reported a value of 43 Pa·s, but the difference could be due to the EPS extraction process, since some authors decrease the viscosity of the bacterial broth, either through dilutions with distilled water or by adjusting pH with H_2SO_4 to increase the production of EPS [9,30].

Table 2. Physicochemical properties of different dissolutions: FucoPol in water, FucoPol with pullulan (2:1 ratio, w/w) and FucoPol with PEO (1:3 ratio, w/w) in ethanol:water (30:70 v/v).

Sample	Viscosity* (Pa·s)	Surface tension (mN/m)	Conductivity (mS/cm)
FucoPol in water	24.8 ± 0.3c	64.20 ± 0.40a	1.55 ± 0.00a
FucoPol + Pullulan, ratio 2:1	38.9 ± 0.1b	41.00 ± 0.40c	0.53 ± 0.00b
FucoPol + PEO, ratio 1:3	98.1 ± 0.5a	43.90 ± 0.10b	0.50 ± 0.01c

Each column represents the mean ± standard deviation of three independent replicas. Different letters (a–c) in each column indicate a significant difference ($p < 0.05$).
*All samples were Newtonian fluids.

The increased viscosity of FucoPol:pullulan solution, 38.9 ± 0.1 Pa·s, is attributed to the addition of pullulan and the higher percentage of solids in the final solution (2.25% in comparison with 1.50% for FucoPol). In addition, ethanol increased the viscosity of the solutions of FucoPol with pullulan and FucoPol with PEO in comparison with the same solutions prepared with water (results not shown). The solution of FucoPol with PEO showed a viscosity of 98.1 ± 0.5 Pa·s. This value was statistically significant in comparison with the previous solutions. This behavior was mainly attributed to the high molecular weight of PEO. FucoPol had a surface tension of 64.20 ± 0.40 mN/m. This value was high and does not ensure stability during the electrohydrodynamic process [31]. A decrease in surface tension occurred when a mixture of water and ethanol (70:30, v/v) was used instead

of pure water, as shown in Table 2. In other words, the solutions with pullulan and PEO showed values of 41.00 ± 0.40 mN/m and 43.90 ± 0.10 mN/m, respectively, since the surface tension of each solution is dependent on the polymer and the solvent used and on the presence of Span 20 [15]. In the same way, conductivity decreased when ethanol was added to the solutions with pullulan and PEO. Highly conductive solutions, such as FucoPol, are extremely unstable in the presence of strong electric fields and led to a high bending instability [32].

3.2. Production of Nanofibers by Electrospinning

In spite of using different processing conditions, it was not possible to obtain fibers using pure FucoPol in water (Figure 1a) and ethanol:water (30:70 v/v) (Figure 1b) due to the low solubility of the biopolymer in water [10–13], which produces a low solid concentration in the solution, as well as the lack of polymer chain entanglements [33]. For this reason, different ratios with other polymers and process conditions were evaluated. Figure 2 shows the micrographs obtained by SEM of the different solutions of FucoPol:pullulan. Figure 2a–e shows fibers with cylindrical structure but with the presence of some beads, which are more visible at a ratio of 1:2 (Figure 2d). Sinuous fibers occur by warping the jet due to the impact with the collector plate, which is also closely related to the viscosity of the solution and the rigidity of the jets [34]. Bead formation occurs mainly due to the high surface tension and viscoelastic properties of the solution, as well as the operating parameters used [19], affecting the homogeneity of the fibers.

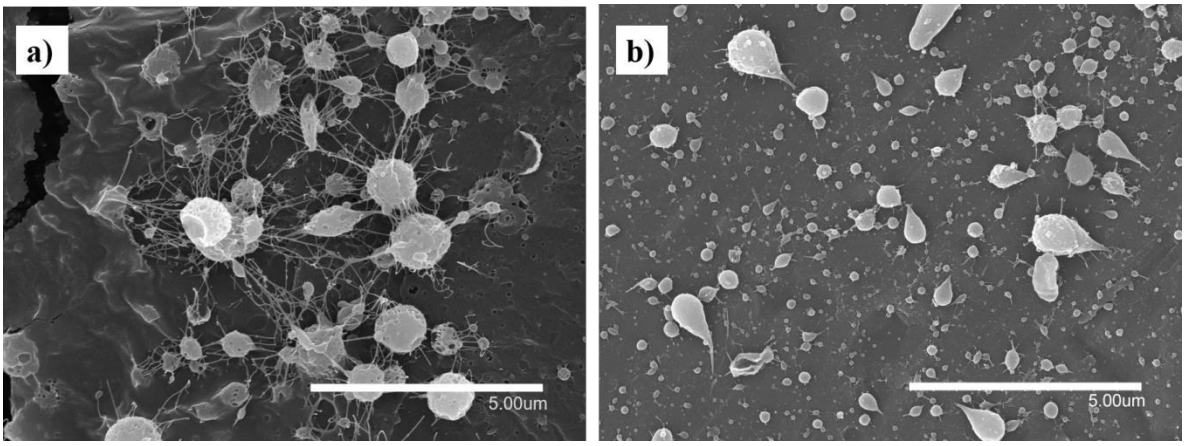

Figure 1. Fibers and capsules of FucoPol in water (a) (optimal conditions: 500 µL/h, 25 cm between collector and needle and 21 kV) and ethanol:water (b) (optimal conditions: 500 µL/h, 15 cm between collector and needle and 15.5 kV in the injector and -3.6 kV in the collector).

On the other hand, pullulan showed uniform and cylindrical fibers with a rough surface, which could be caused by a combination of viscosity of the solution and the ambient conditions. This type of fiber is characteristic of pullulan due to the composition of the polymer. Pullulan has a single bond of maltotriose units interconnected by glycosidic bonds α (1,4) and α (1,6). This structure provides adhesive properties, as well as the ability to form fibers, compression molds and strong oxygen-impermeable films [2]. The studied ratios, shown in Figure 2, did not show significant differences, since the obtained fibers showed similar morphology and nanometric size. Although the different ratios of FucoPol:pullulan showed beads, these fibers were better than the fibers obtained with only FucoPol. FucoPol:pullulan nanofibers with a mass ratio of 2:1 (w/w) were selected to continue the study. These fibers were obtained at a constant flow rate of 250 µL/h, voltages of 23 kV in the injector and −2 kV in the collector and distance between needle and collector of 28 cm.

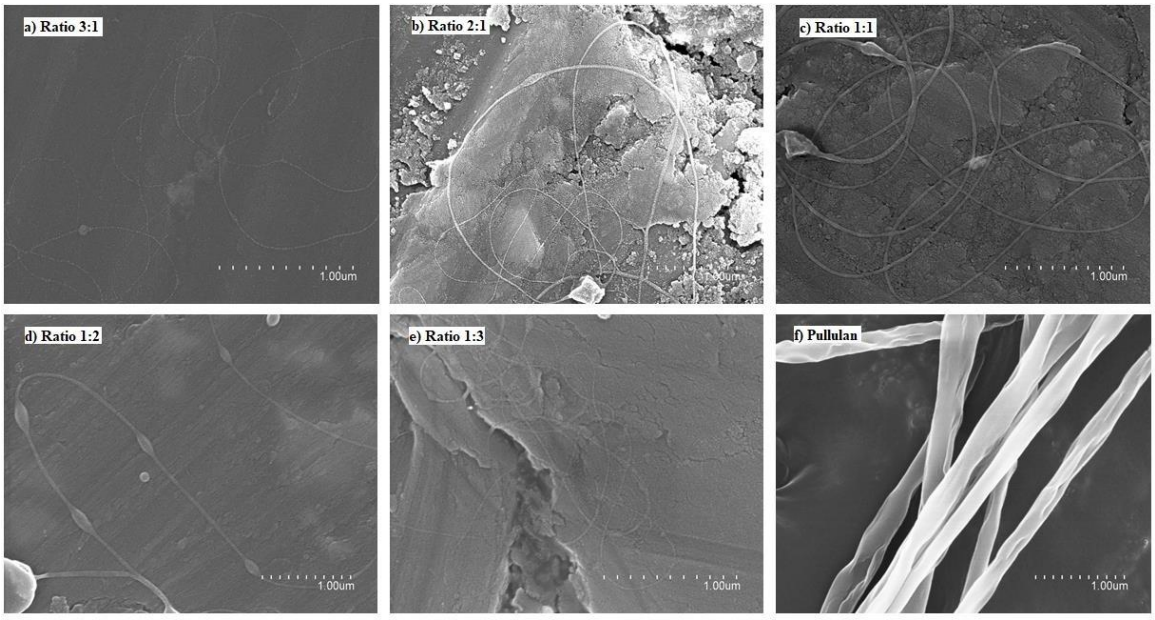

Figure 2. Scanning electron microscopy (SEM) images of the fibers obtained with the FucoPol:Pullulan solutions. a) ratio 3:1, b) ratio 2:1, c) ratio 1:1, d) ratio 1:2, e) ratio 1:3, f) ratio 0:1 (100% pullulan).

Figure 3 shows the micrographs of the different solutions of FucoPol:PEO. Ratios of 3:1 and 1:2 (Figure 3a, d, respectively) showed fibers with a well-defined cylindrical structure and no beads. However, when samples were collected for a long time, fibers and particles were observed, similarly to the fibers obtained with FucoPol:pullulan solutions. Ratios of 2:1 and 1:1 did not show a stable process (Figure 3b and Figure 3c, respectively). Fiber branching observed in Figure 3c, f was due to the high voltage required to electrospin these solutions, which provoked an excess of surface charge on the jet, which was dissipated by branching [35]. However, a ratio of 1:3 led to thick, smooth, continuous and homogeneous fibers due to the higher amount of PEO (Figures 3e and 4). Even if some defects could be detected in Figure 4, they were much less numerous in comparison to the thicker films obtained with the other samples. The solution of FucoPol with PEO (1:3 ratio w/w) showed nanofibers with an average diameter of 0.587 ± 0.200 μm. Those fibers were obtained at a constant flow rate of 300 μL/h, with voltages of 22 kV in the injector and −2 kV in the collector and a distance between the needle and the collector of 28 cm. PEO is considered an electrospinnable polymer [29], since it improves the structural stability and the chargecarrying capacity of the solution, which is crucial for fiber formation [36]. This

result is in agreement with previous studies that showed that the higher viscosity of the solution increases the diameter of fibers [15].

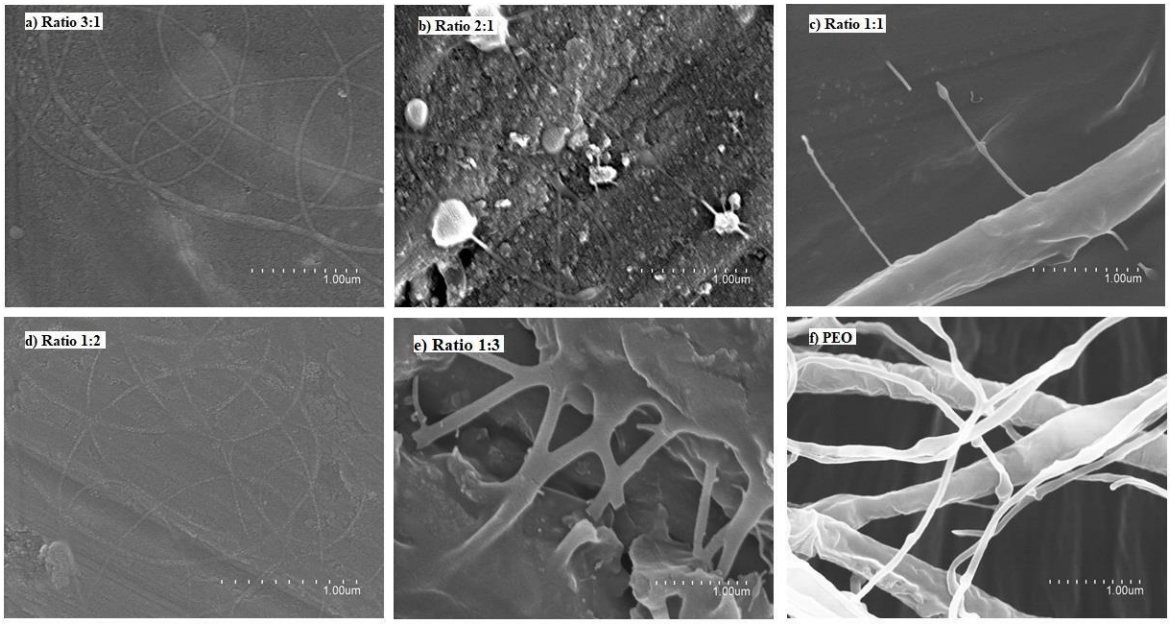

Figure 3. Scanning electron microscopy (SEM) images of the fibers obtained with the FucoPol:PEO solutions. a) ratio 3:1, b) ratio 2:1, c) ratio 1:1, d) ratio 1:2, e) ratio 1:3, f) ratio 0:1 (100% PEO).

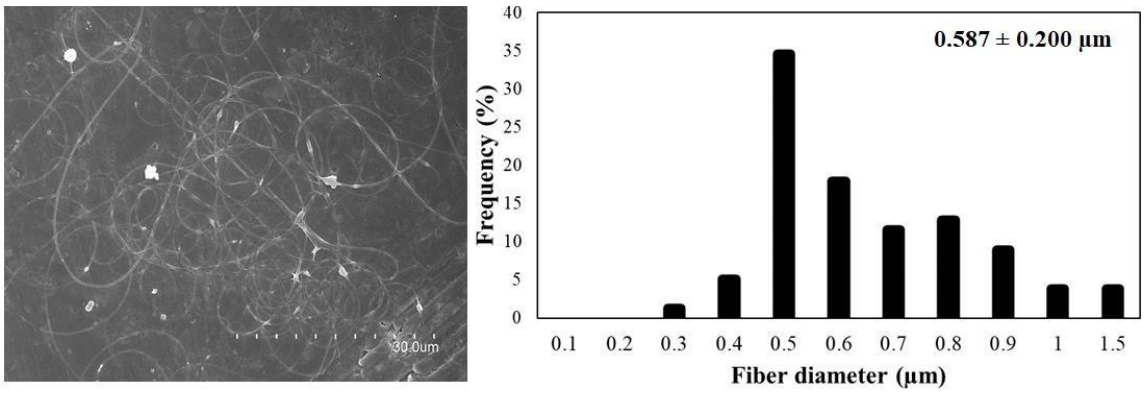

Figure 4. FucoPol:PEO fibers (ratio 1:3, w/w) (left) and the average diameter of the fibers (right).

3.3. Thermal Properties

3.3.1. Thermal Gravimetric Analysis (TGA)

Thermogravimetric curves of FucoPol, FucoPol:pullulan (ratio 2:1, w/w) and FucoPol:PEO (ratio 1:3, w/w), along with TGA curves of pure polymers, which served as references, are shown in Figure 5. FucoPol showed three weight-loss steps (Figure 5f). The first step occurred between 25 and 109 °C, referring to 13% of weight loss, which could be attributed to water evaporation [8,9]. The second step occurred between 220 and 364 °C, referring to 52% of weight, and the third step occurred between 364 and 410 °C, referring to 23% of weight loss. These two steps were attributed to biopolymer thermal degradation [8,37], specifically to decomposition of the polysaccharides side chains [9]. After these three steps, we observed a gradual weight loss, around 10% of total mass. It is important to note that after the electrospinning process, FucoPol showed only two weight-loss steps (Figure 5e), starting from 25–109 °C, corresponding to 4% of weight loss, attributed to the evaporation of water. The second step started from 140–378 °C, referring to 85% of weight loss, and after this, a gradual weight loss. This behavior is thought to be caused by the reduced size of the fibers and the presence of 3% Span 20. The oily and hydrophobic nature [38] of Span 20 leads to a wide range of decomposition temperatures compared to pure FucoPol.

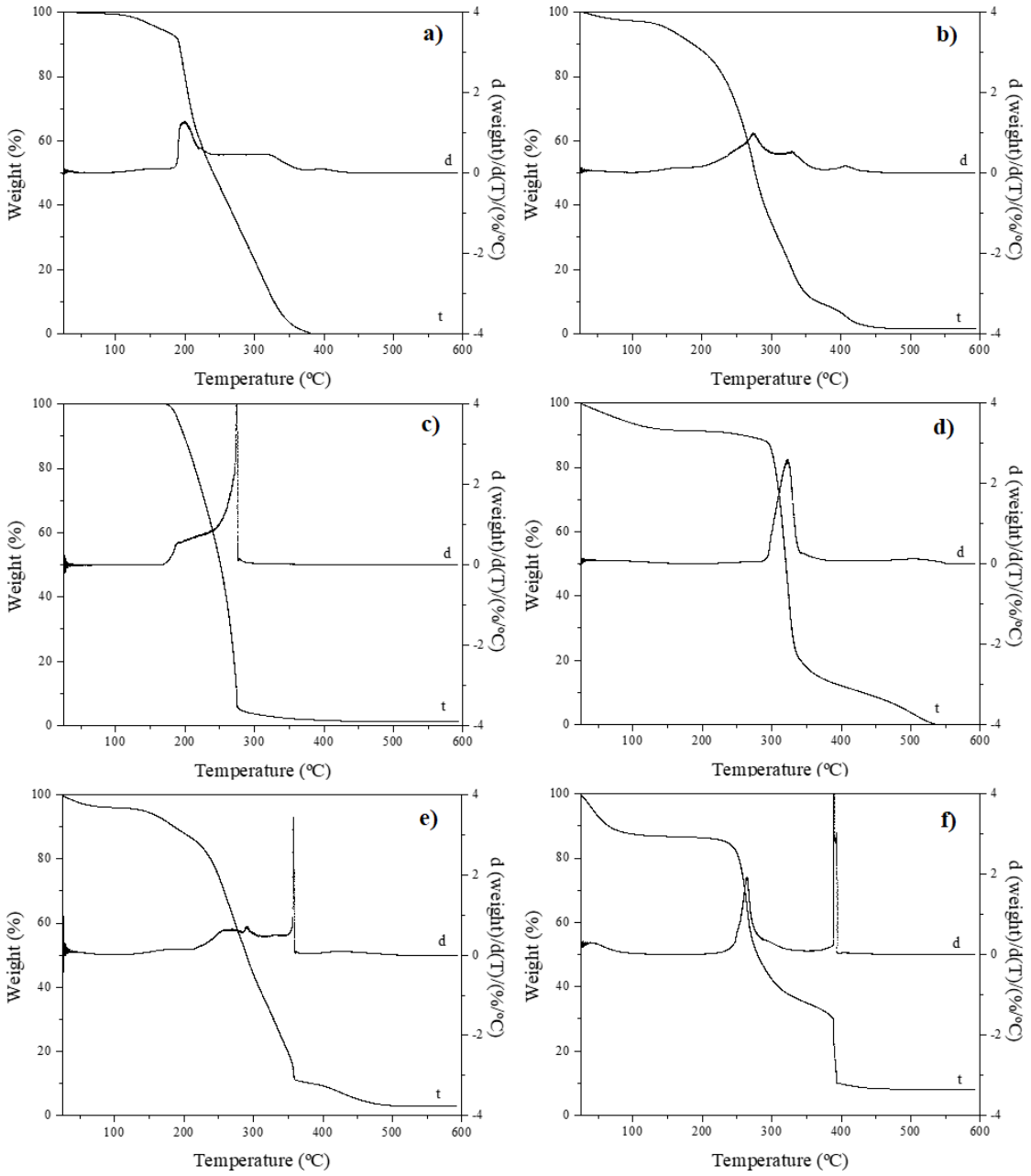

Figure 5. Thermogravimetric analysis of a) FucoPol: PEO fibers, b) FucoPol:Pullulan fibers, c) pure PEO, d) pure Pullulan, e) FucoPol after electrospinning (mixture of fibers and particles), and f) pure FucoPol. Curve t represents thermogram and d is the thermogram derivate.

When it comes to FucoPol:PEO fibers, a similar thermal-degradation curve as for pure PEO is observed (Figure 5c). The thermal decomposition of PEO and FucoPol:PEO fibers consisted of only one weight-loss step. PEO showed 96% of weight loss between 160 and

301 °C, while FucoPol:PEO fibers (Figure 5a) showed a step between 143 and 379 °C with a similar weight loss (97%). The presence of PEO decreased the thermal stability of the fibers in comparison to pure FucoPol nanofibers. Pullulan showed one important weight-loss step from 267 to 362 °C, corresponding to 74% of total weight loss (Figure 5d). Nevertheless, FucoPol:pullulan fibers showed a comparable thermal behavior to that of FucoPol after electrospinning (Figure 5e), attributed to the largest amount of FucoPol among the FucoPol:pullulan fibers (2:1 w/w). Weight loss started from 128 to 369 °C, corresponding to 87% of total weight loss. This study confirms that the obtained nanofibers could be used in multiple applications in which the temperature does not exceed 120 °C. However, this temperature is enough to be subjected to several thermal processes, such as sterilization, as well as to non-thermal technologies, such as electrohydrodynamic processing, which opens a wide range of potential applications, such as pharmaceutics, biomedicine, biosensors, food packaging, agriculture, food or cosmetics, among others.

3.3.2. Differential Scanning Calorimetry (DSC)

DSC curves of fibers are illustrated in Figure 6. The DSC curve of pure FucoPol during the first run showed an endothermic peak at 85 °C, ΔH 113 J/g (Figure 6a), which was also observed by Lourenço et al. [8]. This may be attributed to the evaporation of sorbed water. During the second heating run, stopping at a higher temperature than in the first run, an exothermic peak at 279 °C, ΔH −144 J/g (Figure 6c), was observed, which was attributed to polymer degradation. Additionally, Lourenço et al. reported an exothermic peak at around 270 °C [8]. Unambiguous melting or crystallization events were not discerned in the different heating and cooling ramps, suggesting an amorphous nature of the biopolymer. The same behavior was observed by Guerreiro et al. [39]. In the same way, pullulan showed a similar first-heating thermogram, with a broad peak between 44 and 166 °C instead of a sharp melting point (Figure 6a). This endotherm is also ascribed to moisture evaporation. The same behavior was observed by Singh et al. [40].

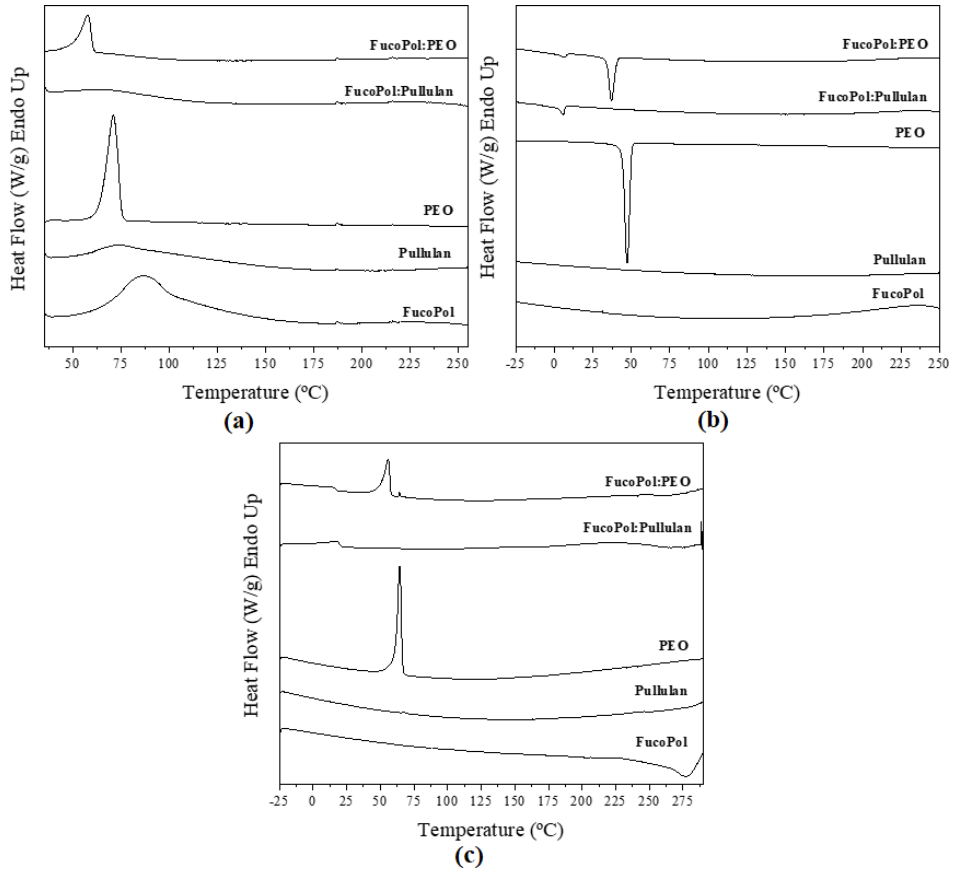

Figure 6. Differential Scanning Calorimetry curves of electrospun fibers and commercial polymers during a) first heating, b) cooling, and c) second heating.

On the other hand, PEO is a semicrystalline polymer [41]. Figure 6a exhibits the melting temperature of PEO at 69 °C, ΔH 151 J/g. Crystallization temperature was 47 °C, ΔH 122 J/g (Figure 6b). Similar results were reported by Balik et al. [42]. The FucoPol:PEO fibers showed similar behavior to that of pure PEO because PEO was the dominant polymer in the solution (1:3 ratio, w/w, Table 1). However, melting and crystallization temperatures and enthalpies corrected for PEO content were reduced, i.e., 58 °C, ΔH 76 J/g and 37 °C, ΔH 63 J/g, respectively, as shown in Figures 6a and 6b. This behavior was attributed to FucoPol impairing the crystallization of the PEO polymer in the blend. Guerreiro et al. [39] reported the formation of dispersed ice crystals in the presence of FucoPol when they studied the cryoprotective properties of FucoPol in water solutions. These authors observed that FucoPol significantly reduced the average size of the formed crystals. Interestingly, during the crystallization and melting runs of the blends, small exothermic and endothermic

events were seen at 10.5 and 17.5 °C, respectively, for FucoPol:pullulan and at 8.1 and 15.5 °C, respectively, for FucoPol:PEO, which may be ascribed to higher hierarchical molecular assemblies induced by blending (see WAXS results below).

3.4. Wide-Angle X-ray Scattering (WAXS)

WAXS allows for the characterization and quantification of the crystallinity present in a given sample through the diffraction patterns measured at wide angles [43]. Results of this analysis are shown in Figure 7. In this context, pure FucoPol and pullulan showed no sharp peaks in the 2θ range, suggesting again a rather amorphous nature [8,44–48]. On the other hand, pure PEO showed a clear crystalline phase with two intense peaks at 19° and at 23° (Figure 7). These observations are consistent with the results obtained by other authors, who reported two characteristic diffraction peaks at 2θ = 19° and 23.5° for crystalline PEO [49] and weak crystalline peaks at around 15°, 26° and 36° [50,51].

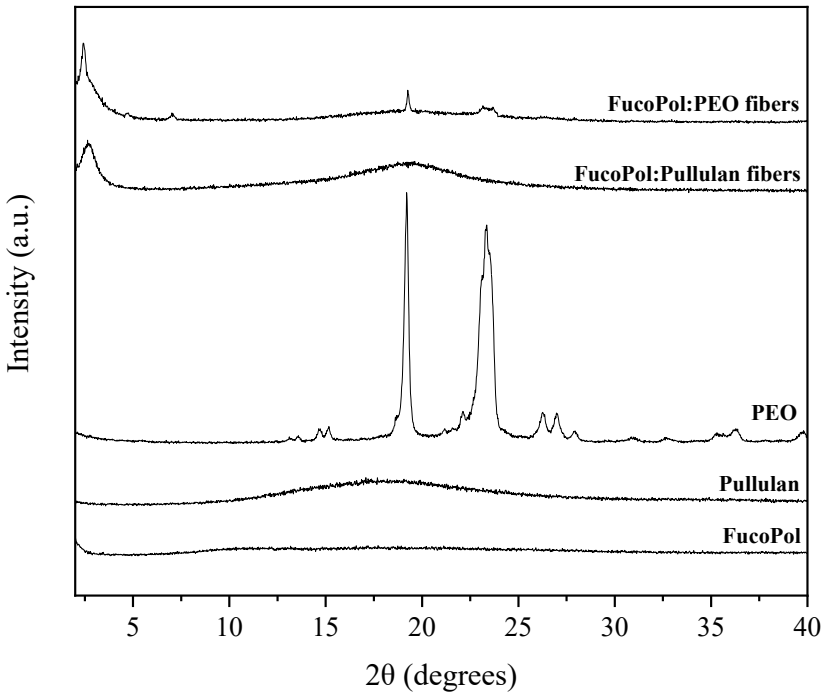

Figure 7. WAXS profiles of fibers of FucoPol with PEO and pullulan, respectively, as well as pure polymers.

3.5. Attenuated Total Reflectance–Fourier Transform Infrared Spectroscopy (ATR-FTIR)

The ATR-FTIR spectra of the fibers that contain FucoPol are presented in Figure 8, along with the spectra of complementary polymers pullulan and PEO for comparison. The broad intense band around 3400 cm^{-1} is common for all samples containing polysaccharides (Figure 8a,b,d,e,g). This band represents O–H stretching of hydroxyls and bound water [55]. This band overlaps in part with the C–H stretching peak of CH_2 groups appearing at 2940 cm^{-1} in the case of FucoPol and pullulan, as shown in Figures 8g and 8d, respectively. FucoPol bands at 1200 and 900 cm^{-1} represent skeletal C–O and C–C vibration bands of glycosidic bonds and pyranoid rings [55]. The band at 1720 cm^{-1} is attributed to the C=O stretching of carbonyls in acyl groups. The band at 1250 cm^{-1} may also be attributed to the C–O–C vibration of acyls and was explored by Freitas et al. [7]. In the same way, the strong bands at 1607 and 1405 cm^{-1}, can be attributed to the asymmetric and symmetric stretchings, respectively, of carboxylates [55]. All peaks shown by FucoPol (Figure 8g) in this study match those reported by Freitas et al. [7] during the characterization of a fucose-containing exopolysaccharide produced by the newly isolated *Enterobacter* strain A47 DSM 23139.

The fibers of FucoPol:PEO and FucoPol:pullulan showed characteristic bands corresponding to the same bands of pure polymers PEO and pullulan, respectively (Figure 8c, d). In addition, the presence of the Span 20 was also observed, since new bands appeared in the spectrum of fibers at ca. 2920 and 2850 cm^{-1}, attributed to CH_2 and CH_3 scissoring [56] of the lipids that form this surfactant, even in FucoPol after electrospinning. The absence of changes in the characteristic bands in the electrospun nanofibers with respect to the pure components proves the absence of chemical reactions and degradation during the applied treatment.

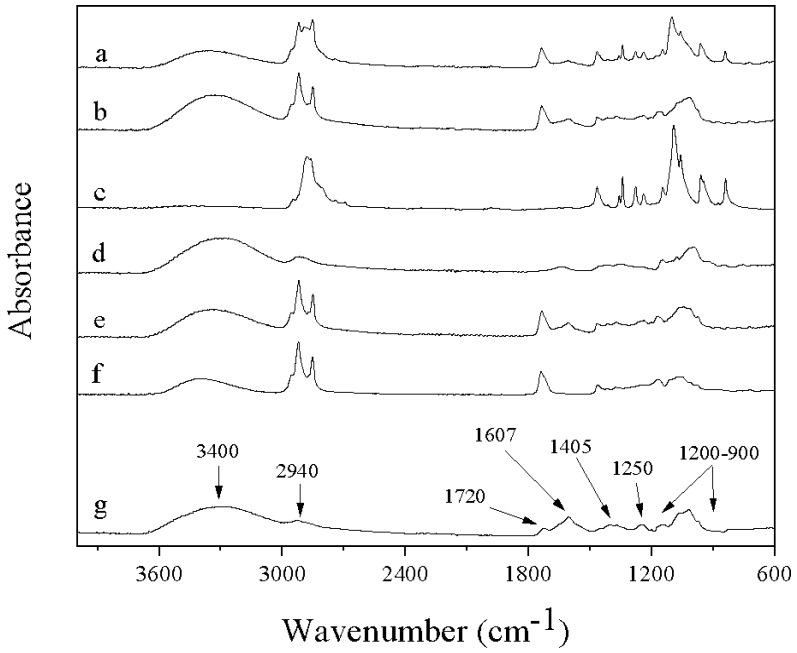

Figure 8. FTIR spectra of (a) FucoPol:PEO fibers, (b) FucoPol:pullulan fibers, (c) pure PEO, (d) pure pullulan, (e) FucoPol after electrospinning (mixture of fibers and particles), (f) Span 20 and (g) pure FucoPol.

4. Conclusions

Electrospun FucoPol nanofibers were not able to be produced from water or alcohol solutions—only by blending with other polymers, such as PEO and pullulan. FucoPol was found to be an amorphous biopolymer stable until 220 °C, but it was not possible to obtain homogeneous nanofibers due to the low water solubility and lack of molecular entanglements. The blend of FucoPol:PEO showed non-agglomerated and homogeneous nanofibers with cylindrical morphology, as well as reduced crystallinity in comparison with pure PEO fibers when normalized for content, and was stable until 140 °C. The blend of FucoPol:pullulan showed an amorphous nature and was stable until 130 °C. Interestingly, the blending components influenced one another in the intermolecular order, since new peaks ascribed to intermolecular hierarchical assemblies were seen by WAXS for FucoPol. The well-known functional properties of FucoPol, together with the possibility to form stable electrospun fibers with controllable morphology and porosity, as well as the interesting structural and thermal properties shown in previous results, opens a new research line concerning the potential applications of FucoPol electrospun fibers in the food

packaging, agricultural, biomedical, pharmaceutical, cosmetic and food industries, among others.

Author Contributions: Conceptualization by J.M.L.; methodology, validation, and formal analysis was carried out by Y.V.-G., M.S., C.P., C.A.V.T., F.F. and J.M.L.; investigation, resources, data curation, writing—original draft preparation, review and editing were performed by Y.V.-G., M.S., C.P., F.F., C.A.V.T., J.A.R.-S., M.C.-S. and J.M.L.; visualization, supervision, project administration and funding acquisition were carried out by C.P., M.C.-S. and J.M.L. All authors have read and agreed to the published version of the manuscript.

Funding: This study was supported by the CYTED thematic network (code 319RT0576), the Spanish Ministry of Science and Innovation (MICI) project RTI-2018-097249-B-C21 and H2020 EU project USABLE PACKAGING (reference number 836884). This work received financial support from FCT— Fundação para a Ciência e a Tecnologia, I.P. (Portugal), in the scope of projects UIDP/04378/2020 and UIDB/04378/2020 of the Research Unit on Applied Molecular Biosciences—UCIBIO, and project LA/P/0140/2020 of the Associate Laboratory Institute for Health and Bioeconomy—i4HB.

Data Availability Statement: No application.

Acknowledgments: Yuliana Vázquez González thanks Consejo Nacional de Ciencia y Tecnología for the fellowship awarded with number 754518. Milan Stojanovic acknowledges the European Institute of Innovation & Technology (EIT) for the fellowship EIT Food KAVA #20272/2020.

Conflicts of Interest: The authors declare no conflict of interest.

References

1. Daba, G.M.; Elnahas, M.O.; Elkhateeb, W.A. International Journal of Biological Macromolecules Contributions of exopolysaccharides from lactic acid bacteria as biotechnological tools in food, pharmaceutical, and medical applications. Int. J. Biol. Macromol. 2021, 173, 79–89. [CrossRef] [PubMed]
2. Singh, R.S.; Saini, G.K.; Kennedy, J.F. Pullulan: Microbial sources, production and applications. Carbohydr. Polym. 2008, 73, 515–531. [CrossRef] [PubMed]
3. Torres, C.A.V.; Marques, R.; Antunes, S.; Alves, V.D.; Sousa, I.; Maria, A.; Oliveira, R.; Freitas, F.; Reis, M.A.M. Kinetics of production and characterization of the fucose-containing exopolysaccharide from Enterobacter A47. J. Biotechnol. 2011, 156, 261–267. [CrossRef] [PubMed]
4. Dsm, A.; Freitas, F.; Alves, V.D.; Torres, C.A.V.; Cruz, M.; Sousa, I.; João, M.; Ramos, A.M.; Reis, M.A.M. Fucose-containing exopolysaccharide produced by the newly isolated. Carbohydr. Polym. 2011, 83, 159–165. [CrossRef]
5. Freitas, F.; Alves, V.D.; Gouveia, A.R.; Grandfils, C.; Reis, M.A.M. Controlled Production of Exopolysaccharides from Enterobacter A47 as a Function of Carbon Source with Demonstration of Their Film and Emulsifying Abilities. Appl. Biochem. Biotechnol. 2014, 172, 641–657. [CrossRef]
6. Araújo, D.; Alves, V.D.; Campos, J.; Coelhoso, I.; Sevrin, C.; Grandfils, C.; Freitas, F.; Reis, M.A.M. International Journal of Biological Macromolecules Assessment of the adhesive properties of the bacterial polysaccharide FucoPol. Int. J. Biol. Macromol. 2016, 92, 383–389. [CrossRef]
7. Freitas, F.; Alves, V.D.; Reis, M.A.M. Advances in bacterial exopolysaccharides: From production to biotechnological applications. Trends Biotechnol. 2011, 29, 388–398. [CrossRef]
8. Lourenc, S.C.; Torres, C.A.V.; Nunes, D.; Duarte, P.; Freitas, F.; Reis, M.A.M.; Fortunato, E.; Moldão-martins, M.; Beirão, L.; Alves, V.D. International Journal of Biological Macromolecules Using a bacterial fucose-rich polysaccharide as encapsulation material of bioactive compounds. Int. J. Biol. Macromol. 2017, 104, 1099–1106. [CrossRef]
9. Concórdio-reis, P.; Pereira, C.V.; Batista, M.P.; Sevrin, C.; Grand, C.; Marques, A.C.; Fortunato, E.; Gaspar, F.B.; Matias, A.A.; Freitas, F.; et al. International Journal of Biological Macromolecules Silver nanocomposites based on the bacterial fucose-rich polysaccharide secreted by Enterobacter A47 for wound dressing applications: Synthesis, characterization and in vitro bioactivity. Int. J. Biol. Macromol. 2020, 163, 959–969. [CrossRef]
10. Ferreira, A.R.V.; Torres, C.A.V.; Freitas, F.; Reis, M.A.M.; Vítor, D.; Coelhoso, I.M. International Journal of Biological Macromolecules Biodegradable films produced from the bacterial polysaccharide FucoPol. Int. J. Biol. Macromol. 2014, 71, 111–116. [CrossRef]
11. Ferreira, A.R.V.; Torres, C.A.V.; Freitas, F.; Sevrin, C.; Grandfils, C.; Reis, M.A.M.; Alves, V.D.; Coelhoso, I.M. Development and characterization of bilayer films of FucoPol and chitosan. Carbohydr. Polym. 2016, 147, 8–15. [CrossRef] [PubMed]
12. Ferreira, A.R.V.; Haapanen, J.; Mäkelä, J.M.; Bratvold, J.E.; Nilsen, O.; Tuominen, M.; Alves, V.D.; Coelhoso, I.M. International Journal of Biological Macromolecules

Comparison of different coating techniques on the properties of FucoPol films. Int. J. Biol. Macromol. 2017, 103, 268–274. [CrossRef] [PubMed]
13. Ferreira, A.R.V.; Bandarra, N.M.; Moldão-martins, M.; Coelhoso, I.M.; Alves, V.D. FucoPol and chitosan bilayer fi lms for walnut kernels and oil preservation. LWT Food Sci. Technol. 2018, 91, 34–39. [CrossRef]
14. Bhardwaj, N.; Kundu, S.C. Electrospinning: A fascinating fi ber fabrication technique. Biotechnol. Adv. 2010, 28, 325–347. [CrossRef]
15. Marcela, L.; Sánchez, D.; Rodriguez, L.; López, M. Electrospinning: La era de las Nanofibras. Rev. Iberoam. Polímeros 2014, 14, 10–27. 16. Bhushani, J.A. Electrospinning and electrospraying techniques: Potential food-based applications. Trends Food Sci. Technol. 2014, 38, 21–33. [CrossRef]
17. Leidy, R.; Ximena, Q.M. Trends in Food Science & Technology Use of electrospinning technique to produce nano fi bres for food industries: A perspective from regulations to characterisations. Trends Food Sci. Technol. 2019, 85, 92–106. [CrossRef]
18. Frenot, A.; Chronakis, I.S. Polymer nanofibers assembled by electrospinning. Curr. Opin. Colloid Interface Sci. 2003, 8, 64–75. [CrossRef]
19. Fong, H.; Chun, I.; Reneker, D.H. Beaded nanofibers formed during electrospinning. Polymer 1999, 40, 4585–4592. [CrossRef]
20. Torres-Giner, S.; Pérez-Masiá, R.; Lagaron, J.M. A review on electrospun polymer nanostructures as advanced bioactive platforms. Polym. Eng. Sci. 2016, 56, 500–527. [CrossRef]
21. Torres-giner, S.; Wilkanowicz, S.; Melendez-rodriguez, B.; Lagaron, J.M. Nanoencapsulation of Aloe vera in Synthetic and Naturally Occurring Polymers by Electrohydrodynamic Processing of Interest in Food Technology and Bioactive Packaging. J. Agric. Food Chem. 2017, 65, 4439–4448. [CrossRef] [PubMed]
22. Wang, S.; Yang, Y.; Zhang, Y.; Fei, X.; Zhou, C.; Zhang, Y.; Li, Y.; Yang, Q.; Song, Y. Fabrication of large-scale superhydrophobic composite films with enhanced tensile properties by multinozzle conveyor belt electrospinning. J. Appl. Polym. Sci. 2014, 131, 39735. [CrossRef]
23. Barhoum, A.; Rasouli, R.; Yousefzadeh, M. Nanofiber Technologies: History and Development. Handbook of Nanofibers; Springer International Publishing AG: Cham, Switzerland, 2019; ISBN 9783319536552.
24. Teck, C. Progress in Polymer Science Nanofiber technology: Current status and emerging developments. Prog. Polym. Sci. 2017, 70, 1–17.
25. Alves, V.D.; Freitas, F.; Torres, C.A.V.; Cruz, M.; Marques, R.; Grandfils, C.; Gonc, M.P.; Oliveira, R.; Reis, M.A.M. Rheological and morphological characterization of the culture broth during exopolysaccharide production by Enterobacter sp. Carbohydr. Polym. 2010, 81, 758–764. [CrossRef]
26. Hilliou, L.; Freitas, F.; Oliveira, R.; Reis, M.A.M.; Lespineux, D.; Grandfils, C.; Alves, V.D. Solution properties of an exopolysaccharide from a Pseudomonas strain obtained using glycerol as sole carbon source. Carbohydr. Polym. 2009, 78, 526–532. [CrossRef]
27. Lidón, E.; Safont, S.; Aldureid, A.; María, J.; Jose, L.; Perez, G.; Cabedo, L. Effect of the Purification Treatment on the Valorization of Natural Cellulosic Residues as Fillers in PHB—Based Composites for Short Shelf Life Applications. Waste Biomass Valorization 2021, 12, 2541–2556. [CrossRef]

28. Deitzel, J.M.; Kleinmeyer, J.; Harris, D.; Tan, N.C.B. The effect of processing variables on the morphology of electrospun nanofibers and textiles. Polymer 2001, 42, 261–272. [CrossRef]
29. Vidinha, R.; Botequim, D.; Borges, J.P. A systematic study of solution and processing parameters on nanofiber morphology using a new electrospinning apparatus A Systematic Study of Solution and Processing Parameters on Nanofiber Morphology Using a New Electrospinning Apparatus. J. Nanosci. Nanotechnol. 2009, 9, 3535–3545. [CrossRef]
30. Li, S.; Xia, H.; Xie, A.; Wang, Z.; Ling, K.; Zhang, Q.; Zou, X. International Journal of Biological Macromolecules Structure of a fucose-rich polysaccharide derived from EPS produced by Kosakonia sp. CCTCC M2018092 and its application in antibacterial film. Int. J. Biol. Macromol. 2020, 159, 295–303. [CrossRef]
31. Jaworek, A. Electrospray droplet sources for thin film deposition. J. Mater. Sci. 2007, 42, 266–297. [CrossRef]
32. Hayati, I.; Bailey, A.I.; Tadros, T.H.F. Investigations into the Mechanisms of Electrohydrodynamic Spraying of Liquids I. Effect of Electric Field and the Environment on Pendant Drops and Factors Affecting the Formation of Stable Jets and Atomization. J. Colloid Interface Sci. 1987, 117, 205–221. [CrossRef]
33. Shenoy, S.L.; Bates, W.D.; Frisch, H.L.; Wnek, G.E. Role of chain entanglements on fiber formation during electrospinning of polymer solutions: Good solvent, non-specific polymer—Polymer interaction limit. Polymer 2005, 46, 3372–3384. [CrossRef]
34. Yu, J.; Qiu, Y.; Zha, X.; Yu, M.; Yu, J.; Rafique, J.; Yin, J. Production of aligned helical polymer nanofibers by electrospinning. Eur. Polym. J. 2008, 44, 2838–2844. [CrossRef]
35. Ti, P. Branching effect and morphology control in electrospun. J. Mater. Res. 2014, 29, 1721–1729. [CrossRef]
36. Francis, L.; Balakrishnan, A.; Sanosh, K.P.; Marsano, E. Characterization and tensile strength of HPC—PEO composite fi bers produced by electrospinning. Mater. Lett. 2010, 64, 1806–1808. [CrossRef]
37. Vendruscolo, C.W.; Ferrero, C.; Pineda, E.A.G.; Silveira, J.L.M.; Freitas, R.A.; Jiménez-castellanos, M.R.; Bresolin, T.M.B. Physicochemical and mechanical characterization of galactomannan from Mimosa scabrella: Effect of drying method. Carbohydr. Polym. 2009, 76, 86–93. [CrossRef]
38. Geng, Q.; Chen, J.; Guo, R.; Zhang, L.; Li, Q.; Yu, X. Salt-assisted aqueous extraction combined with Span 20 allow the obtaining of a high-quality and yield walnut oil. LWT 2020, 121, 108956. [CrossRef]
39. Guerreiro, B.M.; Freitas, F.; Lima, J.C.; Silva, J.C.; Dionísio, M.; Reis, M.A.M. Demonstration of the cryoprotective properties of the fucose-containing polysaccharide FucoPol. Carbohydr. Polym. 2020, 245, 116500. [CrossRef]
40. Sarup, R.; Kaur, N.; Pandey, A.; Kennedy, J.F. Bioresource Technology Reports Hyper-production of pullulan from de-oiled rice bran by Aureobasidium pullulans in a stirred tank reactor and its characterization. Bioresour. Technol. Rep. 2020, 11, 100494. [CrossRef]
41. Lu, C.; Wai, S.; Du, H.; Li, J.; Gan, L.; Zhang, X.; Chu, X.; Yao, Y.; Li, B.; Kang, F. Thermal conductivity of electrospinning chain-aligned polyethylene oxide (PEO). Polymer 2017, 115, 52–59. [CrossRef]
42. Balik, B.A.; Argin, S.; Lagaron, J.M. Preparation and Characterization of Electrospun Pectin-Based Films and Their Application in Sustainable Aroma Barrier Multilayer Packaging. Appl. Sci. 2019, 9, 5136. [CrossRef]

43. Louati, M.; Tahon, J.; Fournier, D.; Stoclet, G.; Takao, M.; Takeshita, M.; Lefebvre, J.; Barrau, S. In-situ SAXS/WAXS investigations of ureidopyrimidinone functionalized semi-crystalline poly (ethylene-co-butylene) supramolecular polymers. Polymer 2021, 228, 123875. [CrossRef]
44. Haghighatpanah, N.; Mirzaee, H.; Khodaiyan, F.; Kennedy, J.F.; Aghakhani, A.; Saeid, S.; Jahanbin, K. Optimization and characterization of pullulan produced by a newly identi fi ed strain of Aureobasidium pullulans. Int. J. Biol. Macromol. 2020, 152, 305–313. [CrossRef] [PubMed]
45. Mao, Y.; Su, Y.; Hsiao, B.S. Probing structure and orientation in polymers using synchrotron small- and wide-angle X-ray scattering techniques. Eur. Polym. J. 2016, 81, 433–446. [CrossRef]
46. Sarup, R.; Kaur, N.; Sharma, R.; Rana, V. International Journal of Biological Macromolecules Carbamoylethyl pullulan: QbD based synthesis, characterization and corneal wound healing potential. Int. J. Biol. Macromol. 2018, 118, 2245–2255. [CrossRef]
47. Trovatti, E.; Fernandes, S.C.M.; Rubatat, L.; Perez, S.; Freire, C.S.R.; Silvestre, A.J.D.; Pascoal, C. Pullulan—Nanofibrillated cellulose composite films with improved thermal and mechanical properties. Compos. Sci. Technol. 2012, 72, 1556–1561. [CrossRef]
48. van Drongelen, M.; Meijer-vissers, T.; Cavallo, D.; Portale, G.; Vanden, G.; Androsch, R. Thermochimica Acta Microfocus wide-angle X-ray scattering of polymers crystallized in a fast scanning chip calorimeter. Thermochim. Acta 2013, 563, 33–37. [CrossRef]
49. Liu, R.; Jin, L.; Lu, D.; Hu, G.; He, L.; Shan, J. Electrochimica Acta Bi-continuous phases structured nanocomposite polymer electrolytes: Facile preparation and electrochemical properties. Electrochim. Acta 2013, 114, 372–378. [CrossRef]
50. Lin, H.; Kai, T.; Freeman, B.D.; Kalakkunnath, S.; Kalika, D.S. The Effect of Cross-Linking on Gas Permeability in Cross-Linked Poly (Ethylene Glycol Diacrylate). Macromolecules 2005, 38, 8381–8393. [CrossRef]
51. Sunderrajan, S.; Freeman, B.D.; Hall, C.K.; Pinnau, I. Propane and propylene sorption in solid polymer electrolytes based on poly (ethylene oxide) and silver salts. J. Membr. Sci. 2001, 182, 1–12. [CrossRef]
52. Michael, D. Structural Hierarchy in Linear Polysaccharides—From the Nano- to Macroscale. Ph.D. Thesis, ETH Zurich, Zurich, Switzerland, 2020.
53. Fittolani, G.; Seeberger, P.H.; Delbianco, M. Helical polysaccharides. Peptide Sci. 2020, 112, e24124. [CrossRef]
54. Khan, M.A.; Zhou, C.; Zheng, P.; Zhao, M.; Liang, L. Improving Physicochemical Stability of Quercetin-Loaded Hollow Zein Particles with Chitosan/Pectin Complex Coating. Antioxidants 2021, 10, 1476. [CrossRef] [PubMed]
55. Mate, P.; Machovic, V.; Synytsya, A. Fourier transform Raman and infrared spectroscopy of pectins. Carbohydr. Polym. 2003, 54, 97–106. [CrossRef]
56. Ali, A.; Talpur, F.N.; Aqeel, M.; Cebeci, A.; Jawaid, S.; Imran, H. Monitoring the Rhizopus oryzae lipase catalyzed hydrolysis of castor oil by ATR-FTIR spectroscopy. J. Mol. Catal. B Enzym. 2015, 113, 56–61. [CrossRef

7.3. Desarrollo de nanofibras antifúngicas a base de goma de anacardo, FucoPol y pululano obtenidas mediante proceso de *electrospinning*

Los resultados correspondientes a la etapa 3 de este proyecto de tesis están contenidos en la siguiente publicación:

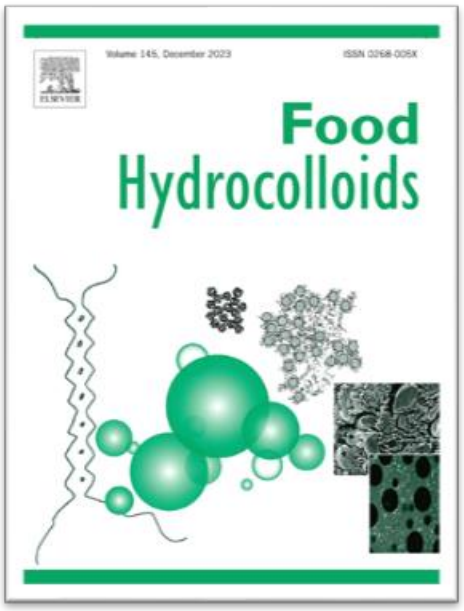

Development of antifungal nanofibers from novel biopolymers by the high-throughput electrospinning process

Vázquez-González, Yuliana, Prieto, Cristina, Ragazzo-Sánchez, Juan Arturo, Calderón-Santoyo, Montserrat, & Lagarón, José María.

Food Hydrocolloids 147 (2024) 109343, DOI: 10.1016/j.foodhyd.2023.109343

Factor de impacto (2023): 11.504

Número de citas: 0

7.3.1. Introducción al tema

Una de las razones del desperdicio de alimentos se relaciona con las enfermedades postcosecha. Estas enfermedades, causadas por diversos microorganismos como hongos fitopatógenos, pueden provocar pérdidas significativas, llegando a representar hasta el 42% de la producción total de frutos y verduras. El control de dichos fitopatógenos convencionalmente se ha realizado mediante control químico; no obstante, esto ha causado preocupación respecto al total de residuos generados y al impacto potencial en la salud humana y el medioambiente. Por tanto, en la actualidad se están desarrollando nuevas estrategias de control más sostenibles. Los agentes de biocontrol (BCA) tales como los microorganismos antagonistas, fueron estudiados por primera vez en 1977 por Tronsmo y Dennis y fue a partir del 2005 en donde se fomentó una gran cantidad de investigación y desarrollo en todo el mundo. Sin embargo, ha tenido un éxito limitado ya que se ha avanzado poco en la implementación comercial debido a una falta de eficacia y viabilidad económica. En este sentido, para aumentar la eficacia de un BCA, el atrapamiento o encapsulación en matrices poliméricas lograría proporcionar protección y estabilidad además de dar lugar a su liberación controlada. De entre las tecnologías de encapsulación, el procesado electrohidrodinámico es una alternativa que permite generar nanofibras electrohiladas a temperatura ambiente, las cuales son estructuras con una gran superficie-volumen lo que las hace matrices más activas y eficientes. Para la obtención de las nanofibras se están estudiando biopolímeros como una alternativa a los polímeros sintéticos, tal es el caso de los polisacáridos, como, por ejemplo, la goma de anacardo, el FucoPol y el pululano quiénes además de ser biopolímeros, están altamente disponibles.

El objetivo de esta investigación fue obtener nanofibras de diferentes biopolímeros mediante el proceso de electrohilado para encapsular *M. caribbica* y demostrar su eficacia como potencial agente antifúngico postcosecha contra hongos de interés comercial. Para ello se llevó a cabo la preparación de soluciones de goma de anacardo y óxido de polietileno, CG:PEO (0.15 g/mL, ratio 5.6:1 p/p), FucoPol y óxido de polietileno, FP:PEO (0.015 g/mL, ratio 1:2 p/p) y pululano (0.15 g/mL p/v). Posterior a ello, a cada una de las soluciones se agregó la levadura *M. caribbica* y se ajustó a la concentración de 1×10^8 células/mL. Las soluciones con y sin *M. caribbica* fueron caracterizadas fisicoquímicamente. Las soluciones se procesaron en un equipo LE-10 y LE-500. Las nanofibras obtenidas fueron caracterizadas

mediante SEM, ATR-FTIR y TGA. Se determinó la viabilidad de *M. caribbica* después del proceso de *electrospinning* y durante 25 días de almacenamiento a 6 y a 25 ºC. Finalmente se evalúo la actividad antifúngica (inhibición de crecimiento micelial y germinación de esporas) frente a 6 hongos de interés comercial, *Botrytis cinerea*, *Penicillium digitatum*, *Penicillium italicum*, *Fusarium oxysporum*, *Trichothecium roseum*, *Colletotrichum gloeosporioides*.

Mediante la técnica SEM se observó que las soluciones de CG:PEO, FP:PEO y pululano mostraron nanofibras cilíndricas, lisas y homogéneas con un tamaño promedio de 719 ± 140 nm, 192 ± 50 nm y 137 ± 20 nm, respectivamente. Mediante ATR-FTIR se mostró que no había interacciones fuertes entre la levadura y los polímeros. En general, las nanofibras de pululano mostraron la más alta viabilidad de *M. caribbica*, aunado a ello éstas mostraron el mayor porcentaje de inhibición frente a los 6 hongos evaluados. Todas las fibras con *M. caribbica* mostraron efecto fungistático frente a la germinación de esporas. Estos resultados prometedores hacen de estas fibras una alternativa interesante para tratamientos postcosecha en el control de enfermedades fúngicas en frutas y vegetales.

Development of Antifungal Electrospun Nanofiber Mats Containing *Meyerozyma caribbica*

Yuliana Vázquez-González[1,2], Cristina Prieto[1,*], Montserrat Calderón-Santoyo[2,*], Juan Arturo Ragazzo-Sánchez[2], José M. Lagarón[1,*].

[1]Novel Materials and Nanotechnology Group, Institute of Agrochemistry and Food Technology (IATA), Spanish Council for Scientific Research (CSIC), Calle Catedrático Agustín Escardino Benlloch 7, 46980 Paterna, Spain; cprieto@iata.csic.es (C.P.); lagaron@iata.csic.es (J.M.L.); yuliana.vg04@gmail.com (Y.V.-G)

[2]Laboratorio Integral de Investigación de Alimentos, Tecnológico Nacional de México-Instituto Tecnológico de Tepic, Av. Tecnológico de Tepic, Av. Tecnológico #2595, C.P. 63175, Tepic, Nayarit, México; yuliana.vg04@gmail.com (Y.V.-G); montserratcalder@gmail.com (M.C.-S); arturoragazzo@hotmail.com (J.A.R.-S)

*Corresponding author: cprieto@iata.csic.es

Abstract

To mitigate vegetable and fruit loss caused by post-harvest fungal diseases, polymeric antifungal coatings encapsulating biocontrol yeasts offer a sustainable alternative. Nanofibers derived from pullulan, cashew gum, FucoPol and poly (ethylene oxide) (PEO), were electrospun and loaded with *Meyerozyma caribbica* (GenBank ID: JQ398674). The morphological, thermal and chemical properties of cashew gum (CG:PEO), FucoPol (FP:PEO), and pullulan nanofibers were characterized. The viability of *M. caribbica* within the fibers and their *in vitro* antifungal activity against six phytopathogens were assessed. Morphological analysis exhibited the presence of nanofibers encapsulating *M. caribbica*. Thermal analysis through TGA demonstrated the biopolymer´s capacity to offer thermal protection to the yeast. ATR-FTIR spectroscopy identified the absence of interactions between the yeast and polymers. Fibers containing *M. caribbica* exhibited *in vitro* fungistatic effects on spore germination. Pullulan nanofibers showed the highest *M. caribbica* viability and the highest percentage of growth inhibition against the evaluated fungi. These promising nanofibers encapsulating biocontrol yeasts could be used as edible coatings, which offer an alternative for post-harvest treatment to control fungal diseases, reducing global food loss.

Keywords: cashew gum, FucoPol, pullulan, electrospinning process, antifungal nanofibers, *M. caribbica*.

1. Introduction

Governmental and international organizations have raised public attention on food loss and waste, and according to the Sustainable Development Goals calls, the objective is to reduce these losses to the half by 2030 (United Nations 2015).

Fruits and vegetables are one of the most consumed commodities globally, accounting for more than 42% of total food wastage (Ganesh, Sridhar, and Vishali 2022). Among them, phytopathogens result in an annual estimated loss of 10–15% of the world's major crops (Peng et al., 2021). Particularly, the predominant postharvest pathogens responsible for spoilage in fruits and vegetables primarily include fungi categorized under the genera *Botrytis*, *Penicillium, Aspergillus, Alternaria, Colletotrichum* spp., and *Rhizopus* (Parafati et al., 2015; Yang et al., 2017), which are naturally present in fruits and vegetables. These pathogenic fungi use different mechanisms to bind to the surface of the host plant. In any case, the penetration of the fungal onto the plant requires the contact and adhesion of the spores to the plant surface. Fungi possess the capability to generate enzymes that modify the plant surface, thereby aiding in adhesion. Subsequently, these phytopathogens induce various forms of rot in the fruit during the post-harvest stage resulting in compromised quality and rendering them unsuitable for sale (Rodrigues et al., 2021). In addition, some fungi species are capable of producing mycotoxins in food and agricultural commodities (Zain, 2011), which can cause adverse health effects to humans and/or livestock.

Addressing these pathogens typically involves the application of chemical fungicides, both pre and post-harvest, directly onto the fruits or vegetables. Nevertheless, the utilization of chemical fungicides has revealed drawbacks such as their harmful impact on human health, the emergence of resistant strains, and their considerable adverse effect on the environment (Shi et al., 2021). Consequently, there has been substantial research devoted to the development of innovative environmentally friendly biocontrol methods (Zhang et al., 2018). Among these novel strategies, certain yeast taxa have garnered attention for their ability to rapid multiplication, synthesis of cell wall-degrading enzymes, induction of host tissue resistance, and production of plant growth promoters. To this extent, yeasts have been used to manage and control postharvest diseases, especially in fruits (El-Tarabily & Sivasithamparam, 2006). One example of these yeasts as biocontrol agents is *Meyerozyma*

caribbica, a yeast naturally present in fruits, which was isolated from mangoes for the first time by Bautista-Rosales et al. (2013), group that also elucidated the different action mechanisms of *M. caribbica* against phytopathogens such as *Colletotrichum gloeosporioides*. Subsequently, different authors have evaluated the antifungal properties of *M. caribbica* against *Colletotrichum gloeosporioides* in other food products such as avocado (González-Gutiérrez et al., 2021; Iñiguez-Moreno et al., 2020) and papaya (Aguirre-Güitrón et al., 2022). It is important to note that, one of the main characteristics of a biocontrol agent is its ability to control a variety of pathogens on different hosts (Droby et al., 2009). However, in order to use them at an industrial level, it is required to ensure their effectivity during their shelf-life and ease their handling. In this sense, the yeast encapsulation into a biopolymeric matrix could be an interesting alternative. Multiple encapsulation techniques are currently available; however, many of these techniques, such as spray drying or coacervation, use high temperature or toxic reactives, which can affect the yeast viability or are difficult to scale up (Anwar & Kunz, 2011). However, electrohydrodynamic technology could be an adequate encapsulation technology (Vázquez-González et al., 2022). Electrohydrodynamic processing, including electrospinning and electrospraying, uses a high-voltage electrostatic field to charge the surface of a polymer solution to produce ultrathin droplets that after solvent evaporation at room temperature form micro and nano structures. This technology does not require the use of temperature or toxic reactives and it is already available at industrial scale. Up to now, Aguirre-Güitrón et al. (2022) assessed the conditions to obtain polymeric microparticles encapsulating *M. caribbica* by an electrospraying process and maintaining its viability. However, the fibers produced by the electrospinning process display structural advantages such as large surface area to volume ratio, optimized diameters, shape and porosity characteristics, which are important for their function as carriers of bioactive ingredients (Haider et al., 2018). The incorporation of encapsulating biopolymers gives in enhanced stability, improved bioavailability of bioactive compounds and a controlled release (Castro Coelho et al., 2021). In this sense, the electrospinning process may be a suitable alternative for the encapsulation of *M. caribbica* into nanofibers in order to provide innovative applications in phytopathogens control. In addition, the use of novel biodegradable polymers can provide viable and environmentally friendly alternatives for agrochemical or food applications (Vázquez-González et al., 2021, 2022).

Therefore, the primary objective of this research was to produce nanofibers using various innovative biopolymers by electrospinning process encapsulating *M. caribbica* and to demonstrate their effectiveness as a potential post-harvest antifungal aid against fungi of commercial concern. The developed antifungal materials could be used in edible antifungal coatings for food or in agricultural applications to reduce food loss. For that purpose, growing interest on microbial polysaccharides has emerged due to the possibility to control microbial metabolism enables a constant production rate of products with low variability of their properties. In this sense, pullulan and FucoPol obtained from *Aureobasidium pullulans* and *Enterobacter* A47, respectively were selected for the *M. caribbica* encapsulation. On the other hand, emphasis has also placed on the natural product extracted in a sustainable and low-cost manner. Cashew gum is a hydrophilic polysaccharide derived from the exudate extracted from the *Anacardium occidentale* tree (Vasconcelos Silva et al., 2019). These polymers were selected due to their bio-based origin, biodegradability, and functional properties (Aceituno-Medina et al., 2013; Botrel et al., 2017; Ferreira et al., 2018; Vázquez-González et al., 2021). In addition, FucoPol and cashew gum exhibits properties that envisage a good potential for use as wall material in encapsulation processes of bioactive compounds (Lourenço et al., 2017; Silva et al., 2018). As previously reported by Grumi et al and Vázquez-González et al, pure cashew gum and FucoPol are not able to form nanofibers on their own by electrospinning process (Grumi, 2021; Vázquez-González et al., 2022), but they can form nanofibers if these polymers are blended with the minimum amount possible of a high molecular weight polymer such as poly (ethylene oxide) (PEO) to improve the formation of nanofibers as it forms hydrogen bonds between ether and hydroxyl groups of polysaccharides and it improves polymeric chain entanglements. The produced fibers were characterized in terms of morphological, thermal, chemical, and *in vitro* antifungal properties against spore germination and mycelial growth.

2. Materials and methods

2.1 Materials

Pullulan (Pul) (Mw ~ 2×10^5 g/mol) was purchased from Hayashibara CO., LTD. (Tokio, Japan), PEO (Mw ~ 4×10^5 g/mol), PEO (Mw ~ 5×10^6 g/mol), phosphate buffered saline (PBS), YPD broth (Yeast Extract Peptone Dextrose) and Span 20 were purchased from Sigma Aldrich (St. Louis, MO, USA), glycerol from PanReac AppliChem (Barcelona,

Spain). FucoPol (FP) (1.1×10^7 g/mol) was produced and purified using the same procedures described by Ferreira et al. (2016). The composition of FP was the same as reported by Vázquez-González et al. (2022). Cashew gum (CG) (2.13×10^4 g/mol) was obtained using the methodology previously described by Silva et al. (2018). The composition was the same as reported by Vázquez-González et al. (2021).

2.2 Antagonistic microorganism

M. caribbica (GenBank ID: JQ398674), isolated from "Ataulfo" mangoes (Bautista-Rosales et al., 2013), was preserved with 20% (v/v) glycerol at -80 °C; and subsequently reactivated in YPD broth. The yeast culture was incubated on a rotary shaker at 28 °C and 110 rpm for 48 h (Bautista-Rosales et al., 2013). Following this incubation period, the cells were collected, and the concentration was adjusted to 1×10^8 cells/mL.

2.3 Fungal strains and culture conditions

Colletotrichum gloeosporioides Pa14 (GenBank ID: MN477464) was isolated from decayed avocado fruit in Nayarit, Mexico (Bautista-Rosales et al., 2013). *Botrytis cinerea* CECT 20973 (BC03 Persoon 1794) was isolated from grapes. *Penicillium digitatum* CECT 21108 (NAV-7 (Persoon) Saccardo 1881) and *Penicillium italicum* CECT 21109 (MAV-1 Wehmer 1894) were isolated from harvested citrus fruit. *Fusarium oxysporum* CECT 20967 (Schlechtendal 1824) was isolated from the root of *Citrus macrophylla*. *Trichothecium roseum* CECT 20223 (Persoon) Link 1809) was isolated from *Diospyros kaki*. All these strains were obtained from the Spanish Type Culture Collection (CECT) from the Universidad de Valencia.

These strains were cultured on pre-filled plates of potato dextrose agar (PDA) (Scharlau, Barcelona, Spain). The strains obtained from CECT were incubated according to their optimal cultivation conditions for CECT strains, i.e., 24 ~ 26 ºC for 7-10 days. Whereas *Colletotrichum gloeosporioides* was cultivated at 28 ºC for 7-10 days.

2.4 Preparation of solutions with *Meyerozyma caribbica* to obtain nanofibers

In order to obtain nanofibers encapsulating *M. caribbica*, different polymeric solutions were used. Three biopolymers were selected, i.e., Pul, FP and CG. The solution of Pul was prepared with a concentration of 15% (w/w). The solution of FP:PEO was prepared using

FucoPol and PEO (Mw ~ 4×10^5 Da) to form nanofibers. However, the formulation of the FP:PEO solution to obtain electrospun nanofibers reported previously by Vázquez-González et al. (2022) has been adapted to encapsulate yeast. In this case, this solution was prepared at a concentration of 0.015 g/mL (ratio 1:2, w/w) with 5% of Span 20 (w/v) using sterile water as solvent. Finally, the solution of CG:PEO was prepared with PEO (Mw ~ 5×10^6 Da) at a concentration of 0.15 g/ml (ratio 5.6:1 w/w) with 1% of Span 20 (w/v) (Grumi, 2021). For this research, PEO with different molecular weights were used due to the mixture of CG:PEO was optimized previously by Grumi (2021). Sterile distilled water was used as solvent. Solutions were prepared in sterile conditions. Sterilization of biopolymers was performed by UV radiation for 30 min to avoid aggressive treatment. However, sterilization with the autoclave (Presoclave III 4001759, J.P. SELECTA, SA, Barcelona, Spain) at 120 ºC for 20 min was required for FP, since this biopolymer contained some residues from *Enterobacter* A47, and it was not possible to sterilize it using only UV radiation. Subsequently, *M. caribbica* was added to each polymeric solution, to give a final concentration of 1×10^8 cells/mL.

2.5 Physicochemical characterization

The solutions with/without *M. caribbica* were subjected to characterization based on electrical conductivity, apparent viscosity, and surface tension. Electrical conductivity was determined using a multiparameter potentiometer (Hanna Instruments HI-4521, Meltrose, MA, USA). Apparent viscosity was measured using a rotational viscosimeter, ROTAVISC lo-vi Complete (IKA, Wilmington, USA). Measurements were performed at 15, 48, and 15 rpm for Pullulan, CG:PEO and FP:PEO solutions, respectively at room temperature. Surface tension was measured with the Force tensiometer model K20 EasyDyne (Krüss GmbH, Hamburg, Germany), with the Wilhelmy plate method. All measurements were performed in triplicate at room temperature (Vázquez-González et al., 2021).

2.6 Electrospinning process

The electrospinning process was carried out using a Fluidnatek® LE-500 equipment from Bioinicia S.L. (Valencia, Spain). Various process conditions were evaluated to achieve a

stable production of continuous fibers containing viable *M. caribbica*. Once the conditions were determined, polymeric solutions containing *M. caribbica* were processed while neat polymeric solutions were used as a control.

For the solution of Pul, the electrospinning parameters were set as follows: a constant flow rate of 500 µL/h, a work distance of 20 cm, and a voltage of 9.7 kV at the injector, and -3 kV at the collector. For the solution of FP:PEO, the electrospinning parameters were as follows: a constant flow rate of 600 µL/h, a work distance of 15 cm, and a voltage of 19 kV at the injector and -1 kV at the collector. The solution of CG:PEO was processed with the following electrospinning parameters: a flow rate of 400 µL/h, a work distance of 28 cm, and a voltage of 20 and -7 kV for the injector and collector, respectively. A 23 gauge needle was used for all solutions. The ambient conditions were monitored and maintained at a temperature of 33 ºC and relative humidity of 28%.

2.7 Attenuated Total Reflectance Fourier Transform Infrared spectroscopy (ATR-FTIR)

ATR-FTIR spectroscopy was employed to investigate potential interactions between the different polymers comprising the nanofibers and *M. caribbica*. The analysis was conducted using a Bruker FTIR Tensor 37 equipment (Rheinstetten, Germany). The samples were positioned on the diamond crystal, and the low-temperature ATR sampling accessory Golden Gate from Specac Ltd (Orpington, UK) was used to ensure proper contact. Spectra were recorded within the wavenumber range of 4000-600 cm^{-1}, averaging 10 scans at a resolution of 4 cm^{-1}. The spectral data analysis was performed using Origin Pro, Version 2019 from OriginLab Corporation (Northampon, MA, USA) (Vázquez-González et al., 2022).

2.8 Scanning Electronic Microscopy (SEM)

The morphology of nanofibers obtained from Pul, CG:PEO, and FP:PEO, both with and without *M. caribbica*, was analyzed using a Hitachi-S-4800 FE-SEM (Hitachi High-Technologies Corporation, Tokyo, Japan) with an electron beam acceleration of 10 kV. The samples, weighing approximately 1.5 mg, were securely mounted on the sampler holder using double-sided carbon tape and the coated with a gold-palladium layer. The fiber diameter distribution was determined by analyzing at least 100 measurements per sample

using Image J Launcher v.1.41 software (National Institutes of Health, Bethesda, MD, USA). In this work, the term nanofiber refers to fibers that have a diameter size bellow the micron.

2.9 Conventional optical microscopy

The presence of *M. caribbica* inside the nanofibers was studied by conventional optical microscopy, for that, the nanofibers were encapsulated in LR-White resin in gelatin capsules and polymerized in a conventional drying stove between 55-60 ºC for 24 h. The blocks were cut to 2 µm with a Diatome diamond blade in an ultramicrotome (UC7, Leica, Wetclar, Germany). To observe the cuts, they were stained with toluidine blue, and the samples were visualized using a conventional microscope (Eclipse 90i, Nikon Instruments Inc., New York, USA).

2.10*In vitro* antifungal assays of nanofibers with *M. caribbica*

2.10.1 Viability of *M. caribbica* after electrospinning process

The nanofibers were collected in sterile tubes after the electrospinning process. The amount of the nanofibers was calculated according to the percentage of solids contained in the polymer solution including the weight of polymers and weight of dried yeast. 1 g of nanofibers was mixed with sterile distilled water in flasks for 1 h. After that, serial dilutions were prepared and 100 µL of sample was spread on YPD Petri dishes. The number of *M. caribbica* colonies were counted after 48 h incubation at 28 °C. Analyses were performed in triplicate for each treatment and the experiment was repeated three times.

2.10.2 *In vitro* inhibition of spore germination of nanofibers with *M. caribbica*

The inhibition of spore germination was determined according to Iñiguez-Moreno et al. (2020) with some modifications. Spore suspension was prepared using PBS, and 10 mL of the suspension was added to each plate to collect the fungus. The agar surface was gently rubbed with a sterile inoculation loop to obtain the spore suspension, which was then filtered through sterile gauze and collected in a falcon tube. The spore concentration was adjusted to 1×10^5 spores/mL by counting under a microscope using a hemocytometer. Fifty microliter

of fungal spores (1×10^5 spores/mL) were spread on PDA disks (1.4 cm) and allowed to dry for 5 minutes in a cabinet. Subsequently, the disks were covered with nanofibers containing *M. caribbica* (Pul, FP:PEO, and CG:PEO). The disks were then incubated under the cultivation conditions specific to CECT strains (24-26 ºC) for 7-10 days. After the incubation period, the nanofibers were absorbed by the PDA disks.

The germination percentage of each evaluated fungus was determined using conventional microscopy. The percentage of germinated spores was measured after 24 h at 26 ºC for *B. cinerea*, after 9 h at 25 ºC for *P. digitatum* and *P. italicum*, after 6 h at 26 ºC for *F. oxysporum*, after 6 h at 25 ºC for *T. roseum,* and after 9.5 h at 25 ºC for *C. gloeosporioides*. In the control group, a minimum of 200 germinated spores was considered. Spores were considered germinated when the length of the germ tube was equal or longer than the spore diameter.

2.10.3 *In vitro* inhibition of mycelial growth of nanofibers with *M. caribbica*

The electrospun materials developed were thought as an edible coating or agricultural aid to fight against pathogenic fungi. The action of this antifungal coating is by direct contact with the fruit, vegetable or plant, allowing the yeast to develop its mechanisms of action against phytopathogens, such as the competition for nutrients and space or the production of volatile compounds. For that reason, an inhibition of mycelial growth test on PDA plates was performed taking into account the growth conditions of each studied fungus (Aguirre-Güitrón et al., 2022; Iñiguez-Moreno et al., 2020).

A total of 100 µL of fungal spores (1×10^5 spores/mL) where evenly spread in the center of each Petri dish and allowed to dry for 5 min in a cabinet. Then, the inoculated PDA Petri dishes were covered with nanofibers containing *M. caribbica* (Pul, FP:PEO, and CG:PEO), which were obtained through the electrospinning process.

Growth diameter was registered for 6 days at 24 ºC for *B. cinerea*, for 8 days at 25 ºC for *P. digitatum*, for 8 days at 25 ºC for *P. italicum*, for 6 days at 26 ºC for *F. oxysporum*, for 8 days at 25 ºC for *T. roseum* and for 7 days at 28 ºC for *C. gloeosporioides*. The percentage of the inhibition of mycelial growth was calculated according to equation 1:

$$Inhibition\ (\%) = \left[\frac{dc-dt}{dc}\right] x\ 100 \qquad Eq.\ 1$$

Where *dc* (cm) is the mean of colony diameter for the control sets and *dt* (cm) is the mean of colony diameter for the different treatments. All tests were done in triplicate. All Petri dishes were covered with parafilm to avoid dehydration.

For both assays, inoculated and uncoated PDA Petri dishes and inoculated and coated with nanofibers without *M. caribbica* PDA Petri dishes were used as control.

2.11 Statistical analysis

The data obtained from the experiment were subjected to statistical analysis using an analysis of variance (ANOVA) test, with a significance level set at $P < 0.05$. For the comparison of means, the Fisher test was employed. The statistical analysis was performed using STATISTICA 12 software (Statsoft Inc., Tulsa, OK, USA).

3 Results and Discussion

3.1 Physicochemical characterization

The physicochemical analysis of the solutions was conducted to assess their suitability for electrospinning. Consequently, both solutions with and without *M. caribbica* yeast were examined. Results are presented in Table 1.

The apparent viscosity of the polymeric solution is an interesting parameter that provides preliminary information about the electrospinnability of a polymeric solution and also is related to the size of the obtained fibers. Samples prepared with Pul showed the lowest apparent viscosity, being this value in concordance with the value reported by other authors for similar concentration (Aguilar-Vázquez et al., 2018) Samples prepared with CG and FP showed larger viscosities, which could affect fiber diameter and the stability of the electrospinning process. Same behavior was observed when PEO was added to CG (Grumi, 2021) and FP solutions (Vázquez-González et al., 2022). The CG solution presented a pseudoplastic behavior, phenomenon previously reported by other authors (Ribeiro et al., 2016). However, FP:PEO solution showed reduced apparent viscosity values in comparison to the values presented before by Vázquez-González et al. (2022) probably due to the lower PEO content in the polymeric solution, the use of water as solvent instead of ethanol, and

also to a possible thermal degradation during the sterilization in the autoclave. The addition of *M. caribbica* to the polymeric solutions did not suppose a significant difference in apparent viscosity, probably due to the low amount of yeast added, as shown in Table 1.

Regarding surface tension, the values of CG:PEO and FP:PEO were found within the surface tension range to have a stable electrospinning process (Vázquez-González et al., 2021, 2022). It is worth mentioning that CG:PEO and FP:PEO solutions showed low surface tension values as a consequence of the content of Span 20 surfactant (1% and 5%, respectively). However, the surface tension of the Pul solution was close to the surface tension of the water, which could affect the stability of the process and the morphology of the obtained fibers. The addition of *M. caribbica* to the polymeric solution had no or little effect in surface tension in the case of CG:PEO and FP:PEO solutions, being more significant in the case of Pul, which could have an effect on the stability of the process.

On the other hand, regarding the conductivity, polymeric solutions showed low conductivity values, being larger in those samples with PEO. The addition of *M. caribbica* showed a significant increase in conductivity in comparison with solutions without yeast (Table 1). This effect was observed by other authors. Aguirre-Güitrón et al. (2022) and Mojaveri et al. (2020) observed an increase in conductivity when adding *M. caribbica* and *Bifidobacterium animalis* subsp *lactis* Bb12, respectively to the polymeric solutions. This increase in conductivity may be due to the presence of different compounds in the cell wall such as a variety of charged ions (Na, K, Ca, and other ions) and biological macromolecules (nucleic acids, amino acids proteins, and other polymers) in the form of dipoles exist in the cells (Zhou et al., 2014). Although conductivity increased by adding *M. caribbica* to the different solutions, the conductivity values were still found in the established conductivity range so that polymeric solutions are suitable for the electrospinning process (Vázquez-González et al., 2021, 2022).

Table 1. Physicochemical characterization of different polymeric solutions without and with *M. caribbica.*

Sample	Apparent Viscosity (cP)	Surface Tension (mN/m)	Conductivity (mS/cm)
Pul	878.40 ± 4.82 b	64.10 ± 0.20 b	0.023 ± 0.000 f
CG:PEO	5747.00 ± 116.77 a	32.80 ± 0.60 c	0.738 ± 0.003 d
FP:PEO	1091.33 ± 458.10 b	28.80 ± 0.20 e	1.140 ± 0.012 c
Pul + *M. caribbica*	606.26 ± 3.36 b	69.40 ± 0.20 a	0.582 ± 0.000 e
CG:PEO + *M. caribbica*	5178.00 ± 691.31 a	31.50 ± 0.60 d	1.219 ± 0.041 b
FP:PEO + *M. caribbica*	746.53 ± 29.40 b	28.20 ± 0.20 e	1.731 ± 0.004 a

* Each column represents the mean ± standard deviation of three independent replicas. Different letters in each column indicate significant difference ($P < 0.05$).

** Pul and FP:PEO solutions were Newtonian solutions, whereas CG:PEO was pseudoplastic. The values shown are the average and standard deviation of the measurements performed at 48 rpm.

3.2 Morphology properties

The fibers obtained with CG:PEO without and with *M. caribbica* (Figure 1a and 1b, respectively) showed smooth and uniform structures. Both samples showed diameter size of 719 ± 140 nm, and no difference in diameter size between nanofibers with yeast and without yeast was found since yeasts were positioned in specific places inside of the fiber. Furthermore, FP:PEO fibers, without and with yeast, showed smooth and uniform structures. However, these fibers were smaller than the CG:PEO nanofibers, 192 ± 50 nm, (Figure 1c and 1d, respectively). As it is well known, the size of nanofibers is determined by both the solution and the operation parameters. In this case, the voltage used for CG:PEO and FP:PEO was similar (20, -7 kV and 19, -1 kV, respectively). However, the total solids content and the apparent viscosity were higher for the CG:PEO solution than in the FP:PEO, which could explain the difference in fiber diameter (Deitzel et al., 2001).

Pul fibers without and with yeast resulted in the smallest diameter (137 ± 20 nm, Figure 1e and 1f, respectively). In addition, Pul showed thin, smooth, and well-defined nanofibers with the presence of some beads (Figure 1e), which could be due to the high surface tension of the solution. Similar results were already reported by several authors (Aceituno-Medina

et al., 2013; Xiao & Lim, 2018), which could be related to the reduced apparent viscosity in comparison with the previous solutions.

In this particular case, nanofibers are preferred to microfibers because they create membranes with a higher degree of porosity, allowing the permeability of volatiles and water vapour produced during the ripening of fruits and vegetables.

Figure 1b, 1d and 1f, showed the presence of *M. caribbica* inside the nanofibers. The encapsulation of the yeast inside the nanofiber during the electrospinning process occurs due to the combination of the uniaxial extensional flow and the surface charges caused by the high voltage electrostatic field applied that attract the high molecular weight molecules to the surface of the solution (de Jesús et al., 2005; Torres-Giner et al., 2016). In the polymeric solution containing *M. caribbica*, the droplet undergoes elongation to form the fiber. The presence of yeast leads to the complete coating of the yeast by the polymer. Subsequently, the fiber formation continues. In this sense, it is clear that only polymers with high molecular weights with enough intermolecular chain entanglements, which can provide viscoelastic properties, would allow the yeast encapsulation (Torres-Giner et al., 2008) .

Additionally, the micrographs obtained by SEM showed that the encapsulation of *M. caribbica* was similar to the encapsulation of probiotics in nanofibers from chitosan/poly (vinyl alcohol) obtained by electrospinning process (Mojaveri et al., 2020).

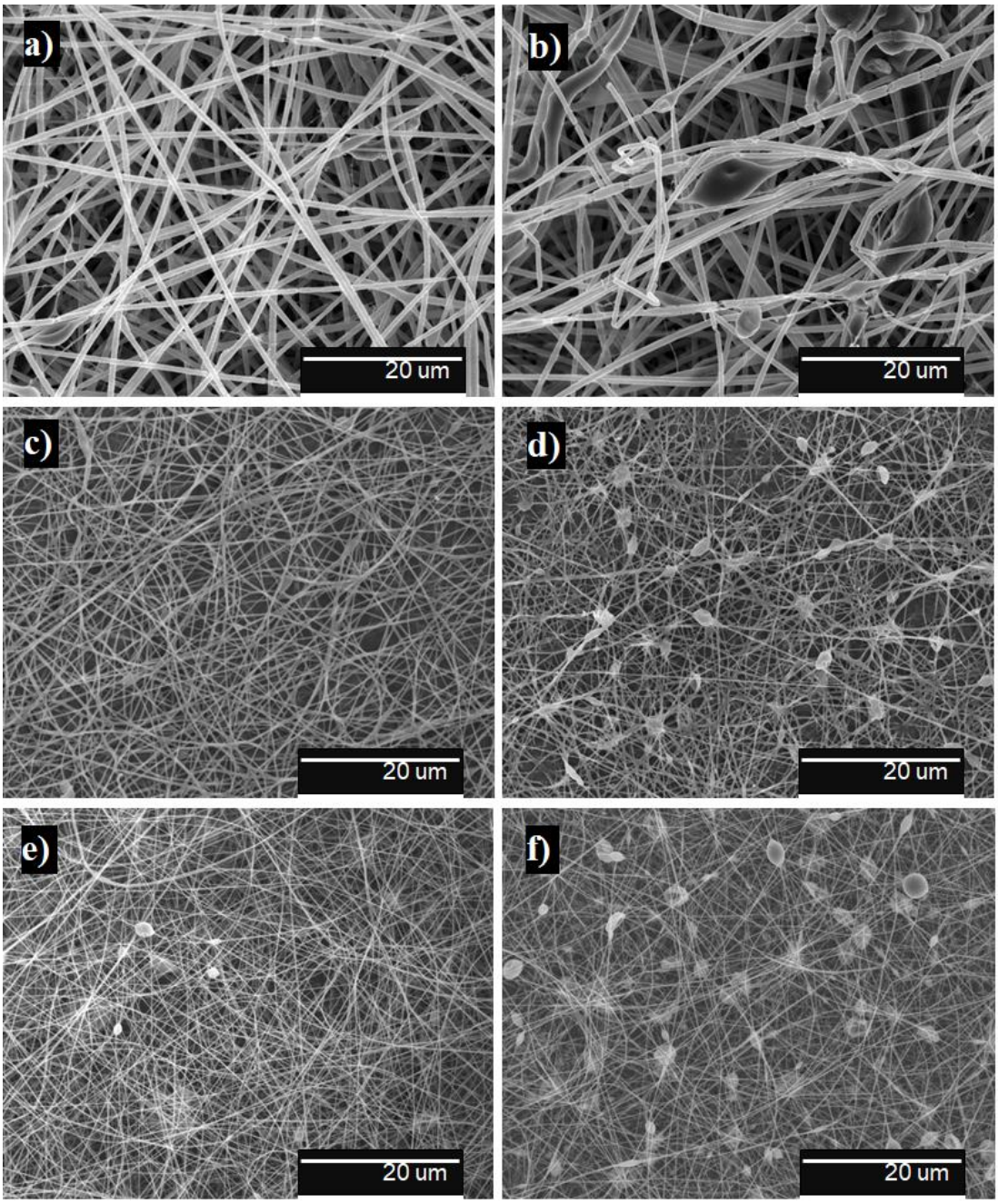

Figure 1. SEM micrographs of the biopolymeric nanofibers obtained by electrospinning. a) CG:PEO nanofibers, b) CG:PEO nanofibers with *M. caribbica*, c) FP:PEO nanofibers, d) FP:PEO nanofibers with *M. caribbica*, e) Pul nanofibers, and, f) Pul nanofibers with *M. caribbica*. Scale bars correspond to 20 µm.

3.3 Distribution of *M. caribbica* inside the nanofibers

The staining of the ultramicrotome cut of the nanofibers with toluidine blue was performed to confirm the presence of the yeast inside the nanofibers, and to differentiate the presence of yeasts from the possible beads formed by the electrospinning process, since the main function of this dye is to selectively dye acid components present in tissues, such as sulfates and phosphate radicals incorporated into the DNA and RNA of cells (Sridharan & Shankar, 2012).

Figure 2 shows the images of the nanofibers encapsulating *M. caribbica*. As it can be appreciated, small, pigmented spots were observed inside the nanofibers, which corresponded to the yeast, and therefore, this confirms the yeast encapsulation into the nanofibers. In addition, it was observed that the yeasts were not placed continuously within the nanofibers.

3.4 Storage stability

The viability of *M. caribbica* in Pul, FP:PEO, and CG:PEO nanofibers was evaluated after the electrospinning process and every 5 days, during 25 days at 6 and 25 ºC. Results are shown in Figure 3. According to this figure, after the electrospinning process, the viability of *M. caribbica* was higher in Pul and FP:PEO nanofibers than in CG:PEO nanofibers. It could be due to obtain CG:PEO nanofibers a high voltage was applied. To obtain the nanofibers of Pul, the applied voltage was 9.7, -3 kV, while, for CG:PEO and FP:PEO, was, 20, -7 kV and 19, -1 kV, respectively. This decrease in cell viability could be due to the electroporation provoked when cell membranes and cell organelles are exposed to electric fields (Guo et al., 2021), which generates hydrophilic pores in the cell membrane increasing the permeability (Novickij et al., 2016). Guo et al. (2021) reported that the nanometer pores start to appear in the dielectric lipid membrane when the transmembrane potential exceeds the threshold, resulting in a leakage of intracellular compounds and cell llysis.

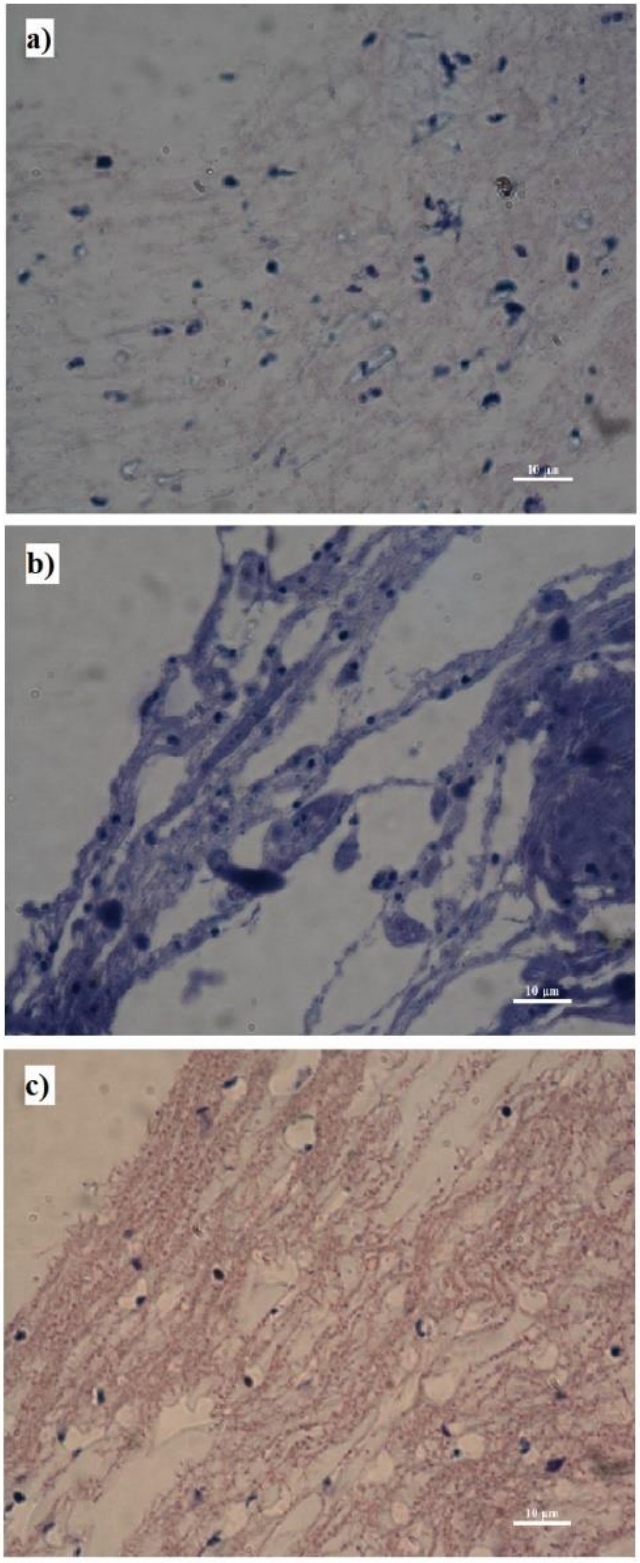

Figure 2. Observation of a) CG: PEO, b) FP:PEO, and c) Pul nanofibers with *M. caribbica* by means of an optical microscope. Images were taken at the scale of 10 µm with a magnification of 80X.

Regarding the storage stability of the yeast at the two storage temperatures, it was observed that the cell density was more affected during storage at 6 ºC than at 26ºC. However, at both temperatures, the loss of viable cells was more visible in CG:PEO and FP:PEO nanofibers as a function of storage time than in Pul nanofibers, although a decrease in the viability of *M. caribbica* in Pul nanofibers was also observed. Nevertheless, Pul nanofibers maintained a higher cell density at both temperatures for the 25 days of evaluation (2.36×10^5 CFU/g and 8.38×10^6 CFU/g, respectively).

In this case, it could be hypothesized that the reduction in cell density in the CG:PEO and FP:PEO nanofibers was due to the fact that the yeast suffered damage after exposure to high voltages. This damage weakens the cell membrane. This phenomenon combined with the storage conditions may have influenced the decrease in cell density.

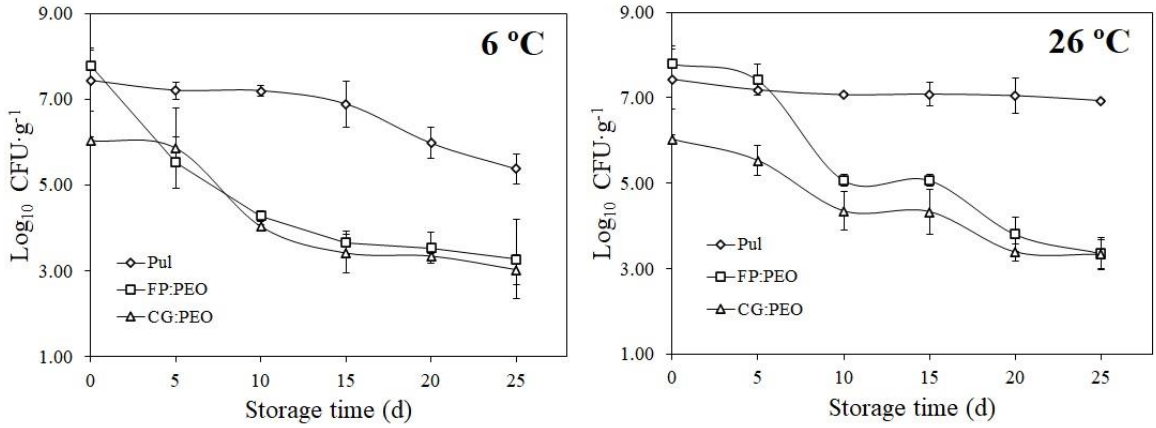

Figure 3. Storage stability of *M. caribbica* in Pul, FP:PEO, and CG:PEO nanofibers obtained by electrospinning process evaluated at 6 and 26 ºC for 25 days. Each point represents the mean ± standard deviation (n = 4).

3.5 ATR-FTIR analysis

Polymeric nanofibers with and without *M. caribbica* were evaluated by ATR-FTIR, and the obtained spectra are shown in Figure 4. FP:PEO nanofibers (Figure 4a) showed also a broad intense band around 3300 cm^{-1} ascribed to the O – H stretching of hydroxyls and bound water (Synytsya et al., 2003) and a band at 2940 cm^{-1} corresponding to the C – H stretching peak

of CH_2 groups. The band at 1720 cm^{-1}, is attributed to the C = O stretching of carbonyls in acyl groups. In the same way, the strong bands at 1607 and 1405 cm^{-1}, can be attributed to the asymmetric and symmetric stretching of carboxylates, respectively (Synytsya et al., 2003). The band at 1250 cm^{-1} may also be attributed to the C – O – C vibration of acyls (Freitas et al., 2011). Bands shown at 1200 and 900 cm^{-1} represent skeletal C – O and C – C vibration bands of glycosidic bonds and pyranoid rings (Synytsya et al., 2003).

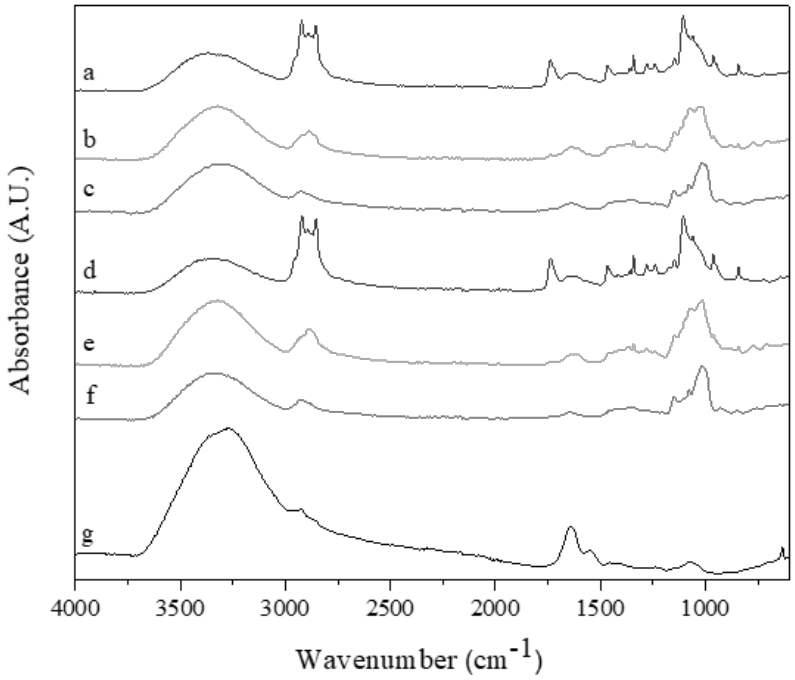

Figure 4. ATR-FTIR spectra of a) FP:PEO nanofibers, b) CG:PEO nanofibers, c) Pul nanofibers and d), e) and f) FP:PEO, CG:PEO and Pul nanofibers with *M. caribbica*, respectively, g) *M. caribbica*.

CG:PEO nanofibers (Figure 4b) showed a broad intense band around 3300 cm^{-1} ascribed to the O – H stretching of hydroxyls and bound water (Synytsya et al., 2003). This band overlaps in part with the C – H stretching peak of CH_2 groups appearing at 2912 cm^{-1}. These nanofibers also showed an absorption peak at 1635 cm^{-1}, due to O-H vibrations from bound water molecules, and a band at ca. 1620 cm^{-1}, attributed to the carboxylate group. The

peaks at 1137, 1060 and 1010 cm^{-1} were due to stretching vibrations of C-O-C from glycosidic bonds and O-H bending of alcohols (da Silva et al., 2009; Vázquez-González et al., 2021).

Pul nanofibers (Figure 4c) showed characteristic bands at 752, 924 and 1150 cm^{-1} assigned to α-1,6 glycosidic bonds, respectively. The peak between 1200 and 1030 cm^{-1} was assigned to the C-O stretching vibration. The band around 2923 cm^{-1} corresponded to the C-H stretching. A broad peak located around 3331 cm^{-1} was attributed to O-H stretching (Aceituno-Medina et al., 2013).

The *M. caribbica* spectrum is shown in Figure 3g. Regions from 950 to 1200 cm^{-1} are characteristic peaks of polysaccharides, they represent the sugars contained in the matrix. Band at 1420 cm^{-1} indicates the presence of β-glucan mainly contained in the cellular wall of yeasts. Also, there were bands at 1400-1750 cm^{-1}, attributed to the presence of proteins principally mannoprotein and chitin in the yeast layer. The band at ca. 3300 cm^{-1} is attributed to the OH stretching vibration of hydroxyls (Liu et al., 2021; Piotrowska & Masek, 2015) .

There was not significant difference between polymeric nanofibers and polymeric nanofibers with *M. caribbica*. This can be attributed to the relatively low percentage of yeast present in each polymeric solution (CG:PEO, 7.25%, Pul, 8.25% and FP:PEO, 23.06%). These percentages were calculated as the percentage of yeast with respect to the solids concentration of the polymeric solutions to adjust the final yeast concentration of 1×10^8 CFU/mL. In addition, *M. caribbica* showed bands and peaks at the same wavelength as the stretching of the functional groups of polymer mixtures, suggesting that the bands of *M. caribbica* were superimposed.

3.6 Antifungal *in vitro* growth assay

3.6.1 Inhibition of mycelial growth

Inhibition of mycelial growth is shown in Figure 6 and Figure 7, corresponding to visual observation and inhibition percentage, respectively. For visual observation, only the results of Pul are shown, as mentioned above, Pul nanofibers showed the greatest viability of

M. caribbica even after 25 days of storage at both evaluated temperatures (Figure 3), and these nanofibers showed the highest inhibition percentage against the 6 different fungi (Figure 7).

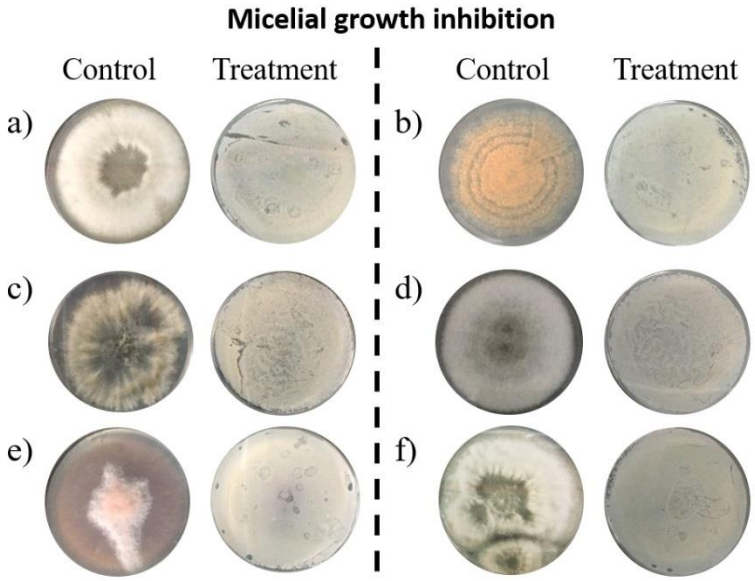

Figure 5. Visual inhibition of mycelial growth caused by Pul nanofibers against 6 different fungi. a) *P. italicum*, b) *T. roseum*, c) *B. cinerea*, d) *C. gloeosporioides*, e) *F. oxysporum* and f) *P. digitatum*. The treatment column refers to the yeasts released from Pul nanofibers.

All polymeric nanofibers with *M. caribbica* after 48 h with 95% relative humidity in a closed environment (Petri dishes with medium Potato Dextrose Agar, PDA) were solubilized releasing *M. caribbica* colonizing Petri dishes. Controls, this is polymeric nanofibers without *M. caribbica,* did not show antifungal activity (results not shown). Therefore, *M. caribbica* did not allow the development of the studied fungi. In the case of *P. italicum* and *P. digitatum*, their mycelium did not fully develop, indeed it showed a slight growth of hyphae compared to controls where a normal growth of a thick mycelium occurred (Figure 6a). This behavior could be attributed to the production of toxins or some enzymes by *M. caribbica*, since it has been reported that, these metabolites could deform the fungal mycelium and could inhibit the fungi spore's germination (Papoutsis et al., 2019). *M. caribbica* has been shown to have

several mechanisms of action against phytopathogens (Bautista-Rosales et al., 2013). However, the competition for nutrients and space are more frequently reported as the prevalent modes of action of yeasts, although other mechanisms were also reported such as the production of volatile compounds (González-Gutiérrez et al., 2021; Iñiguez-Moreno et al., 2020). In addition, more than one mechanism of action may take place at the same time, resulting in a more efficient control of phytopathogens.

On the other hand, unlike *P. italicum* and *P. digitatum*, *T. roseum* and *F. oxysporum* showed an orange and violet spot, respectively without development of mycelium. The pigments shown are characteristic of these fungi and are mostly determined by melanin that accumulates in fungal cell walls and plays vital roles in fungal survival in case of damaging events (Wang et al., 2021).

Additionally, the presence of melanin in the inner layer of appressoria is also indispensable for the build-up of turgor pressure and for the driving force that enables fungi to mechanically break through the host tissue. To this extent, it was observed that the presence of *M. caribbica* decreased melanin production of fungi, thereby, affecting the development of phytopathogens since it has been reported that melanin biosynthesis is vital for the maturation and normal development of the fungal mycelium in different fungi species (Liang et al., 2018).

Figure 7 shows the percentage of inhibition of mycelial growth of different nanofibers against fungi. The inhibition of fungi growth is a complex phenomenon that it is affected by multiple factors:

1. *The type of phytopathogen*: Different results were obtained for the different fungi studied, which could be related with the compatibility of the yeast with the phytopathogen due to factors such as the composition of the cell membrane (glycoproteins, chitin and glucans), the pathogenicity, secretory vesicles transportation, and infectious structures (Hua et al. 2018; Wei et al., 2018).
2. *Viability of the yeast in the nanofibers membrane* (shown in section 3.4). The inhibition test (results shown in Figure 7) was performed during between 6 or 8 days depending on the type of phytopathogen. In this time period, Pullulan was the

formulation that ensured the stability of the yeast during longer storage times at the temperatures of the test. This fact explains the results obtained for Pullulan for all tested fungi, being better than FucoPol:PEO and CG:PEO.

3. *The effect of the polymeric matrix*. Pullulan, cashew gum and FucoPol do not have an antifungal activity (results not shown), however, they can have a role in the competition between yeast and fungi for nutrients or in the generation of volatile compounds (Bautista-Rosales et al., 2013; González-Gutiérrez et al., 2023; Iñiguez-Moreno et al., 2020). This is an interesting aspect that needs to be studied more in depth, and we will focus on it on future works.

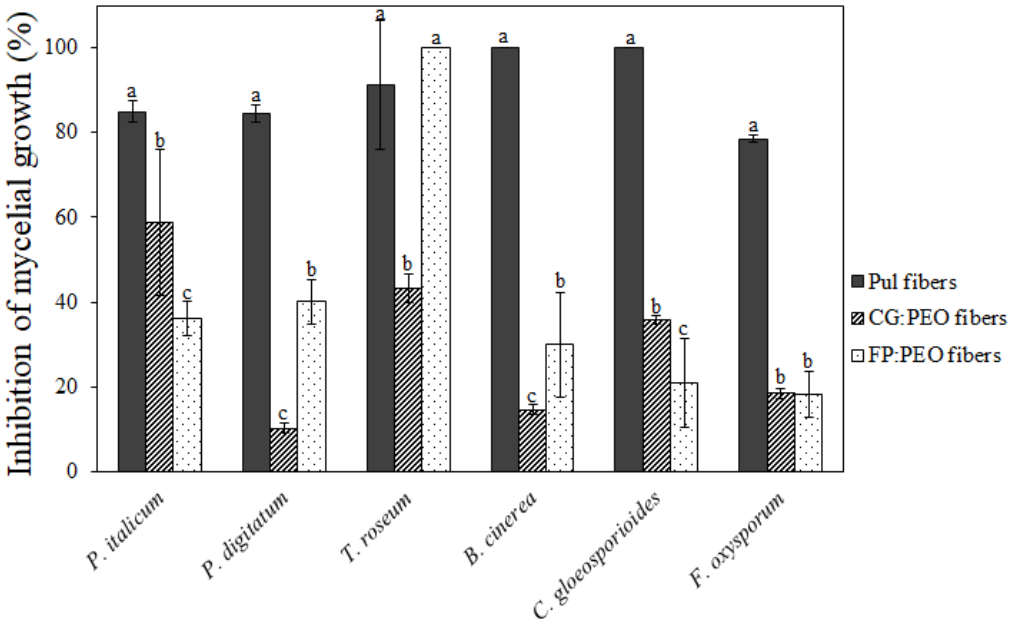

Figure 6. Percentage of inhibition of mycelial growth of different nanofibers against fungi. Error bars indicate standard errors of the means of three repeated experiments. Different letters above the bars indicate significant difference for each fungus according to Fisher LSD range test (p<0.05).

Regarding the nanofibers of CG:PEO and FP:PEO, it was evident that the low percentage of inhibition against fungi was due to the low viability of *M. caribbica* in

nanofibers after electrospinning process. In this sense, it can be hypothesized that a concentration of viable cells lower than 1×10^7 CFU/g will not be enough to inhibit completely the growth of these phytopathogens.

The yeasts have the capacity to colonize surfaces such as fruits' surfaces, which depends on the adaptation to assimilate the necessary carbon sources, mainly saccharose, fructose, and glucose, among others, for survival and multiplication, limiting carbohydrate and amino acids disposition for the phytopathogen fungus (Carmona-Hernandez et al., 2019; Romero et al., 2022). In addition, one characteristic of yeast is non-demanding of specific nutrients. In this sense, nutrients for sustaining yeast after application on fruit surface will be available. Even if these results are very promising, in vivo tests in a model fruit or vegetable will be required.

3.6.2 Inhibition of spore's germination

Inhibition of spore germination is shown in Figure 8. Overall, all treatments showed a fungistatic effect, since after the spore germination time, the spores with the treatment germinated. The results showed by the mycelial growth inhibition assay confirmed the fungistatic effect, as the fungus developed after 24 h.

In this case, FP:PEO nanofibers showed the highest percentage spores germination inhibition (*P. italicum*, 84.2 ± 4.6%, *P. digitatum*, 82.5 ± 3.5% and *T. roseum*, 100.0 ± 1.8%) in comparison with CG:PEO and Pul nanofibers. This phenomenon was caused by the nutrient's depletion provided by yeast, which limits the germination of fungal spores (Bautista-Rosales et al., 2013; Zhang et al., 2020). Additionally, Iñiguez-Moreno et al. (2020) found that the main VOC´s emitted by *M. caribbica* include ethanol, ethyl acetate, isobutyl alcohol, 1-butanol, 3-methyl, 2-methyl, isoamyl acetate, and phenethyl alcohol, suppressed the mycelial growth and sporulation, due to damage to the DNA and cell membranes (Zhang et al., 2020). However, despite the high percentage of spore inhibition, it was not enough to avoid the development of the fungus after the evaluated time.

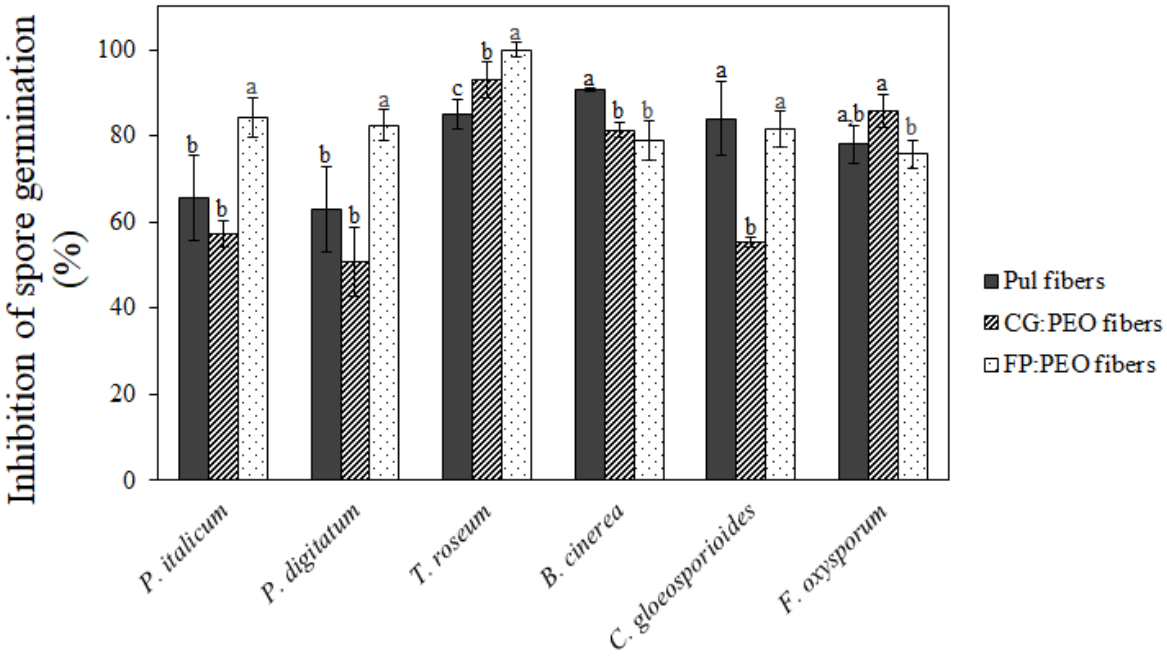

Figure 8. Percentage of inhibition of spore's germination of different fibers against fungi. Error bars indicate standard errors of the means of three repeated experiments. Different letters above the bars indicate significant difference for each fungus according to Fisher LSD range test (p<0.05).

4 Conclusions

Nanofibers of CG:PEO, FP:PEO and Pul encapsulating *M. caribbica* were obtained by the electrospinning process. SEM analysis showed smooth and homogeneous nanofibers, completely covering the yeast *M. caribbica*. CG:PEO, FP:PEO and Pul fibers showed an average size of 719 ± 140 nm, 192 ± 50 nm and 137 ± 20 nm, respectively. Pul nanofibers showed the highest viability of *M. caribbica*, persistent even after 25 days at 26 ºC (8.38×10^6 CFU/mL). For this reason, Pul nanofibers showed the highest antifungal inhibition percentage against the 6 tested fungi. In addition, all the 3 different polymeric nanofibers showed a fungistatic effect against the spores. ATR-FTIR analysis did not show any strong interactions between *M. caribbica* and the used polymers since no peak displacement was observed. TGA analysis confirmed that the thermal stability of the polymeric nanofibers was not affected by the addition of *M. caribbica*. These promising results make biopolymeric electrospun nanofibers a viable alternative to produce biocontrol tools, such as a protective

antifungal coating on the surface of fruits or for agricultural applications. However, other studies are required to evaluate *in vivo* the potential of this novel material, paying special attention to the antifungal properties, the interaction between the polymers (CG:PEO, FP:PEO and Pul) and the surface of the fruits, and the effect of the coating on fruit quality parameters. Additionally, the evaluation of the kinetics of yeast release from nanofibers into the surface of the fruit and the effect of polymer matrix on the antifungal activity of the yeast will be of great interest.

Author Contributions: Conceptualization Y.V.G., C.P., and J.M.L.; data curation, formal analysis, investigation and methodology was carried out by Y.V.G., writing-original draft preparation and writing-review and editing was performed by Y.V.G., C.P., M.C.S., J.A.R.S and visualization, supervision, project administration, funding acquisition was carried out by J.M.L.

Funding: This work was supported by the CYTED thematic network (code 319RT0576), the Agencia Valenciana de Innovación (AVI), projects INNEST/2022/25 and AGROALNEXT/2022/058, the grant PID2021-128749OB-C31 funded by MCIN/AEI/10.13039/501100011033 and by ERDF A way of making Europe,

Acknowledgments: Yuliana Vázquez González thanks Consejo Nacional de Ciencia y Tecnología for the scholarship awarded with number 862248. C. Prieto wants to thank the Valencian Ministry of Innovation, Universities, Science and Digital Society for her postdoctoral grant (CIAPOS/2021/45). The authors thank Dr. Atanu Biswas for the donation of cashew gum. Allow us to also thank to Chemical Department of the Nova University for the donation of FucoPol to carry out this research.

Conflicts of Interest: The authors declare no conflict of interest.

5. References

Aceituno-Medina, M., Lopez-Rubio, A., Mendoza, S., & Lagaron, J. M. (2013). Development of novel ultrathin structures based in amaranth (Amaranthus hypochondriacus) protein isolate through electrospinning. Food Hydrocolloids, 31(2), 289–298. https://doi.org/10.1016/j.foodhyd.2012.11.009

Aguilar-Vázquez, G., Loarca-Piña, G., Figueroa-Cárdenas, J. D., & Mendoza, S. (2018).

Electrospun fibers from blends of pea (Pisum sativum) protein and pullulan. Food Hydrocolloids, 83, 173–181. https://doi.org/10.1016/j.foodhyd.2018.04.051

Aguirre-Güitrón, L., Calderón-Santoyo, M., Lagarón, J. M., Prieto, C., & Ragazzo-Sánchez, J. A. (2022). Formulation of the biological control yeast Meyerozyma caribbica by electrospraying process: effect on postharvest control of anthracnose in mango (Mangifera indica L.) and papaya (Carica papaya L.). Journal of the Science of Food and Agriculture, 102(2), 696–706. https://doi.org/10.1002/jsfa.11400

Anwar, S. H., & Kunz, B. (2011). The influence of drying methods on the stabilization of fish oil microcapsules: Comparison of spray granulation, spray drying, and freeze drying. Journal of Food Engineering, 105(2), 367–378. https://doi.org/10.1016/j.jfoodeng.2011.02.047

Bautista-Rosales, P. U., Calderon-Santoyo, M., Servín-Villegas, R., Ochoa-Álvarez, N. A., & Ragazzo-Sánchez, J. A. (2013). Action mechanisms of the yeast Meyerozyma caribbica for the control of the phytopathogen Colletotrichum gloeosporioides in mangoes. Biological Control, 65(3), 293–301. https://doi.org/10.1016/j.biocontrol.2013.03.010

Botrel, D. A., Borges, S. V., Fernandes, R. V. de B., Antoniassi, R., de Faria-Machado, A. F.,Feitosa, J. P. de A., & de Paula, R. C. M. (2017). Application of cashew tree gum on the production and stability of spray-dried fish oil. Food Chemistry, 221, 1522–1529. https://doi.org/10.1016/j.foodchem.2016.10.141

Carmona-Hernandez, S., Reyes-Pérez, J. J., Chiquito-Contreras, R. G., Rincon-Enriquez, G., Cerdan-Cabrera, C. R., & Hernandez-Montiel, L. G. (2019). Biocontrol of postharvest fruit fungal diseases by bacterial antagonists: A review. Agronomy, 9(3). https://doi.org/10.3390/agronomy9030121

Castro Coelho, S., Nogueiro Estevinho, B., & Rocha, F. (2021). Encapsulation in food industry with emerging electrohydrodynamic techniques: Electrospinning and electrospraying – A review. Food Chemistry, 339(August 2020), 127850. https://doi.org/10.1016/j.foodchem.2020.127850

da Silva, D. A., Feitosa, J. P. A., Paula, H. C. B., & de Paula, R. C. M. (2009). Synthesis and characterization of cashew gum/acrylic acid nanoparticles. Materials Science and Engineering C, 29(2), 437–441. https://doi.org/10.1016/j.msec.2008.08.029

de Jesús, T., Guadarrama-Medina, T. J., Pérez-González, J., & de Vargas, L. (2005). Enhanced melt strength and stretching of linear low-density polyethylene extruded under strong slip conditions. Rheologica Acta, 44(3), 278–286. https://doi.org/10.1007/s00397-004-0409-0

Deitzel, J. M., Kleinmeyer, J., Harris, D., & Beck-Tan, N. C. (2001). The effect of processing variables on the morphology of electrospun nanofibers and textiles. Polymer, 42, 261–272.

Droby, S., Wisniewski, M., Macarisin, D., & Wilson, C. (2009). Twenty years of postharvest biocontrol research: Is it time for a new paradigm? Postharvest Biology and Technology, 52(2), 137–145. https://doi.org/10.1016/j.postharvbio.2008.11.009

El-Tarabily, K. A., & Sivasithamparam, K. (2006). Potential of yeasts as biocontrol agents of soil-borne fungal plant pathogens and as plant growth promoters. Mycoscience, 47(1), 25–35. Ferreira, A. R. V., Torres, C. A. V., Freitas, F., Sevrin, C., Grandfils, C., Reis, M. A. M., Alves, V. D., & Coelhoso, I. M. (2016). Development and characterization of bilayer films of FucoPol and chitosan. Carbohydrate Polymers, 147, 8–15. https://doi.org/10.1016/j.carbpol.2016.03.089

Ferreira, A. R. V., Bandarra, N. M., Moldão-Martins, M., Coelhoso, I. M., & Alves, V. D. (2018). FucoPol and chitosan bilayer films for walnut kernels and oil preservation. LWT – Food Science and Technology, 91(August 2017), 34–39. https://doi.org/10.1016/j.lwt.2018.01.020

Freitas, F., Alves, V. D., & Reis, M. A. M. (2011). Advances in bacterial exopolysaccharides: From production to biotechnological applications. Trends in Biotechnology, 29(8), 388–398. https://doi.org/10.1016/j.tibtech.2011.03.008

Ganesh, K. S., Sridhar, A., & Vishali, S. (2022). Utilization of fruit and vegetable waste to produce value-added products: Conventional utilization and emerging opportunities-A review. Chemosphere, 287(P3), 132221. https://doi.org/10.1016/j.chemosphere.2021.132221

González-Gutiérrez, K. N., Ragazzo-Sánchez, J. A., Barros-Castillo, J. C., Narváez-Zapata, J. A.; Calderón-Santoyo, M. (2023). Yeasts with potential biocontrol of Colletotrichum gloeosporioides in avocado (Persea americana Mill. cv. Hass) and characterization of Yamadazyma mexicana mechanisms. European Journal of Plant Pathology, 165(3), 525–543. https://doi.org/10.1007/s10658-022-02625-4

González-Gutiérrez, K. N., Ragazzo-Sánchez, J. A., &; Calderón-Santoyo, M. (2021). Application of stressed and microencapsulated Meyerozyma caribbica for the control of Colletotrichum gloeosporioides in avocado (Persea americana Mill. cv. Hass). Journal of Plant Diseases and Protection, 128(5), 1243–1251. https://doi.org/10.1007/s41348-021-00487-2

Grumi, M. (2021). DEVELOPMENT AND CHARACTERIZATION OF ELECTROSPUN CASHEW GUM-BASED FILMS FOR FOOD PACKAGING APPLICATIONS. Università degli Studi di Milano, Milan (Italy).

Guo, L., Azam, S. M. R., Guo, Y., Liu, D., & Ma, H. (2021). Germicidal efficacy of the pulsed

magnetic field against pathogens and spoilage microorganisms in food processing: An overview. Food Control, 108496. https://doi.org/10.1016/j.foodcont.2021.108496

Haider, A., Haider, S., & Kang, I. K. (2018). A comprehensive review summarizing the effect of electrospinning parameters and potential applications of nanofibers in biomedical and biotechnology. Arabian Journal of Chemistry, 11(8), 1165–1188. https://doi.org/10.1016/j.arabjc.2015.11.015

Hua, L., Yong, C., Zhanquan, Z., Boqiang, L., Guozheng, Q., & Shiping, T. (2018). Pathogenic

mechanisms and control strategies of Botrytis cinerea causing post-harvest decay in fruits and vegetables. Food Quality and Safety, 2(3), 111–119. https://doi.org/10.1093/fqsafe/fyy016

Iñiguez-Moreno, M., Ragazzo-Sánchez, J. A., Barros-Castillo, J. C., Sandoval-Contreras, T., & Calderón-Santoyo, M. (2020). Sodium alginate coatings added with Meyerozyma caribbica: Postharvest biocontrol of Colletotrichum gloeosporioides in avocado (Persea americana Mill. cv. Hass). Postharvest Biology and Technology, 163(January), 111123. https://doi.org/10.1016/j.postharvbio.2020.111123

Liang, Y., Xiong, W., Steinkellner, S., & Feng, J. (2018). Deficiency of the melanin biosynthesis genes SCD1 and THR1 affects sclerotial development and vegetative growth, but not pathogenicity, in Sclerotinia sclerotiorum. Molecular Plant Pathology, 19(6), 1444–1453. https://doi.org/10.1111/mpp.12627

Liu, Y., Wu, Q., Wu, X., Algharib, S. A., Gong, F., Hu, J., Luo, W., Zhou, M., Pan, Y., Yan, Y. Y., & Wang, Y. (2021). Structure, preparation, modification, and bioactivities of β-glucan and mannan from yeast cell wall: A review. International Journal of Biological Macromolecules, 173, 445–456. https://doi.org/10.1016/j.ijbiomac.2021.01.125

Lourenço, S. C., Torres, C. A. V., Nunes, D., Duarte, P., Freitas, F., Reis, M. A. M., Fortunato, E., Moldão-Martins, M., da Costa, L. B., & Alves, V. D. (2017). Using a bacterial fucose-rich polysaccharide as encapsulation material of bioactive compounds. International Journal of Biological Macromolecules, 104, 1099–1106. https://doi.org/10.1016/j.ijbiomac.2017.07.023

Mojaveri, S. J., Hosseini, S. F., & Gharsallaoui, A. (2020). Viability improvement of Bifidobacterium animalis Bb12 by encapsulation in chitosan/poly(vinyl alcohol) hybrid electrospun fiber mats. Carbohydrate Polymers, 241(April), 116278. https://doi.org/10.1016/j.carbpol.2020.116278

Novickij, V., Grainys, A., Lastauskiene, E., Kananavieiùte, R., Pamedytyte, D., Kalediene, L., Novickij, J., & Miklaveiè, D. (2016). Pulsed Electromagnetic Field Assisted in vitro Electroporation: A Pilot Study. Scientific Reports, 6(September), 1–10. https://doi.org/10.1038/srep33537

Papoutsis, K., Mathioudakis, M. M., Hasperué, J. H., & Ziogas, V. (2019). Non-chemical treatments for preventing the postharvest fungal rotting of citrus caused by Penicillium digitatum (green mold) and Penicillium italicum (blue mold). Trends in Food Science and Technology, 86(March), 479–491. https://doi.org/10.1016/j.tifs.2019.02.053

Parafati, L., Vitale, A., Restuccia, C., & Cirvilleri, G. (2015). Biocontrol ability and action mechanism of food-isolated yeast strains against Botrytis cinerea causing post-harvest bunch rot of table grape. Food Microbiology, 47, 85–92. https://doi.org/10.1016/j.fm.2014.11.013

Peng, Y., Li, S. J., Yan, J., Tang, Y., Cheng, J. P., Gao, A. J., Yao, X., Ruan, J. J., & Xu, B. L. (2021). Research Progress on Phytopathogenic Fungi and Their Role as Biocontrol Agents. Frontiers in Microbiology, 12(May). https://doi.org/10.3389/fmicb.2021.670135

Piotrowska, M., & Masek, A. (2015). Saccharomyces cerevisiae cell wall components as tools for ochratoxin A decontamination. Toxins, 7(4), 1151–1162. https://doi.org/10.3390/toxins7041151

Ribeiro, A. J., De Souza, F. R. L., Bezerra, J. M. N. A., Oliveira, C., Nadvorny, D., De La Roca Soares, M. F., Nunes, L. C. C., Silva-Filho, E. C., Veiga, F., & Soares Sobrinho, J. L. (2016). Gums' based delivery systems: Review on cashew gum and its derivatives. Carbohydrate Polymers, 147, 188–200. https://doi.org/10.1016/j.carbpol.2016.02.042

Rodrigues, J. P., de Souza Coelho, C. C., Soares, A. G., & Freitas-Silva, O. (2021). Current technologies to control fungal diseases in postharvest papaya (Carica papaya L.). Biocatalysis and Agricultural Biotechnology, 36(June). https://doi.org/10.1016/j.bcab.2021.102128

Romero, J., Albertos, I., Díez-m, A., & Poveda, J. (2022). Control of postharvest diseases in berries through edible coatings and bacterial probiotics. Scientia Horticulturae, 304(June). https://doi.org/10.1016/j.scienta.2022.111326

Shi, X. C., Wang, S. Y., Duan, X. C., Wang, Y. Z., Liu, F. Q., & Laborda, P. (2021). Biocontrol strategies for the management of Colletotrichum species in postharvest fruits. Crop Protection, 141(November 2020), 105454. https://doi.org/10.1016/j.cropro.2020.105454

Silva, F., Torres, L., Silva, L., Figueiredo, R., Garruti, D., Araújo, T., Duarte, A., Brito, D., & Ricardo, N. (2018). Cashew gum and maltrodextrin particles for green tea (Camellia sinensis var Assamica) extract encapsulation. Food Chemistry, 261(October 2017), 169–175. https://doi.org/10.1016/j.foodchem.2018.04.028

Sridharan, G., & Shankar, A. (2012). Toluidine blue: a review of its chemistry and clinical utility. J. Oral Maxillofaccial Pathology, 16(2), 251–255. https://doi.org/10.4103/0973-029X.99081

Synytsya, A., Čopíková, J., Matějka, P., & Machovič, V. (2003). Fourier transform Raman and infrared spectroscopy of pectins. Carbohydrate Polymers, 54(1), 97–106. https://doi.org/10.1016/S0144-8617(03)00158-9

Torres-Giner, S., Ocio, M. J., & Lagaron, J. M. (2008). Development of active antimicrobial fiber based chitosan polysaccharide nanostructures using electrospinning. Engineering in Life Sciences, 8(3), 303–314. https://doi.org/10.1002/elsc.200700066

Torres-Giner, Sergio, Pérez-Masiá, R., & Lagaron, J. M. (2016). A review on electrospun polymer nanostructures as advanced bioactive platforms. Polymer Engineering and Science, 56(5), 500–527. https://doi.org/10.1002/pen.24274

United Nations. (2015). https://sdgs.un.org/goals

Vasconcelos Silva, E. de L., Oliveira, A. C. de J., Patriota, Y. B. G., Ribeiro, A. J., Veiga, F., Hallwass, F., Silva-Filho, E. C., da Silva, D. A., Soares, M. F. de L. R., Wanderley, A. G., &Soares-Sobrinho, J. L. (2019). Solvent-free synthesis of acetylated cashew gum for oral delivery system of insulin. Carbohydrate Polymers, 207(November 2018), 601–608. https://doi.org/10.1016/j.carbpol.2018.11.071

Vázquez-González, Y., Prieto, C., Filizoglu, M. F., Ragazzo-Sánchez, J. A., Calderón-Santoyo, M., Furtado, R. F., Cheng, H. N., Biswas, A., & Lagaron, J. M. (2021). Electrosprayed cashew gum microparticles for the encapsulation of highly sensitive bioactive materials. Carbohydrate Polymers, 264(October 2020). https://doi.org/10.1016/j.carbpol.2021.118060

Vázquez-González, Y., Prieto, C., Stojanovic, M., Torres, C. A. V, Freitas, F., Ragazzo-Sánchez, J. A., Calderón-Santoyo, M., & María, L. J. (2022). Preparation and Characterization of Electrospun Polysaccharide FucoPol-Based Nanofiber Systems. 1–15. https://doi.org/https://doi.org/10.3390/nano12030498

Wang, X., Lu, D., & Tian, C. (2021). Analysis of melanin biosynthesis in the plant pathogenic fungus Colletotrichum gloeosporioides. Fungal Biology, 125(9), 679–692. https://doi.org/10.1016/j.funbio.2021.04.004

Wei, M., Ge, Y., Li, C., Chen, Y., Wang, W., Duan, B., & Li, X. (2018). Antifungal activity of ε-poly-L-lysine on Trichothecium roseum in vitro and its mechanisms. Physiological and Molecular Plant Pathology, 103, 23–27. https://doi.org/10.1016/j.pmpp.2018.04.005

Xiao, Q., & Lim, L. T. (2018). Pullulan-alginate fibers produced using free surface electrospinning. International Journal of Biological Macromolecules, 112, 809–817. https://doi.org/10.1016/j.ijbiomac.2018.02.005

Yang, Q., Wang, H., Zhang, H., Zhang, X., Apaliya, M. T., Zheng, X., & Mahunu, G. K. (2017). Effect of Yarrowia lipolytica on postharvest decay of grapes caused by Talaromyces rugulosus and the protein expression profile of T. rugulosus. Postharvest Biology and Technology, 126, 15–22. https://doi.org/10.1016/j.postharvbio.2016.11.015

Zain, M. E. (2011). Impact of mycotoxins on humans and animals. Journal of Saudi Chemical Society, 15(2), 129–144. https://doi.org/10.1016/j.jscs.2010.06.006

Zhang, H., Mahunu, G. K., Castoria, R., Yang, Q., & Apaliya, M. T. (2018). Recent developments in the enhancement of some postharvest biocontrol agents with unconventional chemicals compounds. Trends in Food Science and Technology, 78, 180–187. https://doi.org/10.1016/j.tifs.2018.06.002

Zhang, X., Li, B., Zhang, Z., Chen, Y., & Tian, S. (2020). Antagonistic yeasts: A promising alternative to chemical fungicides for controlling postharvest decay of fruit. Journal of Fungi, 6(3), 1–15. https://doi.org/10.3390/jof6030158

Zhou, H., Ma, H., Wu, & Zhang, H. (2014). Progress in understanding magnetic biological effect in food processing. Food Science, 25(17), 285–289.Aceituno-Medina, M., Mendoza, S., Lagaron, J. M., & López-Rubio, A. (2013). Development and characterization of food-grade electrospun fibers from amaranth protein and pullulan blends. Food Research International, 54(1), 667–674. https://doi.org/10.1016/j.foodres.2013.07.055

7.4. Desarrollo de nanofibras a base de goma de anacardo, FucoPol y pululano obtenidas mediante *Solution Blow Spinning* para el control de antracnosis y su evaluación sobre los parámetros de calidad en aguacates

Los resultados correspondientes a la etapa 4 de este proyecto de tesis están contenidos en el siguiente manuscrito.

A new method to produce antifungal nanofibers and its potential post-harvest application on avocado fruit

Yuliana Vázquez-González[1,2]; Cristina Prieto[2], Jose M. Lagaron[2], Juan Arturo Ragazzo-Sánchez[1], Montserrat Calderón-Santoyo[1,*].

7.4.1. Introducción al tema

Los recubrimientos comestibles han sido ampliamente usados en el tratamiento postcosecha de frutas y vegetales para preservar y mejorar su calidad, evitando el deterioro durante su almacenamiento y distribución.

Para la generación de recubrimientos pueden emplearse biopolímeros, como los polisacáridos y las proteínas, y una variedad de métodos para su aplicación, como recubrimiento por inmersión, recubrimiento en lecho fluidizado, recubrimiento en bandeja, y aspersión, entre otros. A pesar de que son métodos usados para aplicar este tipo de recubrimientos en frutas y vegetales, existen ciertas desventajas acerca de su uso, como daño al alimento por manipulación, una aplicación no homogénea del recubrimiento y además algunas de estas técnicas son altamente costosas, dificultando su aplicación a escala comercial.

El uso de la nanotecnología en el desarrollo de recubrimientos comestibles podría ser una alternativa para alargar la vida útil de frutas y vegetales. En este sentido, nanofibras de proteína de suero de leche, zeína, celulosa y quitosano ya han sido aplicadas en frutas mostrando ventajas sobre los recubrimientos convencionales. Además, cabe resaltar que las nanofibras brindan la capacidad de encapsular ingredientes funcionales, proporcionando estabilidad y protección al ingrediente bioactivo. Una técnica que llama la atención por su simplicidad en su configuración y en su manipulación para generar nanofibras a partir de diversos biopolímeros es *Solution Blow Spinning* (SBS). SBS es una técnica que consiste en la generación de nanofibras inyectando una solución polimérica a través de boquillas concéntricas. La gota polimérica se alarga y es hilada mediante aire comprimido a una presión establecida. La simplicidad de la técnica permite que las fibras se pueden aplicar sobre cualquier superficie, por lo que la aplicación "*in situ*" es una de sus grandes ventajas. Además, es una técnica que tiene lugar a temperatura ambiente y permite la encapsulación de compuestos bioactivos sin afectar a sus propiedades funcionales.

En este sentido, el objetivo de esta investigación fue encontrar las condiciones óptimas de SBS para obtener nanofibras a partir de nuevos biopolímeros que puedan encapsular efectivamente a *M. caribbica* para el control de antracnosis en aguacate. Para ello, se prepararon soluciones de pululano (15 %, w/w), CG:PEO (7.5 %; 0.13:1, w/w) y FP:PEO

(7.5 %; 0.024:1, w/w). Las soluciones poliméricas se ajustaron a una concentración de 1×10^8 células/mL. Las soluciones con y sin *M. caribbica* fueron caracterizadas fisicoquímicamente, para posteriormente procesarlas mediante SBS bajo diferentes condiciones de trabajo. Las nanofibras obtenidas se caracterizaron mediante SEM. Se determinó la viabilidad de *M. caribbica* en las nanofibras aplicadas sobre los aguacates almacenados a diferentes condiciones: 1) 15 días a 25 ºC, 2) 10 días a 6 ºC y 5 días a 25 ºC. Se evaluó la actividad antifúngica *in vitro* e *in vivo* en la inhibición de *C. gloeosporioides*. Finalmente, se evaluó el efecto de las nanofibras sobre los parámetros de calidad de los aguacates. Se obtuvieron fibras homogéneas, continuas y rizadas con tamaños promedio 212 ± 61, 554 ± 223 y 482 ± 175 nm para las fibras de pululano, FP:PEO y CG:PEO, respectivamente. SBS garantizó una alta viabilidad de *M. caribbica* en nanofibras aplicadas sobre los aguacates a ambas condiciones de almacenamiento. *M. caribbica* atrapada en las nanofibras de pululano inhibió por completo el desarrollo de *C. gloeosporioides* en las dos condiciones de almacenamiento. La aplicación de nanofibras no tuvo un efecto sobre parámetros de calidad como el color, acidez titulable y pH, contenido de materia seca, solidos solubles totales y firmeza con respecto al control. *Solution Blow Spinning* fue capaz de formar y aplicar directamente las nanofibras sobre los aguacates sin afectar algunos parámetros de calidad. No obstante, es importante mencionar que las nanofibras pueden modificarse o mejorarse en función a la naturaleza de la matriz alimentaria.

A new method to produce antifungal nanofibers and its potential post-harvest application on avocado fruit

Yuliana Vázquez-González[1,2]; Cristina Prieto[2], Jose M. Lagaron[2], Juan Arturo Ragazzo-Sánchez[1], Montserrat Calderón-Santoyo[1,*].

[1]Laboratorio Integral de Investigación de Alimentos, Tecnológico Nacional de México-Instituto Tecnológico de Tepic, Av. Tecnológico de Tepic, Av. Tecnológico #2595, C.P. 63175, Tepic, Nayarit, México; yvazquezgo@ittepic.edu.mx (Y.V.G); jragazzo@tepic.tecnm.mx (J.A.R.S); mcalderon@tepic.tecnm.mx (M.C.S).

[2]Novel Materials and Nanotechnology Group, Institute of Agrochemistry and Food Technology (IATA), Spanish Council for Scientific Research (CSIC), Calle Catedrático Agustín Escardino Benlloch 7, 46980 Paterna, Spain, cprieto@iata.csic.es (C.P.); lagaron@iata.csic.es (J.M.L.); yvazquezgo@ittepic.edu.mx (Y.V.G).

*Corresponding author: mcalderon@tepic.tecnm.mx

Abstract

Solution Blow Spinning (SBS) is an emerging technology for producing nanofibers with different applications. The simplicity of this process makes SBS a potential technique for applications in post-harvest treatments. In this regard, the principal aim of this work was to find the best conditions to obtain biopolymeric nanofibers that effectively encapsulate biocontrol agents, concretely *Meyerozyma caribbica* that has demonstrated its activity against *Colletotrichum gloeosporioides*, an important fungus that affects fruit and vegetables. Pullulan, FucoPol and cashew gum were selected as biopolymers. Initially, the polymeric solutions were characterized in terms of viscosity and surface tension and processed by SBS to obtain nanofibers with and without the addition of *M. caribbica*. The obtained fibers were characterized in terms of morphology, storage viability at two different temperatures, i.e. 6 ºC and 25 ºC, *in vitro* antifungal activity against *C. gloeosporioides*, and *in vivo* antifungal activity evaluating also the effect of the nanofibers on the quality properties of avocado fruit variety Hass. According to SEM characterization, homogenous, continuous, and curly fibers with average sizes ranging from 151 to 777 nm were obtained. Thanks to the mild processing conditions, a high viability of *M. caribbica* into nanofibers applied by SBS on the avocado surface (8.09 Log_{10} CFU $fruit^{-1}$) was maintained. All nanofibers loaded with *M. caribbica* showed high percentages of inhibition *in vitro*, inhibiting the spore´s germination and mycelial growth at either 6 ºC or 25 ºC. *M. caribbica* entrapped into pullulan nanofibers evaluated as a preventive treatment completely inhibited the growth of *C. gloeosporioides* during the *in vitro* and *in vivo* tests, being better than azoxystrobin, a synthetic fungicide. The application of these nanofibers on avocados did not affect pH, titratable acidity, total soluble solids, weight loss, firmness, and dry matter content of avocados with respect to the control formulation. In view of these results, the SBS technique can be used to successfully entrap *M. caribbica* into nanofibers to control anthracnose caused by *C. gloeosporioides* on the avocado fruit variety "Hass".

Keywords: Solution Blow Spinning, nanofibers, FucoPol, cashew gum, pullulan, post-harvest treatment.

1 Introduction

Post-harvest diseases caused by phytopathogens cause devastating losses of fruit and vegetables during their storage, which could achieve more than 55 % of the production in developing countries (Zhang et al., 2017). Among phytopathogens, *Colletotrichum gloeosporioides* can cause severe economic losses, since this fungus is able to cause anthracnose disease in different fruit such as avocado, banana, papaya, mango, citrus, and strawberry, among others, affecting their production and commercialization (Shi et al., 2021). The conventional control of post-harvest diseases primarily consists of the application of synthetic fungicides. However, its potential threats to food security, their toxicity to human health, collateral damage against environment, in conjunction with fungicide-resistant strains make the search for other alternatives crucial (Shi et al., 2021).

Multiple alternative treatments have been developed to combat post-harvest diseases (Ciofini et al., 2022). Biocontrol agents, particularly yeast *Meyerozyma caribbica*, have garnered special attention due to their efficacy against anthracnose in mango, papaya, and avocado (Aguirre-Güitrón et al., 2022, 2019; Bautista-Rosales et al., 2013; González-Gutiérrez et al., 2021; Iñiguez-Moreno et al., 2021, 2020). *Meyerozyma caribbica's* effectiveness results from multiple mechanisms, including nutrient and space competition, parasitism, the biofilm formation (Bautista-Rosales et al., 2013) and the production of volatile organic compounds (VOC) (Iñiguez-Moreno et al., 2020). However, direct application of yeast can reduce its effectivity due to their sensitivity to various physicochemical factors and the challenge of establishing and maintaining it on the fruits surface (González-Gutiérrez et al., 2021; Iñiguez-Moreno et al., 2020). Combining yeast with a polymeric matrix can offer protection and adhesion to the fruit surface, commonly achieved through particle or coating forms. For example, Aguirre-Güitrón et al. (2022) used electrospraying to encapsulate *M. caribbica* in whey protein concentrate particles, resulting in 53% and 74% inhibition of anthracnose incidence of mango cv. "Ataulfo" and papaya cv. "Maradol", respectively. Additionally, González-Gutiérrez et al. (2021) reported a 45% reduction in lesion diameter on avocado fruit by microencapsulating *M. caribbica* in sodium alginate using spray drying.

However, particle production methods often involve temperature, like spray drying (Eijkelboom et al., 2023) or are challenging to scale up and apply directly to fruits, as in the case of electrospraying (Rostamabadi et al., 2021).

Regarding coatings, Iñiguez-Moreno et al. (2020) performed the application of *M. caribbica* entrapped in sodium alginate coatings on the avocado surface as an anthracnose preventive treatment, reporting a severity reduction of 100%. The effectiveness of *M. caribbica* when applied conventionally, like dipping or panning, can be compromised. Dipping can dilute the foods surface layer and unevenly disperse the yeast. Panning may cause fruit damage. Low gas permeability in coating can affect fruit storage and flavor due to anaerobic conditions (Aayush et al., 2022).

In this sense, the application of a coating made of fibers could be an alternative, since fibers are structures with a large surface-volume, which makes them more active and efficient, with a very high porosity and enhanced physico-mechanical properties (Haider et al., 2018; Torres-Giner et al., 2018). These characteristics make the coating made of nanofibers an interesting alternative for the encapsulation of biocontrol yeasts and their application on the fruit surface. Among the available fiber production techniques stand out the electrospinning process and the meltblown processing. Electrospinning uses high-voltage electrostatic fields to create micro/nanofibers from polymer solutions (Torres-Giner et al., 2018). It can affect biomaterials due to the solvents and voltage used (Medeiros et al., 2009; Oliveira et al., 2011). Meltblowing is a key commercial method for micro/nanofiber non-woven (Monsores et al., 2022). Meltblowing is a melt process for 1-10 μm fibers using high-speed gas/air jets. It is a quicker and cost-effective alternative to electrospinning (Kolbasov et al., 2016; Monsores et al., 2022), but it involves heat, which might impact yeast stability.

Based on these fiber production technologies, a novel process called Solution Blow Spinning (SBS) has been developed to make non-woven polymeric micro and nanofibers (Medeiros et al., 2009). SBS is based on the use of a high-velocity gas flow as a driving force, for the polymeric fiber formation (Khalilur et al., 2021). SBS setup consists of a source of compressed gas (nitrogen, argon, or air), equipped with a pressure regulator, a syringe, a syringe pump to control the flow rate of the polymeric solutions, an injector that consisted of concentric nozzles, and a collector positioned at a fixed working distance from the nozzle.

The polymer solution is pumped through the inner nozzle while high-speed gas flows through the outer concentric nozzle (Medeiros et al., 2009; Santos et al., 2016). As the gas accelerates, it lowers the air pressure at the jets center, causing the polymer solution to accelerate and form a polymeric jet towards the collector. Solvent evaporation at room temperature during flight solidifies the fiber structure (da Silva Parize et al., 2016). This process offers several advantages, is more efficient in producing nanofibers due to a higher solution feeding rate per orifice compared to electrospinning (Dadol et al., 2020; Santos et al., 2016). The simplicity of the SBS setup makes scaling up easier (Dadol et al., 2020). It operates at room temperature, preserving bioactive components. It has been explored for various biomedical applications, including drug delivery, wound dressing, tissue engineering, microfiltration, among others (Lu et al., 2012; Stojanovska et al, 2016). Thus, SBS-produced nanofibers can serve as a polymer matrix to trap microorganisms and be deposited homogeneously as thin and uniform coating on the surface of the fruit.

SBS technology has been used for nanofibers production from polymers such as poly (acrylonitrile), poly (vinylpyrrolidone), poly (lactic acid), poly (lactic acid-co-glycolic acid), and cellulose (Dadol et al., 2020). New biopolymers in the spotlight are FucoPol derived from *Enterobacter* strain A47 (DSM 23139) fermentation (Vázquez-González et al., 2022), cashew gum from *Anacardium occidentale* tree (Vázquez-González et al., 2021), and pullulan, water-soluble microbial polysaccharide produced by *Aureobasidium pullulans* (Xiao and Lim 2018). These materials, including FucoPol, cashew gum, and pullulan are non-toxic, bio-based, and exhibit various techno-functional properties, such as emulsification, gelling, film formation, thickening, and biological functions (Sheng et al., 2022; Vázquez-González et al., 2022, 2021; Xiao and Lim, 2018). As of now, there have been no reported studies on producing nanofibers from FucoPol, cashew gum, and pullulan using the SBS technique and applying them in the food industry, especially in the post-harvest fruit and vegetable management (Monsores et al., 2022; Shen et al., 2022; Tien et al., 2022).

This study aimed to assess the feasibility of producing nanofibers using FucoPol, cashew gum, and pullulan loaded with M. caribbica through the SBS process to control anthracnose in Hass variety avocados. The research involved characterizing the fiber morphology, examining storage viability at 6 ºC and 25 ºC, evaluating *in vitro* antifungal

activity against *C. gloeosporioides*, and assessing *in vivo* antifungal activity. While also considering the impact of the nanofibers on the avocado fruit quality properties.

2 Materials and methods

2.1 Materials

Pullulan (Pul) (Mw ~ 2 × 10^5 Da) was purchased from Hayashibara CO., LTD. (Tokio, Japan), polyethylene oxide (PEO) (Mw ~ 4 × 10^5 Da), phosphate-buffered saline (PBS) and YPD broth (Yeast Extract Peptone Dextrose) was purchased from Sigma Aldrich (St. Louis, MO, USA), FucoPol (FP) (4.4 × 10^6 Da) was provided by the Chemical Department of the Nova University (Lisbon, Portugal), and cashew gum (CG) (2.5 × 10^4 Da) was provided by the Department of Agriculture, Agricultural Research Service (Peoria, IL, USA). Synthetic fungicide Azoxystrobin was purchased from AMISTAR® (Syngenta, Zeneca, Frankfurt, Germany). Glycerol was purchased from Jalmek (San Nicolás de los Garza, Mexico). In this study, healthy and uniform-sized avocados (*Persea americana* Mill. cv. "Hass") weighing approximately 120 g were obtained from Leb Trading Products (Guacamodely S. de R.L. de C.V., Xalisco, Mexico). The avocados were at their physiological maturity stage, characterized by a dry matter content (DMC) of approximately 24%. It is worth mentioning that the avocados did not exhibit any mechanical injury.

2.2 Antagonistic microorganism

M. caribbica (GenBank ID: JQ398674) was previously isolated from "Ataulfo" mangoes by Bautista-Rosales et al. (2013). The yeast was preserved using 20% (v/v) glycerol and stored at -80 °C. For reactivation, the yeast was incubated in yeast peptone dextrose (YPD) broth. The incubation took place on a rotary shaker at 28 °C for 48 h and 110 rpm as described by Bautista-Rosales et al. (2013). Following incubation, the cells were collected, and their concentration was adjusted to 1 × 10^8 cells/mL.

2.3 Preparation and characterization of the polymeric solutions with and without *M. caribbica*

To obtain fibers loaded with *M. caribbica*, different polymeric solutions were prepared using the following polymers: Pul, PEO, FP, and CG. The Pul solution was prepared at a concentration of 15 % (w/w). Two separate solutions of PEO were prepared with FP and CG. The FP:PEO solution had a concentration of 7.5 % (ratio 0.024:1, w/w), while the CG:PEO solution had the same solid concentration but a different ratio of 0.13:1 (w/w). All solutions

were prepared under sterile conditions and sterile water was used as a solvent. CG, PEO, and Pul were irradiated under UV light for 30 min. However, sterilization by autoclaving at 121 ºC for 15 min was necessary for FucoPol due to the presence of residues from *Enterobacter* A47. The solutions were then mixed and adjusted with *M. caribbica*, which was homogenized in PBS at a concentration of 1×10^8 cells mL^{-1}.

The polymeric solutions, with and without *M. caribbica*, were characterized in terms of viscosity and surface tension. The methodology described by Vázquez-González et al. (2021) was followed for these measurements. All measurements were made in triplicate at room temperature.

2.4 Solution Blow Spinning process

The SBS process was carried out in a Fluidnatek® LE-10 (Bioinicia S.L. Valencia, Spain) with an adaptation to provide compressed air. The solutions were placed in a 20 mL plastic syringe connected by a PTFE tube to the two-fluid concentric injector. This injector possessed two inlets, one for the fluid and another for the compressed gas; and an outlet, through the two concentric needles, the inner for the liquid and the outer for the compressed gas. A syringe pump was used to provide the desired liquid flow rate. The air pressure was controlled by a pressure gauge. Air pressure used in this study ranged from 1 bar (14.50 psi) to 8 bar (116.03 psi). Different conditions were evaluated to obtain the fibers as shown in Table 1. For *in vitro* assays, the nanofibers were collected on aluminum foil and circles with diameters of 2 cm and 8 cm were cut for further analysis. For the *in vivo* analysis, avocados were placed into an acrylic structure for further nanofibers deposition and to prevent the nanofibers from exiting the environment. The nanofibers were deposited on the avocados during different periods according to solutions concentrations (Pul 1h, FP:PEO 4 h 10 min, and CG:PEO 3h 46 min) to apply the same amount of solutions.

Table 1. SBS working parameters to obtain nanofibers from Pul, FP:PEO and CG:PEO.

Sample	Flow rate (mL/h)	Pressure (bar)	Work distance (cm)
Pul	5	3	42.5
FP:PEO	2	1	36.5

CG:PEO	3	2	36.5

2.5 Scanning Electronic Microscopy

The morphology of the fibers obtained was analyzed using a Hitachi-S-4800 FE-SEM scanning electron microscope (Hitachi High-Technologies Corporation, Tokyo, Japan) operating at an electron-beam acceleration of 10 kV. Approximately 1.5 mg of the sample was placed on the sample holder using double-sided tape and coated with a gold-palladium layer. To determine the fiber sizes, Image J Launcher v1.41 software (National Institutes of Health, Bethesda, MD, USA) was utilized. The data were based on measurements from a minimum of 100 fibers. It is worth noting that the presence of yeast was not considered in the measurements, as it can potentially overestimate the diameter of nanofibers.

2.6 Evaluation of nanofiber properties

2.6.1 *In vitro* inhibition of spore germination of nanofibers loaded with *M. caribbica*

The inhibition of spore germination was assessed following the methodology outlined by Iñiguez-Moreno et al., (2020). For this, ten mL of saline solution were added to Petri plates containing fungal mycelia with 10 d of growth. The spore suspension was prepared by gently rubbing the agar surface using a sterile inoculation loop. The suspension was then filtered through sterile gauze and collected in a conical tube. The spore concentration was adjusted to 1×10^5 cells mL^{-1} by microscopic counting using a Neubauer Counting Chamber (BlauBrand, Germany). Next, fifty µL of the fungal spores suspension (1×10^5 cells mL^{-1}) were spread onto PDA disks measuring 1.4 cm in diameter. The disks were allowed to dry for five min in a cabinet (Novatech, Model CFLV-120, Kingwood, USA). After the drying period, the disks were then incubated at two different temperatures: 6 ºC, which corresponds to the storage temperature for avocado fruit, and 25 ºC, which represents room temperature. During the incubation period, the nanofibers were absorbed by the PDA disks.

The germination percentage of *C. gloeosporioides* was determined using optical microscopy with a BA 310 microscope (Motic, San Antonio, USA). The percentage of germinated spores was measured after 9.5 h at 25 ºC and after 47 h at 6 ºC. A minimum of 200 germinated spores were considered for the control. Spores were considered germinated based on the criterion that the length of the germ tube was equal to or longer than the diameter of the spore.

2.6.2 *In vitro* inhibition of mycelial growth of nanofibers loaded with *M. caribbica*

The antifungal performance of the nanofibers obtained by SBS process against *C. gloeosporioides* was made on PDA plates. Initially, 100 µL of fungal spores (1×10^5 cells/mL) were spread in the center of Petri dishes and allowed to dry for 5 min in a cabinet (Novatech, Model CFLV-120, Kingwood, USA). Subsequently, the inoculated PDA Petri dishes were covered with nanofibers containing *M. caribbica* (Pul, FP:PEO, and CG:PEO cutted circles with 8 cm of diameter were used for this assay) obtained by the SBS process.

The growth diameter of *C. gloeosporioides* was measured for 8 d at 25 ºC and 10 d at 6 ºC. During this period, the radial growth of the fungal mycelium was monitored. The percentage of inhibition of mycelial growth was calculated using Equation 1:

$$Inhibition\ (\%) = \left[\frac{dc-dt}{dc}\right] x\ 100 \qquad Eq.\ 1$$

Where *dc* (cm) is the average colony diameter for the control sets and *dt* (cm) is the average colony diameter for the different treatments. All tests were done in triplicate.

For both assays, two control groups were included, inoculated and uncoated control and inoculated and coated with nanofibers without *M. caribbica*.

2.7 Evaluation of nanofibers with yeast applied on avocado fruit

2.7.1 Viability of *M. caribbica* in nanofibers during avocado fruit storage

The viability of yeast in the nanofiber coatings was assessed during avocado fruit storage under two different conditions: 1) storage at 25 ºC for 15 d, 2) storage at 6 ºC for 10 d followed by ripening at 25 ºC for 5 d. The coated avocado fruits with nanofibers applied by SBS were initially stored at a temperature of 6 ºC for 10 d to simulate cold storage conditions. After the cold storage period, the fruits were transferred to a ripening condition at 25 ºC for an additional 5 days, replicating the conditions typically experienced at the retail level. To evaluate the viability of *M caribbica* yeast, individual avocado fruits were placed into sterile stomacher bags (Seward, BA6041/CLR) containing 50 mL of PBS. The yeasts in the coatings were removed by sonicating the bags for 90 seconds with a KENDAL sonicator (Model CD 48-20 operating at 50/60 Hz, Middletown, USA). Serial dilutions of the sonicated samples were prepared and spread onto YPD agar plates. The plates were then incubated for 48 h at 28 ºC using an incubator (Model E145-AID, Novatech, USA). After the incubation period, yeast colonies were counted to determine the viability of *M. caribbica* yeast in the coatings.

Each experiment was conducted with three replicates, and the entire process was repeated twice to ensure the reliability of the results (Iñiguez-Moreno et al., 2020).

2.7.2 Curative and preventive treatments using Pul, CG:PEO, and FP:PEO nanofibers with *M. caribbica*

Curative and preventive treatments, based on the methodology described by Iñiguez-Moreno et al. (2020) with certain modifications, were carried out in the study. Avocado fruit was wounded (2 holes per fruit, near to peduncle and in the equatorial zone) with a sterile needle (3 mm deep and 3 mm wide), inoculated with 10 µL of a spore suspension of *C. gloeosporioides* (1×10^5 cells mL^{-1}), and left to dry at room conditions. Curative treatments were performed by first inoculating the fruit with the spore suspension and then leaving the fruit to dry for 6 h, allowing the pathogen infection before applying the appropriate treatment. Preventive treatments were done by first applying the nanofibers to the wounded fruit, leaving the fruit to dry for 6 h at 25 ºC, and then inoculating it with the pathogen spore suspension. Avocado fruit inoculated before or after immersion treatment in sterile water or azoxystrobin water solution were used as controls. The fruit was stored in a camera (Novatech, Model CA-550; Kingwood, USA) with humidifiers (Vitallys Plus, Model VUH-3, Marlborough, USA) to ensure high relative humidity (RH) under two conditions: 1) 25 ºC during 15 d (75 % RH), and 2) 6 ºC (95 % RH) during 10 d and ripened at 25 ºC (75 % RH) during 5 d. Disease incidence (percentage of infected fruit), infected wounds (percentage), and severity (lesion diameter expressed in mm) were evaluated as measurements of the impact of *C. gloeosporioides* infection on avocado fruit. An avocado fruit was considered decayed if at least one of the inoculated wounds showed signs of infection. For this assay, each treatment was replicated twice, with 10 avocado fruits per treatment.

The treatments applied were: (1) control (sterile water); (2) azoxystrobin (800 mg/L according to AMISTAR® Syngenta, Zeneca, Frankfurt, Germany); (3) Pul (15 %); FP:PEO (7.5 %, ratio 1:0.024 w/w); CG:PEO (7.5 %, ratio 1:0.13 w/w), and (4) Pul + yeast, FP:PEO + yeast and CG:PEO + yeast, all polymeric solutions at the same initial concentration, i.e. 15 %, 7.5 % and 7.5 % adjusted at 1×10^8 cells/mL, respectively.

2.8 Effect of Pul, CG:PEO, and FP:PEO nanofibers on the quality properties of avocados

For the assessment of avocado quality, we used a total of 9 fruits evaluated over 12 days at 25 and 12 fruit evaluated over 10 days at 6 ºC and ripening at 25 ºC by 8 days per treatment were used. The test was repeated three time. As controls, we used both distilled water and a synthetic fungicide (azoxystrobin) treatment.

2.8.1 Weight loss

To assess the effect of nanofibers on fruit weight loss, each avocado fruit was weighted individually using a digital balance (Sartorius, TE212, Göttingen, Germany) at the start and end of the experiment. The difference between these measurements was calculated to determine the weight loss for each nanofiber treatment. The weight loss was then expressed as a percentage.

2.8.2 Total soluble solids (TSS)

To determine the TSS content, the technique proposed by Iñiguez-Moreno et al. (2021) was employed. The refractive index of the samples was measured using a manual refractometer (Atago, Model NAR-1T, Tokyo, Japan) at 25 ºC and expressed as percentage.

2.8.3 Titratable acidity (TA) and pH

For TA, 20 g of avocado flesh was weighed and mixed with 100 mL of distilled water to achieve homogenization. Then, the sample was brought to pH 7 by adding 0.1 N NaOH. The neutral sample was brought to pH 8.3 with NaOH. The pH values were measured using a potentiometer (Hanna Instruments, 2210, Woonsocket, USA). The results were expressed in g of tartaric acid per 100 g, with a conversion factor of 0.007 for tartaric acid (Iñiguez-Moreno et al., 2021).

2.8.3 Firmness

To measure the firmness of the whole avocado, two opposite sides of each fruit were selected, and firmness measurements were taken. For the firmness of the avocado flesh, the fruit was cut in half, and one measurement was performed on each half. The measurements were carried out using a digital texture analyzer (Stable Micro Systems, Model TA-XT plus, Surrey, UK). The analysis was performed at a speed of 2 mm/s, using a stainless-steel probe with a puncture diameter of 2 mm. The depth reached during the test was 5 mm. This method

allowed for the assessment of the firmness of both the whole avocado and its flesh, providing information on the texture characteristics of the fruit.

2.8.4 Dry matter content (DMC)

First, the avocado pericarp was removed, then, the fruit was cut into two halves and longitudinal slices of approximately 2 mm thick were cut to obtain a total of 10 g. The sample was dried in a convection drying oven (Novatech, HS60, Kingwood, USA) at 105 ºC until constant weight (Iñiguez-Moreno et al., 2021). The DMC was calculated with equation 2.

$$DMC\ (\%) = (M_1 / M_0)\ 100 \qquad \text{Eq. 2}$$

Where M_1 is the final weight of the sample, and M_0 is the initial weight of the sample.

2.8.5 Color

The pericarp color of the avocado was measured using a colorimeter (Chromameter CR-400, Konica Minolta Sensing Inc., Tokyo, Japan) at two different points of the equatorial zone of the opposite sides of the fruit. The color values were expressed in terms of L^*, a^*, and b^* parameters, which provide information about lightness, redness/greenness, and yellowness/blueness, respectively.

2.8.6 Statistical analysis

Data were analyzed by ANOVA with a *P-value* < 0.05. The Fisher test was used for the comparison of means. STATISTICA 12 software (Statsoft Inc., Tulsa, OK, USA) was used for statistical analysis.

3 Results and Discussion

3.1 Physicochemical characterization of polymeric solutions

SBS generation of nanofibers depends on parameters such as molecular weight of the polymer, concentration, solution viscosity, surface tension, and polymer solution flow rate (Benavides et al., 2012; Dadol et al., 2020; Daristotle et al., 2016). These parameters have direct influence on critical characteristics that enable the formation of a fiber-producing jet of polymer solution (Daristotle et al., 2016. In this sense, the physicochemical characterization of the polymeric solutions was done in order to stablish a relationship between the polymeric solutions and the obtained materials. The viscosity values for each of the polymeric solutions are presented in the Table 2. Pul, CG:PEO and FP:PEO showed significant differences in the viscosity, which are mainly due to the differences in molecular

weight of the polymers used for these formulations. Significant differences in the solutions viscosity were also observed when *M. caribbica* was added to these polymeric solutions. The viscosity for Pul, CG:PEO, and FP:PEO with *M. caribbica* solutions showed a decrease of the viscosity values in comparison with polymeric solutions without *M. caribbica*. This could be due to the solubilization of the yeast pellet into PBS to improve the solubilization in the polymeric solution, which could affect the viscosity of the final polymeric solution. However, no changes in process stability were observed.

Table 2. Physicochemical characterization of polymeric solutions with/without the addition of *M. caribbica*.

Polymeric solutions	Viscosity (cP)	Surface Tension (mN/m)
Pul	675.90 ± 9.54e	59.80 ± 0.20c
CG:PEO	9942.33 ± 323.47b	62.80 ± 0.30b
FP:PEO	12844.67 ± 219.39a	57.10 ± 0.30d
Pul + *M. caribbica*	573.57 ± 3.21f	67.20 ± 0.20a
CG:PEO + *M. caribbica*	7334.00 ± 162.25d	60.10 ± 0.20c
FP:PEO + *M. caribbica*	9219.00 ± 341.17c	57.20 ± 0.40d

*Each column represents the mean ± standard deviation of three independent replicas. Different letters in each column indicate significant difference.

On the other hand, the surface tension of polymeric solutions is determined principally from the solvent used. In this case, water was used as solvent to maintain the viability of *M. caribbica*. It is well known that water is characterized by a high surface tension value, which needs to be overcome to obtain the fiber formation. Additionally, according to Hofmann et al. (2018), surface tension is the main cause for jet instability and breakup. As we can see in the Table 2, surface tension values of 57 to 63 mN/m were obtained. For the different polymer solutions. As we can see there was no significant difference between different polymeric solutions, even when *M. caribbica* was added being these values suitable for SBS process.

3.2 Scanning Electron Microscopy analysis

SEM micrographs of Pul, CG:PEO, and FP:PEO fibers with and without *M. caribbica* produced by SBS technique and fiber diameter are shown in Fig. 1 (a-f). Fibers are uniform, smooth, and have curly appearance with some bundling due to the turbulence of the pressurized gas during the SBS process (Dadol et al., 2020). The presence of some beads could be related to the high surface tension. The nanofibers were placed successfully on the avocado surface by SBS, generating a coating made of nanofibers loaded with *M. caribbica* for the control of *C. gloeosporioides*. This coating was similar to the obtained by other methods such as fluidized-bed, spraying (Aayush et al., 2022) or electrospinning process (Ayón-Macías et al., 2023; Iñiguez-Moreno et al., 2022).

Fibers with mean diameter of 212 ± 61, 482 ± 175, and 554 ± 223 nm were obtained for Pul, CG:PEO and FP:PEO, respectively. Similar mean diameters were obtained for the nanofibers added with *M. caribbica.* Pul nanofibers showed the smallest fiber diameter, due to the low viscosity of the polymeric solution and the high air pressure used (3 bar). It is well-known that a reduced viscosity, produces thinner fibers, but also an increase of the air pressure produces a greater drag force of the polymeric solution reducing the fiber diameter (Lu et al., 2012). Same behavior was observed by Benavides et al. (2012), who obtained nanofibers from SBS and observed a reduction of the average diameter of the fiber from 1.6 to 0.34 μm when the air jet pressure incremented from 10 to 30 psi.

CG and FP did not produce fibers by SBS alone, for this reason PEO, which is a high molecular weight polymer often used as spinning aid (Francis et al. 2010), was added to these formulations. According to literature, it was not possible to produce fibers with PEO of low molecular weight (2×10^5 Da) (Kolbasov et al. 2016). In this study, the use of a high molecular weight PEO (5×10^6 Da) was first tested, but the production of fibers was unsuccessful (results not shown). For that reason, PEO with a middle molecular weight (2×10^5 Da) was used in this research to be blended with CG and FP.

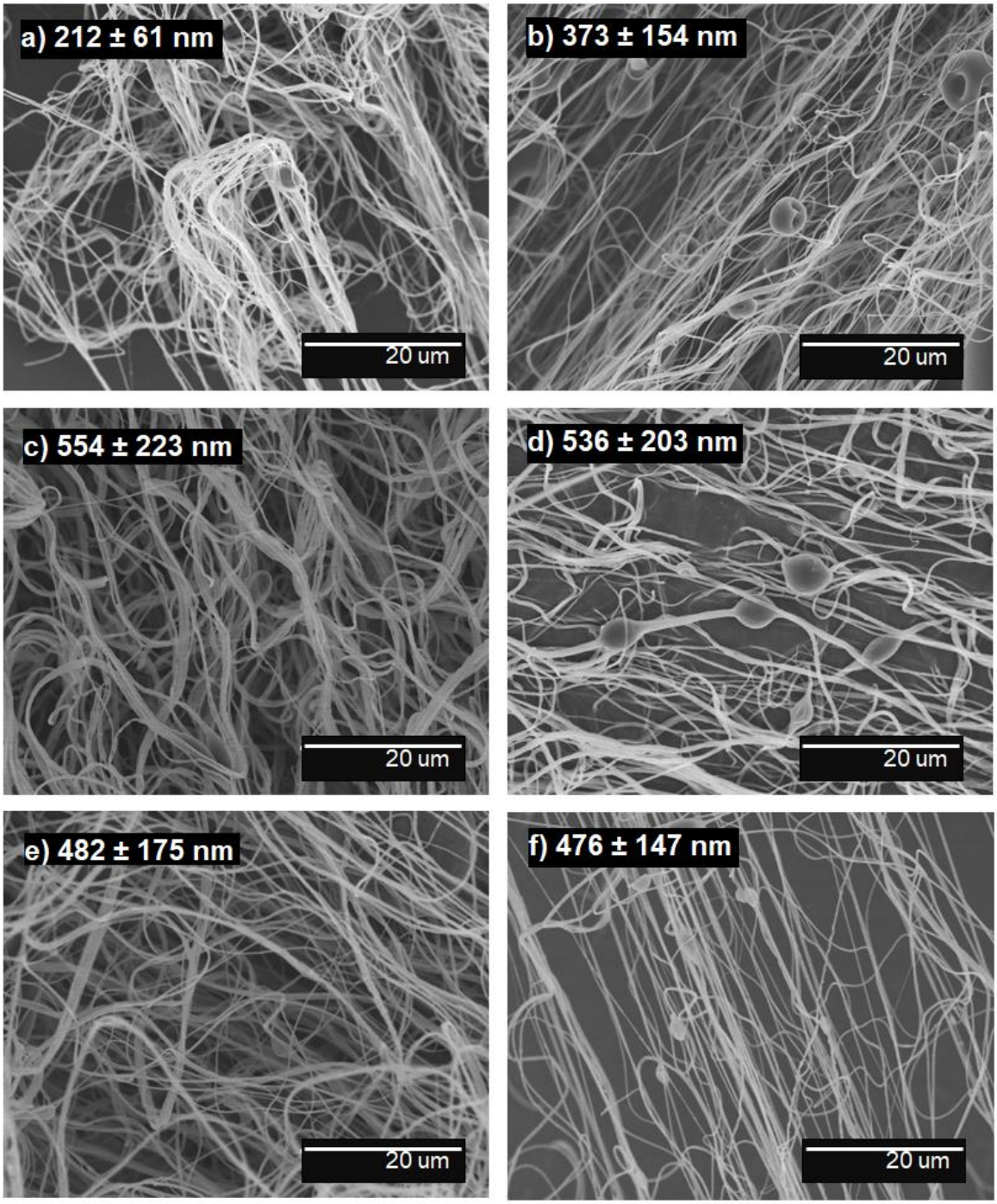

Figure 7. SEM analysis of polymeric fibers obtained by SBS, a) Pul nanofibers, b) Pul nanofibers loaded with *M. caribbica*, c) FP:PEO nanofibers, d) FP:PEO nanofibers loaded with *M. caribbica*, e) CG:PEO nanofibers, f) CG:PEO nanofibers loaded with *M. caribbica*.

SBS of a solution of PEO blended with CG and FP produced slightly larger nanofibers than Pul fibers. Despite these solutions present a higher viscosity, this increase in fiber diameter could be also provoked by a lower gas pressure, a lower flow rate, and a lower working distance. These combination of parameters results in insufficient stretching of the produced fibers (da Silva Parize et al., 2016; Kolbasov et al., 2016).

3.3 *In vitro* antifungal activity

Concerning the spore germination, all nanofibers loaded with *M. caribbica* exhibited high percentages of inhibition, as shown in Table 3. CG:PEO nanofibers presented the highest inhibition percentages in comparison with Pul and FP:PEO nanofibers. In addition, there was no difference between CG:PEO nanofibers tested at 6 or 25 ºC. It is important to note that polymeric nanofibers without *M. caribbica* did not inhibit spore´s germination and mycelial growth of *C. gloeosporioides* (results not shown). The slight major inhibition at 6 ºC of all nanofibers could be due to the low temperature effect in the spore germination (Iñiguez-Moreno et al., 2020). In this sense, inhibition was attributed to the different actions mechanisms of *M. caribbica* against fungi such as competition for space and nutrients, parasitism, biofilms production, and volatile organic compounds (VOC) production (Bautista-Rosales et al., 2013; González-Gutiérrez et al., 2021; Iñiguez-Moreno et al., 2020). In addition, Choińska et al. (2020) reported that due to the method used (no contact between the antagonistic and the pathogen) the antagonistic activity of the yeast strains studied resulted mainly from the production of biologically active VOC. According to Iñiguez-Moreno et al. (2020), a possible compound produced by *M. caribbica* was a phenylethyl alcohol, which together with phenylethyl acetate have been also recognized as effective antifungal volatile compounds (Arrarte et al., 2017). The production of VOC is species-specific and, the antimicrobial action of volatiles should be treated as a synergistic effect with other suggested inhibitory mechanisms against the pathogen (Choińska et al.,2020). Similar behavior was observed by Iñiguez-Moreno et al. (2020), who evaluated a sodium alginate coating loaded with *M. caribbica* produced by casting technique as a postharvest biocontrol of *C. gloeosporioides* in avocado.

Table 3. *In vitro* antifungal activity of nanofibers loaded with *M. caribbica* against *C. gloeosporioides*. The percentage of germinated spores was measured after 9.5 h (25 ºC) and 47 h (6 ºC), whereas the percentage of mycelial growth inhibition was registered after 8 d (25 ºC) and 20 d (6 ºC).

Conditions	Percentage of inhibition (%)			
	Germination		Mycelial growth	
	6 ºC	25 ºC	6 ºC	25 ºC
Pul nanofibers	98.67 ± 1.04Ba	89.17 ± 3.82Bb	100 ± 0.00Aa	85.78 ± 1.33Bb
FP:PEO nanofibers	96.83 ± 1.61Ba	88.33 ± 3.82Bb	99.58 ± 0.72Aa	89.17 ± 4.42ABb
CG:PEO nanofibers	100 ± 0.00Aa	100 ± 0.00Aa	99.38 ± 1.08Aa	96.67 ± 4.71Aa

Values are expressed as means ± standard deviation (n = 6). Values in the same column followed by different capital case letter are significantly different according to Fisher´s LSD test at $p < 0.05$. Values in the same row, comparing germination or mycelial growth, followed by different lower-case letter are significantly different according to Fisher´s LSD test at $p < 0.05$.

In relation to mycelial growth inhibition, Pul, CG:PEO, and FP:PEO loaded with *M. caribbica* did not show differences in the inhibition of *C. gloeosporioides* at 6 ºC. This result agrees with the high inhibition percentage against *C. gloeosporioides* found for all the tested samples at 6 ºC.

These results could be explained because when *M. caribbica* is released from polymeric nanofibers, the yeast is interposed between the pathogen and the substrates, which is more easily taken by the yeast, limiting the growth of *C. gloeosporioides* (Bautista-Rosales et al., 2013). Then, other mechanisms are involved, for example, the biofilm formation, where cells as primary colonizers, exclude other microorganisms, by the production of exopolysaccharides. Also, *M. caribbica* can parasitize hyphae of *C. gloeosporioides*, through the production of enzymes such as glucanases, chitinases, and proteases, which deform the fungal hyphae, provoke vacuolization in mycelium and hyphal lysis (Bautista-Rosales et al., 2013).Other factors, as biosurfactants also produced by yeasts, such as sophorolipids, carbohydrate-protein-lipid complex, mannanoprotein, among others (Amaral et al., 2010), can elicit pores on fungal hyphae and trigger apoptosis by producing reactive oxygen species (ROS). In this sense, the ROS retard normal hyphae development and reduce the disease severity of *C. gloeosporioides* (Wu et al., 2020). In addition, as mentioned above, the production of VOC plays an important role in inhibiting pathogens since this is given through plasmatic membrane damage and rapid denaturation of proteins, with subsequent interference with metabolism impairing respiration and cell lysis (González-Gutiérrez et al., 2021; Iñiguez-Moreno et al., 2020).

3.4 Evaluation of *M. caribbica* in polymeric nanofibers applied on avocado fruit

3.4.1 Viability of *M. caribbica* in nanofibers during storage of avocados

The evolution of the viability of *M. caribbica* in Pul, CG:PEO and FP:PEO nanofibers applied on avocado with time, stored at 25 ºC and at 6 ºC are shown in the Fig. 2. After the SBS process, the viability of *M. caribbica* in all nanofiber formulations was similar to the initial yeast concentration, consequently, no loss of viability was observed during the SBS process. During avocado storage, Pul, CG:PEO, and FP:PEO nanofibers showed similar behavior, since viability of *M. caribbica* was reduced over time showing a final viability of 4.37, 5.73, and 5.52 Log 10 CFU fruit -1 at 25 ºC, respectively. Under mimic conditions (6 ºC, 95 % RH during 10 d and ripened at 25 ºC, 75 % RH during 5 d) avocados showed final

viability of 5.73, 4.41, and 5.90 Log_{10} CFU $fruit^{-1}$ for Pul, CG:PEO, and FP:PEO nanofibers. This loss of viability of *M. caribbica* in nanofibers applied on avocados can be associated with a higher moisture loss at 25 ºC, as observed by Iñiguez-Moreno et al. (2020).

It is important to note that during SBS process, voltage is not involved as it is in electrospinning process, reducing cell viability due to a leakage of intracellular compounds (Guo et al., 2021). In this sense, this is an advantage in the SBS process of living cells and other biomaterials, such as proteins, vitamins, and hormones (Oliveira et al., 2011). Therefore, a high viability of cells is warranted after SBS processing. Some cells have been studied in their encapsulation into nanofibers by SBS obtaining high viability, such as fibroblast and osteoblast cells (Pehlivaner Kara and Ekenseair, 2016), renal epithelial cells (Lu et al., 2012), and bovine dermal fibroblasts (Veazey et al., 2005). Lu et al. (2012) studied a SBS method for the preparation of nanofibers containing cells and their potential industrial bioengineering applications. They observed that living cells had higher rates of survival when using SBS compared to electrospinning process. The SBS technique ensures high viability of cells, simultaneous deposition of cells and material. However, the use of new biological materials for SBS process, merit further investigations because some important parameters in polymers such as concentration, viscosity, and spraying technique may affect cell viability (Daristotle et al., 2016; Pehlivaner Kara and Ekenseair, 2016).

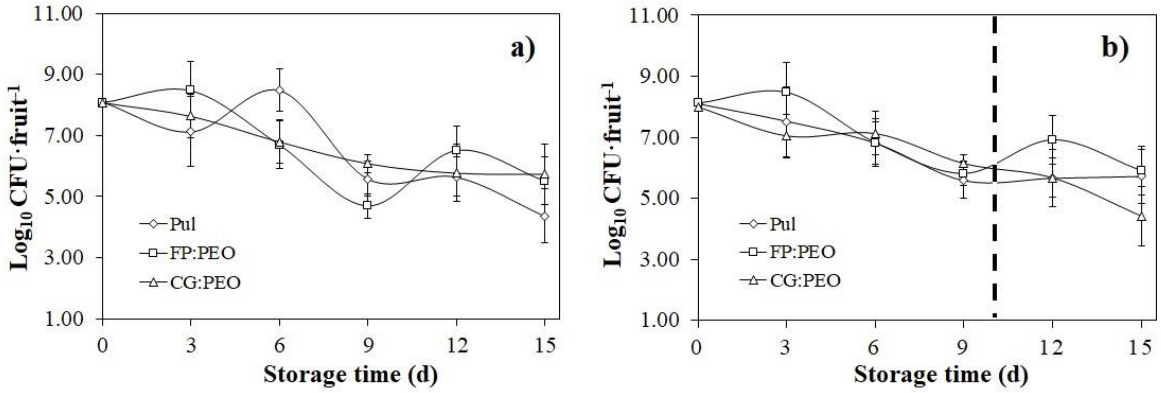

Figure 8. Population dynamics of *Meyerozyma caribbica* in nanofibers applied on avocado Hass fruit. The graph shows the evolution of yeast viability in avocados coated with nanofibers stored at a) 25 ºC during 15 d and b) 6 ºC for 10 d and ripened at 25 ºC for 5 d. Each point represents the mean ± standard deviation (n = 6).

3.4.2 Postharvest protection of avocado fruit with polymeric nanofibers (preventive and curative treatments)

The effectiveness of Pul, CG:PEO, and FP:PEO nanofibers with *M. caribbica* were evaluated against *C. gloeosporioides*. The results of preventive and curative treatments against anthracnose caused by *C. gloeosporioides* in avocado fruit during the storage at 25 ºC for 15 d and at 6 ºC during 10 d and ripened at 25 ºC during 15 d are shown in the Fig. 3 and Fig. 4, respectively. It is important to note that during *in vivo* assays, different conditions such as temperature, relative humidity and interaction between polymeric matrix and cuticle of fruits can influence in the effectiveness of nanofibers against *C. gloeosporioides*. In this sense, in contrast with the *in vitro* results, where CG:PEO was the best formulation, in this *in vivo* assay the nanofibers of Pul loaded with yeast showed the best results as a preventive treatment in the inhibition of *C. gloeosporioides,* compared with the CG:PEO and FP:PEO nanofibers and the synthetic fungicide (azoxystrobin). Pul nanofibers showed a 100% severity reduction with respect to the control (no infected wounds nor diseased fruits observed, Fig. 3, group A, B, C), whereas CG:PEO, FP:PEO and azoxystrobin showed 35%, 50%, 75% at 25 ºC during 15 d, respectively. In some cases, biocontrol agents have better efficacy than synthetic fungicides (Ocampo-Suarez et al., 2017). This important characteristic was mentioned also Shi et al. (2021), who discussed about biocontrol strategies for the management of *Colletotrichum* species in postharvest fruits. On the contrary, when nanofibers were evaluated as a curative treatment, a decrease of effectiveness in comparison with the preventive treatment was observed. Pul nanofibers loaded with *M. caribbica* showed a reduction of severity of 26 % in comparison to the control (Fig. 3, group A).

Regarding FP:PEO nanofibers, they showed a reduction of severity of 28 % (Fig. 3, group A). However, the level of anthracnose protection was higher with CG:PEO nanofibers as a curative treatment, which showed a reduction in severity of 59 %, whereas azoxystrobin showed a severity reduction of 69 % (Fig. 3, group A). However, in both cases, there was not statistically difference with the preventive treatment. A decrease in the effectiveness of nanofibers as curative treatments may be due to the fact that during curative treatments *C. gloeosporioides* is inoculated before the application of nanofibers with yeasts. This allows *C. gloeosporioides* to colonize the wound before *M. caribbica*. After colonization, *C.*

gloeosporioides acquires the necessary nutrients to initiate its mechanisms of infection. During destructive phase, the pathogen secrets toxins and an enzymatic complex responsible for degrading plant tissue (da Silva et al., 2020).

As can be seen in the Fig. 3, all polymeric nanofibers without *M. caribbica* did not show an effect in anthracnose inhibition, the severity, the percentage of incidence of anthracnose and the percentage of infected wounds did not show significant difference with respect to control.

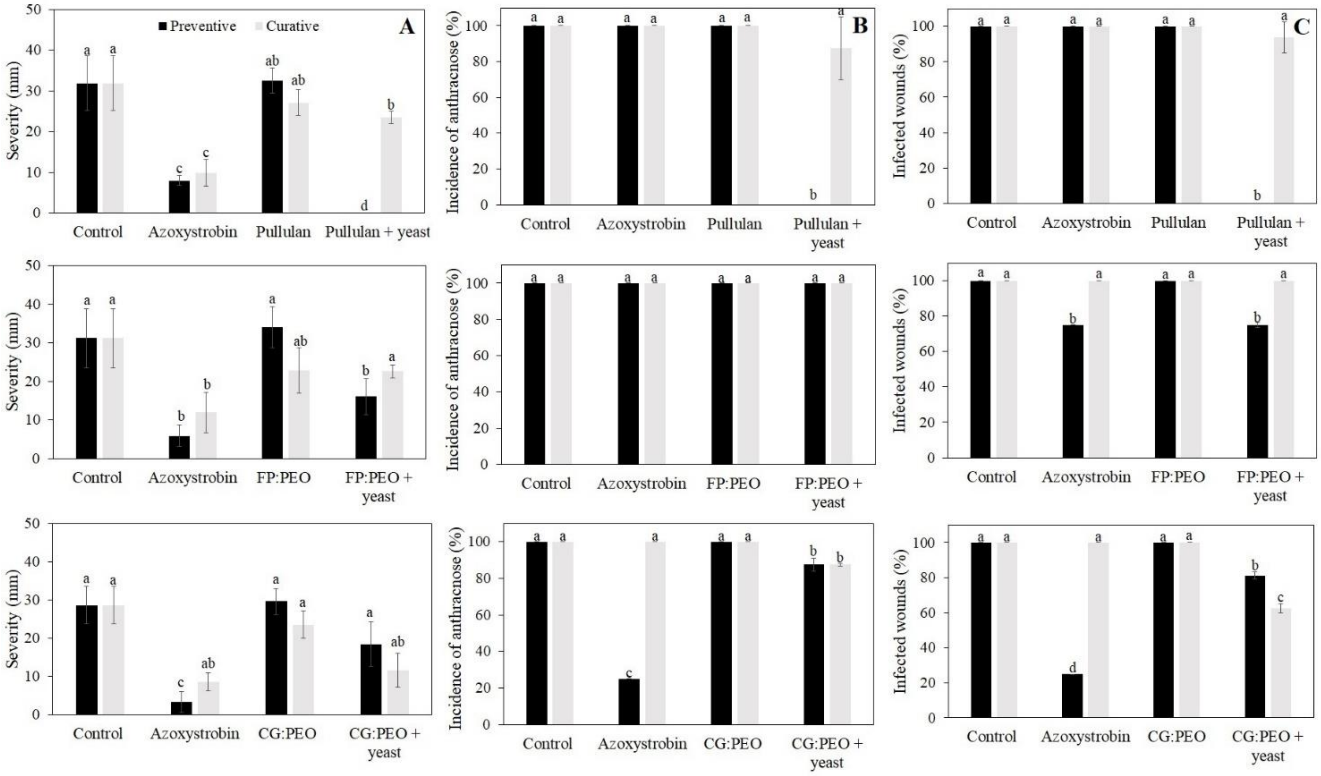

Figure 9. Curative and preventive treatments against *Colletotrichum gloeosporioides* applied on avocado fruit variety Hass. Group A referring to severity, Group B referring to incidence of anthracnose, and Group C, infected wounds.The fruit with curative and preventive treatments were stored at 25 ºC for 15 d. Control (sterile water); Azoxystrobin (synthetic fungicide); Pullulan (15%); FP:PEO (7.5%, ratio 0.024:1 w/w); CG:PEO (7.5%, ratio 0.13:1 w/w), and Pullulan + yeast, FP:PEO + yeast and CG:PEO + yeast, all polymeric solutions at the same initial concentration, i.e. 15%, 7.5% and 7.5% adjusted at 1×10^8 cells mL^{-1}, respectively. Mean values in the same graph followed by different lower-case letter are significantly different according to Fisher´s LSD test at $p < 0.05$. Each bar represents the mean values ± standard deviation (n = 18).

On the other hand, preventive and curative treatments stored at 6 ºC during 10 d and ripened at 25 ºC during 5 d, were more effective in severity reduction (Fig. 4), comparing with treatments stored at 25 ºC for 15 d (Fig. 3). Avocado fruits treated with preventive Pul nanofibers did not show development of anthracnose disease. Even under these storage conditions, CG:PEO and FP:PEO nanofibers did not show completely inhibition of anthracnose caused by *C. gloeosporioides*. The severity was reduced in 42% and 58% for CG:PEO and FP:PEO, respectively, in comparison with the control. As a curative treatment severity was also reduced showing 76%, 60%, and 45% for Pul, CG:PEO and FP:PEO nanofibers, respectively. In general, preventive treatments were more efficient than curative treatments under both tested conditions, similar results were shown by González-Estrada et al. (2017) and Iñiguez-Moreno et al., (2020), who evaluated *M. caribbica* as a biocontrol agent against *P. italicum* and *C. gloeosporioides*, respectively. This behavior is related to the viability of *M. caribbica* in nanofibers and the release of *M. caribbica* from nanofibers into the surface of avocado fruit. High cell density of *M. caribbica* was observed after 6 d of storage in the Pul nanofibers at 25 ºC (Fig. 2a).

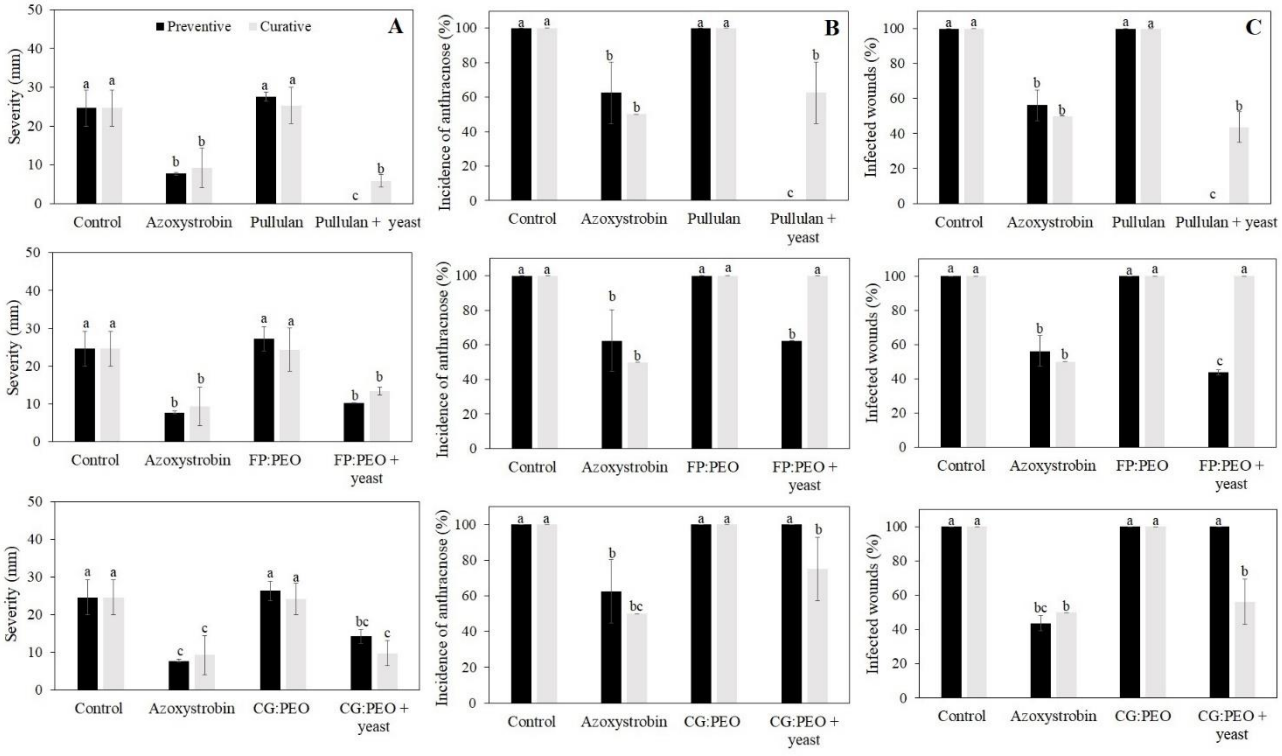

Figure 10. Curative and preventive treatments against *Colletotrichum gloeosporioides* applied on avocado fruit variety Hass. Group A referring to severity, Group B referring to incidence of

anthracnose, and Group C, infected wounds.The fruit with curative and preventive treatments were stored at 6 ºC during 10 d and ripened at 25 ºC during 5 d to simulate the conditions at the retail level. Control (sterile water); Azoxystrobin (800 mg/L according technical sheet; AMISTAR® Syngenta, Zeneca, Frankfurt, Germany); Pullulan (15%); FP:PEO (7.5%, ratio 0.024:1 w/w); CG:PEO (7.5%, ratio 0.13:1 w/w), and Pullulan + yeast, FP:PEO + yeast and CG:PEO + yeast, all polymeric solutions at the same initial concentration, i.e. 15%, 7.5% and 7.5% adjusted at 1×10^8 cells mL^{-1}, respectively. Mean values in the same graph followed by different lower-case letter are significantly different according to Fisher´s LSD test at $p < 0.05$. Mean values in the same graph followed by different lower-case letter are significantly different according to Fisher´s LSD test at $p < 0.05$. Each bar represents the mean values ± standard deviation (n = 18)

In addition to this, Pul is a water-soluble polysaccharide; therefore, it shows high solubility at 100% RH, 28 ºC (Niu et al., 2020). Aceituno-Medina et al. (2013) observed that the fibers with higher Pul content (amaranth protein isolate:pullulan 50:50) were less stable when exposed at 100% RH. These characteristics enhance the rapid release of *M. caribbica* from the Pul nanofibers allowing the yeast establishment owing to its ability to colonize the surface of avocado fruit wound faster than fungus (Iñiguez-Moreno et al., 2020). Although the CG and FP are also water-soluble polysaccharides (Vázquez-González et al., 2024, 2022, 2021), the mixture with PEO showed a strong film formed by hydrogen bonds between the ether groups and hydroxyl groups of CG and FP reducing *M. caribbica* release and retarding the colonization on the avocado surface (Kolbasov et al., 2016; Tien et al., 2022).

3.5 Quality properties of avocados after applying Pul, CG:PEO, and FP:PEO nanofibers loaded with *M. caribbica*.

3.5.1 pH, titratable acidity (TA), and total soluble solids (TSS)

At both stored conditions, pH values increased in the same way in avocado treated with nanofibers (Pul, CG:PEO, and FP:PEO nanofibers) as for controls (sterile water and synthetic fungicide) (Table 4 and Table 5). This result is in line with the results previously showed by Iñiguez-Moreno et al. (2021), who observed an increase in the pH up to 6.6 when they evaluated sodium alginate coatings with *M. caribbica* and impact on quality properties of avocado fruit.

The TA values of avocados with and without nanofibers decreased with storage time and did not show significant differences. Same behavior was observed by Sierra et al. (2019),

who evaluated changes in physicochemical properties of avocado fruits variety Hass. This result could be due to the decrease of organic acids, such as malic acid or citric acid, during the ripening process, since they are primary substrates for respiration, contributing to the reduction of titratable acidity (Ali et al., 2010; Iñiguez-Moreno et al., 2021).

All treatments showed similar TSS values (1 – 1.5 ºBrix) showing an increment of TSS during storage time. During the metabolic activity, α and β amylases hydrolyze starch to simpler disaccharides and monosaccharide, reducing the TA and incrementing the TSS values (Sierra et al., 2019).

3.5.2 Weight loss

Under room temperature storage condition (Table 4), CG:PEO nanofibers with and without *M. caribbica* showed the highest weight loss in comparison with control avocados (sterile water and azoxystrobin). Whereas FP:PEO and Pul nanofibers with and without *M. caribbica* did not show significant statistical difference with control. An increase of temperature contributes to decreasing the water concentration in the atmosphere surrounding the fruit, and, therefore, to increase the transpiration rate (Sierra et al., 2019).

On the other hand, under simulated conditions at retail level (Table 5), CG:PEO, FP:PEO and Pul loaded with *M. caribbica* nanofibers did not show significant statistical difference with control. While, CG:PEO, FP:PEO and Pul without yeast showed a statistical difference in comparison with control avocados (sterile water and azoxystrobin). Permeability of material is a crucial characteristic to modulate respiration process of the fruit (Iñiguez-Moreno et al., 2021). In this sense, CG:PEO can negatively alter the internal atmosphere of the fruit by inducing anaerobic off-flavor development with the restriction of respiratory gas exchange (Saberi et al., 2018). Polysaccharide based coatings have a hydrophilic nature and influence the weight loss in coated fruits due to formation of hydrogen bonds with cuticle of fruits (Moreira et al., 2020). Some research has emphasized also that weight loss is due to the coating solution itself (Ali et al., 2010; Park and Chinnan, 1995; Sucheta et al., 2019). In this sense, Sucheta et al. (2019), observed that due to higher solids in concentration of solution, edible coatings (50% pectin : 50% corn flour, 80% pectin : 20% corn flours) added with beetroot powder (0.4% w/v) were found to be less effective in reducing the evapotranspiration as compared to other non-added coating solutions. The primary reason for

increased weight loss of avocados when they were covered with FP:PEO but to a larger extent with CG:PEO could be that after nanofibers deposition a kind of thick coating was generated on the surface of avocados due to nanofibers are sensitive to moisture. CG:PEO completely covered the surface of the fruit resulting in generation heat and an anaerobic fermentation due to low O_2 concentrations and high CO_2 concentrations (Park and Chinnan, 1995; Sucheta et al., 2019). Similar results were observed by Ali et al. (2010), who observed more weight loss when using 20% gum Arabic compared with a concentration of 10 % to improve postharvest quality of tomato. Also, Park and Chinnan (1995) observed that tomato fruit coated too thickly with a corn-zein film resulted in more weight loss. In addition, the lower gas permeability by FP and CG can also influence. Studies carried out by Ferreira et al. (2016) and Moreira et al. (2020) showed that FP mixed with chitosan and CG mixed with PVA have been shown low water vapor permeability (0.75×10^{-11} and 7×10^{-11} mol/ms Pa) and CO_2 permeability (5.8×10^{-16} mol m/m^{2}sPa and 363 cm^3 m^{-2} day^{-1} at 0.1 Mpa^{-1}, respectively).

The weight loss of avocados increased gradually during the storage time, due to different metabolic processes such as transpiration and respiration (vapor-phase diffusion and to the moisture loss through the stomata) (Bill et al., 2014; Iñiguez-Moreno et al., 2021). Different weight loss under storage conditions evaluated are influenced by all the metabolic processes involved in the degradation of the cell membranes leading to a lower water retention capacity and facilitating the evaporation (Sierra et al., 2019).

3.5.3 Firmness

Firmness is an important attribute of fruit quality and is associated to shelf life. In this sense, CG:PEO, FP:PEO and Pul nanofibers showed a decline of firmness similar to the control, therefore there was not a significant statistical difference in comparison with the controls (sterile water and azoxystrobin) under both storage conditions (Table 4 and Table 5). Regarding the flesh firmness, the same behavior was observed, treatments did not show statistical differences with controls. Softening of fruit is due to deterioration in the cell structure, cell wall composition and intracellular materials and is a biochemical process involving the hydrolysis of pectin and starch enzymes (Ali et al., 2010; Iñiguez-Moreno et al., 2021; Marques et al., 2016). During mimic storage conditions (Table 4), Pul, CG:PEO, and FP:PEO nanofibers with and without *M. caribbica* showed a slightly higher values

compared with control. There is a relation between the weight loss and firmness parameter. As mentioned above (section 3.5.2), the slightly higher values could be due to the low levels of O_2 and high levels of CO_2 limit the activities of these enzymes and allow retention of the firmness during storage (Ali et al., 2010).

Table 4. Quality properties of coated avocado fruit with nanofibers storage during 12 days at 25 ºC.

Physicochemical properties		Storage conditions							
		12 days at 25 ºC							
		Control	Azoxystrobin	Pul	Pul + yeast	CG:PEO	CG:PEO + yeast	FP:PEO	FP:PEO + yeast
Weight loss (%)		4.73 ± 1.29^{b}	4.80 ± 0.41^{b}	6.88 ± 2.64^{b}	7.70 ± 0.40^{b}	25.41 ± 9.17^{a}	22.34 ± 5.38^{a}	11.28 ± 6.43^{b}	6.42 ± 2.57^{b}
TSS (ºBrix)		1.00 ± 0.00^{b}	1.50 ± 0.00^{a}	1.50 ± 0.00^{a}	1.00 ± 0.00^{b}	1.5 ± 0.00^{a}	1.00 ± 0.00^{b}	1.00 ± 0.00^{b}	1.00 ± 0.00^{b}
TA (%)		0.10 ± 0.01^{b}	0.12 ± 0.04^{ab}	0.12 ± 0.00^{ab}	0.12 ± 0.03^{ab}	0.15 ± 0.01^{a}	0.10 ± 0.01^{b}	0.10 ± 0.03^{b}	0.12 ± 0.01^{ab}
pH		6.78 ± 0.08^{ab}	6.66 ± 0.17^{bc}	6.62 ± 0.03^{bc}	6.58 ± 0.17^{bc}	6.53 ± 0.13^{c}	6.78 ± 0.05^{ab}	6.97 ± 0.08^{a}	6.77 ± 0.16^{b}
Fruit firmness (N)		6.07 ± 1.15^{a}	5.74 ± 0.85^{a}	5.84 ± 1.10^{a}	5.32 ± 0.43^{a}	6.69 ± 1.23^{a}	5.08 ± 1.55^{a}	6.57 ± 2.43^{a}	5.79 ± 0.78^{a}
Flesh firmness (N)		0.19 ± 0.04^{ab}	0.18 ± 0.03^{ab}	0.23 ± 0.12^{ab}	0.19 ± 0.05^{ab}	0.14 ± 0.01^{ab}	0.13 ± 0.00^{b}	0.18 ± 0.08^{ab}	0.27 ± 0.13^{a}
DMC (%)		20.25 ± 0.90^{c}	21.76 ± 2.14^{bc}	19.81 ± 0.99^{c}	21.86 ± 2.40^{bc}	28.22 ± 1.80^{a}	25.18 ± 3.01^{ab}	24.50 ± 3.22^{b}	20.43 ± 1.17^{c}
Pericarp	L^*	21.02 ± 0.40^{a}	19.97 ± 0.78^{a}	20.64 ± 2.98^{a}	20.93 ± 1.48^{a}	19.71 ± 1.62^{a}	21.22 ± 1.02^{a}	19.57 ± 1.49^{a}	20.74 ± 0.81^{a}
	a^*	1.97 ± 0.82^{ab}	1.18 ± 0.25^{b}	2.39 ± 1.38^{ab}	2.17 ± 0.64^{ab}	1.84 ± 0.87^{ab}	1.48 ± 0.21^{b}	2.96 ± 0.54^{a}	1.99 ± 0.42^{ab}
	b^*	1.99 ± 0.70^{ac}	1.31 ± 0.15^{c}	2.90 ± 0.83^{ab}	3.27 ± 1.11^{a}	2.39 ± 0.84^{abc}	2.36 ± 0.51^{abc}	2.38 ± 0.84^{abc}	2.80 ± 0.36^{ab}
	ΔE	21.22 ± 0.59^{a}	20.04 ± 0.79^{a}	21.02 ± 3.01^{a}	21.31 ± 1.69^{a}	19.98 ± 1.41^{a}	21.40 ± 1.01^{ab}	19.96 ± 1.38^{b}	21.02 ± 0.81^{ab}

The avocados were immersed in SDW (sterile distilled water), azoxystrobin (800 mg/L). CG:PEO, FP:PEO and Pul nanofibers with and without *M. caribbica* were applied on the avocado´s surface by SBS. Values in the same row, with different lower-case letters, are significantly different according to Fisher´s LSD test at $p < 0.05$. Values are expressed as means ± standard deviation (n = 27). Initial TSS (total soluble solids, %) = 0.50 ± 0.00; TA (titrata ble acidity as percentage of tartaric acid) = 0.15 ± 0.03; pH = 5.89 ± 0.02; Fruit firmness (N) = 21.27 ± 1.52; Flesh firmness (N) = 20.63 ± 1.77; DMC (dry matter content) = 22.21 ± 2.52; Pericarp color L^* = 27.00 ± 2.78, a^* = -6.87 ± 1.88, b^* = 8.47 ± 2.41. ΔE: total color change.

3.5.4 Dry matter content (DMC)

Dry matter content is a crucial parameter for determining avocado maturity and is currently used worldwide (Araújo et al., 2018). CG:PEO nanofibers showed the highest DMC percentage under both storage conditions evaluated (Table 3 and Table 4). This is related to the fact that the ripening process was faster with the application of CG:PEO nanofibers due to the hydrophilic polymers usually have poor water vapor barriers (Iñiguez-Moreno et al., 2021; Moreira et al., 2020). Pul and FP:PEO nanofibers did not show significance statistical difference with controls under both storage conditions.

3.5.5 Color change

Skin color change of avocados, particularly variety "Hass" is important for industry and consumers, since it is an indication of fruit ripeness (Cox et al., 2004). Under both storage conditions luminosity of the pericarp did not show statistical significance in comparison with the controls (sterile water and azoxystrobin, Table 4 and Table 5). This luminosity values were decreased throughout the avocado ripening process. It was observed that the nanofibers application did not affect fruit color, avocados had a black color associated to the epidermis, may be due to chlorophyll degradation (Cox et al., 2004). These results are in line with Correa-Pacheco et al. (2017), who evaluated the effect of nanostructures chitosan and chitosan-thyme essential oil coating on cv Hass avocado quality. The a^* value in the avocado pericarp changed from negative in the unripe fruit to positive at the end of time storage under both conditions. For b^* values also showed no significant differences with respect to the control (Table 4 and Table 5). Similar behavior was observed by Correa-Pacheco et al. (2017); Iñiguez-Moreno et al. (2021); Sierra et al. (2019). Regarding the ΔE values were low and there were not differences between treatments and controls under both storage conditions (Table 4 and Table 5). This means that the application of CG:PEO, FP:PEO and Pul did not prolong ripening process of avocados (Iñiguez-Moreno et al., 2021).

Table 5. Quality properties of coated avocado fruit with nanofibers storage during 10 days at 6 ºC and ripening at 25 ºC by 8 days.

Physicochemical properties		Storage conditions							
		10 days at 6 ºC and ripening at 25 ºC by 8 days							
		Control	Azoxystrobin	Pul	Pul + yeast	CG:PEO	CG:PEO + yeast	FP:PEO	FP:PEO + yeast
Weight loss (%)		10.80 ± 2.64^{de}	11.33 ± 0.46^{cde}	16.89 ± 6.00^{abc}	10.14 ± 0.72^{e}	19.59 ± 3.53^{a}	16.26 ± 3.90^{abcd}	18.08 ± 4.96^{ab}	13.17 ± 1.48^{bcde}
TSS (ºBrix)		0.67 ± 0.29^{a}	0.50 ± 0.00^{a}	0.67 ± 0.29^{a}	0.83 ± 0.29^{a}	0.67 ± 0.29^{a}	0.67 ± 0.29^{a}	0.83 ± 0.29^{a}	0.67 ± 0.29^{a}
TA (%)		0.14 ± 0.01^{a}	0.14 ± 0.02^{a}	0.12 ± 0.01^{ab}	0.11 ± 0.01^{ab}	0.09 ± 0.00^{b}	0.12 ± 0.01^{ab}	0.12 ± 0.02^{ab}	0.12 ± 0.01^{ab}
pH		6.89 ± 0.19^{ab}	6.84 ± 0.18^{ab}	6.96 ± 0.11^{a}	6.83 ± 0.10^{abc}	6.43 ± 0.15^{d}	6.50 ± 0.24^{cd}	6.61 ± 0.31^{bcd}	6.69 ± 0.14^{abcd}
Fruit firmness (N)		4.05 ± 0.48^{b}	4.73 ± 0.89^{b}	6.05 ± 1.17^{ab}	5.60 ± 0.75^{ab}	5.57 ± 2.69^{ab}	6.01 ± 0.82^{ab}	9.31 ± 1.53^{a}	5.99 ± 1.06^{ab}
Flesh firmness (N)		0.27 ± 0.05^{ab}	0.77 ± 0.78^{a}	0.25 ± 0.09^{ab}	0.25 ± 0.01^{ab}	0.60 ± 0.33^{ab}	0.24 ± 0.03^{b}	0.25 ± 0.09^{ab}	0.25 ± 0.01^{ab}
DMC (%)		28.01 ± 6.44^{ab}	26.12 ± 2.46^{b}	24.09 ± 2.95^{b}	27.54 ± 2.22^{b}	26.38 ± 1.57^{b}	33.98 ± 4.94^{a}	23.89 ± 2.18^{b}	27.93 ± 1.63^{b}
Pericarp	L^*	18.55 ± 0.41^{a}	19.29 ± 1.42^{a}	18.87 ± 0.45^{a}	19.15 ± 0.63^{a}	18.40 ± 2.21^{a}	19.40 ± 0.85^{a}	18.43 ± 0.86^{a}	18.57 ± 0.24^{a}
	a^*	1.58 ± 0.45^{a}	1.81 ± 0.95^{a}	1.24 ± 0.10^{a}	1.45 ± 0.56^{a}	1.48 ± 0.25^{a}	1.76 ± 0.58^{a}	1.02 ± 0.17^{a}	1.01 ± 0.12^{a}
	b^*	1.39 ± 0.16^{b}	1.26 ± 0.32^{b}	1.38 ± 0.07^{b}	1.68 ± 0.30^{ab}	2.08 ± 0.59^{a}	1.55 ± 0.19^{ab}	1.40 ± 0.34^{b}	1.26 ± 0.21^{b}
	ΔE	18.68 ± 0.37^{a}	19.41 ± 1.73^{a}	18.96 ± 0.44^{a}	19.29 ± 0.64^{a}	18.58 ± 2.27^{a}	19.55 ± 0.90^{a}	18.51 ± 0.85^{a}	18.64 ± 0.26^{a}

The avocados were immersed in SDW (sterile distilled water), azoxystrobin (800 mg/L). CG:PEO, FP:PEO and Pul nanofibers with and without *M. caribbica* were applied on the avocados surface by Solution Blow Spinning. Values in the same row, with different lower-case letters, are significantly different according to Fisher´s LSD test at $p < 0.05$. Values are expressed as means ± standard deviation (n = 36). Initial TSS (total soluble solids, %) = 0.50 ± 0.00; TA (titrata ble acidity as percentage of tartaric acid) = 0.15 ± 0.02; pH = 6.43 ± 0.06; Fruit firmness (N) = 20.40 ± 1.44; Flesh firmness (N) = 18.05 ± 1.71; DMC (dry matter content) = 29.22 ± 1.25; Pericarp color L^* = 28.15 ± 0.81, a^* = -7.00 ± 0.26, b^* = 9.62 ± 0.69. ΔE: total color change.

4 Conclusions

This is the first report where *M. caribbica* was encapsulated in nanofibers from new polymeric materials such as Pul, CG and FP using SBS technique. Homogenous, continuous, smooth, and curly nanofibers were obtained, with *M. caribbica* effectively encapsulated and distributed within the nanofibers. SBS was able to directly form and apply the nanofibers on avocados. CG:PEO, FP:PEO and Pul nanofibers were effectively adhered to the surface of avocados. The nanofibers could control the growth of *C. gloeosporioides*. However, the Pul nanofibers showed to be the most effective to inhibit the growth of *C. gloeosporioides* under both conditions tested during *in vivo* assay. The application of these nanofibers did not have a negative effect on quality properties of avocados such as pH, TA, TSS, firmness and DMC with respect to the controls (azoxystrobin and distilled water). It is important to mention that CG:PEO nanofibers provoked a high weight loss on avocados, and consequently, optimization may be required depending on the properties of fruits and vegetables. According to these results, the use of *M. caribbica* entrapped into Pul nanofibers by SBS may have great potential to act as a new biocontrol strategy to extending the shelf life of fruits and vegetables.

Author Contributions

Yuliana Vázquez González: perform methodology, validation, formal analysis, writing-original draft preparation and writing-review and editing.

Cristina Prieto: perform visualization, supervision, project administration and funding acquisition, writing-review and editing.

Jose M. Lagaron: perform visualization, supervision, project administration and funding acquisition, providing guidance and support to ensure efficient project execution, as well as reviewing, and editing.

Juan Arturo Ragazzo Sánchez: formal analysis, writing-review and editing.

Montserrat Calderón Santoyo: perform visualization, supervision, project administration and funding acquisition, writing-review and editing.

Funding: This study was supported by the CYTED thematic network (code 319RT0576), the Tecnologico Nacional de Mexico (TecNM) (project 13838.22-P), the Agencia

Valenciana de Innovación (AVI), project INNEST/2022/25, the grant PID2021-128749OB-C31 funded by MCIN/AEI/10.13039/501100011033 and by ERDF A way of making Europe.

Acknowledgments: Yuliana Vázquez González thanks Consejo Nacional de Ciencia y Tecnología for the scholarship awarded with number 862248. Cristina Prieto thanks the Valencian Ministry of Innovation, Universities, Science and Digital Society for her postdoctoral grant (CIAPOS/2021/45). The authors are also thankful to Atanu Biswas, Roselayne Furtado and H. N. Cheng for donate cashew gum polymer and thankful to Chemical Department of the Nova University for donation of FucoPol polymer. Finally, authors thankful Leb Trading Products (Guacamodely) S. de R.L. de C.V. for supplying the avocado fruit for this research.

Conflicts of Interest: The authors declare no conflict of interest.

References:

Aayush, K., McClements, D.J., Sharma, S., Sharma, R., Singh, G.P., Sharma, K., Oberoi, K., 2022. Innovations in the development and application of edible coatings for fresh and minimally processed Apple. Food Control 141, 109188. https://doi.org/10.1016/j.foodcont.2022.109188

Aceituno-Medina, M., Lopez-Rubio, A., Mendoza, S., Lagaron, J.M., 2013. Development of novel ultrathin structures based in amaranth (Amaranthus hypochondriacus) protein isolate through electrospinning. Food Hydrocoll. 31, 289–298. https://doi.org/10.1016/j.foodhyd.2012.11.009

Aguirre-Güitrón, L., Calderón-Santoyo, M., Bautista-Rosales, P.U., Ragazzo-Sánchez, J.A., 2019. Application of powder formulation of Meyerozyma caribbica for postharvest control of Colletotrichum gloeosporioides in mango (Mangifera indica L.). Lwt 113, 108271. https://doi.org/10.1016/j.lwt.2019.108271

Aguirre-Güitrón, L., Calderón-Santoyo, M., Lagarón, J.M., Prieto, C., Ragazzo-Sánchez, J.A.,2022. Formulation of the biological control yeast Meyerozyma caribbica by electrospraying process: effect on postharvest control of anthracnose in mango (Mangifera indica L.) and papaya (Carica papaya L.). J. Sci. Food Agric. 102, 696–706. https://doi.org/10.1002/jsfa.11400

Ali, A., Maqbool, M., Ramachandran, S., Alderson, P.G., 2010. Gum arabic as a novel edible

coating for enhancing shelf-life and improving postharvest quality of tomato (Solanum lycopersicum L.) fruit. Postharvest Biol. Technol. 58, 42–47. https://doi.org/10.1016/j.postharvbio.2010.05.005

Amaral, P.F.F., Coelho, M.A.Z., Marrucho, I.M.J., Coutinho, J.A.P., 2010. Biosurfactants from yeasts: Characteristics, production and application. Adv. Exp. Med. Biol. 672, 236–249. https://doi.org/10.1007/978-1-4419-5979-9_18

Araújo, R.G., Rodriguez-Jasso, R.M., Ruiz, H.A., Pintado, M.M.E., Aguilar, C.N., 2018. Avocado by-products: Nutritional and functional properties. Trends Food Sci. Technol. 80, 51–60. https://doi.org/10.1016/j.tifs.2018.07.027

Arrarte, E., Garmendia, G., Rossini, C., Wisniewski, M., Vero, S., 2017. Volatile organic compounds produced by Antarctic strains of Candida sake play a role in the control of postharvest pathogens of apples. Biol. Control 109, 14–20. https://doi.org/10.1016/j.biocontrol.2017.03.002

Ayón-Macías, K.D., Castañeda-Andrade, A.J., Ragazzo-Sánchez, J.A., Calderón-Santoyo, M., 2023. Application of nanofibers with jackfruit leaf extract via electrospinning to control phytopathogens in Averrhoa carambola L. Polym. Bull. https://doi.org/https://doi.org/10.1007/s00289-023-04815-4.

Bautista-Rosales, P.U., Calderon-Santoyo, M., Servín-Villegas, R., Ochoa-Álvarez, N.A., Ragazzo-Sánchez, J.A., 2013. Action mechanisms of the yeast Meyerozyma caribbica for the control of the phytopathogen Colletotrichum gloeosporioides in mangoes. Biol. Control 65, 293–301. https://doi.org/10.1016/j.biocontrol.2013.03.010

Behrens, A.M., Casey, B.J., Sikorski, M.J., Wu, K.L., Tutak, W., Sandler, A.D., Kofinas, P., 2014. In situ deposition of PLGA nanofibers via solution blow spinning. ACS Macro Lett. 3, 249–254. https://doi.org/10.1021/mz500049x

Benavides, R.E., Jana, S.C., Reneker, D.H., 2012. Nanofibers from scalable gas jet process. ACS Macro Lett. 1, 1032–1036. https://doi.org/10.1021/mz300297g

Bill, M., Sivakumar, D., Thompson, A.K., Korsten, L., 2014. Avocado Fruit Quality Management during the Postharvest Supply Chain. Food Rev. Int. 30, 169–202. https://doi.org/10.1080/87559129.2014.907304

Choińska, R., Piasecka-Jóźwiak, K., Chabłowska, B., Dumka, J., Łukaszewicz, A., 2020. Biocontrol ability and volatile organic compounds production as a putative mode of action of yeast strains isolated from organic grapes and rye grains. Antonie van Leeuwenhoek, Int. J.Gen. Mol. Microbiol. 113, 1135–1146. https://doi.org/10.1007/s10482-020-01420-7

Ciofini, A., Negrini, F., Baroncelli, R., Baraldi, E., 2022. Management of Post-Harvest Anthracnose: Current Approaches and Future Perspectives. Plants 11.https://doi.org/10.3390/plants11141856

Correa-Pacheco, Z.N., Bautista-Baños, S., Valle-Marquina, M.Á., Hernández-López, M., 2017. The Effect of Nanostructured Chitosan and Chitosan-thyme Essential Oil Coatings on Colletotrichum gloeosporioides Growth in vitro and on cv Hass Avocado and Fruit Quality. J. Phytopathol. 165, 297–305. https://doi.org/10.1111/jph.12562

Cox, K.A., McGhie, T.K., White, A., Woolf, A.B., 2004. Skin colour and pigment changes during ripening of "Hass" avocado fruit. Postharvest Biol. Technol. 31, 287–294. https://doi.org/10.1016/j.postharvbio.2003.09.008

da Silva, L.L., Moreno, H.L.A., Correia, H.L.N., Santana, M.F., de Queiroz, M.V., 2020. Colletotrichum: species complexes, lifestyle, and peculiarities of some sources of genetic variability. Appl. Microbiol. Biotechnol. 104, 1891–1904. https://doi.org/10.1007/s00253 020-10363-y

da Silva Parize, D.D., Foschini, M.M., de Oliveira, J.E., Klamczynski, A.P., Glenn, G.M., Marconcini, J.M., Mattoso, L.H.C., 2016. Solution blow spinning: Parameters optimization and effects on the properties of nanofibers from poly(lactic acid)/dimethyl carbonate solutions. J. Mater. Sci. 51, 4627–4638. https://doi.org/10.1007/s10853-016-9778-x

Dadol, G.C., Kilic, A., Tijing, L.D., Lim, K.J.A., Cabatingan, L.K., Tan, N.P.B., Stojanovska, E., Polat, Y., 2020. Solution blow spinning (SBS) and SBS-spun nanofibers: Materials, methods,and applications. Mater. Today Commun. 25, 101656. https://doi.org/10.1016/j.mtcomm.2020.101656

Daristotle, J.L., Behrens, A.M., Sandler, A.D., Kofinas, P., 2016. A Review of the Fundamental Principles and Applications of Solution Blow Spinning. ACS Appl. Mater. Interfaces 8, 34951–34963. https://doi.org/10.1021/acsami.6b12994

Eijkelboom, N.M., van Boven, A.P., Siemons, I., Wilms, P.F.C., Boom, R.M., Kohlus, R., Schutyser, M.A.I., 2023. Particle structure development during spray drying from a single droplet to pilot-scale perspective. J. Food Eng. 337, 111222. https://doi.org/10.1016/j.jfoodeng.2022.111222

Ferreira, A.R.V., Torres, C.A.V., Freitas, F., Sevrin, C., Grandfils, C., Reis, M.A.M., Alves, V.D., Coelhoso, I.M., 2016. Development and characterization of bilayer films of FucoPol and chitosan. Carbohydr. Polym. 147, 8–15. https://doi.org/10.1016/j.carbpol.2016.03.089

Francis, L., Balakrishnan, A., Sanosh, K.P., Marsano, E., 2010. Characterization and tensile strength of HPC-PEO composite fibers produced by electrospinning. Mater. Lett. 64, 1806–1808. https://doi.org/10.1016/j.matlet.2010.05.043

González-Estrada, R.R., Carvajal-Millán, E., Ragazzo-Sánchez, J.A., Bautista-Rosales, P.U., Calderón-Santoyo, M., 2017. Control of blue mold decay on Persian lime: Application of covalently cross-linked arabinoxylans bioactive coatings with antagonistic yeast entrapped. LWT - Food Sci. Technol. 85, 187–196. https://doi.org/10.1016/j.lwt.2017.07.019

González-Gutiérrez, K.N., Ragazzo-Sánchez, J.A., Calderón-Santoyo, M., 2021. Application of stressed and microencapsulated Meyerozyma caribbica for the control of Colletotrichum gloeosporioides in avocado (Persea americana Mill. cv. Hass). J. Plant Dis. Prot. 128, 1243–1251. https://doi.org/10.1007/s41348-021-00487-2

Guo, L., Azam, S.M.R., Guo, Y., Liu, D., Ma, H., 2021. Germicidal efficacy of the pulsed magnetic field against pathogens and spoilage microorganisms in food processing: An overview. Food Control 108496. https://doi.org/10.1016/j.foodcont.2021.108496

Haider, A., Haider, S., Kang, I.K., 2018. A comprehensive review summarizing the effect of electrospinning parameters and potential applications of nanofibers in biomedical and biotechnology. Arab. J. Chem. 11, 1165–1188. https://doi.org/10.1016/j.arabjc.2015.11.015

Hofmann, E., Krüger, K., Haynl, C., Scheibel, T., Trebbin, M., Förster, S., 2018. Microfluidic nozzle device for ultrafine fiber solution blow spinning with precise diameter control. LabChip 18, 2225–2234. https://doi.org/10.1039/c8lc00304a

Iñiguez-Moreno, M., Calderón-Santoyo, M., Barros-Castillo, J.C., Miss-Zacarías, D.M., Díaz, J.A., Ragazzo-Sánchez, J.A., 2022. Nanofibers added with citral: Characterization and their application to postharvest control of Fusarium pseudocircinatum in bananas. J. Food Process. Preserv. 46, 1–10. https://doi.org/10.1111/jfpp.17188

Iñiguez-Moreno, M., Ragazzo-Sánchez, J.A., Barros-Castillo, J.C., Sandoval-Contreras, T., Calderón-Santoyo, M., 2020. Sodium alginate coatings added with Meyerozyma caribbica: Postharvest biocontrol of Colletotrichum gloeosporioides in avocado (Persea americana Mill. cv. Hass). Postharvest Biol. Technol. 163, 111123.https://doi.org/10.1016/j.postharvbio.2020.111123

Iñiguez-Moreno, M., Ragazzo-Sánchez, J.A., Barros-Castillo, J.C., Solís-Pacheco, J.R., Calderón-Santoyo, M., 2021. Characterization of sodium alginate coatings with Meyerozyma caribbica and impact on quality properties of avocado fruit. Lwt 152. https://doi.org/10.1016/j.lwt.2021.112346

Iñiguez-Moreno, M., Ragazzo-sánchez, J.A., Calderón-santoyo, M., 2021. An extensive review of natural polymers used as coatings for postharvest shelf-life extension: Trends and challenges. Polymers (Basel). 13. https://doi.org/10.3390/polym13193271

Khalilur, M., Khan, R., Hassan, M.N., 2021. Solution Blow Spinning (SBS): A Promising Spinning System for Submicron/Nanofibre Production How to cite: Khan MKR, Hassan MN. Solution Blow Spinning (SBS): A Promising Spinning System for Submicron/Nanofibre Production. Textile & Leather Review. Text. Leather Rev. 4, 181–200. https://doi.org/10.31881/TLR

Kolbasov, A., Sinha-Ray, S., Joijode, A., Hassan, M.A., Brown, D., Maze, B., Pourdeyhimi, B., Yarin, A.L., 2016. Industrial-Scale Solution Blowing of Soy Protein Nanofibers. Ind. Eng.Chem. Res. 55, 323–333. https://doi.org/10.1021/acs.iecr.5b04277

Lu, B., He, Y., Duan, H., Zhang, Y., Li, X., Zhu, C., Xie, E., 2012. A new ultrahigh-speed method for the preparation of nanofibers containing living cells: A bridge towards industrial bioengineering applications. Nanoscale 4, 1003–1009. https://doi.org/10.1039/c2nr11430e

Marques, K.M., Galati, V.C., Fernandes, J.D.R., Guimarães, J.E.R., Silva, J.P., Mattiuz, B.H., Mattiuz, C.F.M., 2016. Use of chitosan for the control of postharvest anthracnose and quality in avocados. Acta Hortic. 1120, 225–231. https://doi.org/10.17660/ActaHortic.2016.1120.34

Medeiros, E.S., Glenn, G.M., Klamczynski, A.P., Orts, W.J., Mattoso, L.H.., 2009. Solution Blow Spinning: A New Method to Produce Micro- and Nanofibers from Polymer Solutions. J. Appl. Polym. Sci. 113, 2322–2330. https://doi.org/10.1002/app

Monsores, K.G. de C., Oliveira da Silva, A., Oliveira, S. de S.A., Weber, R.P., Dias, M.L., 2022. Production of nanofibers from solution blow spinning (SBS). J. Mater. Res. Technol. 16, 1824–1831. https://doi.org/10.1016/j.jmrt.2021.12.098

Moreira, B.R., Pereira-Júnior, M.A., Fernandes, K.F., Batista, K.A., 2020. An ecofriendly edible coating using cashew gum polysaccharide and polyvinyl alcohol. Food Biosci. 37, 100722. https://doi.org/10.1016/j.fbio.2020.100722

Niu, B., Shao, P., Feng, S., Qiu, D., Sun, P., 2020. Rheological aspects in fabricating pullulan-whey protein isolate emulsion suitable for electrospraying: Application in improving β-carotene stability. Lwt 129, 109581. https://doi.org/10.1016/j.lwt.2020.109581

Ocampo-Suarez, I.B., López, Z., Calderón-Santoyo, M., Ragazzo-Sánchez, J.A., Knauth, P., 2017. Are biological control agents, isolated from tropical fruits, harmless to potential consumers? Food Chem. Toxicol. 109, 1055–1062. https://doi.org/https://doi.org/10.1016/j.fct.2017.05.010.

Oliveira, J., Moraes, E.A., Costa, R.G.F., Afonso, A.S., Mattoso, L.H.C., Orts, W.J., Medeiros,E.S., 2011. Nano and Submicrometric Fibers of Poly(D,L-Lactide) Obtained by Solution Blow Spinning: Process and Solution Variables. J. Appl. Polym. Sci. 116, 2658–2667. https://doi.org/10.1002/app

Park, H.J., Chinnan, M.S., 1995. Gas and water vapor barrier properties of edible films from protein and cellulosic materials. J. Food Eng. 25, 497–507. https://doi.org/10.1016/0260-8774(94)00029-9

Pehlivaner Kara, M.O., Ekenseair, A.K., 2016. In situ spray deposition of cell-loaded, thermally and chemically gelling hydrogel coatings for tissue regeneration. J. Biomed. Mater. Res. - Part A 104, 2383–2393. https://doi.org/10.1002/jbm.a.35774

Rostamabadi, H., Falsafi, S.R., Rostamabadi, M.M., Assadpour, E., Jafari, S.M., 2021. Electrospraying as a novel process for the synthesis of particles/nanoparticles loaded with poorly water-soluble bioactive molecules. Adv. Colloid Interface Sci. 290. https://doi.org/10.1016/j.cis.2021.102384

Saberi, B., Golding, J.B., Marques, J.R., Pristijono, P., Chockchaisawasdee, S., Scarlett, C.J., Stathopoulos, C.E., 2018. Application of biocomposite edible coatings based on pea starch and guar gum on quality, storability and shelf life of 'Valencia' oranges. Postharvest Biol. Technol. 137, 9–20. https://doi.org/10.1016/j.postharvbio.2017.11.003

Santos, A.M.C., Medeiros, E.L.G., Blaker, J.J., Medeiros, E.S., 2016. Aqueous solution blow spinning of poly(vinyl alcohol) micro- and nanofibers. Mater. Lett. 176, 122–126. https://doi.org/10.1016/j.matlet.2016.04.101

Shen, C., Deng, Z., Rao, J., Yang, Z., Li, Y., Wu, D., Chen, K., 2022. Characterization of glycosylated gelatin/pullulan nanofibers fabricated by multi-fluid mixing solution blow spinning. Int. J. Biol. Macromol. 214, 512–521. https://doi.org/10.1016/j.ijbiomac.2022.06.082

Shi, X.C., Wang, S.Y., Duan, X.C., Wang, Y.Z., Liu, F.Q., Laborda, P., 2021. Biocontrol strategies for the management of Colletotrichum species in postharvest fruits. Crop Prot. 141, 105454. https://doi.org/10.1016/j.cropro.2020.105454

Sierra, N.M., Londoño, A., Gómez, J.M., Herrera, A.O., Castellanos, D.A., 2019. Evaluation and modeling of changes in shelf life, firmness and color of 'Hass' avocado depending on storage temperature. Food Sci. Technol. Int. 25, 370–384. https://doi.org/10.1177/1082013219826825

Stojanovska, E., Canbay, E., Pampal, E.S., Calisir, M.D., Agma, O., Polat, Y., Simsek, R., Gundogdu, N.A.S., Akgul, Y., Kilic, A., 2016. A review on non-electro nanofibre spinning techniques. RSC Adv. 6, 83783–83801. https://doi.org/10.1039/c6ra16986d

Sucheta, Chaturvedi, K., Sharma, N., Yadav, S.K., 2019. Composite edible coatings from commercial pectin, corn flour and beetroot powder minimize post-harvest decay, reduces ripening and improves sensory liking of tomatoes. Int. J. Biol. Macromol. 133, 284–293. https://doi.org/10.1016/j.ijbiomac.2019.04.132

Tien, N.D., Geng, T., Heyward, C.A., Reseland, J.E., Lyngstadaas, S.P., Blaker, J.J., Haugen, H.J., 2022. Solution blow spinning of highly deacetylated chitosan nanofiber scaffolds for dermal wound healing. Biomater. Adv. 137, 212871. https://doi.org/10.1016/j.bioadv.2022.212871

Torres-Giner, S., Hilliou, L., Melendez-Rodriguez, B., Figueroa-Lopez, K.J., Madalena, D., Cabedo, L., Covas, J.A., Vicente, A.A., Lagaron, J.M., 2018. Melt processability, characterization, and antibacterial activity of compression-molded green composite sheets made of poly(3-hydroxybutyrate-co-3-hydroxyvalerate) reinforced with coconut fibers impregnated with oregano essential oil. Food Packag. Shelf Life 17, 39–49. https://doi.org/10.1016/j.fpsl.2018.05.002

Torres-Giner, S., Ocio, M.J., Lagaron, J.M., 2008. Development of active antimicrobial fiber based chitosan polysaccharide nanostructures using electrospinning. Eng. Life Sci. 8, 303 314.https://doi.org/10.1002/elsc.200700066

Vázquez-González, Y., Prieto, C., Calderón-Santoyo, M., Ragazzo-Sánchez, J.A., Lagarón, J.M.,2024. Development of antifungal electrospun nanofiber mats containing Meyerozyma caribbica. Food Hydrocoll. 147. https://doi.org/10.1016/j.foodhyd.2023.109343

Vázquez-González, Y., Prieto, C., Filizoglu, M.F., Ragazzo-Sánchez, J.A., Calderón Santoyo, M., Furtado, R.F., Cheng, H.N., Biswas, A., Lagaron, J.M., 2021. Electrosprayed cashew gum microparticles for the encapsulation of highly sensitive bioactive materials. Carbohydr. Polym.264. https://doi.org/10.1016/j.carbpol.2021.118060

Vázquez-González, Y., Prieto, C., Stojanovic, M., Torres, C.A. V, Freitas, F., Ragazzo Sánchez, J.A., Calderón-Santoyo, M., María, L.J., 2022. Preparation and Characterization of Electrospun Polysaccharide FucoPol-Based Nanofiber Systems 1–15. https://doi.org/https://doi.org/10.3390/nano12030498

Veazey, W.S., Anusavice, K.U., Moore, K., 2005. Mammalian cell delivery via aerosol deposition. J. Biomed. Mater. Res. - Part B Appl. Biomater. 72, 334–338. https://doi.org/10.1002/jbm.b.30159

Wu, J.J., Huang, J.W., Deng, W.L., 2020. Phenylacetic Acid and Methylphenyl Acetate From the Biocontrol Bacterium Bacillus mycoides BM02 Suppress Spore Germination in Fusarium oxysporum f. sp. lycopersici. Front. Microbiol. 11, 1–12. https://doi.org/10.3389/fmicb.2020.569263

Xiao, Q., Lim, L.T., 2018. Pullulan-alginate fibers produced using free surface electrospinning. Int. J. Biol. Macromol. 112, 809–817. https://doi.org/10.1016/j.ijbiomac.2018.02.005

Zhang, H., Mahunu, G.K., Castoria, R., Apaliya, M.T., Yang, Q., 2017. Augmentation of biocontrol agents with physical methods against postharvest diseases of fruits and vegetables. Trends Food Sci. Technol. 69, 36–45. https://doi.org/10.1016/j.tifs.2017.08.020

CAPÍTULO 8. DISCUSIÓN GENERAL

8. DISCUSION GENERAL

El mercado de los aguacates se encuentra entre los de más rápido crecimiento en todo el mundo, siendo México el primer productor y exportador de este fruto (STATISTA, 2023). Sin embargo, debido a su susceptibilidad a enfermedades postcosecha se producen grandes pérdidas económicas. La antracnosis causada por el hongo *Colletotrichum gloeosporioides* es una de las enfermedades más importantes que afecta a este fruto (Bill y cols., 2014).

En este sentido, para controlar las enfermedades postcosecha causadas por hongos fitopatógenos, los microorganismos antagonistas están siendo ampliamente estudiados como alternativa a los tratamientos de fungicidas químicos. Dentro de los microorganismos antagonistas estudiados, cabe destacar la levadura *Meyerozyma caribbica*, la cual ha sido reportada como efectiva como control biológico en mango, en papaya y en aguacate (Iñiguez-Moreno y cols., 2021; González-Gutiérrez y cols., 2021; Aguirre-Güitrón y cols., 2022; Bautista-Rosales y cols., 2013), debido a sus diferentes mecanismos de acción y, además, se ha demostrado su no toxicidad (Ocampo-Suarez y cols., 2017), lo que la hace una alternativa segura. Estos microorganismos se pueden combinar con matrices poliméricas con la finalidad de brindarles protección para mantener su actividad y eficacia contra los fitopatógenos. En este sentido, se están explorando nuevas técnicas y matrices poliméricas que proporcionen la liberación controlada del agente bioactivo y permitan una aplicación directa en el fruto.

Las nanoestructuras biopoliméricas producidas mediante procesos electrohidrodinámicos y aerohidrodinámicos presentan características que las hacen altamente interesantes para esta aplicación (Haider y cols., 2018; Torres-Giner y cols., 2018), por este motivo, el desarrollo de nanofibras biopoliméricas con propiedades antifúngicas para el tratamiento de la antracnosis en aguacate Hass ha sido el objetivo principal de esta tesis.

Así, la primera fase de esta tesis se centró en la realización de un estudio sobre el procesado electrohidrodinámico del primer biopolímero seleccionado: la goma de anacardo. En particular, la goma de anacardo (CG) es un exudado gomoso obtenido del árbol *Anacardium occidentale,* el cual está ampliamente distribuido en la parte nororiental de Brasil. Este biomaterial presenta un alto potencial, debido a que se trata de una materia prima económica, biocompatible, ecológica y altamente biodisponible. Además, es soluble en agua, con buenas propiedades emulsificantes, adhesivas y estabilizantes, y se ha reportado su

actividad mucoadhesiva, antiinflamatoria y antimicrobiana, entre otros (Botrel y cols., 2017; Ribeiro y cols., 2016; Silva y cols., 2012). El estudio realizado en esta primera fase de la tesis fue necesario debido a que, de acuerdo con nuestro conocimiento, el procesado de dicho biomaterial no se había realizado anteriormente mediante esta tecnología. Para este estudio, se desarrollaron formulaciones con propiedades físicoquímicas adecuadas para ser procesadas mediante procesado electrohidrodinámico. Sin embargo, se observó que la CG por sí sola no es capaz de formar nanofibras, y en su lugar se obtuvieron cápsulas esféricas, de superficie lisa, sin concavidades y no presentaron fisuras ni roturas. Con el objetivo de caracterizar las propiedades protectoras de la CG, se llevó a cabo el proceso de encapsulación de un compuesto bioactivo modelo, altamente conocido en el grupo de investigación, el β-caroteno. Las partículas obtenidas encapsulando el β-caroteno, presentaron buenas propiedades morfológicas, cápsulas esféricas y lisas, sin presencia de concavidades y tamaño medio de partícula entre 3 y 6 μm, y de eficiencia de encapsulación, siendo superior al 90%; sin embargo, presentaron baja capacidad de carga, siendo inferior al 0.1%, principalmente debido a la baja solubilidad de este compuesto en casi todos los disolventes convencionales. Esto podría limitar su aplicación; sin embargo, podrían realizarse algunas modificaciones químicas de la goma para mejorar las interacciones entre el compuesto bioactivo y la matriz polimérica, y con ello mejorar la capacidad de carga. Finalmente, bajo un estudio acelerado bajo luz ultravioleta se observó que la CG tiene capacidad de brindar fotoprotección al β-caroteno.

La segunda fase de esta tesis consistió en el estudio sobre la posibilidad de formación de nanofibras electroestiradas con el segundo biopolímero seleccionado, el FucoPol. Este biomaterial es un exopolisacárido producido por el microorganismo *Enterobacter* A477. Se trata de un heteropolisacárido con carácter aniónico e interesantes propiedades funcionales, como emulsificantes, espesante, floculante, filmógena, propiedades adhesivas y fotoprotectoras (Ferreira y cols., 2018; Guerreiro y cols., 2020; Lourenço y cols., 2017). Al igual que con el biopolímero anterior, no se disponía de información bibliográfica sobre la formación de micro o nanoestructuras mediante *electrospinning* a partir de este exopolisacárido. Se obtuvo una película de fibras homogéneo, semitransparente y flexible, sin embargo, al momento de manipularlo mostró ser frágil. El análisis mediante microscopía electrónica demostró que este comportamiento se debía a la presencia de fibras y perlas. Por

tanto, la disolución de FucoPol en agua, por sí misma no formó fibras, debido a la baja solubilidad máxima de este polímero en este disolvente. Por lo tanto, se decidió combinar el FucoPol con polímeros de soporte como el PEO o el pululano. Para la producción de estas fibras, se usó una solución agua:etanol (70:30, v/v), para disminuir la tensión superficial, y con ello generar un proceso más estable de formación de fibras. La observación mediante microscopía electrónica de los materiales obtenidos mostró fibras helicoidales, uniformes y cilíndricas a partir de FP:PEO y FP:Pululano. Además, mediante los análisis de TGA se observó que la presencia de FucoPol aumentó el rango de degradación térmica alrededor de 70 ºC. Los análisis de DSC de las nanofibras de FucoPol y FucoPol:Pululano mostraron su naturaleza amorfa. Un hallazgo importante en esta segunda etapa fue que mediante el análisis WAXS, se observaron nuevos picos por debajo de los 10º, lo que sugiere que la presencia del exopolisacárido FucoPol podría afectar el ensamble jerárquico de este polisacárido con los polímeros de soporte con una estructura helicoidal.

Después del estudio de la CG en la fase 1 y la obtención de nanofibras de FucoPol por *electrospinning* en la fase 2, en la fase 3 se procedió a la formación de nanofibras de Pululano, GC:PEO y FucoPol:PEO adicionadas con *M. caribbica* mediante *electrospinning*. En esta fase, se obtuvieron fibras cilíndricas, lisas y uniformes a partir de las diferentes soluciones poliméricas que contenían a la levadura tal y como se observó mediante SEM. Se realizó un estudio de la morfología interna de las fibras, para lo cual las fibras se embebieron en resina, se realizaron cortes finos con un ultramicrotomo, los cuales se tiñeron y ser observaron en un microscopio óptico. Esto permitió confirmar la presencia de la levadura en las nanofibras. Se hipotetizó que dicha encapsulación se producía cuando la gota se alarga para formar la fibra y la levadura está presente, el polímero recubre completamente la levadura y, después de esto, la formación de fibra continua. De acuerdo con la literatura, solo los polímeros con pesos moleculares adecuados pueden proporcionar propiedades viscoelásticas que permitirán la encapsulación de microorganismos (Torres-Guiner y cols., 2008). En relación con la viabilidad de la levadura, se observó que la pérdida de células viables fue más significativa en las nanofibras de CG:PEO y FP:PEO comparadas con las nanofibras de pululano. Adicionalmente, la formulación con pululano proporcionó una mayor estabilidad de la levadura durante 25 días a ambas temperaturas evaluadas. Finalmente, se observó que las nanofibras de pululano mostraron los porcentajes de inhibición más altos frente a los seis

patógenos estudiados, comparadas con las nanofibras de CG:PEO y FP:PEO. Este fenómeno podría deberse a la mayor viabilidad de *M. caribbica* presentada por las fibras de pululano. Las formulaciones poliméricas estudiadas permitieron la liberación de *M. caribbica* durante la incubación, la cual colonizó toda la placa de Petri e impidió el desarrollo de los hongos gracias a los diferentes mecanismos de acción reportados para esta levadura (Bautista-Rosales y cols., 2013). De acuerdo con el ensayo de germinación de esporas, todos los tratamientos mostraron un efecto fungistático, ya que después del tiempo de germinación de la espora control, las esporas con tratamiento germinaron.

Durante la fase 4, se procedió a obtener nanofibras de Pululano, CG:PEO y FucoPol:PEO adicionadas con *M. caribbica* mediante la técnica *Solution Blow Spinning*. Las fibras obtenidas con las formulaciones estudiadas mostraron ser fibras con una apariencia uniforme, suave y rizada con pequeños agrupamientos debido a la turbulencia del gas presurizado durante el proceso de SBS. A pesar de estos agrupamientos, se pudo observar que *M. caribbica* también fue encapsulada dentro de las nanofibras mediante esta técnica. En relación con la inhibición del crecimiento micelial, todas las nanofibras adicionadas con *M. caribbica* no mostraron diferencia estadísticamente significativa en la inhibición de *C. gloeosporioides* a 6 ºC. Es importante señalar que las nanofibras sin *M. caribbica* no mostraron efecto sobre la germinación de las esporas. En este sentido, se atribuyó la inhibición a diferentes mecanismos de acción de *M. caribbica*. Durante los ensayos *in vivo* de estabilidad en condiciones de almacenamiento del aguacate, las nanofibras de pululano, CG:PEO y FP:PEO mostraron un nivel de protección similar, debido a que la viabilidad de *M. caribbica* se redujo con el tiempo. Esta pérdida de viabilidad de *M. caribbica* en nanofibras aplicadas sobre aguacate puede estar asociada a una mayor pérdida de humedad a 25 ºC (Iñiguez-Moreno y cols., 2020). Las nanofibras de pululano con levaduras mostraron los mejores resultados como tratamiento preventivo en la inhibición de *C. gloesosporioides* comparado con las nanofibras de FP:PEO y CG:PEO; ya que no se observaron heridas infectadas y por ende no hubo desarrollo de la enfermedad. Finalmente, se observó que las nanofibras no mostraron un efecto significativo en los diferentes parámetros de calidad evaluados sobre los aguacates en comparación con los aguacates control.

En conclusión, este trabajo de tesis ha demostrado el uso potencial de dos polisacáridos como material de pared en la encapsulación de compuestos activos como el β-caroteno, y de

agentes de biocontrol, como *M. caribbica*. Estos pueden ser procesados mediante técnicas electrohidrodinámicas como *electrospray* y *electrospinning*, así como a través de un proceso aerohidrodinámico, destacando la técnica *Solution Blow Spinning*. La presencia de *M. caribbica* en las nanofibras, junto con las diversas propiedades mostradas, como la elevada viabilidad de *M. caribbica* después de los procesos de *electrospinning* y *Solution Blow Spinning*, la falta de interacción entre las nanofibras y la levadura, y la ausencia de efectos negativos de las nanofibras en los parámetros de calidad de los frutos de aguacate, sugiere que estas nanofibras tienen un potencial de aplicación en el tratamiento post-cosecha de frutas y vegetales. Esto podría ayudar a controlar e inhibir diversos hongos fitopatógenos que causan pérdidas significativas en la producción de frutas y vegetales, contribuyendo así a la reducción del desperdicio de alimentos.

CAPÍTULO 9. CONCLUSIÓN GENERAL Y PERSPECTIVAS DEL PROYECTO

9. CONCLUSIÓN GENERAL Y PERSPECTIVAS DEL PROYECTO

9.1 Conclusión general

Las enfermedades postcosecha producen anualmente una gran cantidad de desperdicios alimentarios y grandes pérdidas económicas. Por este motivo, la búsqueda de estrategias de control alternativas a los fungicidas químicos se sitúa como uno de los principales temas de interés para la comunidad científica. Existe un gran interés por el estudio de agentes de biocontrol y de nuevas técnicas que permitan la protección de dichos agentes y su aplicación directa. En este contexto, en esta tesis se ha realizado el desarrollo de recubrimientos antifúngicos para el control de antracnosis en aguacate "Hass" (*Persea americana* Mill. cv. Hass).

Para ello, en esta investigación, se logró optimizar soluciones utilizando polisacáridos como la goma de anacardo, el FucoPol y el pululano. Estos polisacáridos demostraron la capacidad de formar micro y nanoestructuras mediante procesos electrohidrodinámicos y aerohidrodinámicos, manteniendo una estabilidad térmica. Las microcápsulas resultantes presentaron una morfología característica, siendo uniformes y sin imperfecciones, al igual que las nanofibras, que se mantuvieron homogéneas, continuas y lisas a nivel nanométrico.

Adicionalmente, las nanofibras desempeñaron un papel crucial al actuar como matrices de soporte para agentes de biocontrol, especialmente la levadura *Meyerozyma caribbica*. Las nanofibras al ser depositadas como una capa protectora activa en diferentes frutos, en particular en aguacate Hass, permiten a la levadura ejercer mecanismos de acción para inhibir el crecimiento de *Colletotrichum gloeosporioides*, sin comprometer los parámetros de calidad del fruto.

Es fundamental destacar que, a pesar de estos resultados prometedores, aún se requiere llevar a cabo investigaciones futuras para lograr la viabilidad comercial de estas nuevas tecnologías. El potencial de estos polisacáridos y sus aplicaciones en la industria de alimentos y agricultura abre un campo para investigaciones y desarrollos adicionales, con el fin de contribuir significativamente a la conservación de alimentos y la seguridad alimentaria.

9.2 Perspectivas del proyecto

Las actividades desarrolladas a lo largo de esta investigación han desempeñado un papel significativo en la expansión de nuestro conocimiento, abriendo perspectivas hacia futuras áreas de estudio. En este contexto, resulta recomendable realizar estudios adicionales sobre propiedades como la barrera frente a gases (O_2 y CO_2), permeabilidad al vapor de agua, cristalinidad, solubilidad en agua, entre otros. Esto con el objetivo de mejorar la compatibilidad de los polisacáridos aplicados ya sea como recubrimientos o como nanofibras en la superficie de los frutos. Además, es esencial dirigir esfuerzos hacia el reconocimiento de estos polisacáridos como "generalmente reconocidos como seguros" (GRAS) por la FDA, lo que facilitaría su implementación a gran escala en la industria alimentaria. A pesar de las numerosas ventajas que presentan las nanoestructuras en comparación con los recubrimientos comestibles convencionales, resulta imperativo evaluar con meticulosidad la posible toxicidad asociada a estas nanoestructuras.

Es pertinente resaltar que, si bien en esta investigación se implementaron nanofibras en aguacates, para futuras aplicaciones en frutos que se consuman con piel resulta imperativo realizar estudios específicos centrados en la actividad gastrointestinal de los alimentos recubiertos con estas nanoestructuras. Un ejemplo de ello podría ser el cultivo de células Caco-2 y la digestión *in vitro* de Caco-2. Estos estudios serán cruciales para garantizar la seguridad y la eficacia de estas tecnologías en la industria alimentaria.

En conjunto, esta investigación marca el comienzo de un camino hacia la aplicación práctica de estas innovadoras tecnologías, sin embargo, para alcanzar el máximo potencial de las ventajas y beneficios que estas tecnologías ofrecen, es crucial llevar a cabo investigaciones adicionales en aspectos como la rentabilidad, el tipo de estructuras obtenidas a partir de nuevos materiales poliméricos, la versatilidad para su aplicación en diversos tipos de frutos, la facilidad de manipulación de dichas tecnologías, así como las regulaciones para la aplicación de nanoestructuras en alimentos, entre otros aspectos relevantes.

CAPÍTULO 10. ANEXOS

10. ANEXOS

Carbohydrate Polymers 264 (2021) 118060

Contents lists available at ScienceDirect

Carbohydrate Polymers

journal homepage: www.elsevier.com/locate/carbpol

Electrosprayed cashew gum microparticles for the encapsulation of highly sensitive bioactive materials

Y. Vázquez-González [a,b], C. Prieto [a,*], M.F. Filizoglu [a,c], J.A. Ragazzo-Sánchez [b], M. Calderón-Santoyo [b], R.F. Furtado [d], H.N. Cheng [e], A. Biswas [f], J.M. Lagaron [a]

[a] Novel Materials and Nanotechnology Group, Institute of Agrochemistry and Food Technology (IATA), Spanish Council for Scientific Research (CSIC), Calle Catedrático Agustín Escardino Benlloch 7, 46980, Paterna, Spain
[b] Laboratorio Integral de Investigación en Alimentos, Tecnológico Nacional de México – Instituto Tecnológico de Tepic, Av. Tecnológico de Tepic, Av. Tecnológico # 2595, C.P. 63195, Tepic, Nayarit, Mexico
[c] Department of Biology, Faculty of Science, İstanbul University, 34134 Vezneciler, İstanbul, Turkey
[d] Embrapa Agroindústria Tropical, Rua Dra. Sara Mesquita 2270, CEP 60511-110, Fortaleza, CE, Brasil
[e] U.S. Department of Agriculture, Agriculture Research Service, Southern Regional Research Center, 1100 Robert E. Lee Blvd., New Orleans, LA, 70124, USA
[f] U.S. Department of Agriculture, Agricultural Research Service, National Center for Agricultural Utilization Research, 1815 N. University St, Peoria, IL, 61604, USA

ARTICLE INFO

Keywords:
Cashew gum polysaccharide
β-Carotene
Electrospray
Microparticles
Encapsulation

ABSTRACT

This study focuses on the production and characterization of electrosprayed cashew gum (CG) microparticles that encapsulate β-carotene. CG is an inexpensive, non-toxic polysaccharide obtained from *Anacardium occidentale* trees. Encapsulation of β-carotene in CG was performed by electrospraying from two emulsion formulations (water : oil ratios 80:20 and 90:10 (v/v)) in which the dispersed phase consisted of β-carotene dissolved in castor oil, and the continuous phase was a CG aqueous solution. Spherical particles with smooth surface and medium size between 3 and 6 μm were obtained. The particles produced from the 90:10 (v/v) emulsion showed a loading capacity of 0.075 ± 0.006 % and a minor amount of extractable β-carotene, 10.75 ± 2.42 %. ATR-FTIR confirmed the absence of interaction between the particles' components. CG demonstrated to offer thermoprotection, and photoprotection for short periods of time. These results make CG a viable candidate to encapsulate bioactive compounds via electrospraying for agricultural, food and pharmaceutical applications.

1. Introduction

Encapsulation may be defined as the process that entraps a bioactive compound into a wall material (Nedovic, Knlusevic, Manojlovic, Levic, & Bugarski, 2011) in order to protect it from different physico-chemical factors (temperature, oxygen, humidity, pH, among others), which may engender its degradation and loss of bioavailability (Sobel, Versic, & Gnonkar, 2014). This technology is of significant interest to the pharmaceutical, cosmetic and biotechnological sectors but has special relevance for the food industry (Nedovic et al., 2011). Multiple encapsulation technologies have been developed so far; the efficiency of the encapsulation process not only depends on the selected technology but also on the characteristics of the wall material. Together, they can improve the core material stability and reduce its volatility, mask undesirable aromas and flavors, avoid migration of the core material to the particle surface, and provide controlled release (Botrel, Borges, Fernandes et al., 2017). The wall material must be biocompatible and biodegradable, form a barrier between the internal phase and its surroundings, provide its release at the desired time, and is approved for use in the final product. In addition, the availability and cost of the wall material are also important (Fernandes et al., 2016). Wall materials can be selected from a wide variety of natural or synthetic polymers. Most of the natural polymers are water soluble and non-toxic, which makes them highly appropriate for the encapsulation of sensitive bioactives (Nedovic et al., 2011). Among the natural polymers, polysaccharides and proteins are the most often used in encapsulation processes. In view

Abbreviations: CG, cashew gum; LC, loading capacity; E|C, extractable β-carotene.

* Corresponding author.
E-mail addresses: yuliana.vg04@gmail.com (Y. Vázquez-González), cprieto@iata.csic.es (C. Prieto), filizoglumf@gmail.com (M.F. Filizoglu), arturoragazzo@hotmail.com (J.A. Ragazzo-Sánchez), montserratcalder@gmail.com (M. Calderón-Santoyo), roselayne.furtado@embrapa.br (R.F. Furtado), hn.cheng@usda.gov (H.N. Cheng), atanu.biswas@usda.gov (A. Biswas), lagaron@iata.csic.es (J.M. Lagaron).

https://doi.org/10.1016/j.carbpol.2021.118060
Received 31 October 2020; Received in revised form 15 March 2021; Accepted 6 April 2021
Available online 10 April 2021

nanomaterials

MDPI

Article

Preparation and Characterization of Electrospun Polysaccharide FucoPol-Based Nanofiber Systems

Yuliana Vázquez-González [1,2], Cristina Prieto [1,*], Milan Stojanovic [1,†], Cristiana A. V. Torres [3,4], Filomena Freitas [3,4], Juan Arturo Ragazzo-Sánchez [2], Montserrat Calderón-Santoyo [2,*] and Jose M. Lagaron [1,*]

1 Novel Materials and Nanotechnology Group, Institute of Agrochemistry and Food Technology (IATA), Spanish Council for Scientific Research (CSIC), Calle Catedrático Agustín Escardino Benlloch 7, 46980 Paterna, Spain; yuliana.vg04@gmail.com (Y.V.-G.); milan87stojanovic@gmail.com (M.S.)
2 Laboratorio Integral de Investigación de Alimentos, Tecnológico Nacional de México-Instituto Tecnológico de Tepic, Av. Tecnológico #2595, Tepic 63195, Mexico; arturoragazzo@hotmail.com
3 UCIBIO-Applied Molecular Biosciences Unit, Department of Chemistry, School of Science and Technology, NOVA University Lisbon, 2819-516 Caparica, Portugal; c.torres@fct.unl.pt (C.A.V.T.); a4406@fct.unl.pt (F.F.)
4 Associate Laboratory i4HB—Institute for Health and Bioeconomy, School of Science and Technology, NOVA University Lisbon, 2819-516 Caparica, Portugal
* Correspondence: cprieto@iata.csic.es (C.P.); montserratcalder@gmail.com (M.C.-S.); lagaron@iata.csic.es (J.M.L.); Tel.: +34-963-900-022 (C.P. & J.M.L.)
† On leave from the Department of Food Technology and Biochemistry, Faculty of Agriculture, University of Belgrade, 11000 Belgrade, Serbia.

Abstract: The electrospinnability of FucoPol, a bacterial exopolysaccharide, is presented for the first time, evaluated alone and in combination with other polymers, such as polyethylene oxide (PEO) and pullulan. The obtained fibers were characterized in terms of their morphological, structural and thermal properties. Pure FucoPol fibers could not be obtained due to FucoPol's low water solubility and a lack of molecular entanglements. Nanofibers were obtained via blending with PEO and pullulan. FucoPol:PEO (1:3 *w/w*) showed fibers with well-defined cylindrical structure, since the higher molecular weight of PEO helps the continuity of the erupted jet towards the collector, forming stable fibers. WAXS, DSC and TGA showed that FucoPol is an amorphous biopolymer, stable until 220 °C, whereas FucoPol-PEO fibers were stable until 140 °C, and FucoPol:pullulan fibers were stable until 130 °C. Interestingly, blended components influenced one another in intermolecular order, since new peaks associated to intermolecular hierarchical assemblies were seen by WAXS. These results make FucoPol-based systems viable candidates for production of nanofibers for packaging, agriculture, biomedicine, pharmacy and cosmetic applications.

Keywords: FucoPol; exopolysaccharide; electrospinning process; nanofibers; characterization

Citation: Vázquez-González, Y.; Prieto, C.; Stojanovic, M.; Torres, C.A.V.; Freitas, F.; Ragazzo-Sánchez, J.A.; Calderón-Santoyo, M.; Lagaron, J.M. Preparation and Characterization of Electrospun Polysaccharide FucoPol-Based Nanofiber Systems. *Nanomaterials* **2022**, *12*, 498. https://doi.org/10.3390/nano12030498

Academic Editor: Takuya Kitaoka

Received: 30 December 2021
Accepted: 29 January 2022
Published: 31 January 2022

1. Introduction

Exopolysaccharides (EPS) are water-soluble, non-toxic, high-molecular-weight polymeric carbohydrate structures composed monosaccharide units joined together by glycosidic bonds [1]. EPS can be homopolysaccharides when composed of a single type of monosaccharide, for example, pullulan; or heteropolysaccharides if they are composed of two or more sugars with different ratios, such as FucoPol [2].

FucoPol is an EPS produced by *Enterobacter* A47, using glycerol as the sole carbon source [3]. It is a high-molecular-weight (4.19×10^6–5.80×10^6) heteropolysaccharide composed of sugar residues [fucose (32–36 mol %), galactose (25–26 mol %), glucose (28–34 mol %) and glucuronic acid (9–10 mol %)], as well as acyl groups [pyruvate (13–14 wt.%), succinate (3 wt.%) and acetate (3–5 wt.%)] [4]. It has an anionic character, with interesting functional properties, including emulsion, film-forming [5], thickening, and flocculating capacity; biological activity and adhesive and photoprotective properties [6,7].

Food Hydrocolloids 147 (2024) 109343

Contents lists available at ScienceDirect

Food Hydrocolloids

journal homepage: www.elsevier.com/locate/foodhyd

Development of antifungal electrospun nanofiber mats containing *Meyerozyma caribbica*

Yuliana Vázquez-González [a, b], Cristina Prieto [a, *], Montserrat Calderón-Santoyo [b, **], Juan Arturo Ragazzo-Sánchez [b], José M. Lagarón [a, ***]

[a] Novel Materials and Nanotechnology Group, Institute of Agrochemistry and Food Technology (IATA), Spanish Council for Scientific Research (CSIC), Calle Catedrático Agustín Escardino Benlloch 7, 46980, Paterna, Spain

[b] Laboratorio Integral de Investigación de Alimentos, Tecnológico Nacional de México-Instituto Tecnológico de Tepic, Av. Tecnológico de Tepic, Av. Tecnológico #2595, C.P. 63175, Tepic, Nayarit, Mexico

ARTICLE INFO

Keywords:
Cashew gum
FucoPol
Pullulan
Electrospinning process
Antifungal nanofibers
M. caribbica

ABSTRACT

To mitigate vegetable and fruit loss caused by post-harvest fungal diseases, polymeric antifungal coatings encapsulating biocontrol yeasts offer a sustainable alternative. Nanofibers derived from pullulan, cashew gum, FucoPol and poly (ethylene oxide) (PEO), were electrospun and loaded with *Meyerozyma caribbica* (GenBank ID: JQ398674). The morphological, thermal and chemical properties of cashew gum (CG:PEO), FucoPol (FP:PEO), and pullulan nanofibers were characterized. The viability of *M. caribbica* within the fibers and their *in vitro* antifungal activity against six phytopathogens were assessed. Morphological analysis exhibited the presence of nanofibers encapsulating *M. caribbica*. ATR-FTIR spectroscopy identified the absence of interactions between the yeast and polymers. Fibers containing *M. caribbica* exhibited *in vitro* fungistatic effects on spore germination. Pullulan nanofibers showed the highest *M. caribbica* viability and the highest percentage of growth inhibition against the evaluated fungi. These promising nanofibers encapsulating biocontrol yeasts could be used as edible coatings or agricultural aids, which offer an alternative for post-harvest treatment to control fungal diseases, reducing global food loss.

1. Introduction

Governmental and international organizations have raised public attention on food loss and waste, and according to the Sustainable Development Goals calls, the objective is to reduce these losses to the half by 2030 (*United Nations*, 2015).

Fruits and vegetables are one of the most consumed commodities globally, accounting for more than 42% of total food wastage (Ganesh et al., 2022). Among them, phytopathogens result in an annual estimated loss of 10–15% of the world's major crops (Peng et al., 2021). Particularly, the predominant postharvest pathogens responsible for spoilage in fruits and vegetables primarily include fungi categorized under the genera *Botrytis*, *Penicillium*, *Aspergillus*, *Alternaria*, *Colletotrichum* spp., and *Rhizopus* (Parafati et al., 2015; Yang et al., 2017), which are naturally present in fruits and vegetables. These pathogenic fungi use different mechanisms to bind to the surface of the host plant. In any case, the penetration of the fungal onto the plant requires the contact and adhesion of the spores to the plant surface. Fungi possess the capability to generate enzymes that modify the plant surface, thereby aiding in adhesion. Subsequently, these phytopathogens induce various forms of rot in the fruit during the post-harvest stage resulting in compromised quality and rendering them unsuitable for sale (Rodrigues et al., 2021). In addition, some fungi species are capable of producing mycotoxins in food and agricultural commodities (Zain, 2011), which can cause adverse health effects to humans and/or livestock.

Addressing these pathogens typically involves the application of chemical fungicides, both pre and post-harvest, directly onto the fruits or vegetables. Nevertheless, the utilization of chemical fungicides has revealed drawbacks such as their harmful impact on human health, the emergence of resistant strains, and their considerable adverse effect on

* Corresponding author.
** Corresponding author.
*** Corresponding author.
E-mail addresses: yuliana.vg04@gmail.com (Y. Vázquez-González), cprieto@iata.csic.es (C. Prieto), mcalderon@tepic.tecnm.mx, montserratcalder@gmail.com (M. Calderón-Santoyo), arturoragazzo@hotmail.com (J.A. Ragazzo-Sánchez), lagaron@iata.csic.es (J.M. Lagarón).

https://doi.org/10.1016/j.foodhyd.2023.109343
Received 15 July 2023; Received in revised form 8 September 2023; Accepted 25 September 2023
Available online 27 September 2023

CAPÍTULO 11. REFERENCIAS

11. REFERENCIAS

Aayush, K., McClements, D. J., Sharma, S., Sharma, R., Singh, G. P., Sharma, K., & Oberoi, K. (2022). Innovations in the development and application of edible coatings for fresh and minimally processed Apple. *Food Control*, *141*(May), 109188. https://doi.org/10.1016/j.foodcont.2022.109188

Abdulsamad, A., Bhatia, P. G., & Ojile, J. E. (2006). Emulsifying and suspending properties of cashew gum. *Nigerian Journal of Pharmaceutical Research*, *5*(1), 40–47.

Aceituno-Medina, M., Lopez-Rubio, A., Mendoza, S., & Lagaron, J. M. (2013). Development of novel ultrathin structures based in amaranth (Amaranthus hypochondriacus) protein isolate through electrospinning. *Food Hydrocolloids*, *31*(2), 289–298. https://doi.org/10.1016/j.foodhyd.2012.11.009

Agrios, G. (2005). *Plant Pathology*. Academic Press.

Aguirre-Güitrón, L., Calderón-Santoyo, M., Bautista-Rosales, P. U., & Ragazzo-Sánchez, J. A. (2019). Application of powder formulation of Meyerozyma caribbica for postharvest control of Colletotrichum gloeosporioides in mango (Mangifera indica L.). *Lwt*, *113*(July 2018), 108271. https://doi.org/10.1016/j.lwt.2019.108271

Aguirre-Güitrón, L., Calderón-Santoyo, M., Lagarón, J. M., Prieto, C., & Ragazzo-Sánchez, J. A. (2022). Formulation of the biological control yeast Meyerozyma caribbica by electrospraying process: effect on postharvest control of anthracnose in mango (Mangifera indica L.) and papaya (Carica papaya L.). *Journal of the Science of Food and Agriculture*, *102*(2), 696–706. https://doi.org/10.1002/jsfa.11400

Aguirre-Güitrón, L., Calderón-Santoyo, M., Ortiz-Basurto, R. I., Bautista-Rosales, P. U., & Ragazzo-Sánchez, J. A. (2018). Optimisation of the spray drying process of formulating the post-harvest biocontrol agent Meyerozyma caribbica. *Biocontrol Science and Technology*, *3157*(May). https://doi.org/10.1080/09583157.2018.1468997

Alvarez, L. D., Moreno, A. O., & Ochoa, F. G. (2012). Tropical and sub-tropical fruits: Postharvest physiology, processing and Packaging. In M. Siddiq (Ed.), *Tropical and sub-tropical fruits [catalog] /* (Oxford: Wi). https://doi.org/10.5962/bhl.title.140794

Andrady, A. L. (2008). *Science and technology of polymer nanofibers*. John Wiley.

Aytac, Z., Yildiz, Z. I., Kayaci-Senirmak, F., Tekinay, T., & Uyar, T. (2017). Electrospinning of cyclodextrin/linalool-inclusion complex nanofibers: Fast-dissolving nanofibrous web

with prolonged release and antibacterial activity. *Food Chemistry*, *231*, 192–201. https://doi.org/10.1016/j.foodchem.2017.03.113

Ballesteros, L. F., Ramirez, M. J., Orrego, C. E., Teixeira, J. A., & Mussatto, S. I. (2017). Encapsulation of antioxidant phenolic compounds extracted from spent coffee grounds by freeze-drying and spray-drying using different coating materials. *Food Chemistry*, *237*, 623–631. https://doi.org/10.1016/j.foodchem.2017.05.142

Barhoum, A., Pal, K., Rahier, H., Uludag, H., Kim, I. S., & Bechelany, M. (2019). Nanofibers as new-generation materials: From spinning and nano-spinning fabrication techniques to emerging applications. *Applied Materials Today*, *17*, 1–35. https://doi.org/10.1016/j.apmt.2019.06.015

Bautista-Rosales, P. U., Calderon-Santoyo, M., Servín-Villegas, R., Ochoa-Álvarez, N. A., & Ragazzo-Sánchez, J. A. (2013). Action mechanisms of the yeast Meyerozyma caribbica for the control of the phytopathogen Colletotrichum gloeosporioides in mangoes. *Biological Control*, *65*(3), 293–301. https://doi.org/10.1016/j.biocontrol.2013.03.010

Benavides, R. E., Jana, S. C., & Reneker, D. H. (2012). Nanofibers from scalable gas jet process. *ACS Macro Letters*, *1*(8), 1032–1036. https://doi.org/10.1021/mz300297g

Bill, M., Sivakumar, D., Thompson, A. K., & Korsten, L. (2014). Avocado Fruit Quality Management during the Postharvest Supply Chain. *Food Reviews International*, *30*(3), 169–202. https://doi.org/10.1080/87559129.2014.907304

Botrel, D. A., Borges, S. V., Fernandes, R. V. de B., Antoniassi, R., de Faria-Machado, A. F., Feitosa, J. P. de A., & de Paula, R. C. M. (2017). Application of cashew tree gum on the production and stability of spray-dried fish oil. *Food Chemistry*, *221*, 1522–1529. https://doi.org/10.1016/j.foodchem.2016.10.141

Calderón-Santoyo, M., Iñiguez-Moreno, M., Barros-Castillo, J. C., Miss-Zacarías, D. M., Díaz, J. A., & Ragazzo-Sánchez, J. A. (2022). Microencapsulation of citral with Arabic gum and sodium alginate for the control of Fusarium pseudocircinatum in bananas. *Iranian Polymer Journal (English Edition)*, *31*(5), 665–676. https://doi.org/10.1007/s13726-022-01033-z

Cruz-Salas, C. N., Prieto, C., Calderón-Santoyo, M., Lagarón, J. M., & Ragazzo-Sánchez, J. A. (2019). Micro-and nanostructures of agave fructans to stabilize compounds of high

biological value via electrohydrodynamic processing. *Nanomaterials*, *9*(12), 1–12. https://doi.org/10.3390/nano9121659

Dahn, E. K., Ploetz, R. C., Coates, L. M., & Pegg, K. G. (2013). *Foliar, fruit and soilborn diseases* (A. W. Schaffer, B., Wolstenholme, B.N., Whiley (ed.); CABI Publi).

Damasceno, C. L., Duarte, E. A. A., dos Santos, L. B. P. R., de Oliveira, T. A. S., de Jesus, F. N., de Oliveira, L. M., Góes-Neto, A., & Soares, A. C. F. (2019). Postharvest biocontrol of anthracnose in bananas by endophytic and soil rhizosphere bacteria associated with sisal (Agave sisalana) in Brazil. *Biological Control*, *137*(June), 104016. https://doi.org/10.1016/j.biocontrol.2019.104016

Daristotle, J. L., Behrens, A. M., Sandler, A. D., & Kofinas, P. (2016). A Review of the Fundamental Principles and Applications of Solution Blow Spinning. *ACS Applied Materials and Interfaces*, *8*(51), 34951–34963. https://doi.org/10.1021/acsami.6b12994

Das, B., Dutta, S., Nayak, A. K., & Nanda, U. (2014). Zinc alginate-carboxymethyl cashew gum microbeads for prolonged drug release: Development and optimization. *International Journal of Biological Macromolecules*, *70*, 506–515. https://doi.org/10.1016/j.ijbiomac.2014.07.030

Deitzel, J. M., Kleinmeyer, J., Harris, D., & Beck-Tan, N. C. (2001). The effect of processing variables on the morphology of electrospun nanofibers and textiles. *Polymer*, *42*, 261–272.

Deng, L., Kang, X., Liu, Y., Feng, F., & Zhang, H. (2017). Effects of surfactants on the formation of gelatin nanofibres for controlled release of curcumin. In *Food Chemistry* (Vol. 231). https://doi.org/10.1016/j.foodchem.2017.03.027

Droby, S., Wisniewski, M., Macarisin, D., & Wilson, C. (2009). Twenty years of postharvest biocontrol research: Is it time for a new paradigm? *Postharvest Biology and Technology*, *52*(2), 137–145. https://doi.org/10.1016/j.postharvbio.2008.11.009

Erben, J., Jencova, V., Chvojka, J., Blazkova, L., Strnadova, K., Modrak, M., & Kostakova, E. K. (2016). The combination of meltblown technology and electrospinning - The influence of the ratio of micro and nanofibers on cell viability. *Materials Letters*, *173*, 153–157. https://doi.org/10.1016/j.matlet.2016.02.147

Faleiro, M. L. (2011). *The mode of antibacterial action of essential oil*. Science against Microbial Pathogens: Communicating Current Research and Technological Advances,

Brow Walker Press.

FAO. (2023). *Tackling food loss and waste: A triple win opportunity*. https://www.fao.org/newsroom/detail/FAO-UNEP-agriculture-environment-food-loss-waste-day-2022/en

Ferreira, A. R. V., Torres, C. A. V., Freitas, F., Reis, M. A. M., Alves, V. D., & Coelhoso, I. M. (2014). Biodegradable films produced from the bacterial polysaccharide FucoPol. *International Journal of Biological Macromolecules*, *71*, 111–116. https://doi.org/10.1016/j.ijbiomac.2014.04.022

Ferreira, A. R. V., Bandarra, N. M., Moldão-Martins, M., Coelhoso, I. M., & Alves, V. D. (2018). FucoPol and chitosan bilayer films for walnut kernels and oil preservation. *LWT - Food Science and Technology*, *91*(August 2017), 34–39. https://doi.org/10.1016/j.lwt.2018.01.020

Freitas, F., Alves, V. D., Gouveia, A. R., Pinheiro, C., Torres, C. A. V., Grandfils, C., & Reis, M. A. M. (2014). Controlled production of exopolysaccharides from enterobacter A47 as a function of carbon source with demonstration of their film and emulsifying abilities. *Applied Biochemistry and Biotechnology*, *172*(2), 641–657. https://doi.org/10.1007/s12010-013-0560-0

Freitas, F., Alves, V. D., Torres, C. A. V., Cruz, M., Sousa, I., Melo, M. J., Ramos, A. M., & Reis, M. A. M. (2011). Fucose-containing exopolysaccharide produced by the newly isolated Enterobacter strain A47 DSM 23139. *Carbohydrate Polymers*, *83*(1), 159–165. https://doi.org/10.1016/j.carbpol.2010.07.034

Freitas, T. K. F. S., Almeida, C. A., Manholer, D. D., Geraldino, H. C. L., de Souza, M. T. F., & García, J. C. (2017). Review of Utilization Plant-Based Coagulants as Alternatives to Textile Wastewater Treatment. *Detox Fashion*, 27–79. https://doi.org/Freitas, T. K. F. S., Almeida, C. A., Manholer, D. D., Geraldino, H. C. L., de Souza, M. T. F., & Garcia, J. C. (2017). Review of Utilization Plant-Based Coagulants as Alternatives to Textile Wastewater Treatment. Detox Fashion, 27–79. doi:10.1007/978-981-10-4780-0_2

García-Moreno, P. J., Özdemir, N., Stephansen, K., Mateiu, R. V., Echegoyen, Y., Lagaron, J. M., Chronakis, I. S., & Jacobsen, C. (2017). Development of carbohydrate-based nano-microstructures loaded with fish oil by using electrohydrodynamic processing.

Food Hydrocolloids, *69*, 273–285. https://doi.org/10.1016/j.foodhyd.2017.02.013

Gaviria-Hernández, V., Patiño-Hoyos, L. F., & Saldarriaga-Cardona, A. (2013). Evaluación in vitro de fungicidas comerciales para el control de Colletotrichum spp., en mora de castilla. *Corpoica Ciencia y Tecnología Agropecuaria*, *14*(1), 67. https://doi.org/10.21930/rcta.vol14_num1_art:344

González-Estrada, R. R., Carvajal-Millán, E., Ragazzo-Sánchez, J. A., Bautista-Rosales, P. U., & Calderón-Santoyo, M. (2017). Control of blue mold decay on Persian lime: Application of covalently cross-linked arabinoxylans bioactive coatings with antagonistic yeast entrapped. *LWT - Food Science and Technology*, *85*, 187–196. https://doi.org/10.1016/j.lwt.2017.07.019

González-Estrada, Ramsés R., Calderón-Santoyo, M., Ragazzo-Sánchez, J. A., Peyron, S., & Chalier, P. (2017). Antimicrobial soy protein isolate-based films: physical characterisation, active agent retention and antifungal properties against *Penicillium italicum*. *International Journal of Food Science & Technology*, 1–9. https://doi.org/10.1111/ijfs.13664

González-Estrada, Ramsés Ramón, Ascencio-Valle, F. de J., Ragazzo-Sánchez, J. A., & Calderón-Santoyo, M. (2017). Use of a marine yeast as a biocontrol agent of the novel pathogen Penicillium citrinum on Persian lime. *Emirates Journal of Food and Agriculture*, *29*(2), 114–122. https://doi.org/10.9755/ejfa.2016-09-1273

González-Gutérrez, K. N., Ragazzo-Sánchez, J. A., Barros-Castillo, J. C., Narváez-Zapata, J. A., & Calderón-Santoyo, M. (2023). Yeasts with potential biocontrol of Colletotrichum gloeosporioides in avocado (Persea americana Mill. cv. Hass) and characterization of Yamadazyma mexicana mechanisms. *European Journal of Plant Pathology*, *165*, 525–543. https://doi.org/https://doi.org/10.1007/s10658-022-02625-4

González-Gutiérrez, K. N., Ragazzo-Sánchez, J. A., & Calderón-Santoyo, M. (2021). Application of stressed and microencapsulated Meyerozyma caribbica for the control of Colletotrichum gloeosporioides in avocado (Persea americana Mill. cv. Hass). *Journal of Plant Diseases and Protection*, *128*(5), 1243–1251. https://doi.org/10.1007/s41348-021-00487-2

Grumi, M. (2021). *DEVELOPMENT AND CHARACTERIZATION OF ELECTROSPUN CASHEW GUM-BASED FILMS FOR FOOD PACKAGING APPLICATIONS*.

Università degli Studi di Milano, Milan (Italy).

Guerreiro, B. M., Freitas, F., Lima, J. C., Silva, J. C., Dionísio, M., & Reis, M. A. M. (2020). Demonstration of the cryoprotective properties of the fucose-containing polysaccharide FucoPol. *Carbohydrate Polymers*, *245*(May), 116500. https://doi.org/10.1016/j.carbpol.2020.116500

Gyedu-Akoto, E., Oduro, I., Amoah, F. M., Oldham, J. H., Ellis, W. O., Opoku-Ameyaw, K., & Hakeem, R. B. (2008). Physicochemical properties of cashew tree gum. *African Journal of Food Science*, *2*, 60–64.

Haider, A., Haider, S., & Kang, I. K. (2018). A comprehensive review summarizing the effect of electrospinning parameters and potential applications of nanofibers in biomedical and biotechnology. *Arabian Journal of Chemistry*, *11*(8), 1165–1188. https://doi.org/10.1016/j.arabjc.2015.11.015

Hassan, M. A., Yeom, B. Y., Wilkie, A., Pourdeyhimi, B., & Khan, S. A. (2013). Fabrication of nanofiber meltblown membranes and their filtration properties. *Journal of Membrane Science*, *427*, 336–344. https://doi.org/10.1016/j.memsci.2012.09.050

Herrera-Balandrano, D. D., Wang, S., Wang, C., Shi, X., Liu, F., & Laborda, P. (2023). Antagonistic mechanisms of yeasts Meyerozyma guilliermondii and M . caribbica for the control of plant pathogens : A review. *Biological Control*, *April*, 105333. https://doi.org/10.1016/j.biocontrol.2023.105333

Iñiguez-Moreno, M., Calderón-Santoyo, M., Barros-Castillo, J. C., Miss-Zacarías, D. M., Díaz, J. A., & Ragazzo-Sánchez, J. A. (2022). Nanofibers added with citral: Characterization and their application to postharvest control of Fusarium pseudocircinatum in bananas. *Journal of Food Processing and Preservation*, *46*(12), 1–10. https://doi.org/10.1111/jfpp.17188

Iñiguez-Moreno, M., Ragazzo-Sánchez, J. A., Barros-Castillo, J. C., Sandoval-Contreras, T., & Calderón-Santoyo, M. (2020). Sodium alginate coatings added with Meyerozyma caribbica: Postharvest biocontrol of Colletotrichum gloeosporioides in avocado (Persea americana Mill. cv. Hass). *Postharvest Biology and Technology*, *163*(January), 111123. https://doi.org/10.1016/j.postharvbio.2020.111123

Iñiguez-Moreno, M., Ragazzo-Sánchez, J. A., Barros-Castillo, J. C., Solís-Pacheco, J. R., & Calderón-Santoyo, M. (2021). Characterization of sodium alginate coatings with

Meyerozyma caribbica and impact on quality properties of avocado fruit. *Lwt*, *152*(April). https://doi.org/10.1016/j.lwt.2021.112346

Karim, M. R., Lee, H. W., Kim, R., Ji, B. C., Cho, J. W., Son, T. W., Oh, W., & Yeum, J. H. (2009). Preparation and characterization of electrospun pullulan/montmorillonite nanofiber mats in aqueous solution. *Carbohydrate Polymers*, *78*(2), 336–342. https://doi.org/10.1016/j.carbpol.2009.04.024

Khalilur, M., Khan, R., & Hassan, M. N. (2021). Solution Blow Spinning (SBS): A Promising Spinning System for Submicron/Nanofibre Production How to cite: Khan MKR, Hassan MN. Solution Blow Spinning (SBS): A Promising Spinning System for Submicron/Nanofibre Production. Textile & Leather Review. *Textile & Leather Review*, *4*(3), 181–200. https://doi.org/10.31881/TLR

Khan, K., Schutyser, M., Schroën, K., & Boom, R. (2012). The potential of electrospraying for hydrophobic film coating on foods. *Journal of Food Engineering*, *108*(3), 410–416. https://doi.org/10.1016/j.jfoodeng.2011.09.005

Kong, L., & Ziegler, G. R. (2014). Rheological aspects in fabricating pullulan fibers by electro-wet-spinning. *Food Hydrocolloids*, *38*, 220–226. https://doi.org/10.1016/j.foodhyd.2013.12.016

Kumar, A. S., Mody, K., & Jha, B. (2007). Bacterial exopolysaccharides - A perception. *Journal of Basic Microbiology*, *47*(2), 103–117. https://doi.org/10.1002/jobm.200610203

Lim, B. C., Lim, J. W., & Ho, Y. C. (2018). Garden cress mucilage as a potential emerging biopolymer for improving turbidity removal in water treatment. *Process Safety and Environmental Protection*, *119*, 233–241. https://doi.org/10.1016/j.psep.2018.08.015

Liu, X., Fang, W., Liu, L., Yu, T., Lou, B., & Zheng, X. (2010). Biological control of postharvest sour rot of citrus by two antagonistic yeasts. *Letters in Applied Microbiology*, *51*(1), 30–35. https://doi.org/10.1111/j.1472-765X.2010.02851.x

López-Cruz, R., Ragazzo-Sánchez, J. A., & Calderón-Santoyo, M. (2020). Microencapsulation of Meyerozyma guilliermondii by spray drying using sodium alginate and soy protein isolate as wall materials: a biocontrol formulation for anthracnose disease of mango. *Biocontrol Science and Technology*, *0*(0), 1116–1132. https://doi.org/10.1080/09583157.2020.1793910

Lourenço, S. C., Torres, C. A. V., Nunes, D., Duarte, P., Freitas, F., Reis, M. A. M., Fortunato, E., Moldão-Martins, M., da Costa, L. B., & Alves, V. D. (2017). Using a bacterial fucose-rich polysaccharide as encapsulation material of bioactive compounds. *International Journal of Biological Macromolecules*, *104*, 1099–1106. https://doi.org/10.1016/j.ijbiomac.2017.07.023

Magalhães, V. S. M., Ferreira, L. M. D. F., & Silva, C. (2021). Causes and mitigation strategies of food loss and waste: A systematic literature review and framework development. *Sustainable Production and Consumption*, *28*, 1580–1599. https://doi.org/10.1016/j.spc.2021.08.004

Mahapatra, S., & Banerjee, D. (2012). Structural elucidation and bioactivity of a novel exopolysaccharide from endophytic Fusarium solani SD5. *Carbohydrate Polymers*, *90*(1), 683–689. https://doi.org/10.1016/j.carbpol.2012.05.097

Medeiros, E. S., Glenn, G. M., Klamczynski, A. P., Orts, W. J., & Mattoso, L. H. . (2009). Solution Blow Spinning: A New Method to Produce Micro- and Nanofibers from Polymer Solutions. *Journal of Applied Polymer Science*, *113*, 2322–2330. https://doi.org/10.1002/app

Moncayo-Martínez, D. C. (2013). Desarrollo de un recubrimiento comestible a partir de un biopolimero para prolongar la vida útil de frutas frescas. In *Universidad Nacional de Colombia Programa interfacultades, Maestría en Ciencia y Tecnología Alimentos*. http://www.bdigital.unal.edu.co/44864/1/24336979.2013.pdf

Morton, J. F. (2004). *Fruits of Warm Climates* (Creative R). https://pdfs.semanticscholar.org/7441/0024de07be2cd9df3aed4de068d6862e1db4.pdf

Ningtyas, D. W., Bhandari, B., Bansal, N., & Prakash, S. (2019). The viability of probiotic Lactobacillus rhamnosus (non-encapsulated and encapsulated) in functional reduced-fat cream cheese and its textural properties during storage. *Food Control*, *100*, 8–16. https://doi.org/10.1016/j.foodcont.2018.12.048

Nwodo, U. U., Green, E., & Okoh, A. I. (2012). Bacterial exopolysaccharides: Functionality and prospects. *International Journal of Molecular Sciences*, *13*(11), 14002–14015. https://doi.org/10.3390/ijms131114002

O'Sullivan, J. J., Norwood, E. A., O'Mahony, J. A., & Kelly, A. L. (2019). Atomisation technologies used in spray drying in the dairy industry: A review. *Journal of Food*

Engineering, *243*, 57–69. https://doi.org/10.1016/j.jfoodeng.2018.08.027

Ocampo-Suarez, I. B., López, Z., Calderón-Santoyo, M., Ragazzo-Sánchez, J. A., & Knauth, P. (2017). Are biological control agents, isolated from tropical fruits, harmless to potential consumers? *Food Chemical Toxicology*, *109*, 1055–1062. https://doi.org/https://doi. org/10.1016/j.fct.2017.05.010.

Ocampo-Suarez, I. B., Sanchez-Salas, J. L., Ragazzo-Sánchez, J. A., & Calderón-Santoyo, M. (2017). Evaluation of the toxicity and pathogenicity of biocontrol agents in murine models, chicken embryos and dermal irritation in rabbits. *Toxicology Research*, *6*(2), 188–198. https://doi.org/10.1039/c6tx00275g

Olorunsola, E. O., Bhatia, P. G., Tytler, B. A., & Adikwu, M. U. (2016). Thermochemical Properties of Hydrophilic Polymers from Cashew and Khaya Exudates and Their Implications on Drug Delivery. *Journal of Drug Delivery*, *2016*, 1–7. https://doi.org/10.1155/2016/7496585

Olvera-Gracia, M., Aguilar-Hernández, J. R., & Kryshtab, T. (2013). Procesamiento de micro y nanofibras de polipirrol/óxido de polietileno/nylon-6 por la técnica de electrohilado**Citación estilo Chicago Olvera-Gracia, Manuel, Jorge Ricardo Aguilar-Hernández, Tetyana Kryshtab. Procesamiento de micro y nanofibras de polipi. *Ingeniería, Investigación y Tecnología*, *14*(4), 575–581. https://doi.org/10.1016/s1405-7743(13)72267-4

ONU. (2023a). *International Day of Awareness on Food Loss and Waste Reduction*. https://www.un.org/en/observances/end-food-waste-day

ONU. (2023b). *Los Objetivos de Desarrollo Sostenible en México*. https://mexico.un.org/es/sdgs/12

Ooi, V. E., & Liu, F. (2000). Immunomodulation and anti-cancer activity of polysaccharide-protein complexes. *Curr Med Chem*, *7*, 715–729.

Pérez-Masiá, R., López-Rubio, A., & Lagarón, J. M. (2013). Development of zein-based heat-management structures for smart food packaging. *Food Hydrocolloids*, *30*(1), 182–191. https://doi.org/10.1016/j.foodhyd.2012.05.010

Pérez, G. (2012). *Extracción de compuestos activos de plantas para su aplicación en recubrimientos comestibles para controlar prodredumbre gris en la fresa* [Universidad Nacional Autónoma de México].

file:///C:/Users/VAZQUEZ/Desktop/PROYECTO_MAESTRÍA/JACK LEAF/extracc de compues.unam.pdf

Ramírez-Gil, J. G., Henao-Rojas, J. C., & Morales-Osorio, J. G. (2021). Postharvest diseases and disorders in avocado cv. Hass and their relationship to preharvest management practices. *Heliyon*, *7*(1), e05905. https://doi.org/10.1016/j.heliyon.2021.e05905

Ramos-Hernández, J. A., Ragazzo-Sanchez, J. A., Calderón-Santoyo, M., Ortiz-Basurto, R. I., Prieto, C., & Lagaron, J. M. (2018). Use of electrosprayed agave fructans as nanoencapsulating hydrocolloids for bioactives. *Nanomaterials*, *8*(11), 1–11. https://doi.org/10.3390/nano8110868

Ribeiro, A. J., De Souza, F. R. L., Bezerra, J. M. N. A., Oliveira, C., Nadvorny, D., De La Roca Soares, M. F., Nunes, L. C. C., Silva-Filho, E. C., Veiga, F., & Soares Sobrinho, J. L. (2016). Gums' based delivery systems: Review on cashew gum and its derivatives. *Carbohydrate Polymers*, *147*, 188–200. https://doi.org/10.1016/j.carbpol.2016.02.042

Ricaurte, L., & Quintanilla-Carvajal, X. M. (2019). Use of electrospinning technique to produce nanofibers for food industries: a perspective from regulations to characterisations. *Trends in Food Science & Technology*. https://doi.org/10.1016/j.tifs.2019.01.006

Rodriguez, A., Troncoso, R., Sánchez, A., González, D., Ruiz, E., Zamora, R., Ceceña, C., Grimaldo, O., & Aviles, M. (2015). Efecto antifúngico de extractos fenólicos y de carotenoidesde chiltepín (Capsicum annum var. glabriusculum) en Alternaria alternata and Fusarium oxysporum. *Revista Argentina de Microbiología*, *47*(1), 72–77. https://doi.org/10.1016/j.ram.2014.12.005

Rohasmizah, H., & Azizah, M. (2022). Pectin-based edible coatings and nanoemulsion for the preservation of fruits and vegetables: A review. *Applied Food Research*, *2*(2), 100221. https://doi.org/10.1016/j.afres.2022.100221

Romero, J., Albertos, I., Díez-m, A., & Poveda, J. (2022). Control of postharvest diseases in berries through edible coatings and bacterial probiotics. *Scientia Horticulturae*, *304*(June). https://doi.org/10.1016/j.scienta.2022.111326

Santos, A. M. C., Medeiros, E. L. G., Blaker, J. J., & Medeiros, E. S. (2016). Aqueous solution blow spinning of poly(vinyl alcohol) micro- and nanofibers. *Materials Letters*, *176*, 122–126. https://doi.org/10.1016/j.matlet.2016.04.101

Sharma, R. R., Singh, D., & Singh, R. (2009). Biological control of postharvest diseases of fruits and vegetables by microbial antagonists : A review. *Biological Control*, *50*(3), 205–221. https://doi.org/10.1016/j.biocontrol.2009.05.001

Shukla, A., Mehta, K., Parmar, J., Pandya, J., & Saraf, M. (2019). Depicting the exemplary knowledge of microbial exopolysaccharides in a nutshell. *European Polymer Journal*, *119*(July), 298–310. https://doi.org/10.1016/j.eurpolymj.2019.07.044

SIAP. (2021). *SIAP*. Servicio de Información Agroalimentaria y Pesquera. https://nube.siap.gob.mx/cierreagricola/

Silva, B. D. S., Ulhoa, C. J., Batista, K. A., Di Medeiros, M. C., Filho, R. R. D. S., Yamashita, F., & Fernandes, K. F. (2012). Biodegradable and bioactive CGP/PVA film for fungal growth inhibition. *Carbohydrate Polymers*, *89*(3), 964–970. https://doi.org/10.1016/j.carbpol.2012.04.052

Silva, D. A., Feitosa, J. P. A., Maciel, J. S., Paula, H. C. B., & de Paula, R. C. M. (2006). Characterization of crosslinked cashew gum derivatives. *Carbohydrate Polymers*, *66*(1), 16–26. https://doi.org/10.1016/j.carbpol.2006.02.021

Silva, F., Torres, L., Silva, L., Figueiredo, R., Garruti, D., Araújo, T., Duarte, A., Brito, D., & Ricardo, N. (2018). Cashew gum and maltrodextrin particles for green tea (Camellia sinensis var Assamica) extract encapsulation. *Food Chemistry*, *261*(October 2017), 169–175. https://doi.org/10.1016/j.foodchem.2018.04.028

Singh, R., Paul, D., & Jain, R. K. (2006). Biofilms: implications in bioremediation. *Trends in Microbiology*, *14*(9), 389–397. https://doi.org/10.1016/j.tim.2006.07.001

Singh, R. S., Saini, G. K., & Kennedy, J. F. (2008). Pullulan: Microbial sources, production and applications. *Carbohydrate Polymers*, *73*(4), 515–531. https://doi.org/10.1016/j.carbpol.2008.01.003

Sousa, H. C., Braga, M. E. M., & Sosnik, A. (2015). *Biomateriales aplicados al diseño de sistemas terapéuticos avanzados*. Imprensa da Universidade de Coimbra. https://doi.org/http://dx.doi.org/10.14195/978-989-26-0881-5

STATISTA. (2023). *STATISTA*. Producción de Aguacate En El Mundo 2012-2021. https://es.statista.com/estadisticas/528382/produccion-de-aguacate-en-el-mundo/#:~:text=En 2021%2C la producción mundial,en todo el periodo estudiado.

Tariq, S., Wani, S., Rasool, W., Shafi, K., Bhat, M. A., Prabhakar, A., Shalla, A. H., &

Rather, M. A. (2019). A comprehensive review of the antibacterial, antifungal and antiviral potential of essential oils and their chemical constituents against drug-resistant microbial pathogens. *Microbial Pathogenesis*, *134*(March), 103580. https://doi.org/10.1016/j.micpath.2019.103580

Torres-Giner, S., Hilliou, L., Melendez-Rodriguez, B., Figueroa-Lopez, K. J., Madalena, D., Cabedo, L., Covas, J. A., Vicente, A. A., & Lagaron, J. M. (2018). Melt processability, characterization, and antibacterial activity of compression-molded green composite sheets made of poly(3-hydroxybutyrate-co-3-hydroxyvalerate) reinforced with coconut fibers impregnated with oregano essential oil. *Food Packaging and Shelf Life*, *17*(March), 39–49. https://doi.org/10.1016/j.fpsl.2018.05.002

Torres, C. A. V., Marques, R., Antunes, S., Alves, V. D., Sousa, I., Ramos, A. M., Oliveira, R., Freitas, F., & Reis, M. A. M. (2011). Kinetics of production and characterization of the fucose-containing exopolysaccharide from Enterobacter A47. *Journal of Biotechnology*, *156*(4), 261–267. https://doi.org/10.1016/j.jbiotec.2011.06.024

Tripathi, P., & Dubey, N. K. (2004). Exploitation of natural products as an alternative strategy to control postharvest fungal rotting of fruit and vegetables. *Postharvest Biology and Technology*, *32*(3), 235–245. https://doi.org/10.1016/j.postharvbio.2003.11.005

Tronsmo, A., & Dennis, C. (1977). The use of Trichoderma species to control strawberry rot. *Dutch Journal of Phytopathology*, *83*, 449–455. https://doi.org/doi: 10.1007 / bf03041462

USDA. (2023). *U.S. DEPARTMENT OF AGRICULTURE*. https://www.usda.gov/

Vázquez-González, Y., Ragazzo-Sánchez, J. A., & Calderón-Santoyo, M. (2020). Characterization and antifungal activity of jackfruit (Artocarpus heterophyllus Lam.) leaf extract obtained using conventional and emerging technologies. *Food Chemistry*, *330*(June), 127211. https://doi.org/10.1016/j.foodchem.2020.127211

Wilson, C. L., & Pusey, P. L. (1985). Potential for Biological Control of Postharvest Plant Diseases. *Plant Disease*, *69*(5), 375–378.

Wiyono, S., & Widodo. (2013). Powder formulation of antagonistic yeasts,cryptococcus albidus and cryptococcus terreusas biofungicides. *Biotropia*, *20*(1), 19–28. https://doi.org/10.11598/btb.2013.20.1.264

Zaeim, D., Sarabi-Jamab, M., Ghorani, B., Kadkhodaee, R., & Tromp, R. H. (2018). Electrospray-assisted drying of live probiotics in acacia gum microparticles matrix. *Carbohydrate Polymers*, *183*(July 2017), 183–191. https://doi.org/10.1016/j.carbpol.2017.12.001

Zhou, Y., Li, W., Zeng, J., & Shao, Y. (2018). Mechanisms of action of the yeast Debaryomyces nepalensis for control of the pathogen Colletotrichum gloeosporioides in mango fruit. *Biological Control*, *123*, 111–119. https://doi.org/10.1016/j.biocontrol.2018.05.014